The preparation of lanthanide macrocyclic complexes for use as MRI and luminescence contrast agents

Amanda E. Sparke

A thesis submitted for the degree of Doctor of Philosophy

The University of Hull
Department of Chemistry

Abstract

Multimodality imaging agents have the potential to be detected in both MRI and optical imaging experiments allowing for visualisation of biological systems from the cellular level up to the whole body. Lanthanide complexes have shown great promise as components of compounds that can act as either MRI contrast agents or luminescent imaging agents dependent on the metal centre incorporated (e.g. gadolinium(III) or europium(III)/terbium(III) respectively).

This thesis describes the design, synthesis and characterisation of multimodality lanthanide imaging agents. The synthesis of a series of lanthanide chelators based on DO3A bearing a benzimidazole or a benzyl derivative that can act as both a chromophore unit and a linking group for conjugation that has the functionality to couple to an optical dye (either rhodamine or BODIPY derivatives) is discussed.

A series of lanthanide complexes with either a nitro- or amino-benzyl benzimidazole DO3A chelator or with an aminobenzyl DO3A chelator have been prepared. A number of strategies have been attempted to couple the complexes to an optical dye to form a multimodality imaging agent.

Physical properties and cellular uptake of the lanthanide complexes have been investigated. It was shown that the benzimidazole ligands can sensitise the luminescence of both the europium(III) and terbium(III) metal ions. Relaxation rates of the gadolinium(III) benzimidazole DO3A complexes are comparable to that of commercial contrast agents. The relaxivity of the gadolinium(III) complex formed with the ligand 1,4,7-tris(carboxymethyl)-10-(1-(4-nitrobenzyl)-2-methyl benzimidazole)-1,4,7,10-tetraazacyclododecane **(34)** is 6.22 mM^{-1} s^{-1}, with the relaxivity of the gadolinium(III) complex formed with 1,4,7-tris(carboxymethyl)-10-(1-(4-aminobenzyl)-2-methyl benzimidazole)-1,4,7,10-tetraazacyclododecane **(37)** was found to be lower at 4.51 mM^{-1} s^{-1}. The luminescence lifetimes of the europium(III) and terbium(III) complexes in H_2O and D_2O were used to calculate the number of coordinated water

molecules in aqueous solution [q = 1.19 for the europium(III) complex of **(34)**, 0.7-0.8 for the europium(III) complex of **(37)** and 1.25 for the terbium(III) complexes of **(34)**]

Table of Contents

List of Figures

List of Tables

Acknowledgments

I would firstly like to thank my supervisors Dr Steve Archibald and Dr Anne-Marie Seymour for their help and support towards the completion of this thesis. I wish to thank the following people Dr Mark Lorch, Dr Rob Lewis, Dr Mark Lowe, Dr Peter Gibb, Abid Khan, Dr Ross Boyle and Huguette Savoie for their help with NMR, MRI, luminescence properties and fluorescence imaging studies. Another thanks go to Dr Jon Silversides and Ryan Mewis for their crystal structure analysis.

A massive thanks goes to Dr Lizzie lewis and Chris Welch for being there and for keeping me motivated when things were going bad, which was most of the time. There are many people I would like to thank and as I do not have enough space for individual comments and they would mainly be insulting so I am going to list you all, though I guess the biggest thanks is for putting up with my many rants and overall general grumpiness! These include Grazia, Dave, Mark, Graeme, Sushil, Christina, Cary, Aaron, Kay, Andy, Jumper Dave, Ruth, Chris, Dana, Emma, Bob, Carol, Mark, Joe, Ionnais, Alistair, Pete, Neil, Hayley, Phil, Nigel, Dunja, Jessica, Ashwin, Dave, Kath, Jan, Paul, Steve, Tim, Hayley, Pete, Neil, Amy, Katie, Martin, Millie, Jake, Becki, Arnoud and to anyone else I probably have forgotten.

The biggest thanks go to Matt and my Mum and Dad with the rest of my family for their help and support during this stressful time. The last thanks of course goes to the most important things in my life, my dogs Alfie and Charlie.

I would also like to thank the Clinical Biosciences Institute at the University of Hull for funding.

Declarations

Except where specific reference is made to other sources, the work presented in this thesis is the work of the author. It has not been submitted, in whole or in part, for any other degree.

Amanda E. Sparke

Abbreviations

Abbreviation	Meaning
Φ	Quantum yield
τ	Emission lifetime
τ_m	Residency time (inner sphere)
τ_m'	Residency time (outer sphere)
τ_R	Tumbling correlation rate
B_0	Magnetic field direction
1B4M-DTPA	2-(4-isothiocyanatobenzyl)-6-methyldiethylenetriamine pentaacetic acid
Bipy	2,2'-Bipyridine
BODIPY	Boron dipyrromethene
DCM	Dichloromethane
DDQ	Dichlorodicyanoquinine
DEPT	Distortionless enhanced polarisation transfer
DMAP	4-(dimethylamino)pyridine
DMF	Dimethylformamide
DOTA	1,4,7,10-Tetraazacyclododecane-1,4,7,10-tetraacetate
DTPA	Diethylenetriaminepentaacetate
DTTA	Diethylenetriamine –*N,N',N'',N'''*-tetraacetate
(Eu(TMT)-AP$_3$)	Europium(III) terpyridine-bis(methyl-enamine) tetraacetic acid chelate
GRID	Gd(DTPA)-tetramethyl rhodamine amine dextran
K_{ML}	Stability constant
K^*_{ML}	pH dependent stability constant
H(2,2)	*N,N,N',N''*-tetrakis-(2-aminoethyl)-ethane-1,2-diamine
H221AM	2-hydroxyisophthalamide
H_4DO3A-P	1,4,7,10-tetraazacyclododecane-4,7,10-triacetic-1-[1,2]
1,2-HOPO	1-hydroxypyridine-2-one
HOPO	Hydroxypyridinone
HSA	Human serum albumin
LDA	Lithium diisopropylamine
M_0	Net magnetization
MLCT	Metal ligand charge transfer
MRI	Magnetic Resonance Imaging
MS-325	((trisodium-((2-(R)-[(4,4-diphenylcyclohexyl) phosphonooxymethyl] diethylenetriaminepentaacetato) (aquo) gadolinium(III)))
(MTTA-europium(III)	europium(III) [4'-(10-methyl-9-anthryl)-2,2':6',2''-tetrpyridine-6,6'-diyl]bis(methylenenitrilo)tetrakis(acetate)
NIH 3T3	Mouse fibroplasts
NMR	Nuclear Magnetic Resonance
PAMAM	5-Polyamidoamine
PBR	Peripheral benzodiazepene receptor
PS	Phospholipid phosphatidylserine
PSI	Polysuccinimide

q	Water bound molecule (inner sphere)
q'	Water bound molecule (outer sphere)
r	Gd-H distance (inner sphere)
r'	Gd-H distance (outer sphere)
rf	Radio frequency
RT	Room temperature
S_1	Singlet state
T_1	Triplet state
T_1	Longitudinal or spin-lattice relaxation
T_2	Transverse or spin-spin relaxation
TACN	Triazacyclononane
TDP	1,1-thiocarbonyldi-2(1H)-pyridone
TEA	Triethylamine
THF	Tetrahydrofuran
t.l.c.	Thin layer chromatography
Tosyl chloride	*p*-toluenesulfonyl chloride
TREN	Tris-(2-aminoethyl)-amine
W_0	Lamour frequency
Z_{eff}	Effective nuclear charge

1. Introduction

1.1 General Introduction

In recent years magnetic resonance imaging (MRI) and optical imaging have been used extensively in the study of biological function at an anatomical and cellular level. MRI has been used to study the human body at an anatomical level to identify abnormalities like cancerous tissues as well as understanding the process of diseases such as cardiac failure. Optical imaging has been used to probe cellular functions including apoptosis (programmed cell death). The technique is restricted to a cellular level due to limited tissue penetration, where as MRI techniques are better suited to an anatomical level because of lower image resolution. Typically images for MRI and optical imaging are shown in figure 1.

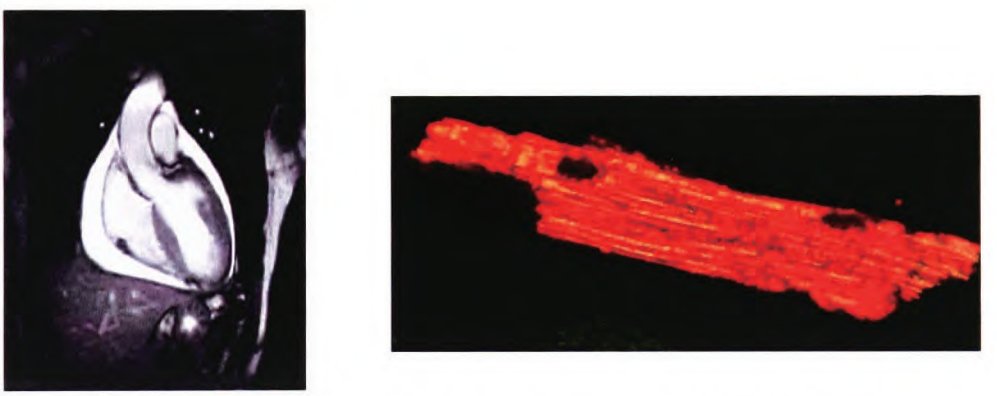

Figure 1 MRI picture of the heart (left) and an optical image of a heart cell (right)

Multimodality imaging agents have the potential to act as both MRI and optical imaging agents allowing for visualisation of biological systems on different scales and varying resolution.[1 2] They can be further modified to target specific cell types or physiological processes. This will allow the same biological specimen to be visualised from cellular up to a whole organism level, and the additional ability to target cell or tissue types may ultimately provide a greater understanding of the human body, which in turn could lead to improved treatment of diseases.

Lanthanides have shown great promise as components of contrast agents that have the ability to act as both MRI agents [e.g. gadolinium(III)] and optical

agents when sensitised by a chromophore [e.g. europium(III) or terbium(III)). Gadolinium(III)] compounds are used as MRI contrast agents due to their long electron spin relaxation times and high magnetic field, while luminescent lanthanide ions such as europium(III) and terbium(III) are used for optical imaging as they have suitable wavelength emissions (visible) and long lived excited states.[3 4]

Lanthanide ions are toxic to the body and need to be chelated to a ligand in order to be used *in vivo*. Common chelator designs that have been exploited are based on incorporating a cyclen macrocycle unit 1,4,7,10-tetraazacyclododecane-1,4,7,10-tetraacetic acid, (DOTA) and a linear chelator diethylenetriaminepentaacetatic acid (DTPA). They are both know to form lanthanide ion complexes of high stability and are shown in figure 2.[5]

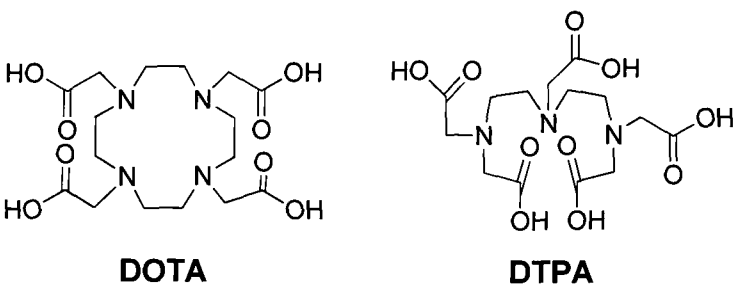

Figure 2 The polyaminocarboxylic acid ligands DOTA and DTPA

The application of MRI contrast agents relies on the ability of the gadolinium(III) centre to influence the relaxivity of water molecules that results in an enhancement of the image quality. For lanthanide complexes to be used as luminescent agents a chromophore group needs to be incorporated onto the lanthanide(III) chelator. The chromophore is required to either sensitise the luminescence of the lanthanide metal centre [europium(III), terbium(III)], or could be a separate optical dye in a multimodal agent incorporating gadolinium(III).[2 6]

The purpose of this work is to synthesise a range of multimodal lanthanide contrast agents that can be used in both MRI and optical imaging experiments and also specifically localise within a cell. The strategy to achieve this is to incorporate a linker unit between the chelated lanthanide and a functional unit

that is either an optical dye or causes cellular localisation/uptake. This linking unit could sensitise lanthanide luminescence [for example: europium(III)/ terbium(III)/ ytterbium(III)] or act simply as a linker between the MRI contrast agent component [gadolinium(III)] and an optical dye (see figure 3).

Figure 3 Design template for dual modality imaging agents

1.2 The lanthanides

The lanthanides are a family of highly electropositive metals in period 6, composed of a series of fifteen elements in the *f*-block that correspond to the filling of the seven 4*f* orbitals (table 1).[7]

$_{57}$La	$_{58}$Ce	$_{59}$Pr	$_{60}$Nd	$_{61}$Pm	$_{62}$Sm	$_{63}$Eu	$_{64}$Gd	$_{65}$Tb	$_{66}$Dy	$_{67}$Ho	$_{68}$Er	$_{69}$Tm	$_{70}$Yb	$_{71}$Lu

Table 1 Lanthanide metal ions

The chemistry of the lanthanides is dominated by their +3 oxidation state. Lanthanides have low charge densities, which leads to their compounds being predominantly ionic in character. The ionic radii of the lanthanides decrease steadily across the row and this is termed 'the lanthanide contraction' as shown in figure 4.

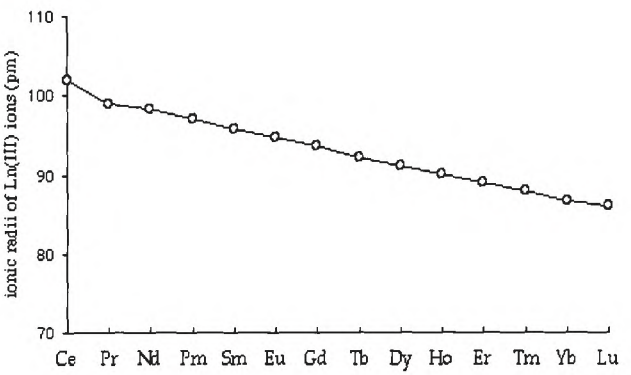

Figure 4 Ionic radii of the lanthanide ions across the period

The lanthanide contraction is caused by the increase in effective nuclear charge (Z_{eff}) across the series due to the poor shielding ability of the 4f electrons. The lanthanide ions are classed as being hard in character, they tend to bond to O, N and F-donors and often have high coordination numbers ranging from 9-12.[8] This preference for hard donors is thought to be because the 4f orbitals are too contracted to play any significant role in the bonding in lanthanide complexes. Thus, ligand-field stabilization energies are small and probably play little role in determining the geometry of complexes. Due to the unique properties of the lanthanides, they have found many uses in magnetic and luminescent materials.[7] Some key properties are summarised in table 2.

Ln^{3+}	$4f^n$	ground level	colour	g $[J(J+1)]^{1/2}$	μ_{obs}
Ce	1	$^2F_{5/2}$	colourless	2.54	2.3-2.5
Pr	2	$^3H_4$	green	3.58	3.4-3.6
Nd	3	$^4I_{9/2}$	lilac	3.62	3.5-3.6
Pm	4	$^5I_4$	pink	2.68	-
Sm	5	$^6H_{5/2}$	yellow	0.85	1.4-1.7
Eu	6	$^7F_0$	pale pink	0	3.3-3.5
Gd	7	$^8S_{7/2}$	colourless	7.94	7.9-8.0
Tb	8	$^7F_6$	pale pink	9.72	9.5-9.8
Dy	9	$^6H_{15/2}$	yellow	10.65	10.4-10.6
Ho	10	$^5I_8$	yellow	10.60	10.4-10.7
Er	11	$^4I_{15/2}$	rose-pink	9.58	9.4-9.6
Tm	12	$^3H_6$	pale green	7.56	7.1-7.5
Yb	13	$^2F_{7/2}$	colourless	4.54	4.3-4.9
Lu	14	$^1S_0$	colourless	0	0

Table 2 Summary of the properties of Ln(III) ions, where g $[J(J+1)]^{1/2}$ is the calculated magnetic moment and μ_{obs} is the observed magnetic moment

Gadolinium(III) is widely used in MRI contrast agents due to its magnetic properties, and because it has 7 unpaired electrons. Even though dysprosium(III) or holmium(III) look like better candidates to be used as MRI contrast agents because they have larger magnetic moments, the asymmetry of these electronic states leads to a very rapid electron spin relaxation. The gadolinium(III) symmetric S state is a more exploitable environment for electron spins and results in a slower electronic relaxation rate and a more effective MRI agents.[7] Another application of the lanthanides is their potential use as components of luminescent imaging agents. Luminescent lanthanides have a partially filled 4*f* shell and can not be directly excited, therefore lanthanide emission is produced by the energy transfer from the excited state of a chromophore onto the metal centre. This results in the different energies levels of the lanthanide electronic terms, as shown in figure 5. These properties result in long wavelength emissions and relatively long lived excited states for the lanthanides in solution. As the emissions occur from symmetry forbidden excited states the lanthanides are only weakly emissive.[9]

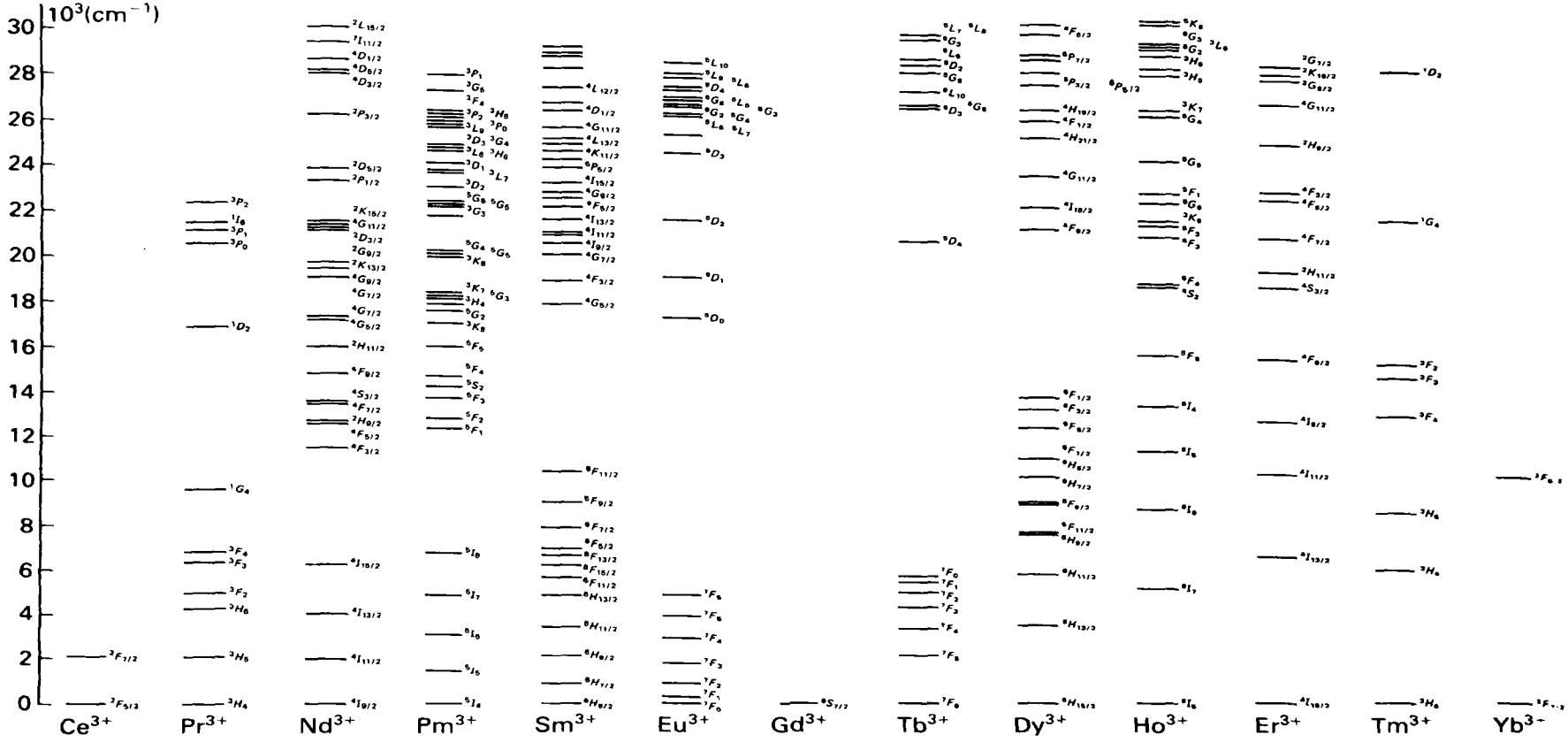

Figure 5 The lanthanide energy levels[8]

Ln	Excited State[a]	τ_{Rad}/ms[b]	End State	Luminescent type[c]	λ/nm[d]	Emission colour
Pr	$^1G_4$	n.a.	$^3H_{4-6}$	P	1300	NIR
	$^1D_2$	n.a.	$^3F_{2-4}$	P	890, 1060	NIR
	$^3P_0$	n.a.	$^3H_{4-6}$	F	525-680	Orange
Nd	$^4F_{3/2}$	0.42	$^4I_{9/2-15/2}$	F	1060	NIR
Sm	$^4G_{5/2}$	6.26	$^6H_{5/2-15/2}$	P	590	Orange
Eu	$^5D_0$	9.67	$^7F_{0-6}$	P	620	Red
Gd	$^6P_{7/2}$	10.9	$^8S_{7/2}$	P	312	UV
Tb	$^5D_4$	9.02	$^7F_{6-0}$	P	550	Green
Dy	$^4F_{9/2}$	1.85	$^6H_{15/2-5/2}$	P	570	Yellow - orange
Ho	$^5F_5$	n.a.	$^5I_{8-4}$	F	970, 1450	NIR
	$^5S_2$	0.37	$^5I_{8-4}$	F	540	Green
Er	$^4S_{3/2}$	0.66	$^4I_{15/2-9/2}$	F		
	$^4I_{3/2}$	n.a.	$^4I_{15/2}$	F	1530	NIR
Tm	$^1G_4$	n.a.	$^3H_{6-4}$	P		
Yb	$^2F_{5/2}$	1.2	$^2F_{7/2}$	F	980	NIR

Table 3 Main luminescent transitions of trivalent lanthanide(III) aquo ions[10]

[a] Most luminescent excited state. [b] Radiative lifetimes of the excited state for aquo ions. [c] F= Fluorescence , P = Phosphorescence. [d] Approximate wavelength of most intense emission lines (or emission range).

1.3 Current commercial contrast agents

Lanthanide metal complexes have found use in many areas of research, including in the area of diagnostic medicine with the development of gadolinium(III) complexes for use as MRI contrast agents, and europium(III) and terbium(III) complexes being investigated as luminescent biological probes.[14 15]

The advantage of MRI over other medical imaging techniques, such as X-ray, is to differentiate between soft tissues and this has increased its use in the clinical field. One of the main parameters in the production of a MR image is the proton relaxation time (T_1 and T_2). When there is poor contrast between healthy and pathological regions due to small variations in relaxation times, a contrast agent is used to alter the relaxation times of water protons within the tissue. In 1999 approximately 30% of all MRI scans used a contrast agent, but this has increased to around 40 - 50% at present.[16] T_1 commercial contrast agents incoporate gadolinium(III) and manganese(II) ions and a positive image enhancement is observed *i.e.* brighter, while T_2 contrast agents are usually based on iron(III) oxide particles and a negative image effect is observed *i.e.* darker.[5] Gadolinium(III) contrast agents affect the image by altering the relaxation times of the water protons within the tissue and lead to the enhancement of the brightness in the image. As free gadolinium(III) ions are toxic, they are therefore chelated to a ligand, with commercially used chelators including DOTA and DTPA.[5] There are currently around eight gadolinium(III) contrast agents that are licensed for clinical use, see figure 6.

Complex	Brand Name	Company
$[GdDTPA(H_2O)]^{2-}$	Magnevist®	Schering
$[GdDOTA\ (H_2O)]^{-}$	Dotarem®	Guerbet
$[GdHPDO3A\ (H_2O)]$	ProHance®	Bracco
[GdDO3A-butrol (H_2O)]	Gadovist®	Schering
[GdDTPA-BMA(H_2O)]	Omniscan®	Nycomed-Amersham
[GdDTPA-BMEA(H_2O)]	OptiMARK®	Mallinckrodt
$[GdBOPTA(H_2O)]^{2-}$	MultiHance®	Bracco
$[GdEOB\text{-}DTPA\ (H_2O)]^{2-}$	Eovist®	Schering

Table 4 Contrast agents that are licensed for clinical use

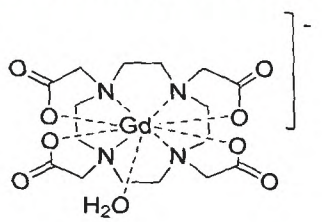

$[GdDOTA\ (H_2O)]^{-}$

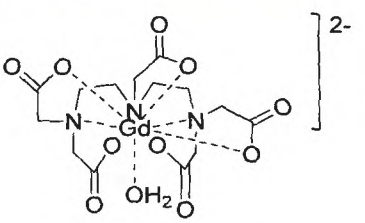

$[GdDTPA(H_2O)]^{2-}$

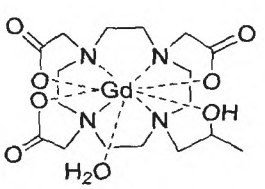

$[GdHPDO3A\ (H_2O)]$

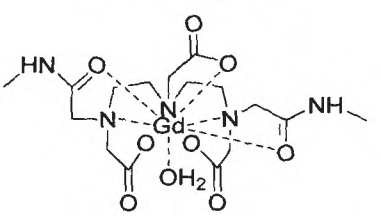

[GdDTPA-BMA(H_2O)]

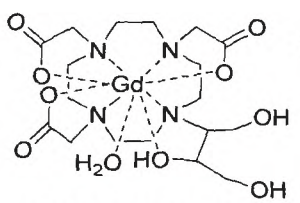

[GdDO$_3$A-butrol (H_2O)]

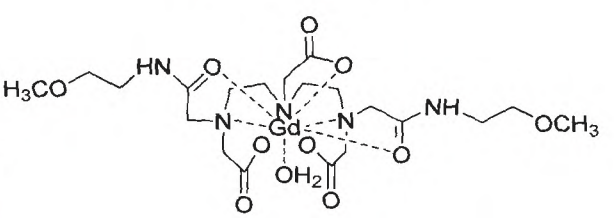

[GdDTPA-BMEA(H_2O)]

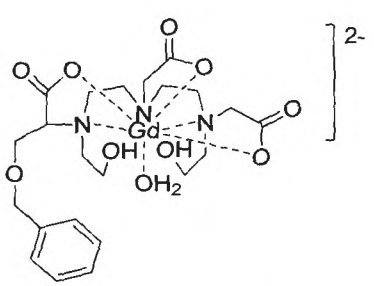

$[GdBOPTA(H_2O)]^{2-}$

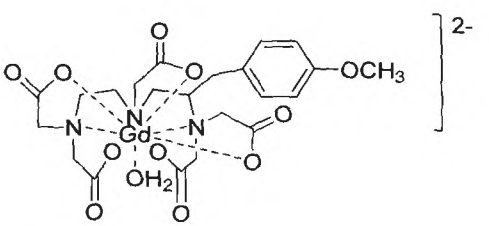

$[GdEOB\text{-}DTPA\ (H_2O)]^{2-}$

Figure 6 Contrast agents that are licensed for clinical use

The development of new MRI contrast agents is currently being investigated with the aim of increasing the relaxivity of contrast agents to improve image quality, to improve their sensitivity and also to target specific markers within the body, *i.e.* apoptosis.[14 17]

1.4 Magnetic resonance imaging

Magnetic Resonance Imaging (MRI) involves the natural production of net magnetization that occurs in the body when a magnetic field is applied. The net magnetization causes protons in the human body to align in the direction of the magnetic field (B_0). This includes any atom that contains a spin and the one commonly used to probe the body is hydrogen (^1H). It is found in all tissues in the human body as they contain both fats and water with the relaxation of protons in these molecules forming the basis of the MRI signal.

The proton can be viewed as a small magnet; because it has spin, and a positively charged nucleus, therefore having a local magnetic field. A bar magnet has magnitude and orientation to this magnetic field (i.e. north and south pole), this is the same for the proton, with its spin having an axis of rotation with definite orientation and magnitude, and can be described in terms of a vector (figure 7).

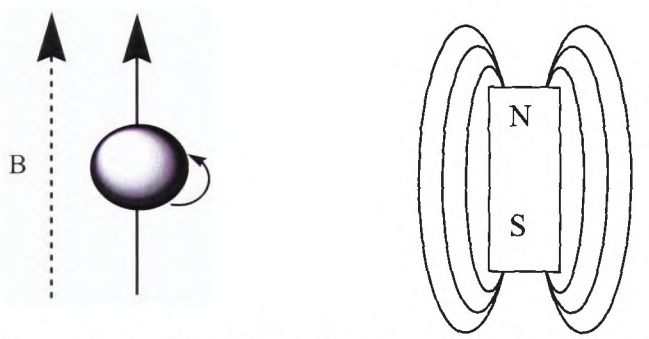

Figure 7 Diagram to show the positive charge on the nucleus producing a magnetic field orientated parallel to the axis of rotation and its analogy to a bar magnet

MR measurements involve a collection of similar spins. When there is no magnetic field applied, the spin vectors in the tissue are orientated randomly, on application of a strong magnetic field the spin vectors align themselves parallel with the externally applied field B_0, thus making the tissue a weak magnet (figure 8).[18]

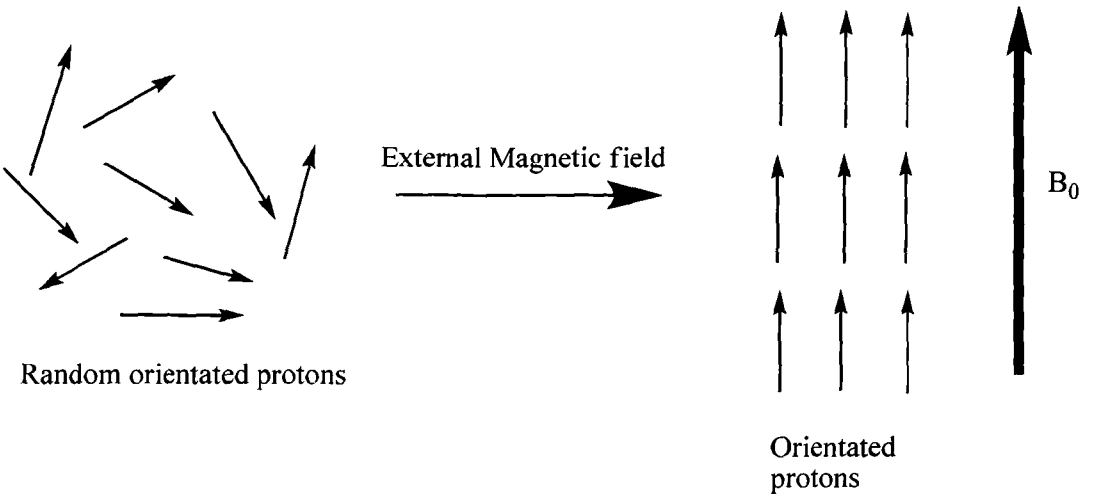

Figure 8 Diagram to show the effect of an applied magnetic field B_0 on the set of individual protons in fluid or tissue

The individual protons are not stationary in one position, and precess about the magnetic field. The precession is tilted slightly away from the axis of the magnetic field, but the axis of rotation is always parallel to B_0, and is defined as being in the z direction (figure 9).[19]

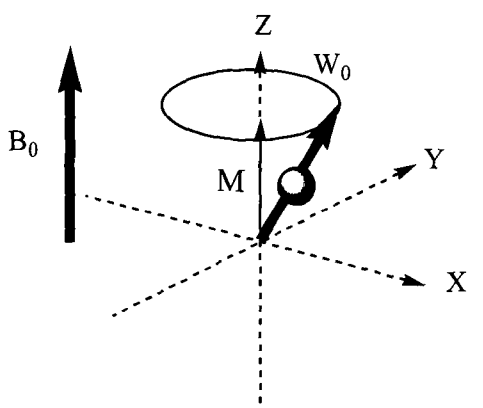

Figure 9 Showing a proton precessing about the magnetic field direction. The precessional axis is parallel to the main magnet field B_0, in the z direction, with a frequency of precession of W_0 (also known as Larmor frequency), and a net magnetization of M

In the z component there are spins in two orientations, parallel (spin up), and anti-parallel (spin down). Protons can swap between the two by simply gaining or losing energy. The energy difference between the two spins is directly

proportional to the strength of the external magnetic field. In equilibrium the protons are all out of phase with each other, and are either parallel or anti-parallel to magnetic field B_0. The vector sum is called the net magnetization M_0, which is aligned exactly with the main field B_0. The entire field of MRI is based on the manipulation of this M value from the longitudinal to the transverse component, and allowing it to relax back. MRI involves a short pulse of radio frequency (rf) energy that contains many frequencies spread over a narrow range or bandwidth, causing protons to absorb the energy at a particular frequency. The frequency absorbed is proportional to the magnetic field B_0 (the Larmor equation $\omega_0 = \gamma B_0$). Absorption of rf energy frequency (ω_0) at a 90^0 pulse, causes M to rotate into the xy plane (M_1), perpendicular to B_0 (figure 10).[19]

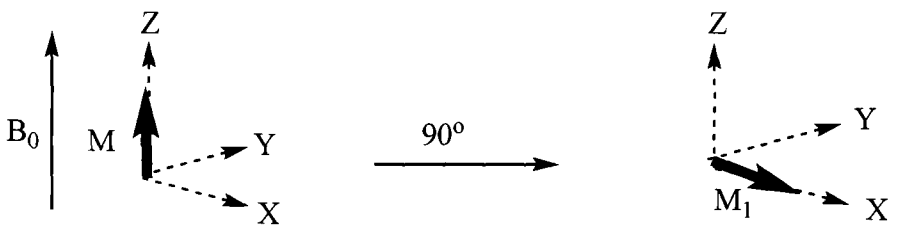

Figure 10 Diagram to show the effect of a 90° excitation pulse

When the rf pulse stops, the protons start to re-align themselves from M_1 and return to their equilibrium position M. A conducting wire detects the changes in the net magnetization M, because protons induce a voltage in the wire due to the changing field producing a radio frequency, and therefore producing a MRI signal.[18]

The process of the net magnetization M, returning to the z plane is known as relaxation. Important parameters in MRI are the T_1 relaxation times and the T_2 relaxation times. T_1 relaxation provides the mechanism by which protons give up their energy to return to the z-component, and hence get an increase in the return in longitudinal magnetization. The excited protons do not transfer their energy to another spin, they actually release it to the surrounding lattice, and this energy does not contribute to the spin excitation. For these reasons, T_1 relaxation may also be known as longitudinal or spin-lattice relaxation. T_2 relaxation is the process where the energy of one proton is transferred to a

nearby proton and the absorbed energy remains as spin excited. This is also known as spin-spin relaxation, or transverse relaxation time. Protons are contained in both fats and water with both longitudinal and transverse relaxation occurring rather rapidly in fats compared to water. As a result, fat protons have short T_1 relaxation times. In comparison protons in water molecules do not decay as efficiently as those in fat protons, because of their high mobility, and reduced ability to give up their energy to the lattice as effectively.[20] In a MR image, you want to relax the water protons, and not fat protons. Contrast agents work by improving the MRI image, but do not directly interact with fat molecules and therefore will only affect water molecules.

1.5 Gadolinium(III) contrast agents

Contrast agents are used in medical imaging when there is poor contrast between healthy and pathological tissues due to small variation in relaxation times. Consequently, this has led to improvements in medical diagnosis by providing better tissue characterisation with greater sensitivity and specificity. Gadolinium(III) acts as a T_1 contrast agent by increasing the signal observed and resulting in a brighter area of the image where the contrast agent is located. Gadolinium(III) is toxic in the body as its ionic radii is very similar to that of calcium(II), as a result it can disrupt calcium signalling pathways and hence it needs to be chelated by a polydentate ligand. An important feature of gadolinium(III) contrast agents is that they should have at least one bound water molecule (q) so that it can be relaxed more rapidly and then undergo rapid exchange with water molecules in the bulk. This exchange is required to be rapid as the image obtained is representative of the relaxivity. Other factors that can affect relaxivity are shown in figure 11 and include the number of inner-sphere water molecules (q), their residency time (τ_m) and Gd-H distance (r), the 2nd-sphere water (q') with its residency time (τ_m'), and Gd-H distance (r'); and the tumbling correlation rate, (τ_R).[21 22]

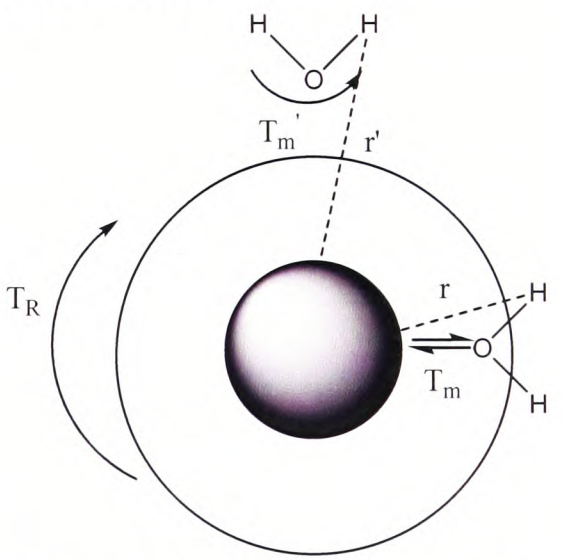

Figure 11 Illustration of the different parameters that influence relaxivity

Designing gadolinium compounds that are able to accommodate a greater number of bound water molecules q, have an optimally short water residence

time (τ_m), and a slower tumbling rate (τ_R) should lead to an increase in the relaxivity of the contrast agent.

1.5.1 Increase the number of bound water molecules (q)

An increase in the number of bound water molecules (where $q \geq 1$) would result in a more efficient inner sphere relaxivity and an enhancement in the overall proton relaxation rate and image quality.[16] Forming gadolinium(III) complexes with 2- to 3- coordinated water molecules, can cause a decrease in their thermodynamic stability and lead to leaching of the gadolinium(III) ion therefore making it toxic. However, there are some examples of stable gadolinium(III) complexes with two bound water molecules, which offer comparable stability to current clinical agents and lead to an increase in relaxivity.[23] [24] Raymond and co-workers have reported a family of gadolinium(III) agents based on tris-(2-aminoethyl)-amine hydroxypyridinone that show a relaxivity of 10.5 mM^{-1} s^{-1}, while Merbach and co-workers have given an account of a dinuclear gadolinium(III) substituted with diethylenetriamine *–N,N',N'',N'''*-tetraacetate (DTTA) that is linked by the formation of a supramolcular complex with iron(III) (figure 12).[25] [26]

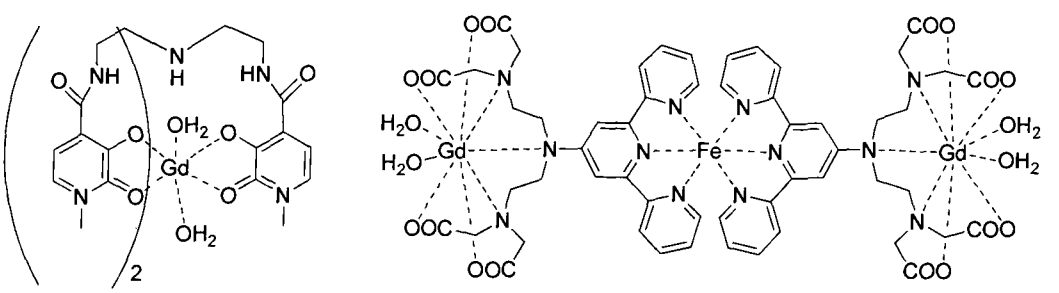

Figure 12 Gadolinium(III) agents based on hydroxypyridinone (left) and a dinuclear gadolinium(III) substituted with DTTA (right)

Raymond and co-workers have further developed the hydroxypyridinone (HOPO) complexes by replacing the tris-(2-aminoethyl)-amine (TREN) with triazacyclonane (TACN) as the ligand cap.[25] These stable complexes have three bound water molecules (q = 3) with relaxation enhancement of 12.5 $mM^{-1}s^{-1}$. These complexes (figure 13) have also been shown to have improved water

solubility with over 1000-fold increase compared to the parent TREN series. However, such agents have not undergone extensive stability analysis so questions might arise about how they will respond under physiological conditions .

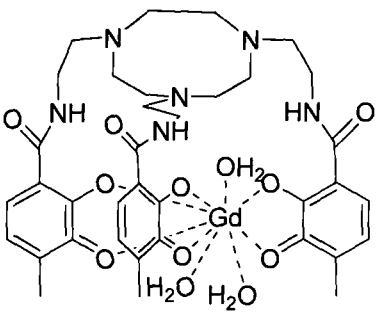

Figure 13 The molecular structure of Gd- TACN- 1,2-HOPO

Merbach and co-workers have also reported another supramolecular gadolinium(III) complex where the number of gadolinium(III) centres has been increased from 2 to 6 by switching to a 2,2'-bipyridine (figure 14) from the terpyridine used in their previous complex (figure 12), to form a metallostar, which results in an increase in the number of inner sphere bound water molecules (q) see figure 14.[26] The relaxivity reported is 33.6 $mM^{-1}s^{-1}$ at 40 MHz. The increase in relaxivity is also due to the formation on the supramolecular structure, that leads to a reduction in the tumbling rate.

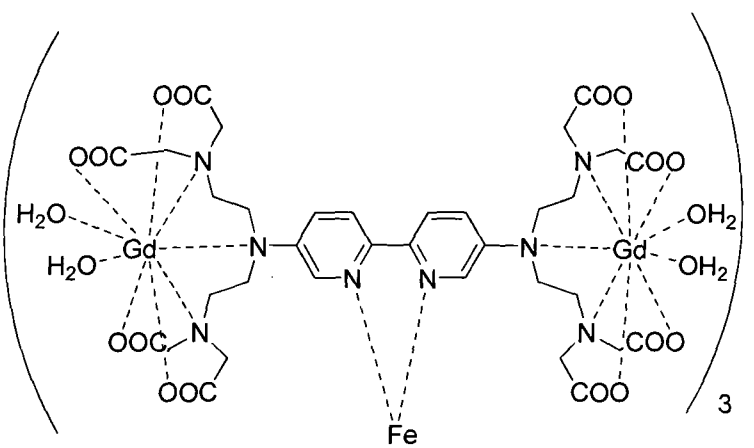

Figure 14 The structure of the metallostar molecular framework

Both Raymond and co-workers and Merbach and co-workers have presented novel gadolinium(III) complexes which clearly show that altering the number of

inner sphere water molecules can lead to significantly higher relaxivity values, and will result in brighter and better defined MRI images. Parker and co-workers have also investigated a supramolecular structure to alter the number of water molecules, however here, the number of outer sphere water molecules (q') has also been increased.[27] Here, a medium molecular weight conjugate that incorporates a sugar moiety dendritic wedge attached to a central gadolinium(III) complex has been synthesised. The compound is known to contribute to the 2nd sphere water molecule exchange and has been shown to have a relaxivity of 23.5 $Mm^{-1}s^{-1}$ (298 K, pH 7, 20 MHz). This molecule can be renally excreted and should be cleared from the blood pool quickly after injection due to the presence of the sugar moieties.

1.5.2 Multiple gadolinium(III) centres

Incorporating a number of gadolinium(III) ions in a molecular system can increase the relaxivity of a gadolinium MRI contrast agent and allow a lower concentration of gadolinium(III) contrast agent to produce a useful enhancement in the MR image.[28] There are a number of approaches to tackle this challenge, including the metallostar structures that Merbach and co-workers have produced (figure 14).[26] Alexander and co-workers have formed a tetranuclear Gd-DO3A showing a 5.86 times enhancement in relaxivity compared to $[Gd(DO3A)(H_2O)_2)_8]$.[29] While other approaches involve the production of multi gadolinium(III) centres by forming micelles and nanoparticles. One such approach by Delville and co-workers uses either noncovalent or covalent binding of low-molecular weight Gd-DTPA chelates to metal oxide particles (SiO_2, Al_2O_3).[30] This has a relaxivity of 42 $mM^{-1}s^{-1}$ (4.7 T) for the silica doped nanoparticles, and by incorporating a rhodamine based dye they have shown that these agents are able to penetrate the cell membrane. An example has been been produced by Cho and co-workers, where a biocompatiable polysuccinimide (PSI) derivatives is conjugated with Gd-DTPA to form micelles, although no relaxivity data has been published yet.[31] More data is required to understand the effect these type of contrast agents will have *in vivo*, as micelle formation might be affected by physiological conditions and this could influence the overall relaxivity.

Another line of approach is to form dendrimer based gadolinium(III) contrast agents.[32] There are numerous examples in the literature with a number of reviews on such compounds.[33 34] Merbach and co-workers have synthesised a DTPA based chelate containing a phosphinate group conjugated to a generation 5 polyamidoamine (PAMAM) dendrimer *via* benzylthiourea linkages (figure 15).[35 36] The relaxivity here was shown to be 26.8 $mM^{-1}s^{-1}$ at 37°C, 4.7 T, but this could potentially be increased if a way could be found to fully load the PAMAM G5 dendrimer with Gd-DTPA (currently only loading of 49% has been achieved).

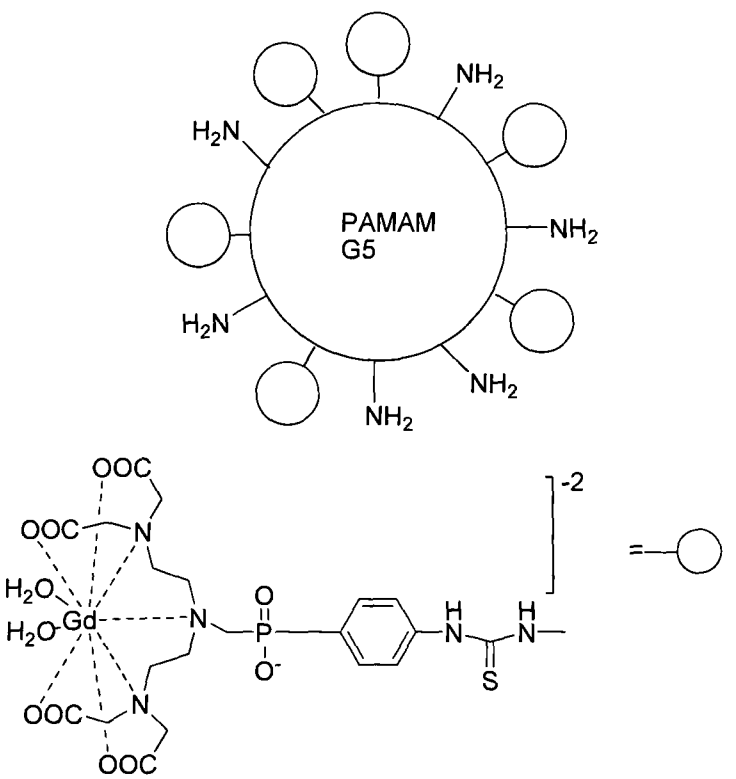

Figure 15 Gadolinium(III) based dendritic complex based on PAMAM G5

Brechbiel and co-workers have also formed a dendritic MRI agent based on PAMAM G4, which is shown in figure 16.[37] This utilises a fourth generation polyaminoamido dendrimer bearing 2-(4-isothiocyanatobenzyl)-6-methyldiethylenetriamine pentaacetic acid (1B4M-DTPA) chealator complexed with gadolinium(III). Compared to the Merbach and co-workers complex, a much greater number of gadolinium(III) complexes are attached to the PAMAM

G4 dendrimer with 50 – 57 present per molecule. The compound was shown to be a potential vascular contrast agent to target intravascular agents with angiogenesis.

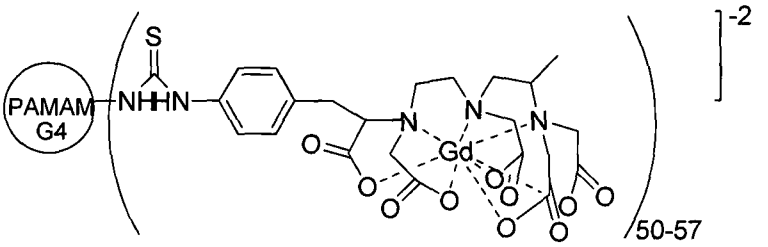

Figure 16 Gd-B4M-DTPA-functionalized PAMAM G4 dendrimers

Dendritic gadolinium(III) compounds have huge potential as MRI contrast agents as they increase the number of gadolinium(III) ions on a single molecule which in turn leads to an increase in the relaxivity.[38] They are also known to alter the route of excretion and the potential function of the agent. Smaller dendrimer based contrast agents of less than 60 kD in molecular weight, are found to be excreted from the kidneys and have shown potential as blood pool contrast agents. The larger dendrimer based contrast agents are generally processed by the liver and have potential as lymphatic imaging compounds.[38]

1.5.3 Responsive MRI contrast agents

While relaxivity is one way to expand the potential applications of a gadolinium(III) contrast agent, another way is to produce molecules that can respond to changes in their environment leading to the variation in the relaxivity, thus reporting on their environment. This event could be a change in physiological pH, metal ion concentration, enzyme activity or partial pressure of oxygen.[13 39-42] The contrast agent will respond to physiological changes by either 'switching on' (increase in relaxivity), or by 'switching off' (decrease in relaxivity) allowing physiological or diseased states to be identified. There are a number of examples in the literature of pH dependent probes.[43 44] The motivation for these studies stems from the fact that tumour tissue is more acidic, with pH values at around 6.8 – 6.9, while with healthy tissue this is around pH 7.4. Agents that can differentiate between the two have great

potential for pH mapping and locating tumour tissue. A number of approaches have been investigated to produce pH sensitive agents, including reversible intermolecular and intramolecular anion binding, and changes in water or proton exchange rates. Parker and co-workers have formed an agent based on (Gd-DO3Aala) where to produce a variation in relaxivity due to pH, a reversible intermolecular anion binding event occurs as shown in figure 17.[45] Here, the gadolinium(III) complex is coordinated to seven donors from the ligand and possesses two water bound molecules (q = 2). Displacement of the two water molecules by endogenous anions, results in a decrease in relaxivity. The Gd-DO3Aala showed about a 280% increase in relaxivity between pH 8 and 6 from 1.9 $mM^{-1} s^{-1}$ (q = 0) and 7.2 $mM^{-1} s^{-1}$ (q = 2) at 20 MHz respectively.

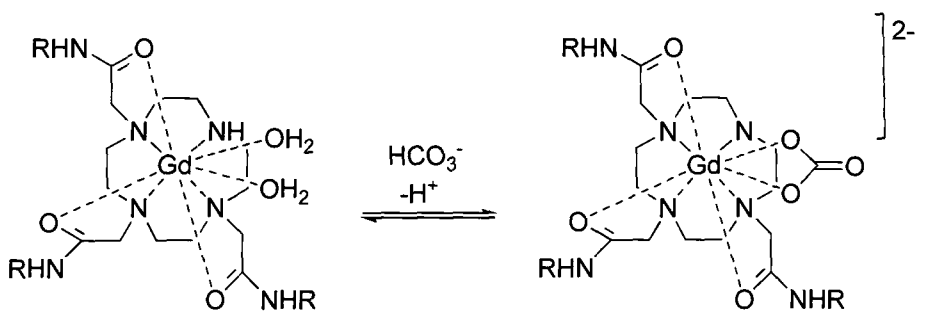

Figure 17 Gd-DO3Aala where R = $CH(CH_3)CO_2^-$ showing intermolecular anion binding on a pH sensitive probe

Another approach is a reversible intramolecular anion coordination, such as the gadolinium(III) compound Gd-SaDO3A.[46] Changes in pH affect the hydration state which causes changes in relaxivity. This occurs because the sulphonamide group is protonated at lower pH (pH 5.5) and hence is not bound to the gadolinium(III) centre, which allows water molecules to complete the hydration sphere (q = 2) and leads to a relaxivity of 8.5 $mM^{-1} s^{-1}$. While at pH 8, the sulphonamide is not protonated and is able to displace the water molecules and bind to the gadolinium(III) (q = 0) leading to a decrease in the relaxivity (2.8 $mM^{-1} s^{-1}$) (figure 18).

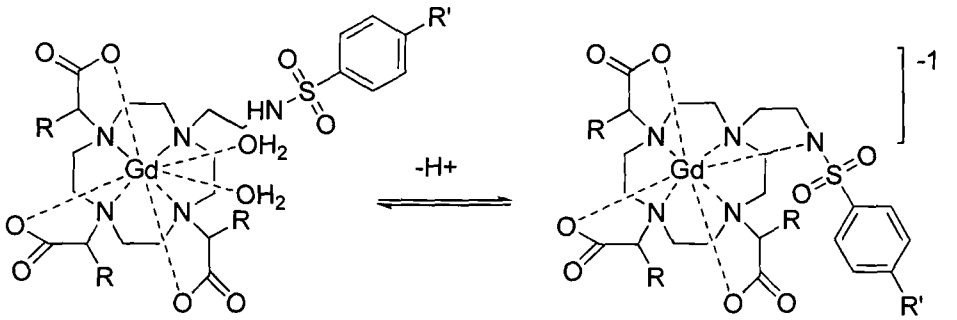

Figure 18 Gd-SaDO3A R = $(CH_3)_2CO_2^-$, R' = CH_3 showing intramolecular anion binding on a pH sensitive probe.

Sherry and co-workers have formed a pH activated contrast agent that has a response dependent on changes in proton exchange rates.[47] Gd-DOTA-4AmP (figure 19) has been used to map tissue pH with a relaxivity of 5.3 mM^{-1} s^{-1} at pH 6.3 (where q = 1) and 3.4 mM^{-1} s^{-1} at pH 9 (where q= 0). It is postulated that the pH responsive changes are due to protonation of the phosphonates that are believed to form a hydrogen bonded network that provides a catalytic pathway for the exchange of bound water protons with the bulk water. The compound has been shown to target the kidneys and identify the acidic regions.[48]

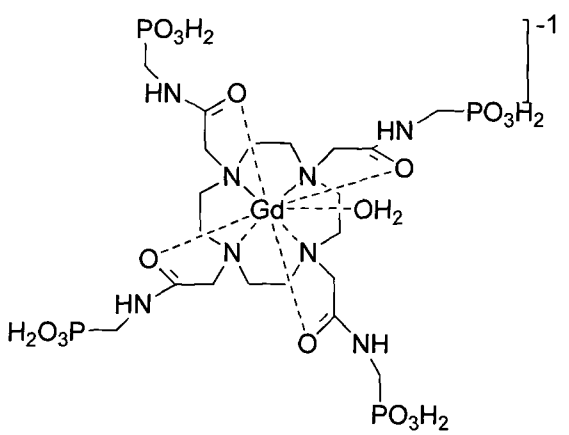

Figure 19 Structure of Gd-DOTA-4AmP

These above compounds have shown that responses to variations in pH can result in an alteration of relaxivity. However, these compounds do not show sufficient sensitivity to differentiate between healthy and tumour tissue. Another area of research is to form MRI agents that can be activated by the

presence of metal ions such as calcium(II) and zinc(II). Meade and co-workers have synthesised a molecule that displays an alteration of relaxation properties in response to a physiological changes in calcium(II) concentration (figure 20).[49] Calcium(II) (which plays an important role in signal transduction) binds to the carboxylates from the imidodiacetates allowing water access to the gadolinium(III) centres and increasing relaxivity from 3.3 mM^{-1} s^{-1} to 5.8 mM^{-1} s^{-1}.

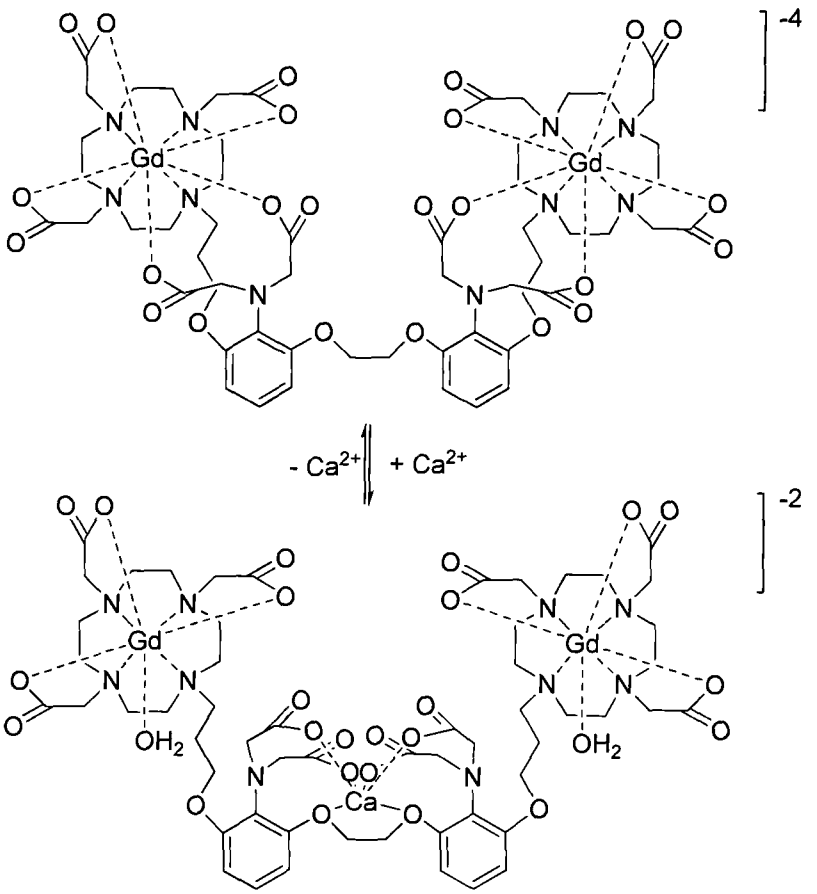

Figure 20 Proposed conformational change of a calcium activated MRI agent

Meade and co-workers have also formed a MRI agent that can monitor enzyme activity through changes in relaxivity properties (figure 21).[50] In this case, Gd-DO3A bears a pendant β-glucuronic acid moiety linked to the macrocycle by a self immolative linker. In the presence of the enzyme β-glucuronidase, the β-glucuronic acid is cleaved to allow the water to access the gadolinium(III) ion, resulting in a 20% increase in relaxivity.[51]

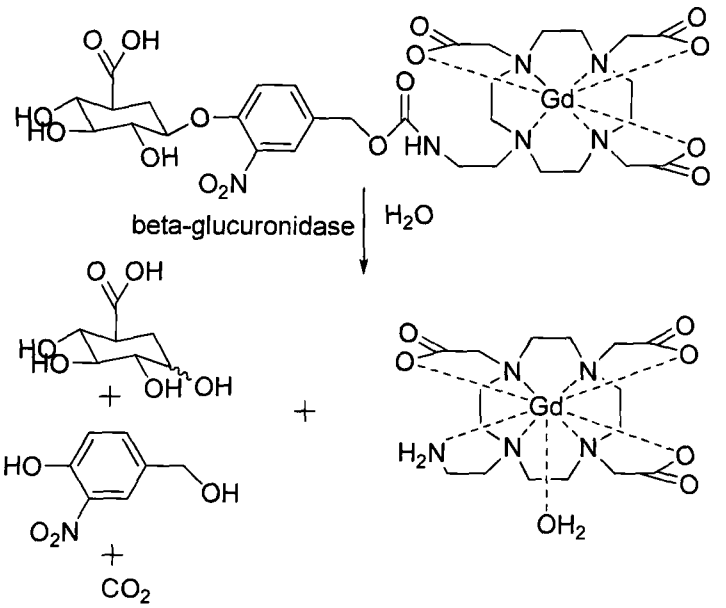

Figure 21 An enzyme activated MRI contrast agent

Meade's enzyme active contrast agent is irreversible, which may be an issue with specific monitoring of enzyme activity, as one β-glucuronidase enzyme could cleave the β-glucuronic acid linker on multiple gadolinium(III) contrast agents.

1.5.4 Targeted MRI agents

Most MRI agents distribute around the intravascular and interstitial space and can be classed as non-specific agents. Therefore there is great scope for designing agents that can target specific events and detect abnormalities to improve diagnostic accuracy.[52] [53-56] Typical target areas or events in the body for example include tumours, heart failure and cellular uptake.[57] [58-61] These agents could target and locate within a region e.g. cancerous tissue, and allow physicians to easily identify the disease. There are many approaches to target different tissues within the body including the use of antibodies and polypeptides.[54] [62] Meade and co-workers have formed a progesterone modified DTPA based contrast agent that is able to target over expressed hormone receptors in cancers (figure 22).[63] The relaxivity of this molecule was shown to

be 4.73 mM^{-1} s^{-1} at 4.7 T and *in vivo*, was shown to accumulate in the intracellular space resulting in a signal intensity increase.

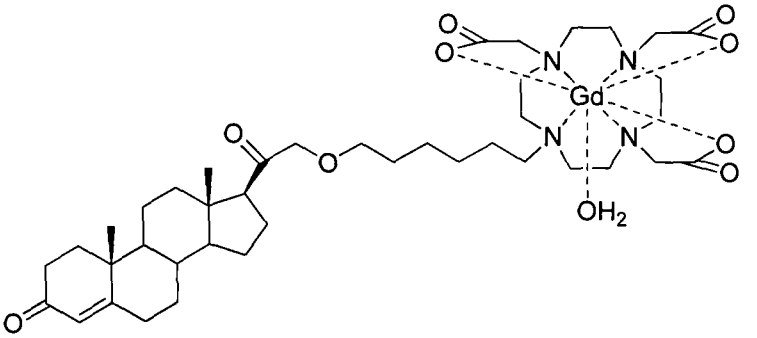

Figure 22 Structure of the progesterone conjugated MRI contrast agent

Another approach involves exploiting the interaction between avidin and biotin to form a supramolecular structure that would give target specific agents for angiogenesis (formation of new blood vessels).[64 65] A number of research groups have investigated the synthesis of MRI contrast agents that can target human serum albumin (HSA) and have the potential to be used as angiography contrast agents.[66 67, 68] Such an example has been developed by Caravan and co-workers where the amphiphilic gadolinium(III) complex MS-325 ((trisodium-((2-(R)-[(4,4-diphenylcyclohexyl)phosphonooxymethyl]-diethylenetriaminepentaacetato) (aquo) gadolinium(III))) has been produced (figure 23).[69] This agent has been shown to assess blockages in arteries by targeting HSA in the plasma. This targeting of HSA allows the complex to stay in the plasma compartment and extends the circulation time, hence results in better image differentiation of the blood vessels. Also by binding to HSA, the gadolinium(III) complex increases its relaxivity because of the slow rotation of the complex-protein unit, with a relaxivity value of 6.84 mM^{-1} s^{-1} at 4.7 T.

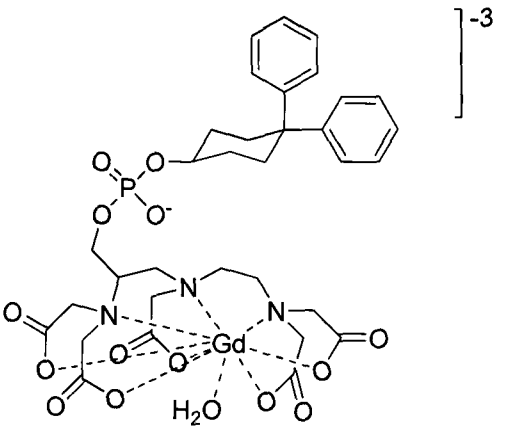

Figure 23 Structure of gadolinium(III) MS-325

Significant progress has occurred in the synthesis of novel MRI agents. Current investigations include increasing the number of bound water molecules on the gadolinium(III) metal centre, an increase in the number of gadolinium(III) metal centres (i.e. dendrimers and micelles etc) and the synthesis of responsive and targeted gadolinium(III) contrast agents. Presently, the number of new gadolinium(III) agents that have been clinically accepted is limited as they must be shown to be cost effective and non-toxic.

1.6 Lanthanide Luminescence

There are many examples of organic luminescent molecular probes that are used in imaging applications which are based on heterocyclic dyes such as rhodamine and MitoTracker (figure 24).[70]

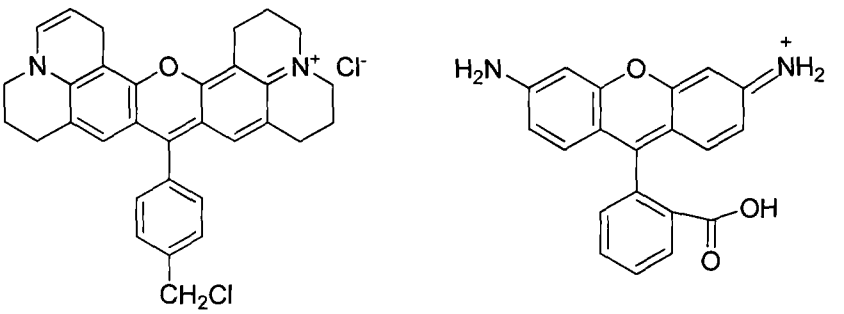

MitoTracker Red CMXRos Rhodamine

Figure 24 MitoTracker and Rhodamine luminescent molecular probes

They typically have short lived singlet excited states with lifetimes less than 10 ns, broad absorption and emission bandwidths in the order of tens of nm, and they usually have small Stokes shifts. Luminescent lanthanide complexes have the advantage of 'delayed fluorescence' and hence provide an opportunity to probe biological systems with the interference from biological chromophores removed by time gating. Lanthanide complexes have been exploited for their luminescence properties and have shown great potential as materials for liquid crystal displays, organic light emitting diodes and as biological probes.[71] Lanthanides have very low excitation coefficients ($\leq 1\ M^{-1}\ cm^{-1}$) because the f - f transitions are Laporte forbidden and the 4f electrons are effectively shielded by the 5p and 6s electrons. For this reason, lanthanides need a highly absorbing chromophore to be able to act as a luminescent agent. The chromophore absorbs the excitation, followed by energy transfer onto the metal centre and finally leading to a metal centred sensitised luminescence.

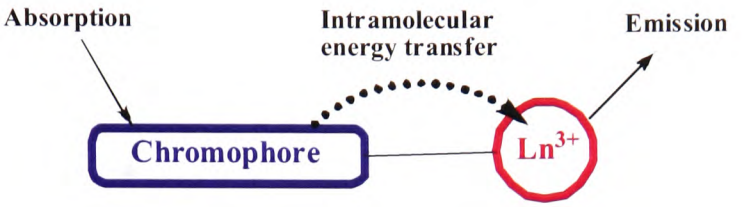

Figure 25 Schematic to show the energy transfer processes to sensitise emission

Figure 25 gives a very simple model of what occurs to allow lanthanide emission via sensitisation, this can also be shown in terms of the energy levels *i.e.* Jablonski diagram. The sensitisation pathway involves absorption of energy by the antenna into its excited singlet state (S_1). This is followed by intersystem crossing of the chromophore to its triplet states, then energy transfer onto the lanthanide(III) metal ion and finally results in the metal ion sensitised luminescence when the transition to the ground state occurs. Figure 26 shows the typical process for an europium(III) ion. The triplet state of the antenna transfers its energy onto the $^5D_0$ followed by the internal conversion to the ground states ^7F_J (J = 0 – 4) resulting in emission. As a consequence typical europium(III) emission bands are observed at about 580, 595, 615, 655 and 700 nm.

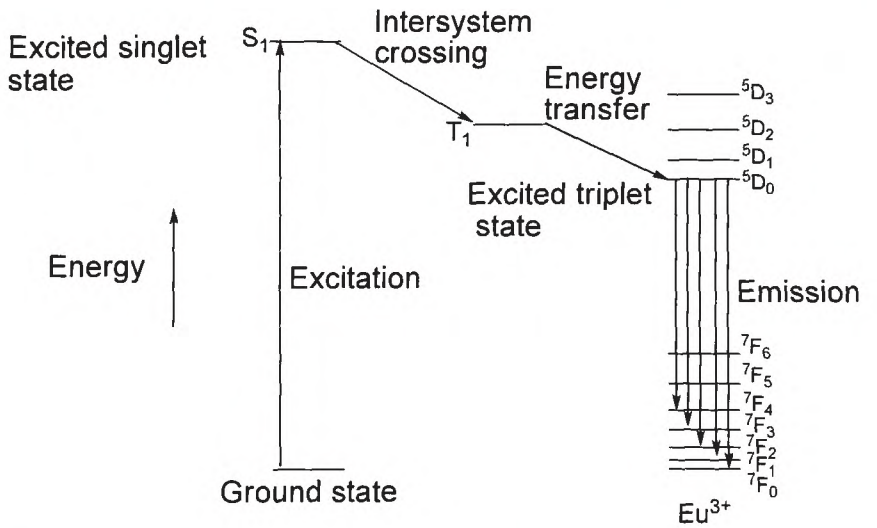

Figure 26 The sensitisation pathway of lanthanide luminescence for europium(III)

The wavelengths of the lanthanide emissions are relatively long with europium(III) emitting in the red and terbium(III) in the green region of the visible spectrum, while neodymium(III) and ytterbium(III) emit in the near

infra-red region. They also have excited state lifetimes that occur in the milli or sub-microsecond for europium(III) and terbium(III) while neodymium(III) and ytterbium(III) are micro or submicro second range. These lifetimes are much longer than most organic chromophores, with singlet excited state (S_1) lifetimes within 10 ns. As a result of this, the lanthanide emission can be distinguished from fluorescence emission because of this 'delayed fluorescence' by using a time-gated luminescence microscope. During a time gated luminescence experiment (figure 27), the short lived background fluorescence decays to negligible levels during an appropriate 'delay time'. These experiments therefore record after a 'x' gated time, leaving just lanthanide metal centre emission and removing the scattered light and short lived fluorescence from organic chromophores.[72]

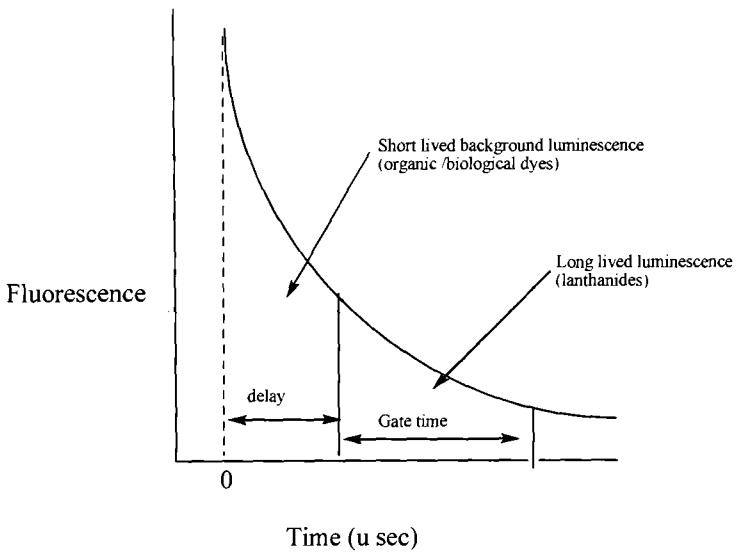

Figure 27 Principles behind time-resolved long-lived luminescence

Time-gated experiments can be used to probe biological environments with lanthanide probes, as the lanthanide luminescence allows for the fluorescence from biological chromophores to be removed, hence offering greater reliability in monitoring biological systems with more clearly defined images.[8 10]

1.7 Luminescent lanthanide complex design

To design luminescent lanthanide complexes for imaging, the number of bound water molecules ideally should be zero (q = 0) to prevent the loss of energy by non-radiative transfer processes (quenching) and the sensitising antenna has to be close to the lanthanide metal centre to allow for fast and efficient energy transfer. The luminescence from lanthanide excited states can be quenched by radiative or through non-radiative deactivation to the ground state. Non-radiative processes are promoted by high frequency vibration modes of nearby or coordinated solvent molecules (X-H). The quenching is therefore increased (i.e. decrease in luminescence) by the co-ordination of water molecules (when q > 0). This is because of the abundance of O-H oscillators that result in the overlap of energy levels and stretching vibrations. Other vibrational overtones that are known to quench luminescence include N-H, C-H and C=O, although not as efficiently as O-H. While deuterated oscillators (i.e. O-D, C-D, N-D) are less effective at quenching luminescence as they are of lower frequency and require more energy to interact with excited states of the lanthanide metal ion.

Another issue is the choice of chromophore, it needs to absorb light efficiently at a suitable wavelength and possess a fast intersystem crossing to the triplet state (S_1 to T_1) to allow for efficient energy population of that state. The energy of the chromophore has to be higher than the energy of the lanthanide excited state for the sensitisation process to be thermodynamically favourable.[73] For europium(III) and terbium(III) the energy acceptor levels are at 581 nm and 490 nm respectively, which means the triplet energy state should be higher then 455 nm preventing thermally activated energy back energy transfer onto the chromophore interfering with lanthanide luminescence. Therefore, the chromophore needs to have a high triplet energy and a small $S_1 - T_1$ energy gap to allow for excitation to occur in the range of 300 – 430 nm.[74]

1.7.1 Sensitisation of lanthanide luminescence by a chromophore

As shown in section 1.5, a chromophore can be incorporated onto a lanthanide chelator to sensitise the luminescence of the lanthanide metal to result in long-lived emission. A number of approaches to form novel luminescent lanthanide complexes involve the attachment of the chromophore to either a polydentate ligand such as DTPA, or a macrocyclic ligand such as DOTA (figure 2).[75] [76] Attachment of the chromophore, can influence the excitation properties and may lead to a more efficient overlap between the lanthanide metal ion excited state and chromophore triplet state. Couchet *et al.* have formed a europium(III) complex based on a bis(pyridine) DTPA structure (figure 28).[4] The 2,2'-bipyridine chromophore does not co-ordinate to the metal centre and acts purely to sensitise the europium(III) metal centre. The system produces quantum yields (Φ) of 2.8% and emission lifetimes (τ) of 0.58 ms both in water (excitation at 285 nm, pH 8.6, 295 K). While Werts *et al.* have synthesised a system, again based on DTPA, and incorporated fluorescein, with a ytterbium(III) metal ion (figure 28).[74] Ytterbium(III) is known to emit in the near-infrared region and is much lower in energy. Emission lifetimes (τ) of 1.91 ms in water were observed after excitation at 510 nm.

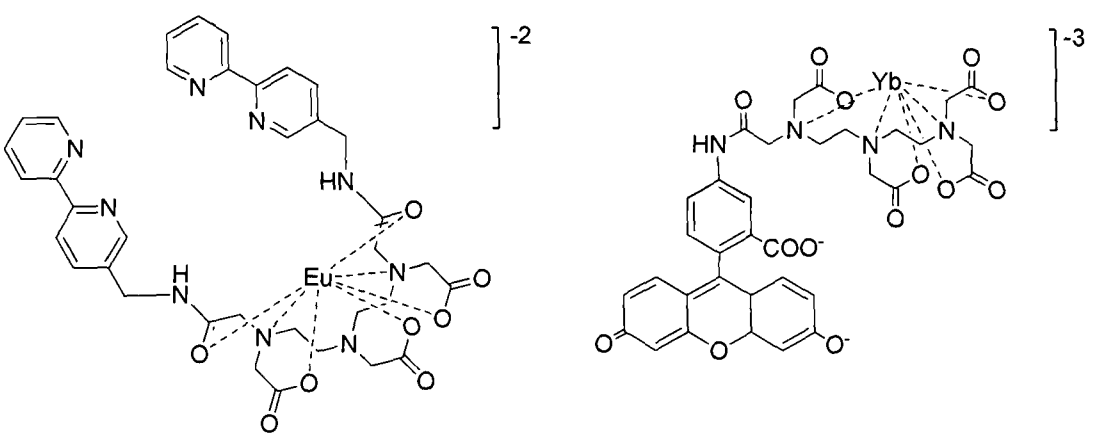

Figure 28 Structures of europium(III) 2,2'-bipyridine DTPA (left) and ytterbium(III) DTPA fluorescein (right)

There are numerous examples in the literature of molecules based upon DOTA as the chelating ligand.[77] [78-80] One example involves the incorporation of azaxanthone sensitising chromophores with europium(III) and terbium(III) complexed to DO3A (figure 29).[81] The emission lifetimes are reported as 0.57 ms and 1.82 ms, with quantum yields of 6.9% and 24% for europium(III) and terbium(III) respectively. Thus showing that with azaxanthone as the chromophore, the terbium(III) shows greater sensitisation and leads to an enhanced luminescence.

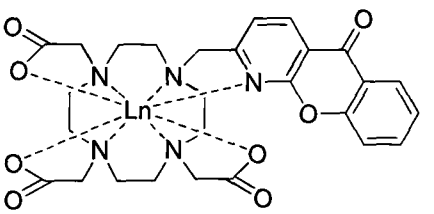

Figure 29 Azaxanthone DO3A sensitising ligand (where Ln = europium(III) and terbium(III))

The chromophore unit can also have a dual function, as it is able to sensitise and encapsulate the lanthanide metal ion.[82] Raymond and co-workers have been involved in synthesising a range of octadentate ligands that form luminescent lanthanide complexes.[24] Carrying on the work based on 1-hydroxypyridine-2-one (1,2-HOPO) derivatives, a europium(III) H(2,2) (*N,N,N',N''*-tetrakis-(2-aminoethyl)-ethane-1,2-diamine)-1,2-HOPO that has a emission lifetime of 738 μs and quantum yield of 3.6% has been reported (figure 30).[83] The molecule contains no bound water molecules and this leads to an improvement in its luminescent properties. Another lanthanide metal ion complex is again based on H(2,2), however this time it contains four 2-hydroxyisophthalamide chelating groups (H221AM), with the europium(III) and terbium(III) complexes formed (figure 30).[84] The emission lifetimes have been found to be 1271 μs (Tb(III)) and 784 μs (europium(III)) while the quantum yields are 63% (terbium(III)) and 2.3 % (europium(III)). This ligand architecture is able to sensitise the different lanthanide ions, with a strong preference for terbium(III), probably due to the energy gap between the chromophore and metal centre being the best match.

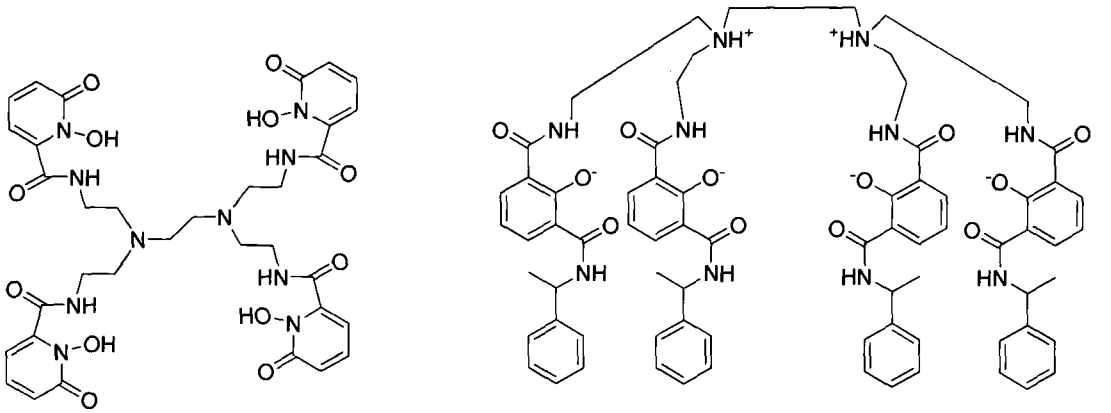

Figure 30 Two chelating ligands of H(2,2)-1,2-HOPO (left) and H221AM (right)

1.7.2 Lanthanide luminescence sensitised by transition metal complexes

Ruthenium and chromium complexes have been used as chromophores for lanthanide sensitisation as they are known to possess intense, low energy and tunable charge transfer absorption bands making them a good alternative to organic based chromophores like fluoroscein.[85 86]

Gunnlaugsson and co-workers have produced a mixed-lanthanide-transition metal (f-d) complex based on a cyclen-ruthenium coordination conjugate (figure 31).[87] The cyclen unit bears a 1,10-phenanthroline moiety that is complexed to a Ru-bipyridine (bipy), with both the ytterbium(III) and neodyium(III) complexes formed.

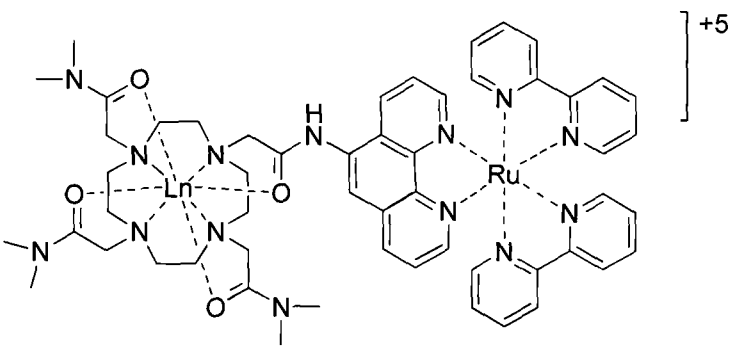

Figure 31 Structures of ytterbium(III) and neodyium(III) complexes of the $Ru(bipy)_2$ conjugate

Complexation of the $Ru(bipy)_2$ conjugate leads to lanthanide luminescence in the NIR through excitation by metal to ligand charge transfer (MLCT) transitions through the chromophore. These complexes lead to intense emission bands as the lanthanide metal centre can effectively be sensitised by the chromophore or by the MLCT band.[87] Another approach is to use transition metals to form supramolecular structures, which will in turn enhances the luminescence because of the increase in the number of lanthanide metal ions. Nagano and co-workers have developed a luminescent lanthanide sensor for zinc(II) based on a europium(III) DTPA unit with a quinoyl moiety as the antenna (figure 32).[88]

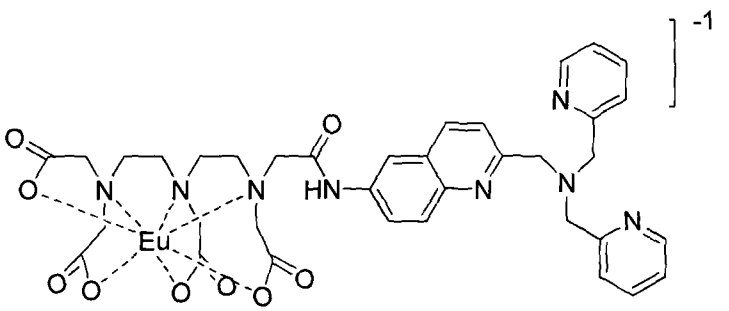

Figure 32 Structure of europium(III) *N*-[*N*-(2-*N*,*N* -bis(2-pyridylmethyl)-aminomethylquinolin-6-yl)carbamoylmethyl]-*N*,*N*',*N*'',*N*'''-diethylenetriaminetetraacetic acid

Upon addition of zinc(II), changes occur in the time delayed emission (8.5 fold increase upon addition of 1.0 equivalents of zinc(II) with a large Stokes shift of > 250 nm), absorbance (3 peaks of 330, 318, and 249 nm change to 2 peaks of 320 and 253 nm) and fluorescence spectra [increase of fluorescence intensity up to 1.0 equivalents of zinc(II)]. These changes occur because there is a photophysical change in the quinoyl moiety upon addition of zinc(II), which in turn leads to a decrease in the number of bound water molecules from 1.42 to 1.22, and results in a change luminescence decay (τ) in D_2O from 2.03 to 2.23 ms.

1.7.3 Multinuclear lanthanide complexes

Multinuclear lanthanide f-f architectures have shown great promise as luminescent complexes.[89, 90, 91] Gunnlaugsson and co-workers have formed a bis-cyclen dinuclear lanthanide complex with lanthanum(III), europium(III) and

terbium(III), see figure 33.[92] However here, the chromophore is a less effective *para*-xylene unit, which weakly sensitises the lanthanide metal ion. To enhance the lanthanide emission, carboxylate anions are added e.g. pimelic acid, that can cause a displacement of the metal bound water molecules. The displacement causes the formation of a self assembly ternary complex between the carboxylate and lanthanide metal ion. Upon coordination of pimelic acid it was shown that a 13% luminescent enhancement occurs with the terbium(III) complex.

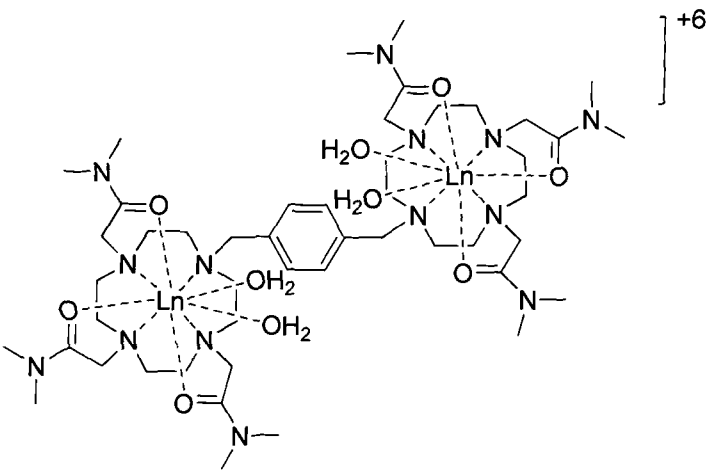

Figure 33 Structure of the bis-cyclen lanthanide complex where Ln = europium(III), terbium(III), lanthanum(III)

A more interesting approach is to form mixed lanthanide complexes. Tremblay and co-workers have done this by producing a cocktail of terbium(III) and europium(III) complexes based on DTPA and containing the chromophore carbostyril 124 (figure 34).[93]

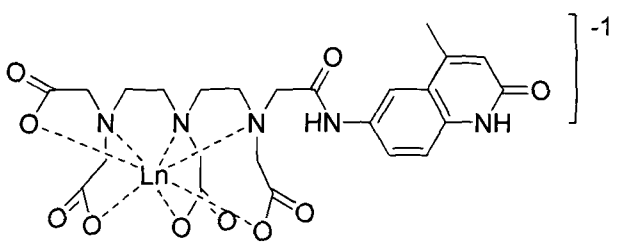

Figure 34 Structure of the Ln-DTPA carbostyril complex, where Ln = europium(III) or terbium(III)

Faulkner and co-workers have produced a mixed luminescent lanthanide complex that bears two DO3A and one DTPA ligands as shown in figure 35.[94] This trinuclear complex contains two terbium(III) ions that are sensitised by the

ytterbium(III) ion. The two terbium(III) ions are coordinated to DO3A, and the ytterbium(III) binds to the DTPA unit.

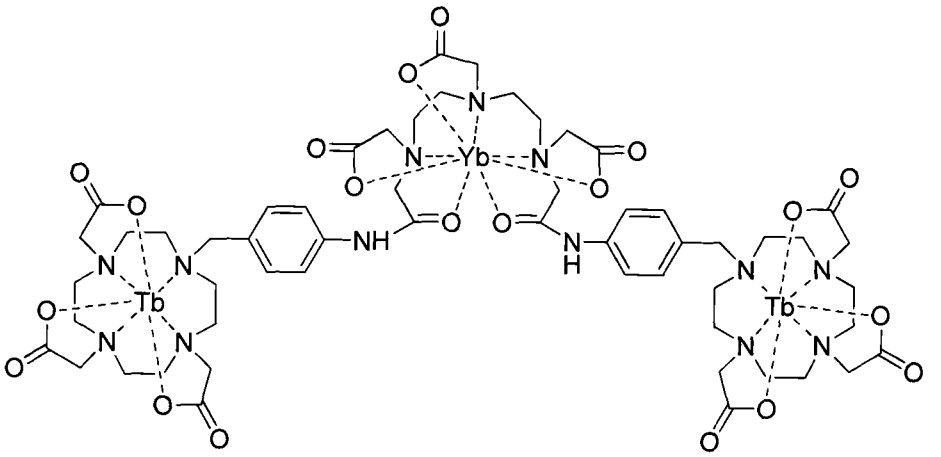

Figure 35 Structure of the ytterbium(III)/terbium(III) complex

The near-IR emission from ytterbium(III) gave lifetimes of 1.8 (water) and 5.2 μs (deuterium oxide). This system is luminescent in both the visible (terbium(III) emission) and near-IR (ytterbium(III) emission) region. Ytterbium(III) is excited at 488 nm and results in near-IR emission at 980 nm with lifetimes of 4.2 μs in D_2O.

1.7.4 Responsive luminescence lanthanide agents

Lanthanide complexes that can modulate lanthanide emission by external inputs such as pH, $^1O_2$ partial pressure and presence of selective ions have great potential to act as sensors for environmental and biological sensing. This will allow for monitoring of environmental or biological stimuli by effectively switching 'on' or 'off' the luminescence.[95] [96] Parker and co-workers have formed a Eu-DO3A based unit containing a 2-methyl quinoline moiety that acts as both a chromophore and receptor (figure 36).[97] In basic conditions the lanthanide emission is 'switched off' while in acidic conditions the emission is 'switched on'. The emission starts to decrease when the pH gets to above 4.5 and leads to a significant decrease at pH 9, above which the emission is completely quenched. This is believed to be associated with the deprotonation of the quinoline nitrogen. The complex has been incorporated into a hydrogel

and has been shown to retain its properties, and shows promise as a fluorescent pH sensor.[98]

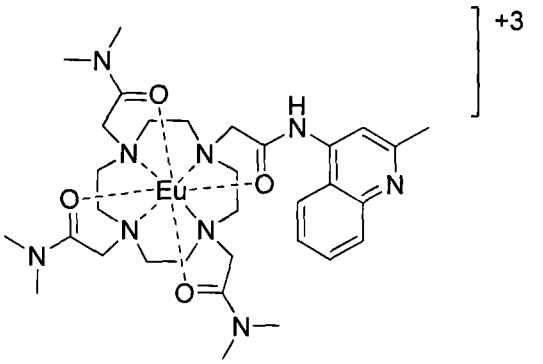

Figure 36 A pH sensor based on Eu-DO3A based unit containing 2-methyl quinoline

Yuan and co-workers have produced a europium(III) complex of the ligand [4'-(10-methyl-9-anthryl)-2,2':6',2''-tetrpyridine-6,6'-diyl]bis(methylenenitrilo) tetrakis(acetate), (MTTA- europium(III)) which is able to probe singlet oxygen ($^1O_2$) concentration (figure 37).[99] Singlet oxygen is important as a probe for biological sensors because it is a toxic species that is associated with cell signalling cascades, and the destruction of malignant cells. This complex can specifically react with $^1O_2$ and form an endoperoxide [EP-MTTA-europium(III)] that is accompanied by an increase in luminescence quantum yield of 0.9 to 13.8% and lifetime of 0.8 to 1.29 ms. The variation in emission properties in the presence of singlet oxygen suggests it could be applied as a sensor for biological changes e.g. apoptosis.

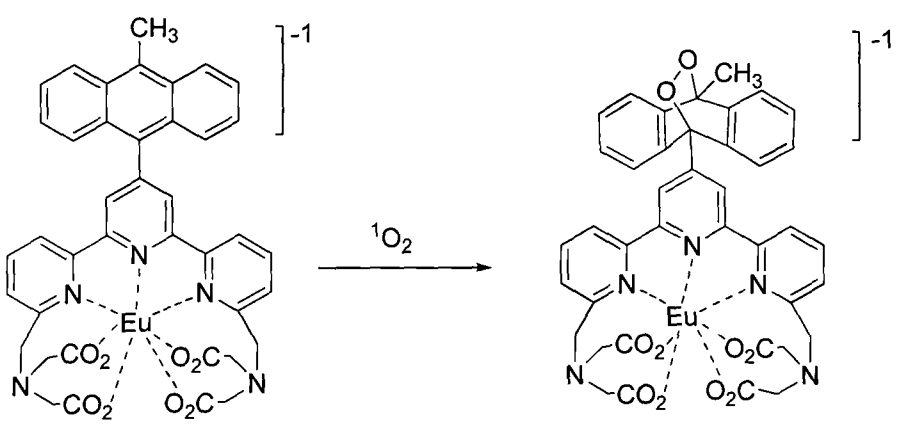

Figure 37 The singlet oxygen sensor based on a europium(III) complex

A number of research groups have investigated lanthanide complexes that show an alteration in the luminescent properties upon binding of an anion.[100] Faulkner and co-workers have reported a series of ytterbium(III) and neodymium(III) complexes of DO3A that can interact with a carboxylate or phosphonate containing molecule that acts as a chromophore and results in 'switching on' of the lanthanide emission (figure 38).[101] This is a very similar system to Gunnlaugsson and co-workers bis-cyclen complex discussed in section 1.6.3, where an increase in luminescence occurs upon the interaction of an anion (figure 33).[92]

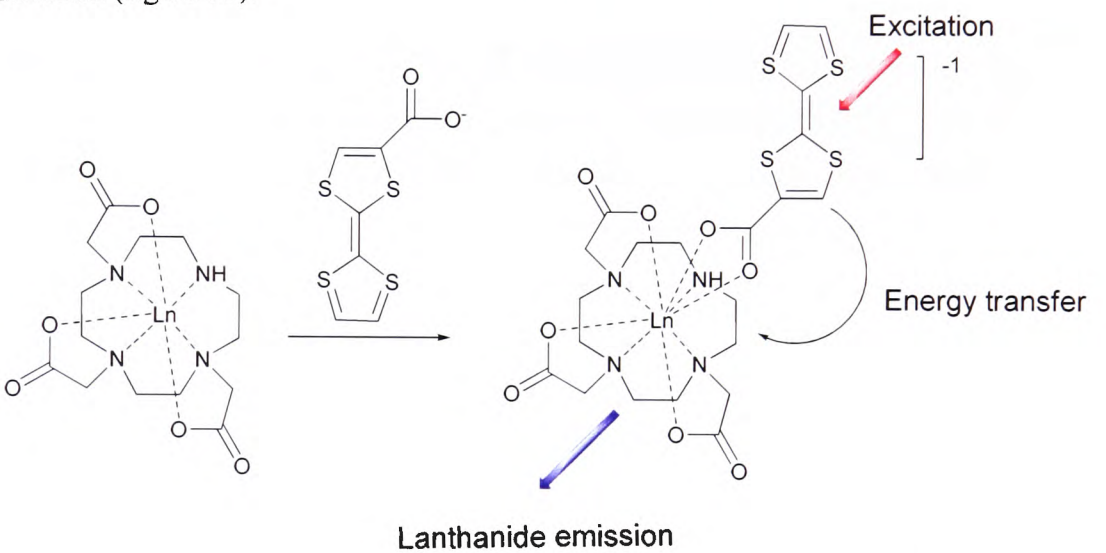

Figure 38 Self assembly of the DO3A based complex where upon interaction of a anion can lead to lanthanide emission, where Ln = ytterbium(III) and neodymium(III)

1.7.5 Targeted luminescent lanthanide agents

For imaging biological systems and sensing applications, it is a major advantage to understand cellular localisation and to be able to target cells *in vivo* with lanthanide complexes. Parker and co-workers have produced numerous lanthanide complexes that can used for cellular imaging (figure 39).[102] One such example is based on cyclen and bears a tetraazatriphenylene chromophore, it is taken up by mouse fibroblasts (NIH 3T3) cells. The europium(III) complex has an absorbance maximum at 340 nm and emits with a millisecond lifetime in the range of 480 to 720 nm.[103 104]

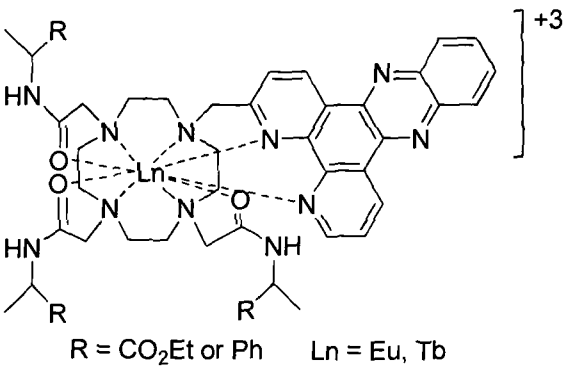

Figure 39 The lanthanide complex bearing a tetraazatriphenylene chromophore synthesised by Parker and co-workers[104]

Romieu and co-workers have formed an aminopropargyl derivative of the terpyridine-bis(methyl-enamine) tetraacetic acid chelate (Eu(TMT)-AP_3) that has been used for fluorescent labelling of proteins and peptides.[105] It contains a capase-3 enzyme substrate dye that is able to detect capase-3 (a component known to be involved in apoptosis) (figure 40). In the presence of caspse-3, (Eu(TMT)-AP_3)capase-3 enzyme substrate conjugate is cleaved and results in an increase in lanthanide luminescence. However, it has been shown that after cleavage, (Eu(TMT)-AP_3) does not maintain its original photophysical properties, and more work will be needed to improve the properties of these compounds.

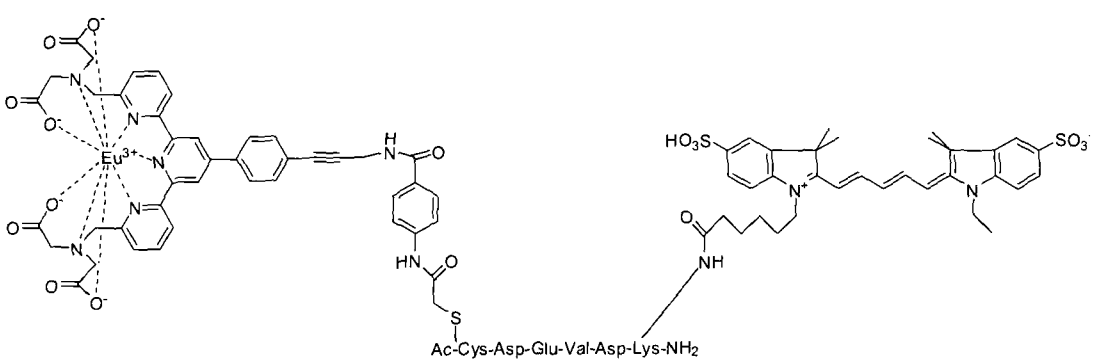

Figure 40 Structure of (Eu(TMT)-AP_3)capase-3 enzyme substrate

1.8 Multimodal imaging agents

Development of multimodal lanthanide imaging agents that can be imaged by both MRI and by fluorescence microscopy, and target cellular function are a major target for development in the area of biological imaging agents. Multimodal imaging agents will help in the understanding of disease states by allowing targeting units to localise in diseased tissue, and through simultaneous MRI visualizing the body and high resolution fluorescence imaging, the mechanism of diseases may be understood.

There are a number of contrast agents that show the potential to be able to target specific tissues or cell types and be visualised by either MRI or luminescence spectroscopy.[1, 73, 106] However, there are a limited number of compounds that are able to do all three. Mishra *et al.* have formed a Gd-DO3A-ethylenediamine complex that bears a fluorescent dye (figure 41).[107] In this design, the gadolinium(III) unit acts as an MRI contrast component, while the fluorescein unit allows the complex to be detected by fluorescence microscopy when it is taken up by cells. The compound has a relaxivity value of 5.36 $s^{-1}mM^{-1}$ at pH 7.4, and has been shown to be taken up by cells (3T3 mouse fibroblasts) using fluorescence microscopy and labelled cell pellet MRI experiments.

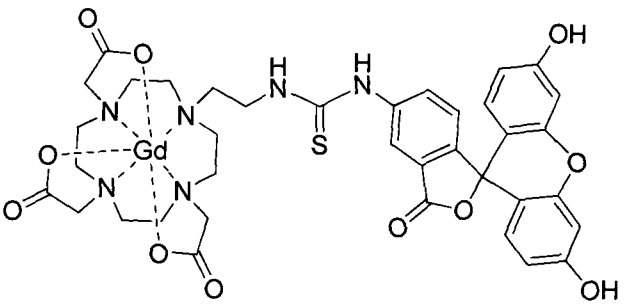

Figure 41 Structure of the Gd-DO3A fluorsecein complex

Bornhop and co-workers have gone for a different approach in forming multimodal lanthanide agents.[108] Here, a 'cocktail' of europium(III)/gadolinium(III) peripheral benzodaiezpene receptor (PBR) mediated cyclen agents (PK11195) have been produced (figure 42). PBR is a

protein that is located in the mitochondria and is associated with a number of biological functions including immunomodulation and apoptosis. PBR has been identified as a factor in Alzheimers and Huntingtons disease. A 'cocktail' solution of 40% Eu-PK11195 and 60% Gd-PK11195 has been shown to localise within the mitochondria in the cells (glioblastoma cells) using fluorescence microscopy, and an increase in the relaxivity is observed in cell pellet MRI experiments, also showing cellular uptake has occurred. The Gd-PK11195 complex has relaxivity of 5.94 mM^{-1} s^{-1}, which is comparable to the known contrast agent Magnevist (6.45 mM^{-1} s^{-1}, 4.7 T) with the added ability to target cells.

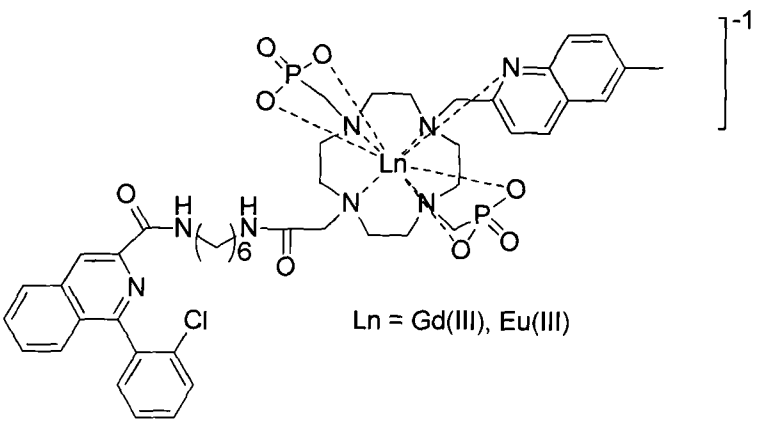

Figure 42 Structure of Ln-PK11195

Meade and co-workers have published an interesting compound Gd(DTPA)-tetramethyl rhodamine amine dextran (GRID), that has been show to track stem cell transplants (figure 43).[109] This is a similar design to a compound used in the work of Mishra *et al.* as the gadolinium(III) component can be used to image through MRI, the rhodamine unit can be detected using fluorescence microscopy, and cell targeting is achieved via the dextran unit.[107] This compound has been shown to accumulate in cells (MHP36) by the use of fluorescence microscopy and a MRI cell pellet experiment. Further studies have also indicated that GRID is able to locate within cells and remain detectable for up to 7 days.[109]

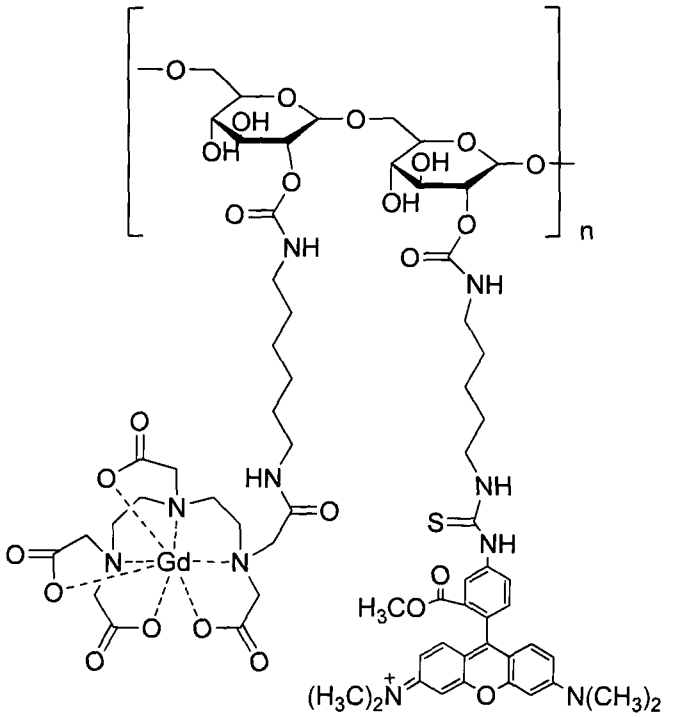

Figure 43 Structure of GRID

Cell grafts of GRID loaded cells have been inserted into an animal brain. MRI has shown that the grafted region can easily be located, with histology studies carried out using fluorescence microscopy also matching the grafted regions.[2]

An interesting method exploited in the formation of multimodality agents is the use of lipids with annexin A5 to form supramolecular structures. Annexin A5 is known to detect the expression of phospholipid phosphatidylserine (PS) which is associated with apoptosis. Nicolay and co-workers have formed a Gd-DTPA-bis(stearylamide)lipid that contains a lipid biolayer of pegylated liposomes to form micelles with annexin A5 covalently coupled (figure 44).[6] Also incorporated into the bilayer are fluorescent lipids that allows for fluorescent imaging. The study showed that these annexin A5 lipid nanoparticles have the ability to target and locate in apoptotic cells as detected using MR and fluorescent imaging experiments. Strijkers and co-workers have formed annexin A5 conjugates with quantum dots that contain a paramagnetic lipid coating (figure 44).[6] The quantum dots act as a fluorescent dye, annexin A5 targets apoptotic cells, the lipid bilayer makes it water soluble and the Gd-

DTPA incorporated into the bilayer allows for MRI image contrast. The agent has been shown to target apoptotic cells by MRI and fluorescent imaging.

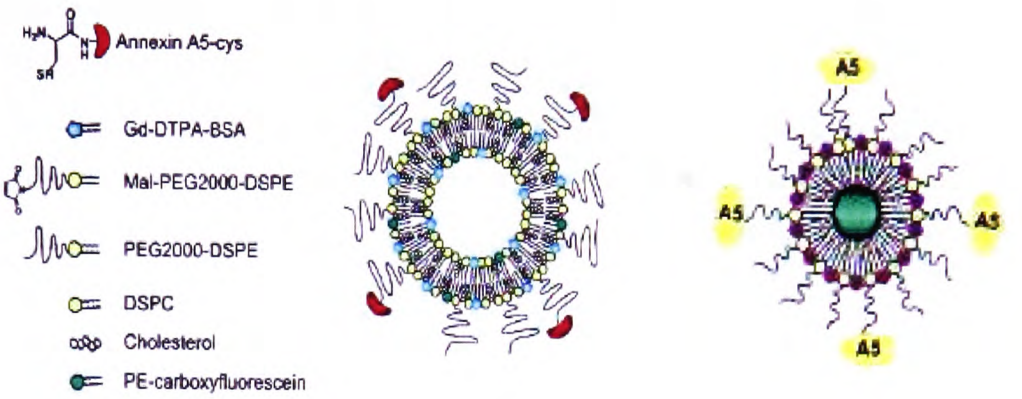

Figure 44 Structures of the annexin A5 supramolecular structures, Nicolay and co-workers complex (left) and Strijkers and co-workers (right)[110 6]

It is clear from the number of publications in the area of lanthanide contrast agents as imaging probes that it is an area of major current interest. Important developments have been made in the performance of gadolinium(III) contrast agents in MRI and luminescent lanthanide metal ion compounds for use as dyes in fluorescence microscopy. Multimodal contrast agents that have the potential to target biological tissue and provide the opportunity to do simultaneous visualisation (MRI and luminescence) also show great promise. There is still a long way to go before they could be accepted for clinical trials and commercial applications. Comprehensive *in vivo* and *in vitro* pharmacological and toxicological analyses must firstly be undertaken to assess safety and efficacy of potential contrast agents.

1.9 Purpose of work

The overall aim of the work presented in this thesis is the design, synthesis and characterisation of multimodality lanthanide imaging agents. The research involves the synthesis of a series of lanthanide chelators based on DO3A **(31)** (chapter 4) bearing a benzimidazole derivative **(7)** (chapter 2) that can act as both a chromophore unit and a linking group for conjugation and that has functionality to couple to an optical dye (either rhodamine or BODIPY derivatives as discussed in chapter 3). The role of the DO3A chelator is to successfully bind the lanthanide ion to prevent release of this toxic metal centre. The benzimidazole derivative was developed as it can act as a chromophore to sensitise the lanthanide metal ion. Simultaneous work was performed on an alternative to the benzimidazole derivatives in their role as a chromophore/linker group, the benzyl derivative (4-nitrobenzylbromide) that has previously been characterised.[78] Optical dyes based on rhodamine and BODIPY have been designed to efficiently conjugate to the chromophore/linker groups, and to function as a highly fluorescent dyes and to influence localisation within the cell.

Other researchers have successfully exploited DO3A-based chelators in the preparation of lanthanide imaging agents, however DO3A benzimidazole chelators have not been previously investigated. Benzimidazole has a number of highly appropriate properties for use in lanthanide chelators. It can coordinate to the metal centre via the N-donor, act as a sensitising chromophore and be functionalised through the N-H group to attach targeting biomolecules or optical dyes. Benzimidazole synthesis is well known in the literature, although limited research has been carried out to prepare precursors that allow for the linkage of two molecules, for example DO3A and the further attachment of a fluorescent dye [rhodamine and boron dipyromethenes (BODIPY)] (figure 45). In this work, lanthanide complexes of DO3A bearing a benzimidazole precursor have been prepared and characterised, and further investigations to form complexes bearing a fluorescent dye to produce multimodal contrast agents for MRI and luminescence imaging have also been carried out.

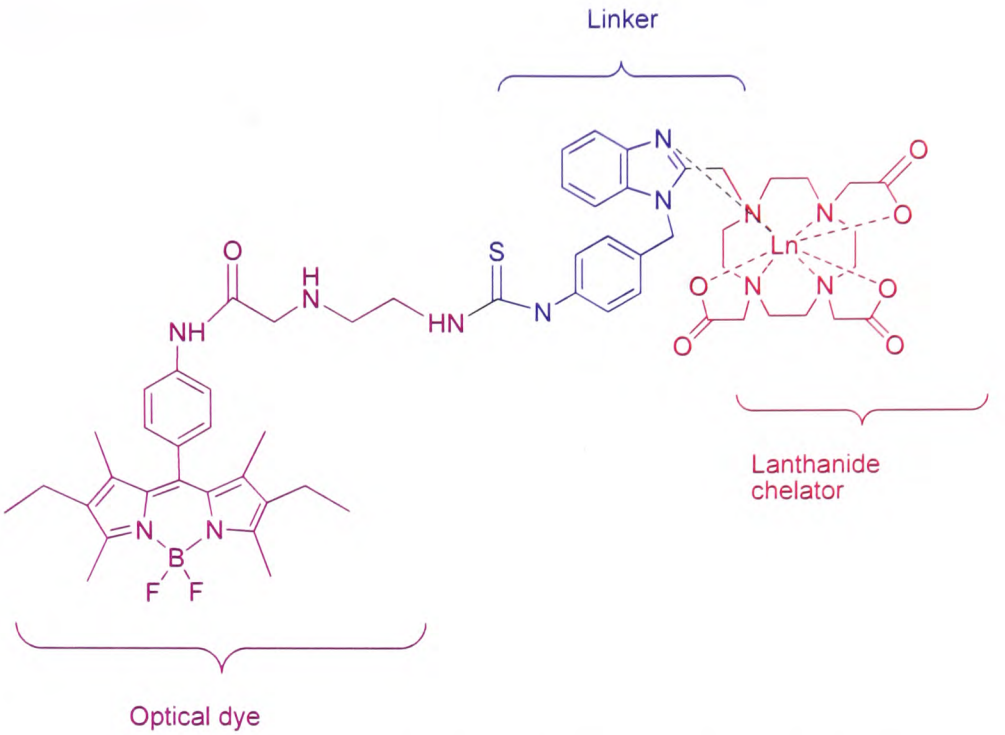

Figure 45 A proposed multimodal lanthanide complex (Ln-DO3A (chelator) in red, benzimidazole precursor in blue (linking unit), and BODIPY (optical dye) in purple

2. Synthesis of benzimidazole derivatives

2.1 Introduction

For a luminescent lanthanide contrast agent to function efficiently and emit fluorescence of a detectable intensity, a chromophore group is required to sensitise the lanthanide metal centre. In the literature, there are many reported examples of different organic chromophores that can efficiently absorb and transfer energy to sensitise lanthanide metal centres, for example 1,10-phenanthroline and anthracene as shown in figure 46.[87 111] The benzimidazole group can also be used as a sensitising chromophore (figure 47) with the additional advantage that it can be N-substituted at the 1-position and C-substituted at the 2-position to allow for further functionality to be incorporated.

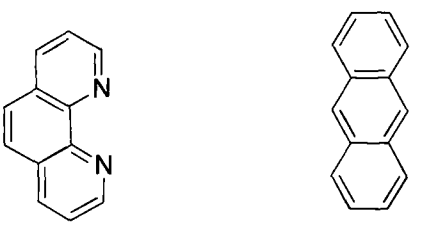

1,10-phenanthroline anthracene

Figure 46 Structure of typical organic chromophores used to sensitise the emission of lanthanide ions, 1,10-phenanthroline and anthracene

This chapter focuses on discussion of the methodology used to synthesise benzimidazole derivatives that can be used as both a chromophore unit to sensitise lanthanide metal ions and as a linker group to allow for conjugation to optical dyes (discussed in chapter 3).

2.1.1 Benzimidazole

A benzimidazole unit consists of a phenyl ring fused to an imidazole ring as shown in figure 47. This unit has the potential to be used as an organic chromophore for lanthanide sensitisation due to the highly conjugated π system and well characterised procedures for functionalisation to facilitate incorporation into a chelating ligand.

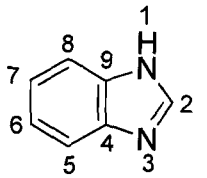

Figure 47 Molecular structure of benzimidazole

Benzimidazole containing compounds are present in nature and one of the most well known systems is (5,6-dimethyl-1-(α-D-ribofuranosyl)benzimidazole, which is an integral part of the structure of vitamin B_{12}. More recently benzimidazole based compounds have been incorporated into pharmaceutical agents and have been used as DNA intercalators.[112 113] For example, 2-[(4-diarylmethoxy)phenyl]-benzimidazole has been identified as a potential inhibitor for the infectious disease hepatitis C, and other substituted benzimidazoles have shown promise as DNA intercalating chemotherapeutic agents for the treatment of cancer.[114 115, 116]

Benzimidazoles have been used as components of metal chelating ligands and more specifically in ligands used to form luminescent lanthanide complexes. This has been successfully exploited by Yang *et al.* in a study where a series of tripodal liands based on bis(2-benzimidazolylmethyl)(2-pyridylmethyl)amine and bis(2-pyridylmethyl)(2-benzimidazolemethyl)amine (figure 48) were synthesised and the gadolinium(III), praesodymium(III), ytterbium(III), europium(III) and terbium(III) complexes prepared.[117]

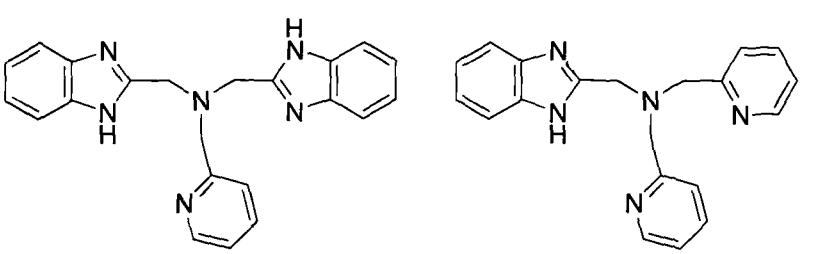

Figure 48 Structure of two tripodal ligands; bis(2-benzimidazolylmethyl)(2-pyridylmethyl)amine (left) and bis(2-pyridylmethyl)(2-benzimidazolemethyl)amine (right)

2.2 Strategy for the preparation of multi-functional benzimidazole derivatives

The advantage of the benzimidazole unit is that it has the potential for multi-functionalisation. It can act as a sentising chromophore unit but it can also be used as a linking group to attach optical dyes to a chelating ligand, which will either be directly detected or offer alternative wavelengths for lanthanide sensitisation. To prepare a benzimidazole that can act as a dual functional component, a number of key synthetic steps are needed. These steps include: 1) attachment of the benzimidazole to the chelating ligand via the carbon at the 2-position to allow for the formation of a 5-membered chelate ring on coordination of the metal centre, 2) attachment of additional functional groups at the 1-position for linking an optical dye and 3) coordination of a metal centre with binding via the N-donor at the 3-position.

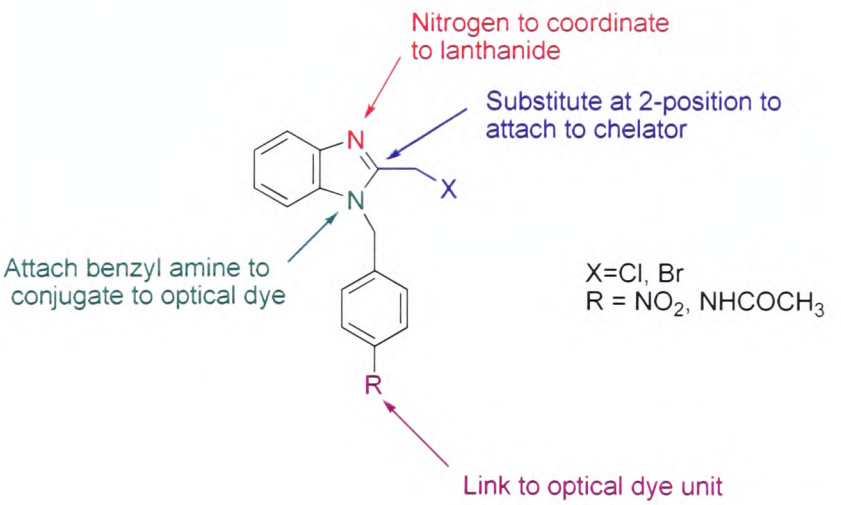

Figure 49 Target multi-functional benzimidazole derivative

A target multi-functional benzimidazole is depicted in figure 49. Each of these reactions is considered in turn. A key step in this process is the initial attachment of either a nitro benzyl or amide benzyl group onto the N at the 1-position. The nitro or amide functionality can be converted to an amine at a later stage (see chapter 4). Substitution of the carbon at the 2-position can be facilitated via the formation of a methyl halide that will react with the secondary amine on the DO3A chelator **(31)**. Formation of the benzimidazole derivative

can be achieved using chloroacetic acid (modified Philips method) or orthoesters as reagents.[118] The remaining nitrogen at the 3-position will ultimately coordinate to the lanthanide metal ion, potentially allowing for efficient sensitisation via the benzimidazole chromophore as it will be directly bound to the metal centre.

2.2.1 Synthetic methodology to produce multi-functional benzimidazole derivatives

The synthesis of benzimidazole derivatives that are functionalised at both the 1- and 2-position (figure 48), can involve a two-step process with either a cyclisation step to form the benzimidazole unit carried out first, or the initial attachment of a nitro or amide benzyl group onto the nitrogen at the 1-position. Previous work has shown that either step can be undertaken first, and the two proposed methods are shown in figure 50. Method 1 involves the mono substitution of one of the amines on the phenylenediamine, followed by the cyclisation to yield the benzimidazole compound. While method 2 carries out the cyclisation first, followed by a nucleophilic substitution of the amine at the 1-position. Both of these methods have been exploited in the literature in the synthesis of benzimidazole derivatives with the desired functional groups.[119 120]

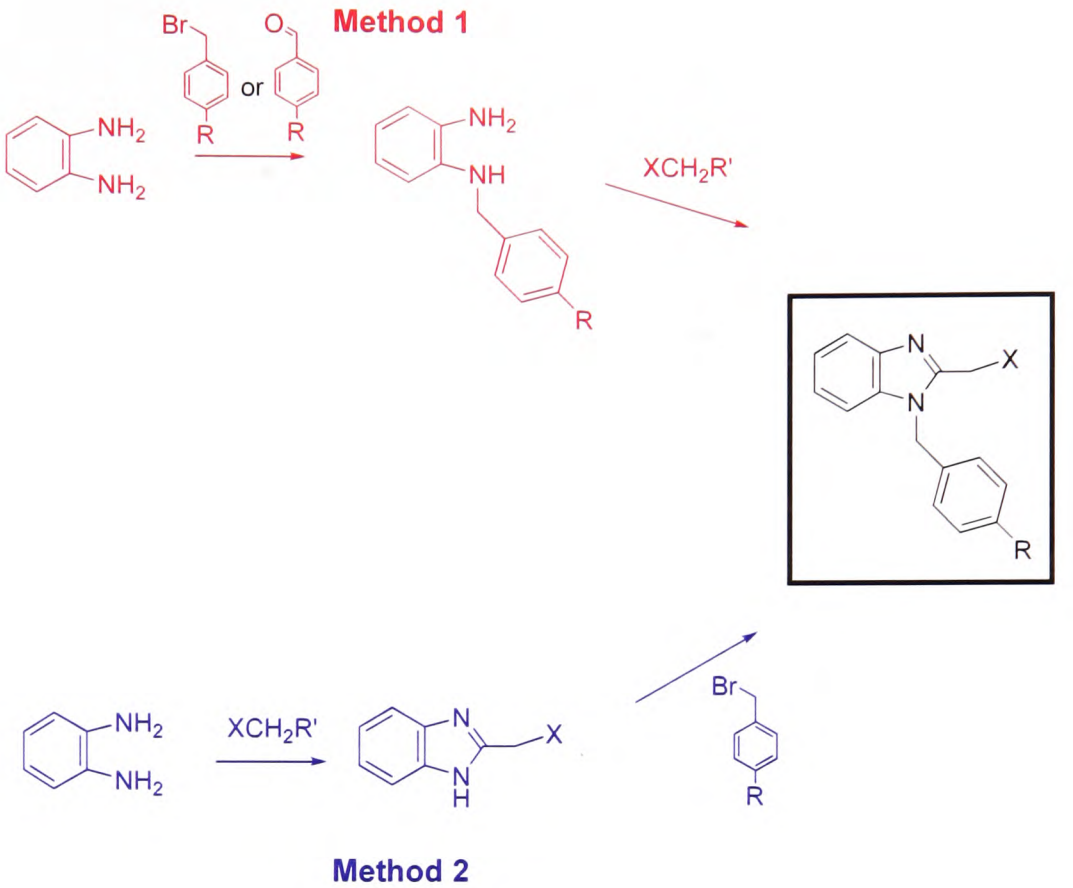

Figure 50 Two potential strategies to synthesise benzimidazole precursors (where R = $NHCOCH_3$ or NO_2, R' = $CNHOCH_3$, or COOH, X = OH, Cl or Br,)

Methods to synthesise benzimidazoles substituted at the 1-position are well documented in the literature. This can involve nucleophilic substitution at the nitrogen with either an alkyl halide or an acid chloride.[121 122]

2.2.2 Strategy for the cyclisation step to form benzimidazole derivatives

In the literature a variety of different routes are reported for the synthesis of benzimidazole derivatives that have been functionalised at the 2-position, including the formation of the 5-membered ring using carboxylic acids, solid-phase routes, nitroanilines, and orthoesters.[123 124-128] Representative examples of these reactions are summarised in figure 51.

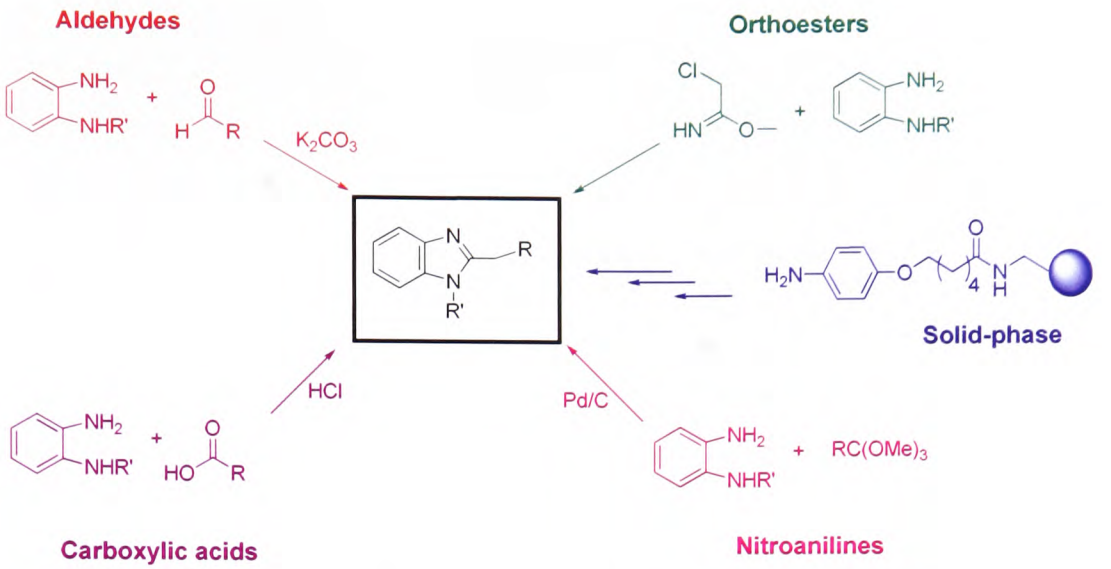

Figure 51 Summary of reactions to synthesis benzimidazole derivatives

While both the nitroaniline and the solid-phase route provide interesting alternatives in the synthesis of benzimidazoles, in this case they are not suitable. The solid-phase route would give products that do not contain the desired functionality and both methods involve multi-step reactions with expensive precursors. The synthesis of benzimidazoles using aldehydes was considered. Das *et al.* have reported the synthesis of a series of benzimidazole derivatives that were obtained by treating 1,2-phenylenediamine with substituted aldehydes in the presence of (bromodimethyl)sulfonium bromide at room temperature, with percentage yields of 72 – 91% (figure 52).[129] Similarly Gogoi *et al.* have combined a series of substituted aldehydes with 1,2-phenylenediamine in water in the presence of potassium carbonate, iodine and potassium iodide (figure 52).[130]

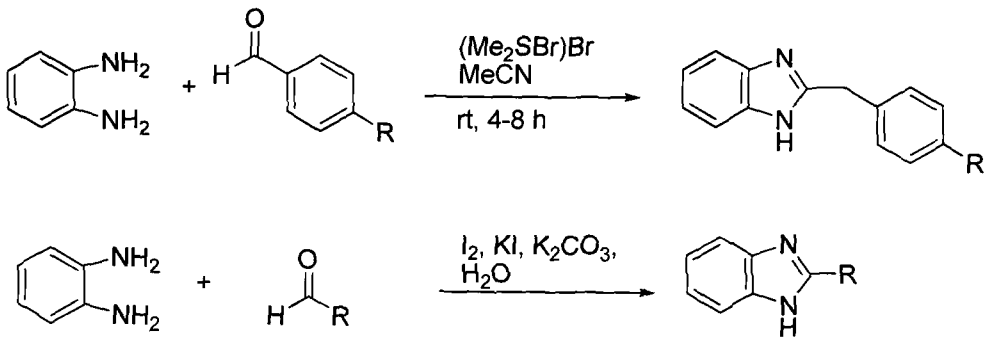

Figure 52 Synthesis of benzimidazoles using (bromodimethyl)sulfonium bromide (top), and potassium carbonate, iodine and potassium iodide (bottom)

A search of the available chemicals database did not reveal any suitable substituted aldehyde derivatives that were commercially available. As a result, this was not investigated further. Efforts then focused on the carboxylic acid and orthoester routes.

Section 2.3-2.5 details the results obtained using method 1 and section 2.6 contains the results obtained using method 2. A discussion of the synthesis of benzimidazole precursors is also presented.

2.3 Synthesis of benzimidazole derivatives – method 1

Method 1 involves the mono alkylation of 1,2-phenylenediamine with a benzyl derivative, where R^2 is an aldehyde (imine formation followed by reduction) or an alkyl bromide group, followed by the cyclisation to form the benzimidazole derivative by reaction with either a carboxylic acid or orthoester. The general synthetic scheme for method 1 is shown in figure 53.

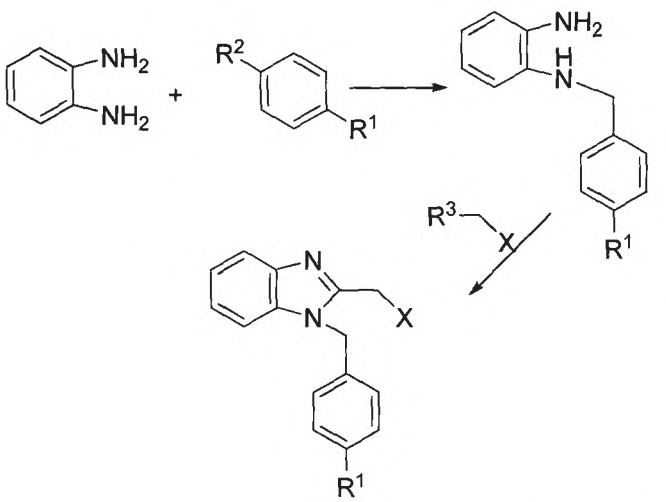

Figure 53 Synthetic route to a benzimidazole derivativised at N1(where R^1 = $NHCOCH_3$ or NO_2, R^2 = CH_2Br or CHO(needs to be reduced before cyclisation), R^3 = $CNHOCH_3$, or COOH and X = Cl or Br)

Hérault *et al.* have employed this strategy in the synthesis of 2-ferrocenyl-*N*-n-butylbenzimidazole by functionalising the phenyl unit first, then treating the molecule with ferrocene carboxaldehyde to form the benzimidazole compound.[121] The reaction involves aromatic nucleophilic substitution of n-butyl amine onto 2-bromonitrobenzene, followed by reduction of the nitro group to form an amine and finally condensation with ferrocene carboxaldehyde to give the benzimidazole functionalised ferrocene in 63% overall yield. The reaction is shown in figure 54.

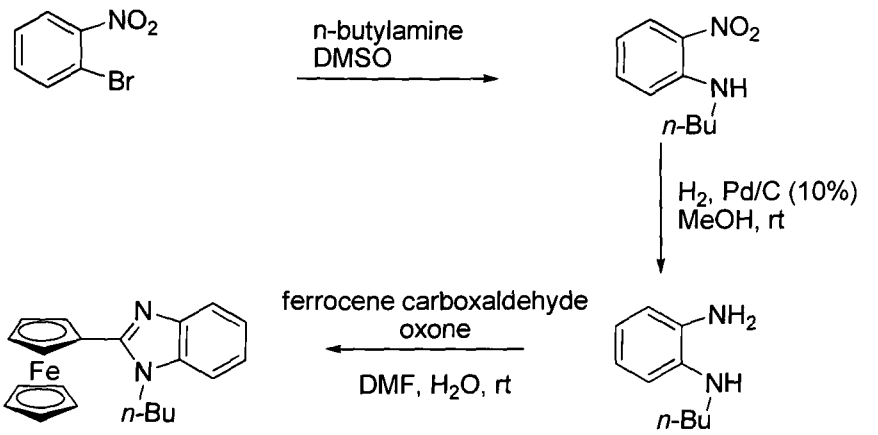

Figure 54 Synthesis of 2-ferrocenyl-*N*-n-butylbenzimidazole

The next stage in the synthetic scheme involves the cyclisation of the substituted phenylenediamine to form the benzimidazole precursor. The proposed method involves a modification of the Phillips synthesis where the benzimidazole precursor is condensed with either chloroacetic acid or chloroacetimidate orthoesters.[131 132]

2.4 Synthesis of amide bearing benzimidazoles

The initial strategy involved the use of an amide derivative that can be readily converted to an amine at a later stage by acid hydrolysis. This would be carried out after the attachment of the benzimidazole to the DO3A chelator **(31)**, thus both the acid arms and amine site can be deprotected at the same time. This offers an advantage over the route using the nitro compound because there are fewer steps in the overall synthetic scheme (the nitro group must be reduced in a separate step to the deprotection of the acid arms).

2.4.1 Attempted synthesis of 1-(4-acetamidobenzyl)-2-chloromethyl benzimidazole (3)

The synthetic scheme for the preparation of 1-(4-acetamidobenzyl)-2-chloromethyl benzimidazole **(3)** is shown in figure 55. The amide group is sensitive to acidic conditions, and so the use of carboxylic acids to form the imidazole ring would lead to early deprotection of the amide. The use of orthoesters (such as methyl chloroacetimidate hydrochloride) was investigated due to the milder conditions for benzimidazole synthesis.

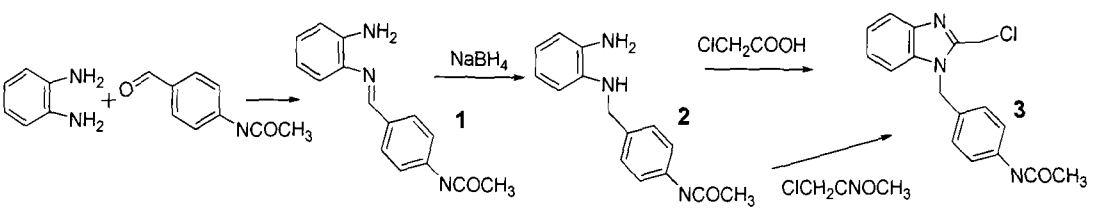

Figure 55 Synthetic scheme for the synthesis of the benzimidazole unit 1-(4-acetamidobenzyl)-2-chloromethyl benzimidazole **(3)**

The first step in the synthesis of 1-(4-acetamidobenzyl)-2-chloromethyl benzimidazole **(3)**, involved the mono-alkylation of 1,2-phenylenediamine with 4-acetamidobenzaldehyde to form 1-(4-acetamidomethylene)phenylenediamine **(1)**.

2.4.2 N-substitution reactions of 1,2-phenylenediamine

The potential problem associated with the N-substitution reactions of 1,2-phenylenediamine is the possibility that multiple alkylation may occur, resulting in the formation of secondary, tertiary or quaternised amines on either one or both of the nitrogens. Some possible multiple alkylation products are shown in figure 56.

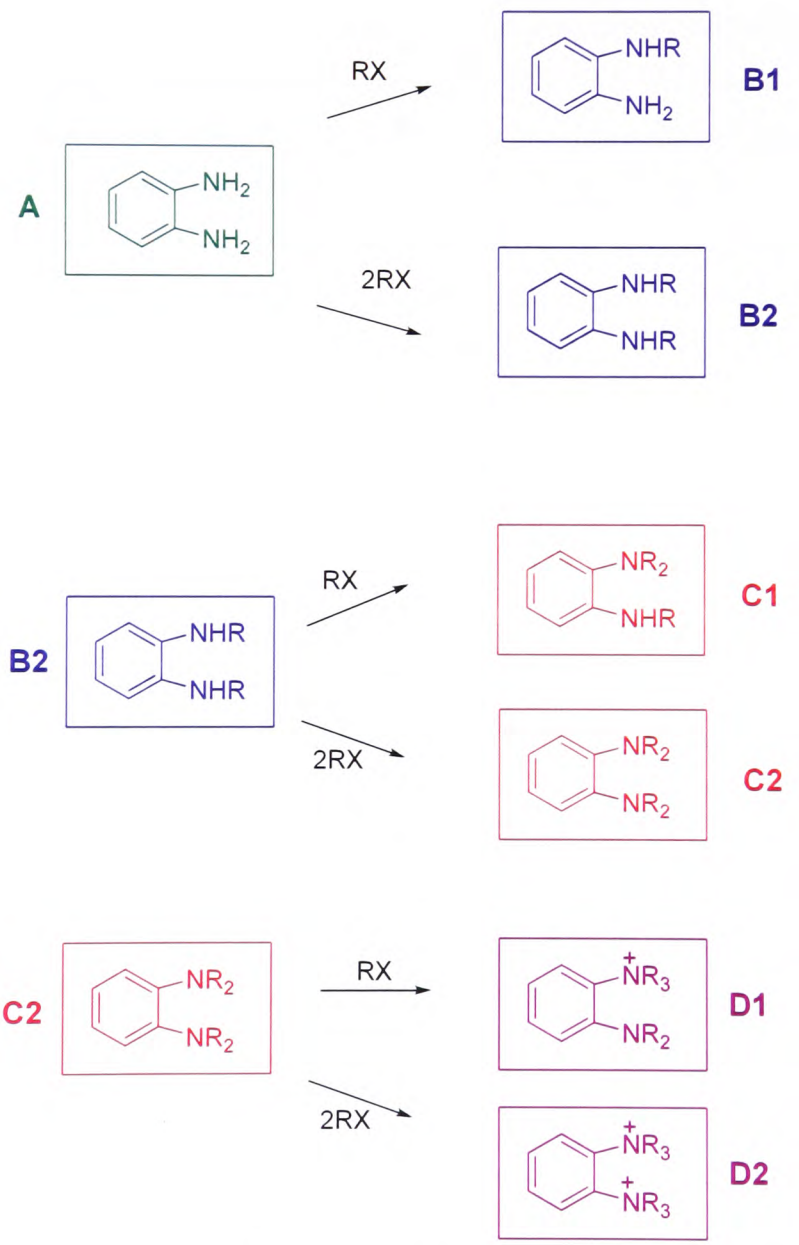

Figure 56 Possible reactions leading to multiple alkylation of the amines on 1,2-phenylenediamine

The presence of a small excess of the alkylating agent, can result in the formation of a mixture of the alklylated amines (B-D). To prevent multiple alkylation, an excess of the 1,2-phenylenediamine can be used, which encourages the formation of the mono-alkylated product (B1) over the multi-alkylated products.[133]

2.4.3 N-substitution reactions of 1,2-phenylenediamine with 4-acetamidobenzaldehyde (2)

The initial attempt to prepare 1-(4-acetamidomethylene)phenylenediamine involved adding 4-acetamidobenzaldehyde to a 3-fold excess of 1,2-phenylenediamine and stirring for 4 hours at room temperature, followed by heating at reflux for 20 minutes. The ^{1}H NMR spectrum was not consistent with the desired product, instead showing a mixture of products alongside the starting material. Imine bonds are known to be susceptible to hydrolysis, either upon heating to reflux or due to the presence of water, and so it was thought that the desired product was degrading during the reaction. Therefore, the reaction conditions were altered to avoid heating and the mixture was stirred with molecular sieves to remove any water formed in the reaction. The reaction was monitored by thin layer chromatography (t.l.c.) and the optimum conditions were found to be stirring for 72 hours with 3Å molecular sieves, followed by removal of the solvent and maintaining the temperature below 40°C. The compound was then recrystallised from the minimum amount of ethanol, and the resulting yellow solid was collected in a 69% yield. The presence of the desired product was confirmed by ^{1}H NMR spectroscopy, and the key feature was the characteristic imine proton observed at 6.86 ppm. The reduction of the imine bond to an amine bond to form 1-(4-acetamidomethyl)phenylenediamine **(2)**, was achieved using sodium borohydride. The ^{1}H NMR spectrum confirmed the disappearance of the imine proton at 6.86 ppm and showed the formation of a CH_2 peak at 4.51 ppm.

2.4.4 Cyclisation of the benzimidazole using substituted orthoesters

A known synthetic procedure used to produce benzimidazole containing compounds involves using orthoesters as precursors. For example, Musser *et al.* have utilised othoesters in the development of benzimidazoles as incorporation into pharmaceutical agents used for inhibitors of leukoriene D_4 antagonists.[131] This reseach group treated *N*-methyl-2-phenylenediamine with chloroacetamidate to produce benzimidazole precursors in *ca.* 70% yield (figure 57). Alternatively, Yasui *et al.* used methyl 2,2,2-trichloroacetimidate to form 4,4'-dibromo-6,6'-dimethyl-2,2'-bisbenzimidazole in *ca.* 80% yield (figure 57).[134]

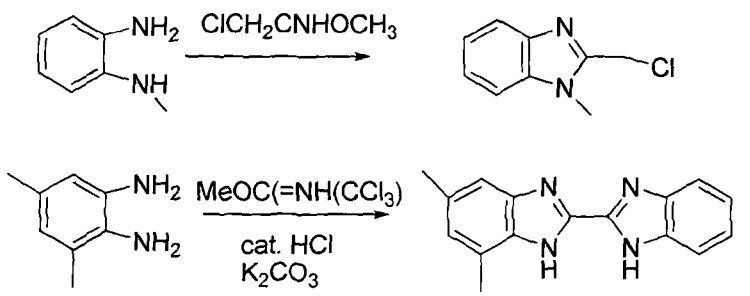

Figure 57 The synthesis of benzimidazoles using orthoesters by Musser *et al.* (top) and by Yasui *et al.*[131] [134]

Orthoesters such as methyl chloroacetimidate hydrochloride are also known to form benzimidazoles on reaction with 1,2-phenylenediamine.[135]

2.4.5 Preparation of (4-acetamidobenzyl)-2-chloromethyl benzimidazole (3)

To form 1-(4-acetamidobenzyl)-2-chloromethyl benzimidazole **(3)** using the orthoester route, methyl chloroacetimidate hydrochloride is required, which can be readily synthesised by a variety of methods.[135] The two routes that were investigated are identified in figure 58.

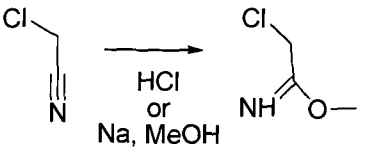

Figure 58 The proposed synthesis of methyl chloroacetimidate hydrochloride

The initial route explored was that reported by McElvain *et al.*, where dry hydrogen chloride gas was bubbled through an ice cooled solution of chloroacetonitrile in dry ethanol, followed by the addition of diethyl ether, which resulted in the formation of a white precipitate.[136] The second method published by Schaefer *et al.* involves sodium methoxide being stirred with chloroacetonitrile overnight.[137] In both cases the 1-(4-acetamidomethyl)phenylenediamine (**2**) was then added to the reaction mixture and heated at reflux overnight, under an inert atmosphere. The literature reported yields of 30% and 71% yields respectively, however, with these starting materials neither method produced the desired product according to analysis by proton and carbon NMR spectroscopy and mass spectrometry (electrospray). Instead the analytical data suggests that 2-chloro-acetimidic acid methyl ester hydrochloride has possibly hydrolysed leaving (**2**) to react with the chloride and form unwanted by-products. Therefore, the synthesis of nitro benzyl ring benzimidazole derivatives was investigated.

2.5 Synthesis of nitro benzyl benzimidazoles

As the synthesis of benzimidazole derivatives with an appended benzylamide group were problematic, efforts were concentrated on synthesis of the nitro benzyl benzimidazoles. The strategy involved the preparation of the phenylenediamine precursor 1-(4-nitrobenzyl)phenylenediamine **(5)** with the attachment of either 4-nitrobenzylbromide, or 4-nitrobenzaldehyde (which forms an imine linkage that is then reduced to an amine) to phenylenediamine. This can then be converted to a benzimidazole derivative that contains a reactive moiety at the 2-position. The research focused on the preparation of the chloromethyl benzimidazole derivative **(7)**.

2.5.1 Synthesis of 1-(4-nitrobenzyl)phenylenediamine (5)

Synthesis of the nitro-functionalised benzyl benzimidazole 1-(4-nitrobenzyl)-2-chloromethyl benzimidazole **(7)** was investigated using a number of routes. The synthetic routes utilised are shown in figure 59.

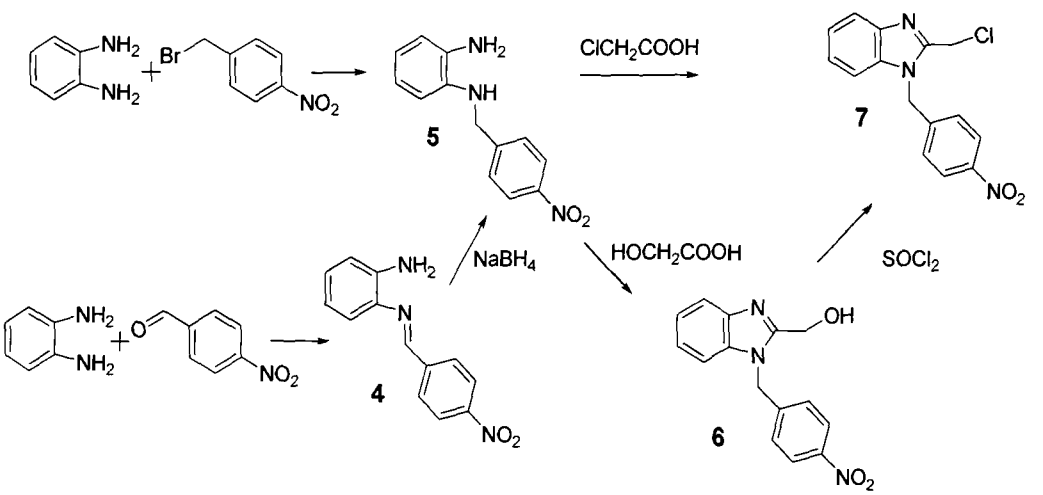

Figure 59 Scheme showing the synthesis of 1-(4-nitrobenzyl)-2-chloromethyl benzimidazole **(7)**

The initial aim was to form 1-(4-nitrobenzyl)phenylenediamine **(5)** either by a Schiff's base condensation with 4-nitrobenzaldehyde followed by the reduction

or a single step reaction with 4-nitrobenzylbromide. Using the optimised protocol for the amide compounds, 4-nitrobenzaldehyde in methanol was added to 1,2-phenylenediamine in methanol in the presence of 3 Å molecular sieves and allowed to stir for 72 hours at room temperature. The solution was filtered and the solvent removed, to yield a red solid. To remove unwanted starting material, the compound was re-crystallised from ethanol, and the precipitated solid was collected to give 1-(4-nitrophenylmethylene)phenylenediamine **(4)** in 71% yield. The ^{1}H NMR spectrum corresponds to the desired product with the aromatic protons observed in the range 6.81 - 8.32 ppm and integrating to 8 protons. The imine proton (C***H***N) appears as a singlet at 6.81 ppm with an integration value of one. The imine was then reduced to the amine by the addition of an excess of sodium borohydride in small portions to a solution of **(4)**, followed by heating at reflux for 4 hours. The reaction was quenched with water and then the product extracted into dichloromethane. A white solid was isolated in 48% yield. Successful reduction was confirmed by ^{1}H NMR spectroscopy, which showed the loss of the imine peak at 6.81 ppm and the formation of a CH_2 peak at 4.46 ppm (integration value of 2). The aromatic CH peaks are in the range of 6.46 – 8.19 ppm. The overall yield of the two steps was 60%, taking a total of five days to synthesise **(5)**. As an alternative to using 4-nitrobenzyaldehyde in the reaction with phenylenediamine, 4-nitrobenzylbromide was used to form **(5)** in a single step reaction. In this reaction, 4-nitrobenzylbromide was added dropwise in methanol to a 5-fold excess of 1,2-phenylenediamine and the reaction mixture allowed to stir for 4 hours, the solvent was removed and the product recrystallised from the minimum amount of ethanol. The recrystallised product was purfied using flash column chromatography on silica with dichloromethane as the eluent to give a red/orange solid in yields of *ca.* 60%. Attempts were made to perform flash column chromatography directly on the crude reaction material, but it was found that the recrystallisation removed starting material that was not easily separated by chromatography alone due to its similar r.f. value to the product. The electrospray mass spectrum contained the molecular ion peak of **(5)**. In the ^{1}HNMR spectrum, the singlet peak at 4.38 ppm arises from the CH_2NH, and a double doublet at 6.39 ppm and a multiplet at 6.65 ppm correspond to the aromatic protons on the phenylenediamine component. The two triplets at 7.49

ppm and 8.0 ppm correspond to the aromatic protons on the other phenyl ring. Single crystal X-ray crystallographic analysis was carried out on samples of 1-(4-nitrobenzyl)-2-chloromethyl benzimidazole and the structure determined. An ORTEP plot of the structure of 1-(4-nitrobenzyl)phenylenediamine **(5)** is shown in figure 60.

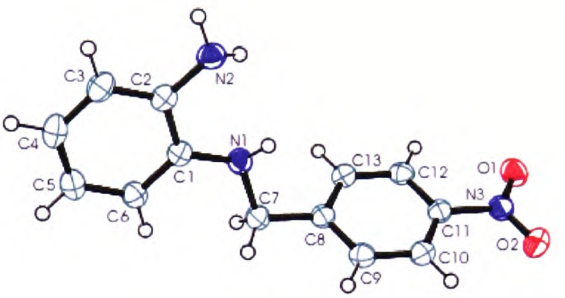

Figure 60 The molecular structure of 1-(4-nitrobenzyl)phenylenediamine, showing the atom labelling and 50% probability ellipsoids for non-H atoms

Bond length (Å)		**Bond and torsion angles (°)**	
C1 - N1	1.3961 (18)	C1 - N1 - C7	119.22 (11)
C2 - N2	1.3998 (19)	N1 - C7 - C8 - C13	-64.36 (17)
C7 - N1	1.4570 (19)	C6 - C1 - N1 -C7	-9.2 (2)
C11 – N3	1.4678 (18)		
N3 - O2	1.2242 (18)		
N3 - O1	1.2268 (17)		

Table 5 Selected bond lengths and bond and torsion angles of 1-(4-nitrobenzyl)phenylenediamine

The crystal structure of 1-(4-nitrobenzyl)phenylenediamine is characterised by the hydrogen-bonded dimers (N1 – H14···O1^{i} and N2 – H16···O2^{i}) as indicated in table 5. This dimer locks the secondary amine group containing the N1 atom into a chiral form, and it contains both the enantiomeric forms of the molecule. The hydrogen bonding is combined with π-π stacking, and results in one-dimensional chains running parallel to the *b* axis. This π-π stacking occurs between the benzene ring (mean plane-plane distance = 3.29 Å) of the nitrobenzyl groups of dimers in adjacent unit cells (figure 61 and 62).

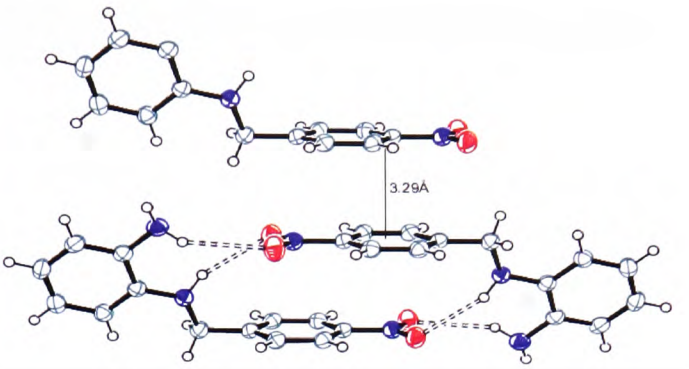

Figure 61 The hydrogen bonded (dashed lines) dimers and π-π stacking between dimeric units of 1-(4-nitrobenzyl)phenylenediamine

D-H···*A*	**D-H**	**H···*A***	**D···*A***	**D-H···*A***
N1-H14···O1^{i}	0.92 (2)	2.43 (2)	3.3005 (18)	158.3 (15)
N2-H16···O2^{i}	0.91 (2)	2.62 (2)	3.4277 (19)	148.0 (18)

Table 6 Hydrogen-bond geometry (Å, °) of 1-(4-nitrobenzyl)phenylenediamine, where the symmetry code: (i) –x +1, -y + 2, -z

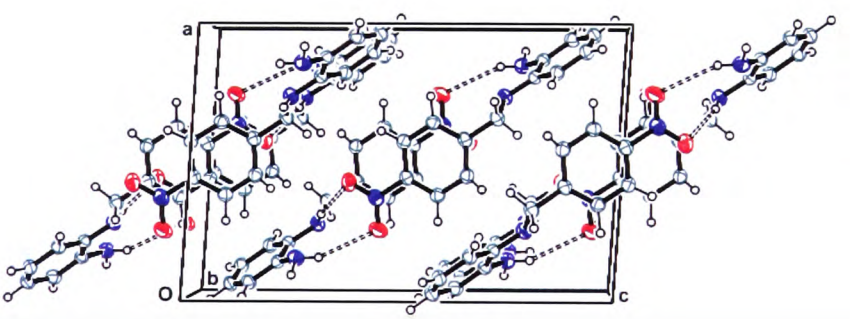

Figure 62 The crystal packing, viewed along the *b* axis of 1-(4-nitrobenzyl)phenylenediamine

2.5.2 Cyclisation to form benzimidazoles using carboxylic acids

There is a great deal of interest in the use of carboxylic acids to form benzimidazoles under acidic conditions.[138] A large number of publications have reported the use of substituted acetic acid derivatives in reactions with 1,2-phenylenediamine using 5 M HCl as the solvent.[121] The solution is heated at reflux, followed by an alkaline work up at 0°C that causes precipitation of the desired compound. In particular, Wilson *et al.* have used this method to form a series of substituted benzimidazoles in *ca.* 80% yield (figure 63).[132]

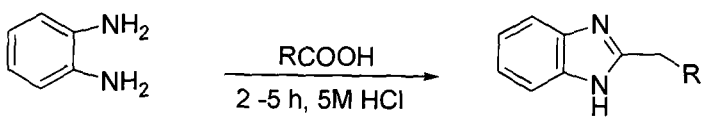

Figure 63 Synthesis of substituted benzimidazoles using carboxylic acids

All of these literature methods are based on modifications of the Philips method. The proposed mechanism for the formation of the benzimidazole unit using this method is shown in figure 64.

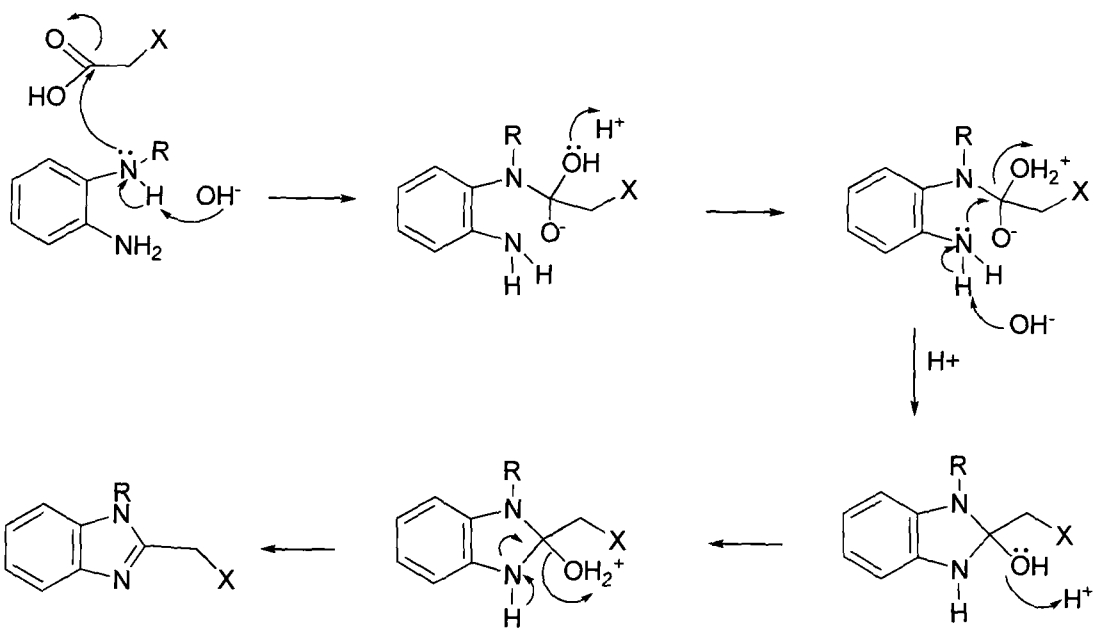

Figure 64 Proposed mechanism for the reaction of substituted 1,2-phenylenediamine with a carboxylic acid R=$CH_2C_6H_4NHCOCH_3$, X = Cl, Br or OH

The role of the acid is to act as a catalyst, activating the carbonyl group by the protonation of the oxygen to form a carbonium ion. With the electron deficiency at the carbon ion on the acetic acid moiety, the lone pair on the nitrogen is able to attack the carbonium ion resulting in a dehydration reaction to form the benzimidazole compound.

2.5.3 Synthesis of 1-(4-nitrobenzyl)-2-chloromethyl benzimidazole (7)

Initial efforts to synthesise 1-(4-nitrobenzyl)-2-chloromethyl benzimidazole **(7)** involved using the modified Philips procedure. There are numerous reports of phenylenediamine derivatives being converted to a chloromethyl benzimidazole group using chloroacetic acid.[139 122, 132, 140] These procedures describe heating a mixture of 1,2-phenylenediamine and chloroacetic acid to reflux in 5N HCl with reaction times varying from 4 to 24 hours. The product is then precipitated out with aqueous ammonia solution in an ice bath. While there is the extensive literature suggesting that this procedure works for a variety phenylenediamine analogues, all attempts to form the nitrobenzyl benzimidazole derivative **(7)** proved unsuccessful. Numerous efforts were made, with variations in reaction times and the molarity of the HCl solution. However, after several attempts it became apparent from the ^{1}H NMR spectrum that a mixture of products was isolated on each occasion. The mass spectral (electrospray) data showed a peak at m/z = 302, corresponding to the desired product **(7)**, and another peak at 282. It is proposed that the work up itself was causing the problem rather than the reaction. In the work up, aqueous ammonia solution was partially displacing the chloride causing the formation of 1-(4-nitrobenzyl)-2-aminomethyl benzimidazole (peak of 282). The reaction was repeated using sodium hydroxide solution, and instead of the amine displacing the chloride, this time a mixture of the chloromethyl and the hydroxymethyl benzimidazole was formed. The mass spectrometry data again showed that the desired compound had been formed, with a peak at m/z = 302 corresponding to product **(7)** but there was also a peak at m/z = 283 representing the hydroxyl product. The literature does suggest that the work up needs to be kept below 15°C, and the reaction was

performed cold by placing the vessel in an ice bath. In practice, however, it was difficult to maintain the reduced temperature in solution as the work up involves the neutralisation of the acid, therefore a lot of heat was generated and this might have led to the formation of the by product. To avoid the problems encounted in the work up, an alterative route was investigated that involved using glycolic acid instead of chloroacetic acid. Thionyl chloride could then be used to convert the hydroxymethyl group to the chloromethyl equivalent. A number of research groups have used this type of route to produce chloro derivatives, possibly due to the same issue that was encountered in this work.[139]

The method used to form 1-(4-nitrobenzyl)-2-hydroxymethyl benzimidazole **(6)** is virtually the same as that used in the attempted preparation of **(7)**, however in this case glycolic acid was used and slightly longer reaction times were required, resulting in a yield of 77%. The ^{1}H NMR spectrum clearly shows the CH_2OH singlet peak at 4.83 ppm, and the CH_2 benzyl peak located at 5.69 ppm. The aromatic CH peaks are in the range of 7.29 to 8.1 ppm, but not all individual peaks are distinguishable due to overlap forming a large multiplet at 7.29 ppm with an integration of 5 [(the other two peaks are at 7.6 ppm (doublet with an integration of 1) and 8.1 ppm (double triplet, integration of 2)]. The ^{13}C NMR spectrum contains 13 carbons, with the peaks at 46.9 ppm and 57.0 ppm corresponding to the two CH_2 peaks.

The hydroxyl group was then readily converted to the chloride to give 1-(4-nitrobenzyl)-2-chloromethyl benzimidazole **(7)** by stirring **(6)** with thionyl chloride for 24 hours. The resulting cream solid was isolated in a yield of 68%. There is a clear difference in the ^{1}H NMR spectrum of **(7)** compared to **(6)** with the shift of the CH_2 peak from 4.83 ppm to 6.32 ppm, because the hydroxide has been displaced by a chloride causing an increase in the electron withdrawing character and resulting in the CH_2 shifting down field. The ^{13}C NMR spectrum shows a shift in the CH_2 peak to 32.9 ppm. The X-ray crystal structure has also been obtained. An ORTEP plot of the structure of 1-(4-nitrobenzylmethyl)-2-chloromethyl benzimidazolium chloride **(7)**.HCl is shown in figure 65.

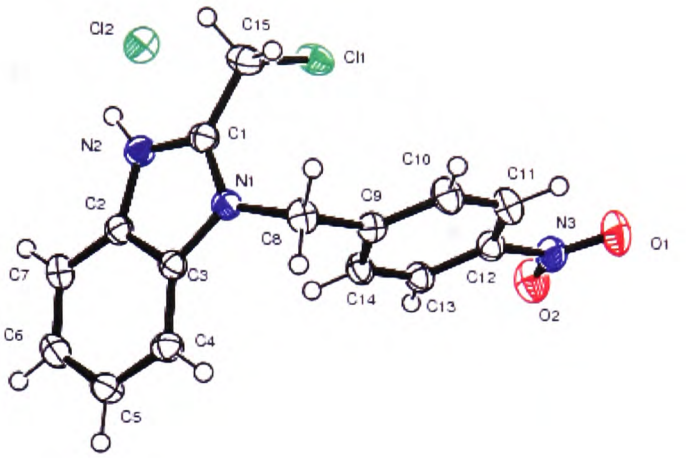

Figure 65 The molecular structure of 1-(4-nitrobenzylmethyl)-2-chloromethyl benzimidazolium chloride **(7)**.HCl, showing the atom labelling and 50% probability ellipsoids for non-H atoms.

In the crystal structure of 1-(4-nitrobenzylmethyl)-2-chloromethyl benzimidazolium chloride **(7)**.HCl, there are no hydrogen-bonded dimers as were observed in the phenylenediamine structure **(7)**.HCl. As shown in table 7, the bond lengths are very similar to those observed in the phenylenediamine structure, with some slight variation in bond angles due to the formation of the benzimidazole unit.

Bond length (Å)		**Bond and torsion angle (°)**	
C(1) – N(1)	1.345 (3)	N(2) – C(1) – N(1)	109.8 (2)
C(1) – N(2)	1.328 (4)	N(2) – C(1) – N(15)	123.3 (3)
C(2) – N(2)	1.384 (3)	N(1) – C(1) – C(15)	126.8 (3)
C(3) – N(1)	1.390 (3)	C(1) – C(15) – Cl(1)	110.15 (18)
C(1) – C(15)	1.481 (4)	N(1)-C(3)-C(2)	106.3 (2)
C(15) – Cl(1)	1.801 (3)	N(1)-C(3)-C(4)	132.6 (2)

Table 7 Selective bond length and bond and torsion angle for 1-(4-nitrobenzylmethyl)-2-chloromethyl benzimidazolium chloride **(7)**.HCl

A view of the crystal packing is shown in figure 66, in this case no π-stacking or edge to face phenyl interactions are observed.

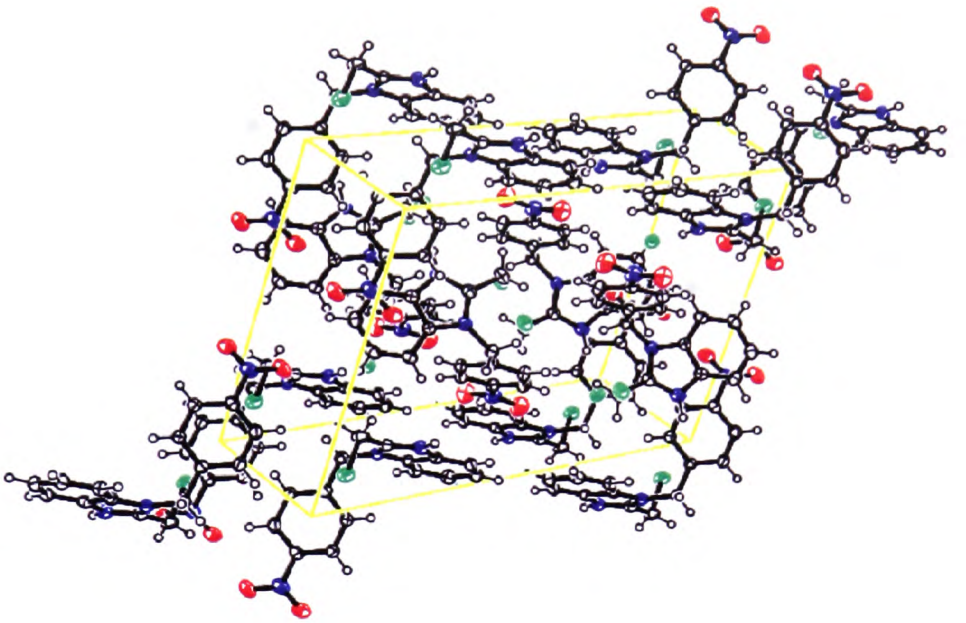

Figure 66 The crystal packing view along the *b* axis for 1-(4-nitrobenzylmethyl)-2-chloromethyl benzimidazolium chloride (**7**).HCl

2.5.4 The attempted preparation of 1-(4-nitrobenzyl)-2-iodomethyl benzimidazole (8)

A number of research groups have shown that a chloroalkyl group can be readily converted to an iodoalkyl group. The reason for converting the chloro to an iodo, is that it will be a better leaving group. This should make **(8)** more effective at undergoing nucleophilic substitution reactions with DO3A compared to **(7)**. The reaction conditions reported by Charmant *et al.* were used.[141] The chloro derivative was added to a solution of sodium iodide in acetone and heated at reflux for 6 hours. The reaction mixture was then cooled to room temperature and washed with water, after which the organic layer was collected and the solvent removed. The reaction scheme is shown in figure 67.

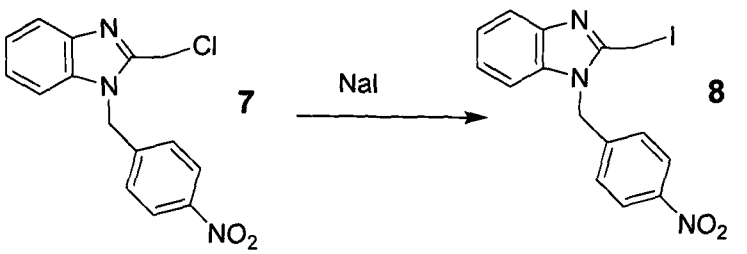

Figure 67 Attempted synthesis of 1-(4-nitrobenzyl)-2-iodomethyl benzimidazole **(8)**

The product **(8)** was not isolated as a single species using this procedure according to analysis of the ^{1}H NMR spectrum, which suggested a mixture of compounds had formed. As the iodide ion is such a good leaving group, the reaction shown in figure 67 could be reversible, thus giving a mixture of **(7)** and **(8)**. Therefore, no further efforts were made to isolate **(8)**.

2.5.5 The synthesis of 1-(4-nitrobenzyl)-2-methylpyridine benzimidazolium chloride (9)

The potential of **(7)** to undergo a nucleophilic substitution reaction with an amine was investigated by reaction with pyridine. The nitrogen atom in the pyridine is planar and trigonal with the lone pair in the plane of the ring. This is nucleophilic because the lone pair of electrons cannot be delocalized around the ring. However, pyridine is less nucleophilic then the secondary amine position on DO3A, therefore if the reaction with pyridine was successful, the reaction between **(7)** and DO3A **(31)** should occur. A modified version of the procedure reported by Iemura *et al.* was used, where **(7)** was dissolved in pyridine and heated at reflux for 30 min.[142] The solvent was removed under reduced pressure, and the resulting cream solid was recrystallised from methanol to give 1-(4-nitrobenzyl)-2-methylpyridine benzimidazolium chloride **(9)** as a white solid in 52% yield. The reaction scheme is shown in figure 68.

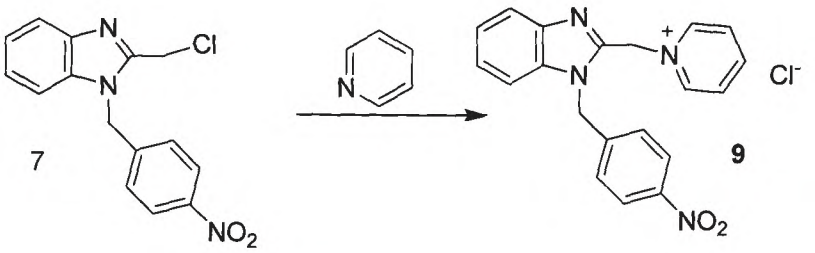

Figure 68 Synthesis of 1-(4-nitrobenzyl)-2-methylpyridine benzimidazolium chloride **(9)**

The ^{1}H NMR spectrum showed two singlets at 6.14 and 6.97 ppm (each having an integration value of 2) that represent the two CH_2 groups. In the aromatic region there are 5 peaks from 7.3 – 9.67 ppm and with a total integration of 13 protons. The ^{13}C NMR spectrum shows 13 peaks, with those at 46.83 and 56.03 ppm assigned to represent the CH_2 peaks, and the other 11 peaks in the region of 110.33 – 146.65 ppm representing the CH and C peaks. The electrospray mass spectrometry data shows the molecular ion peak, and the X-ray crystal structure was also obtained. An ORTEP plot of the structure of 1-(4-nitrobenzyl)-2-methylpyridine benzimidazole is shown in figure 69.

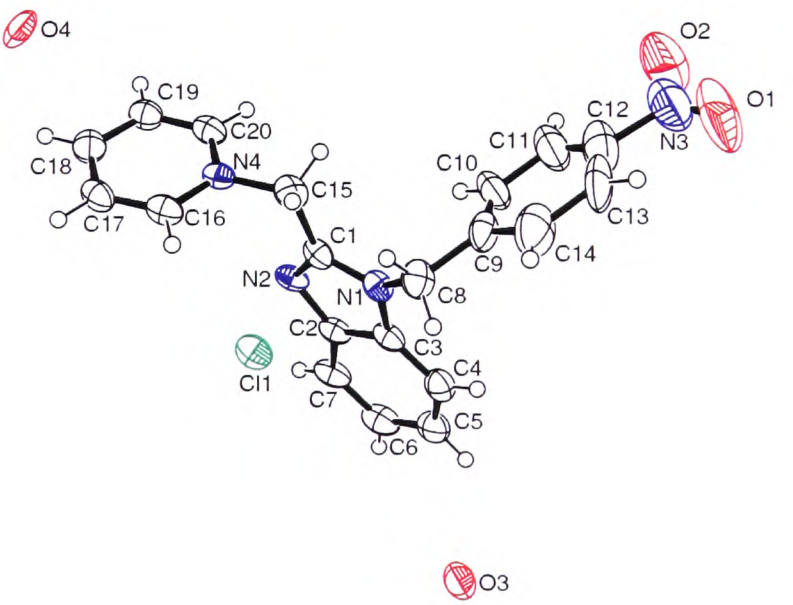

Figure 69 The molecular structure of 1-(4-nitrobenzyl)-2-methylpyridine benzimidazolium chloride, showing the atom labelling and 50% probability ellipsoids for non-H atoms.

The crystal structure of 1-(4-nitrobenzyl)-2-methylpyridine benzimidazolium chloride shows no clear π-stacking or edge to face phenyl interactions, similar to the crystal structure for **(7)**.HCl. The bond lengths in the two structures are similar, however, there is variation in some bond angles. N2-C1-N1 is 109.8° for **(7)**.HCl and 114.1° for **(9)**, and N2-C1-C15 is 123.3° for **(7)**.HCl and 125.4 for **(9)**. An even larger difference can be seen for the angle N1-C1-C15 as this decreases from 126.8 for **(7)**.HCl to 120.4° for **(9)**. These differences may be due to the steric bulk of the pyridyl group.

Bond length Å		**Bond and torsion angle °**	
C(1) – N(1)	1.366(5)	N(2) – C(1) – N(1)	114.1(3)
C(1) – N(2)	1.306(4)	N(2) – C(1) – N(15)	125.4(4)
C(2) – N(2)	1.388(5)	N(1) – C(1) – C(15)	120.4(3)
C(3) – N(1)	1.388(5)	C(1) – C(15) – N(4)	111.5(3)
C(1) – C(15)	1.486(5)	N(1)-C(3)-C(2)	110.4(3)
C(15) – N(4)	1.472(6)	N(1)-C(3)-C(4)	130.9(4)

Table 8 Selected bond lengths and bond and torsion angles for 1-(4-nitrobenzyl)-2-methylpyridine benzimidazolium chloride

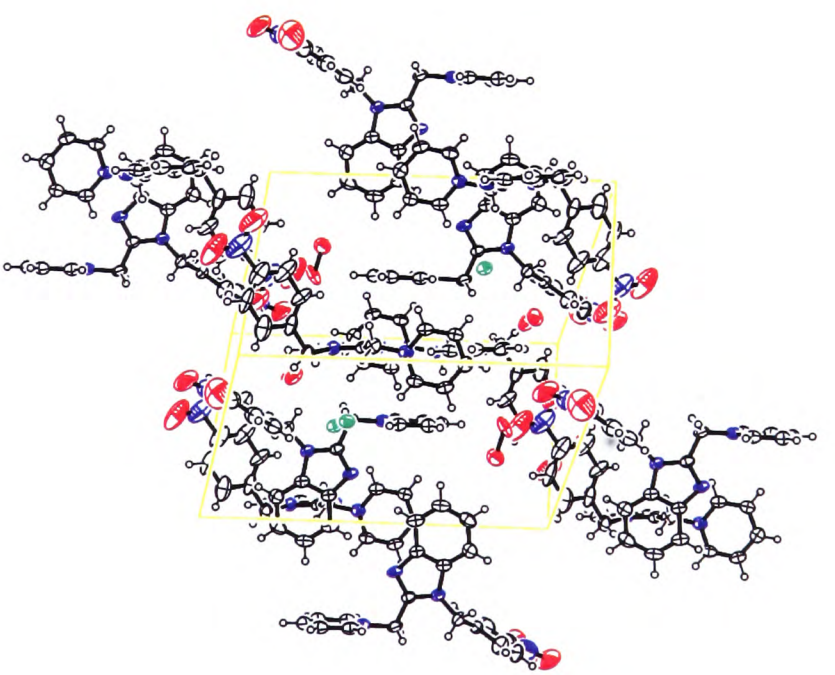

Figure 70 Packing diagram for the crystal structure of 1-(4-nitrobenzyl)-2-methylpyridine benzimidazolium chloride

This section detailed the preparation and characterisation of benzimidazole derivatives using method 1. This route was successfully used to prepare the desired compound 1-(4-nitrobenzyl)-2-chloromethyl benzimidazole (**7**). The next section (2.6) contains a discussion of the attempted synthesis of benzimidazole derivatives using method 2.

2.6 Synthesis of benzimidazole derivatives – method 2

The previous sections (2.4-2.5) described the synthesis of benzimidazole precursors by initial functionalisation of the 1,2-phenylenediamine followed by a cyclisation reaction to form the benzimidazole molecule (method 1). This section contains a discussion of an alternative method to form benzimidazole molecules (method 2). This will initially use a cyclisation reaction to form the benzimidazole compound, for example, a condensation reaction between 1,2-phenylenediamine and an acetic acid derivative (chloroacetic acid), followed by substitution, (e.g. with nitrobenzyl bromide), at the benzimidazole amine.

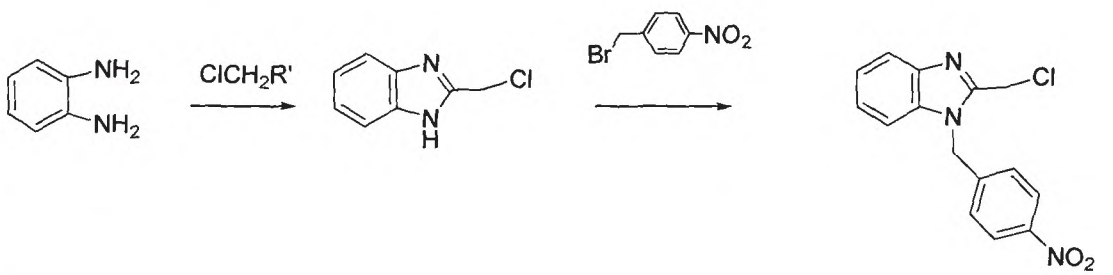

Figure 71 Proposed synthetic strategy to produce novel benzimidazole precursors using method 2 (where R' = $CNHOCH_3$, or COOH)

2.6.1 Synthetic methods used to produce benzimidazole derivatives using method 2

A number of research groups have investigated the substitution of groups directly onto the N1 position on the benzimidazole (method 2). Raban *et al.* have attached a 2,4-dinitrobenzenesulfenyl chloride onto the benzimidazole unit in about 95% yields (figure 72).[122] An alternative method is reported by Li *et al.* where they have reacted methyl iodide with benzimidazole in the presence of potassium carbonate using DMF as solvent, giving the product in yields greater than 70% (figure 72).[143]

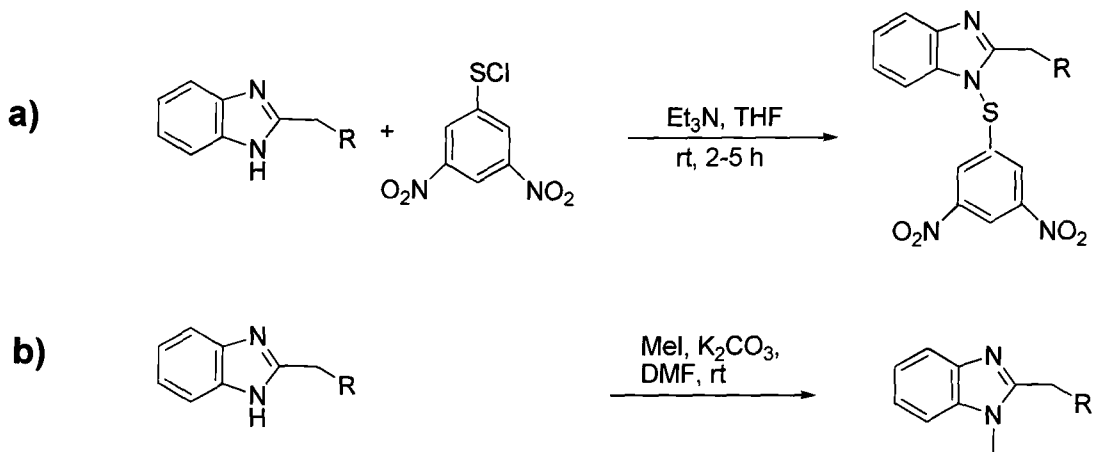

Figure 72 Direct functionalisation of the the benzimidazole nitrogen: Raban *et al.* (a), Li *et al.* (b) [122, 143]

Wang *et al.* have attached a methyl group to the N1-position as part of a route to alkylate both of the nitrogen positions, the N-3 position was subsequently reacted with ethyl 6-(trifluoromethylsulfonyloxy)hexanoate in 87% yield (figure 73).[144]

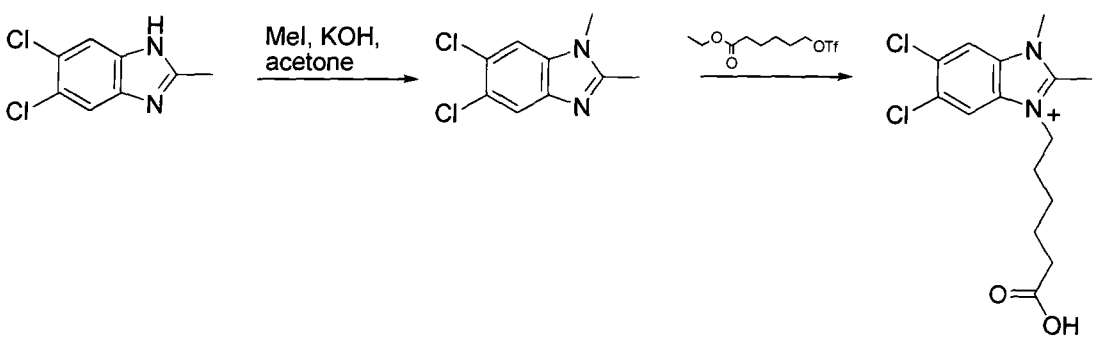

Figure 73 Functionalisation of the the benzimidazole nitrogen at both the N1 and N3 position

A related approach has been employed by Li *et al.* where 1,2-phenylenediamine and 3-phthalimidopropionic acid were suspended in polyphosphoric acid to form 2-[2-(1H-benzoimidazol-2-yl)-ethyl]-isoindole-1,3-dione, which could then be reacted with a variety of reagents allowing substitution to occur at the N-1 position on the benzimidazole.[145] Using this methodology, this group has shown that a number of novel benzimidazole compounds can be synthesised. For example, 4-methylbenzoyl chloride, 4-methylbenzyl chloride and *p*-

toluenesulfonyl chloride (tosyl chloride) were reacted to form benzimidazole derivatives using dry dichloromethane as solvent, and 4-(dimethyl-amino)pyridine (DMAP) as a base, see figure 74.

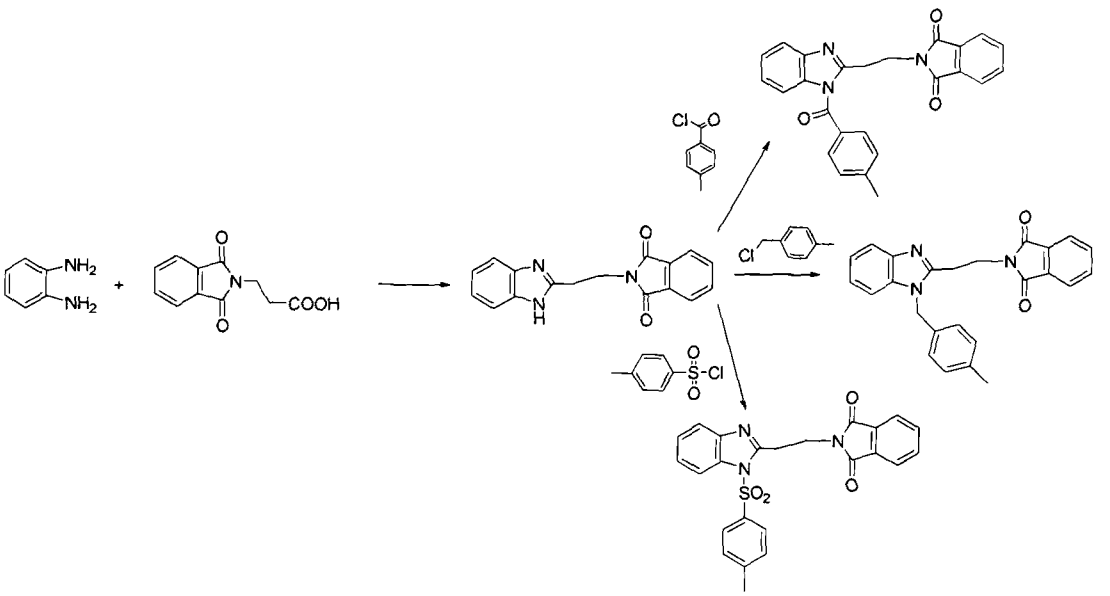

Figure 74 Reaction scheme showing the synthetic routes investigated by Li *et al.*[145]

The wealth of reactions show that this route is well characterised and potentially could be used to produce the target benzimidazole derivative for this work. This section includes the discussion of the synthetic procedures used in the synthesis of 2-chloromethyl benzimidazole and the attempts to attach a 4-nitrobenzyl group onto the N1-position.

2.6.2 Synthesis of 2-chloromethyl benzimidazole (10)

The synthesis of 1-(4-nitrobenzyl)-2-chloromethyl benzimidazole **(7)** involves the initial preparation of 2-chloromethyl benzimidazole **(10)**, using either chloroacetic acid, or methyl chloroacetimidate hydrochloride (figure 75).[132] This intermediate can then be treated with the nitrobenzyl bromide in the presence of base.[146]

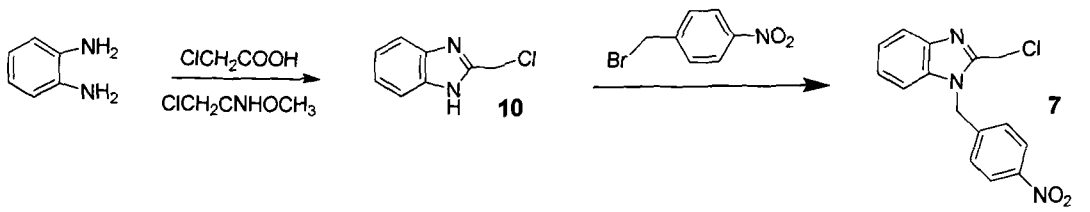

Figure 75 The attempted synthesis of 1-(4-nitrobenzyl)-2-chloromethyl benzimidazole **(7)** using method 2

The synthesis of **(10)** was initially attempted by using a modified version of the procedure employed by Bloom *et al.*, where 1,2-phenylenediamine and chloroacetic acid were suspended in 5 N hydrochloric acid, and heated at reflux for 18 hours.[138] The solution was cooled to 0°C using a salt ice bath and the pH adjusted with ammonium hydroxide solution to cause formation of a precipitate that was collected by filtration. As with previous attempts to synthesise **(7)** using method 1, this reaction failed to yield any pure product. The ^{1}H NMR spectrum appeared to show a mixture of products had been formed, which is likely to be a combination of **(10)** and 2-aminomethyl benzimidazole (due to the basic work up). Attempts were also made to exploit the orthoester route using methyl chloroacetimidate hydrochloride.[137] The procedure was the same as was used in the attempted synthesis of **(3)**, where methyl chloroacetimidate hydrochloride is formed *in situ*, and then allowed to stir for 24 hours with 1,2-phenylenediamine under an atmosphere of nitrogen. Again, this route did not produce the desired compound, as was shown by analysis of the ^{1}H NMR spectrum. This was unexpected as 2-chloromethyl benzimidazole **(10)** can be purchased from Aldrich and should be relatively easy to produce.

2.6.3 Synthesis of 2-chloromethyl benzimidazole derivatives (7)

Numerous attempts were made to synthesise **(7)** from purchased **(10)** by substituting 4-nitrobenzyl bromide onto the N1-position. Initial efforts involved the use of triethylamine (TEA) as the base, and varying the reaction conditions, with 4-nitrobenzylbromide dissolved in dichloromethane and added dropwise to a solution of 2-chloromethyl benzimidazole in dichloromethane with a drop of

TEA. This mixture was allowed to stir for 24 hours at room temperature. The solvent was then removed, which resulted in the formation of a brown solid. Analysis showed that the desired product had not been formed using this procedure. This was believed to be the result of using conditions that were not sufficiently forcing to cause the formation of the desired compound and therefore the procedure was repeated.

On this occasion, the reaction mixture was heated at reflux for 3 hours after being stirred for 24 hours, and the solvent was changed to tetrahydrofuran, since this is more polar and should favour the substitution reaction. A similar method has been used by Raban *et al.* (figure 72), where 2,4-dinitrobenzenesulfenyl chloride was treated with 1,2-phenylenediamine in the presence of TEA and tetrahydrofuran to form *N*-[(2,4-dinitrophenyl)thiol]-2-chloromethyl)-5(6)-chlorobenzimidazole with a crude yield of 96%.[122] In an analogous manner, 2-chloromethyl benzimidazole and 4-nitrobenzylbromide were mixed in tetrahydrofuran with a drop of TEA and reaction mixture was stirred at room temperature for 24 hours, followed by heating at reflux for 3 hours. The solvent was removed and purification attempted by flash chromatography (dichloromethane with an increasing gradient of methanol from 0% to 10%). Chromatography proved unsuccessful in isolating the desired compound, possibly because once again the resulting solid was a mixture of materials that had similar r.f. values. One explanation for the difficulties in forming the desired compound is that the TEA might be reacting with the starting material *i.e.* at the methyl chloride position, and preventing the reaction from going to completion. 2-Chloromethyl benzimidazole is not very soluble in tetrahydrofuran, and while the TEA increased the solubility it may also have caused formation of by products.

Therefore, an alternative option involved using an even higher polarity solvent such as dimethylformamide that will fully dissolve the 2-chloromethyl benzimidazole, and changing the base to potassium carbonate, which will remove the possibility of an amine base reacting with the chloromethyl group. Thomas *et al.* have used a related procedure to form methyl 4'-[(butyl-1*H*-benzimidazol-1-yl)methyl]biphenyl-2-carboxylate.[147] This procedure involved

reacting 2-butylbenzimidazole with a slight excess of methyl 4-(bromomethyl)biphenyl-2-carboxylate and potassium carbonate in dimethylformamide with heating at 100°C. Dichloromethane was then added, and the insoluble material removed, resulting in 45% yields after further purification by flash chromatography. The modified procedure used herein involved reacting 2-chloromethyl benzimidazole, 4-nitrobenzylbromide (in a slight excess) and potassium carbonate dissolved in dimethylformamide while heating to reflux for 3 hours.[147] Upon addition of dichloromethane, a precipitate resulted which was then removed by filtration, and the filtrate was evaporated to dryness to give a solid. Analysis by ^{1}H NMR spectroscopy suggested that the desired compound had not been synthesised in a pure form and a mixture of products had been isolated.

Alternative strategies were then considered, Yu *et al.* have managed to attach a number of alkyl groups to the N-1 position on 2-hydroxymethyl benzimidazole by using sodium hydride as base with dimethylformamide as the solvent.[148] A modified version of this procedure was attempted. Sodium hydride was added in small portions to a solution of 4-nitrobenzylbromide and 2-chloromethyl benzimidazole in dimethylformamide over a period of 30 minutes. The reaction was allowed to stir for 1 week at room temperature and the progress of the reaction monitored by t.l.c. After a week stirring, no compound was separated on the t.l.c. plate that might correspond to possible product formation and so the reaction was heated at reflux for 3 hours. The elevated temperature resulted in the formation of a number of new compounds that were observed by t.l.c. The resultant solid did not appear to consist of the desired compound **(7)** based on ^{1}H NMR spectrscopy. It appears that leaving the reagents to stir at room temperature is not sufficient to cause a reaction, however heating to reflux causes the formation of multiple products. The reaction was repeated, varying the conditions, using potassium carbonate as the base (a less powerful base), and acetone as the solvent (a less polar solvent). 4-Nitrobenzylbromide and 2-chloromethyl benzimidazole were reacted under these conditions with heating at reflux for 24 hours. Following the removal of the solvent, the ^{1}H NMR spectrum again showed that a mixture of products had formed with no identifiable peaks that could be assigned to the desired compound **(7)**.

Further investigations were conducted, this time employing lithium diisopropylamide, (LDA), as the base, since it will react at low temperatures and should readily deprotonate the amine on the benzimidazole to allow for the reaction with the 4-nitrobenzylbromide. The first attempt involved using 2-chloromethyl benzimidazole dissolved in dry tetrahydrofuran with the reaction mixture cooled to −30°C under in an inert atmosphere. While **(10)** does not dissolve fully in tetrahydrofuran, the product does, so it was anticipated that if the reaction occurred, the product could easily be separated from the starting material and other reagents at the work up stage. LDA was then added dropwise over 5 minutes, and the reaction mixture allowed to stir at −30°C for 15 minutes, during which time the solution became clear. After 15 minutes, 4-nitrobenzylbromide was added dropwise in dry tetrahydrofuran, and the reaction mixture was allowed to warm to room temperature and stirred over night under a nitrogen atmosphere, which led to formation of some precipitate. Following the removal of the solvent, the ^{1}H NMR spectrum indicated that the reaction had not gone to completion, with a mixture of starting material and product being obtained, probably due to the lack of solubility of **(10)** in tetrahydrofuran. Attempts to purify the material by re-crystallisation, or washing with tetrahydrofuran proved to be unsuccessful. The reaction was repeated, using the same conditions as before, except this time LDA was stirred with 2-chloromethyl benzimidazole for 2 hours instead of 15 minutes to allow abstraction of the proton on the amine. Further analysis showed that a mixture of products was present that could not be identified or purified.

The aim of this approach was to provide a more reactive alkyl halide (4-nitrobenzylbromide) compared to the chloromethyl group on the benzimidazole and hence in the presence of base the reaction at N1 would occur with the nitrobenzyl reagent rather than this 'self reaction' to give a polymeric compound. However, it is likely that the 'self reaction' did occur when stirring with LDA for 2 hours. The other problems with this synthetic strategy appeared to be the low solubility of the benzimidazole starting material, leading to incomplete reaction, and the fact that the N1 nitrogen position was not as reactive as expected. The choice of solvent seemed to be very important to the reaction with polar solvents such as pyridine and dimethylformamide preferred

due to improved solubility, however, the starting material is partially soluble in less polar solvents such as tetrahydrofuran and dichloromethane in the presence of TEA. It is likely that deprotonation of the starting material was increasing the solubility. The reaction to form the desired product produces acid, which, if insufficient base was present, could have reprotonated unreacted starting material causing it to precipitate and preventing the reaction from going to completion. A further by-product that could have formed is the bis-alkylated compound where the N2 position on the imidazole ring is quaternised resulting in a mixture of starting material and mono and di-substituted products. Wang *et al.* have observed such reactions, see figure 73.[144]

As discussed already it is possible that reaction could occur between two molecules of starting material (alkyl chloride reacting at the N1 position). One way to prevent this would be to use an alternate starting material in the substitution reaction with nitrobenzyl bromide, such as 2-hydroxymethyl benzimidazole. Attempting this reaction would clarify the role of the 'self reaction' in the unsuccessful synthesis. The resulting compound could be converted to **(7)** by treatment with thionyl chloride. However, as method 1 was used successfully to produce the desired benzimidazole compound 1-(4-nitrobenzyl)-2-chloromethyl benzimidazole **(7)**, method 2 was not investigated further.

2.7 Conclusions

Two methods were investigated to synthesise 1-(4-nitrobenzyl)-2-chloromethyl benzimidazole **(7)**. While issues were encountered with both methods, the formation of the *N*-alkylated benzimidazoles was more successful using the cyclisation of alykylated diaminobenzene (method 1) rather than alkylation of the pre-formed benzimidazole (method 2). Method 1 was used to successfully produce the target compound **(7)**. It proved to be much more challenging to get method 2 to proceed cleanly and isolation of a single product was not achieved.

Initial attempts to synthesise 1-(4-aminobenzyl)-2-chloromethyl benzimidazole **(3)** using method 1, were carried out using an amidobenzyl group which can subsequently be converted to the amine compound by acid hydrolysis. The precursor 1-(4-amidobenzyl)phenylenediamine **(2)** was accessible from the Schiff's base condensation reaction between 1,2-phenylenediamine and 4-acetamido benzaldehyde to form **(1)**, followed by the reduction of the imine to the amine to give **(2)**. However, difficulties then arose in finding a suitable method to convert it to the benzimidazole derivative **(3)**. The use of methyl chloroacetimidate hydrochloride resulted in unwanted by products, possibly due to the hydrolysis of the starting material. Efforts were then focused on the synthesis of 1-(4-nitrobenzyl)-2-chloromethyl benzimidazole **(7)**. The precursor compound 1-(4-nitrobenzyl)phenylenediamine **(5)** can be synthesised using a related procedure by reacting 1,2-phenylenediamine and 4-nitrobenzylaldehyde, followed by reduction of the imine to the amine using sodium borohydride. However an improved synthesis was investigated and optimised, reacting 1,2-phenylenediamine and 4-nitrobenzylbromide to give the formation of **(5)** in a single step.

The cyclisation reaction to form benzimidazole compound **(7)** was initially attempted by treatment of **(10)** with chloroacetic acid in 5 N hydrochloric acid, but this led to a mixture of by-products due to partial displacement of the chloro group with either an amino or hydroxo group in the work up. Therefore, an alternative route to synthesise this compound from 1-(4-nitrobenzyl)-2-

hydroxymethyl benzimidazole **(6)** was investigated **(6)** was synthesised by the treatment of **(5)** with glycolic acid in 5 N hydrochloric acid solution, followed by the conversion of the hydroxide to the chloride by reaction with thionyl chloride. Overall, the characterisation of an efficient route to produce, 1-(4-nitrobenzyl)-2-chloromethyl benzimidazole **(7)** with full characterisation was achieved. This compound is a key precursor in the synthesis of dual functionalised benzimidazole containing chelators.

3. Synthesis of optical dyes

3.1 Introduction

There are many examples of organic optical dyes that are frequently used to study biological function. Examples of some widely used fluorescent dyes include ethidium bromide, Alexa Fluor dyes, and fluorescein. The structures of these compounds are given in figure 76.

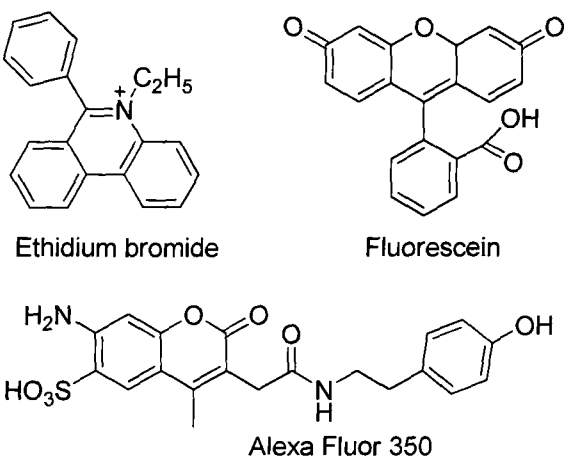

Figure 76 Structures of widely used fluorescent dyes

Such dyes function by undergoing a process of fluorescence, where the molecule becomes excited to a higher energy state (excited state) via the absorption of light *i.e.* excitation. The molecule undergoes a decay process back to the lowest energy excited state. This is followed by the return of the optical dye to the ground state and results in the emission of light, as shown in figure 77.

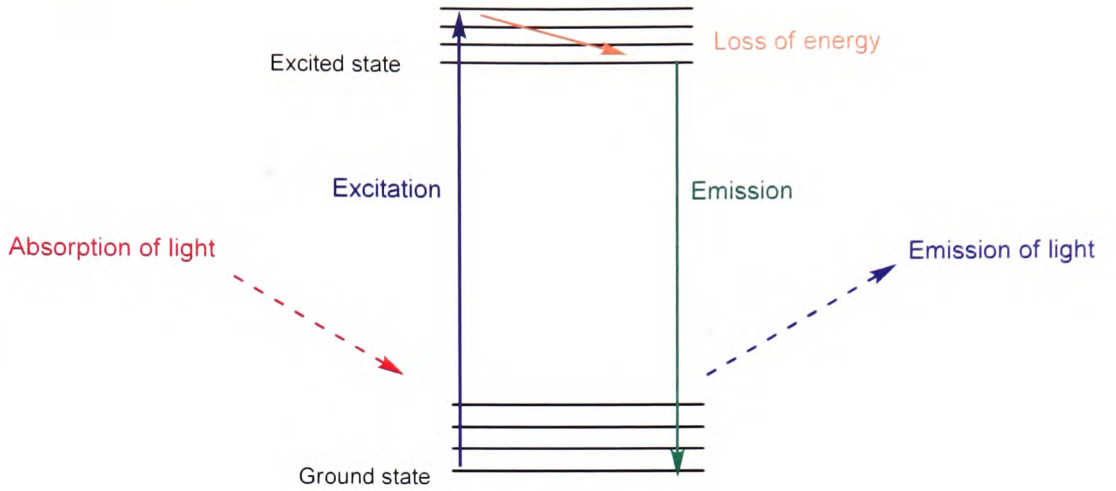

Figure 77 The process of fluorescence for an optical dye

The emitted light is of lower energy and of longer wavelength than the absorbed light, hence the colour of the light that is emitted can be different from the colour of the light that has been absorbed. Optical dyes can undergo this process repeatedly, and are commonly used in the study of biological function. However, they are susceptible to photobleaching where a high intensity illumination can cause structural instabilities and may lead to degradation of the molecule over time.[69]

Common dyes used for this application include those based on rhodamine and boron dipyrromethenes (BODIPY). They can both be used to obtain optical images of biological systems, as they are known to be taken up into cells and are relatively non- cytotoxic. Rhodamine based agents are hydrophobic cationic dyes that can penetrate cell membranes. In particular, dyes of this type have been shown to target functional mitochondria. Rhodamine dyes are attracted to the mitochondria as they have a negative membrane potential and can be used to study mitochondrial function *i.e.* their role in the apoptotic cascade. When the membrane potential is lost (a result of apoptosis), the dye is no longer localised and this change can be observed using confocal microscopy.[149, 150, 151] Structurally, BODIPY dyes are based on the complexation of dipyrrins with boron. They have high fluorescence quantum yields, with tunable emission

maxima wavelengths and have good photochemical stability which has resulted in their uses for biological staining, see figure 78 for general structures.[152]

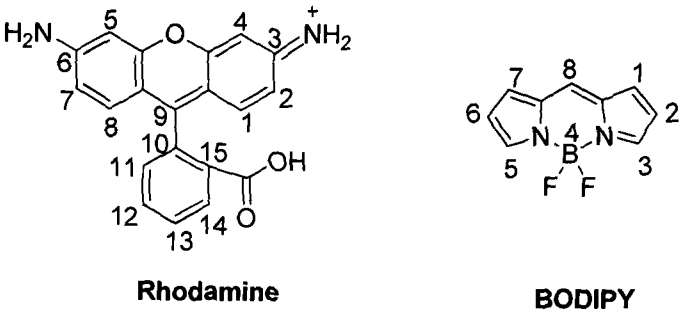

Figure 78 The general structures of rhodamine (left), and BODIPY (right) based dyes

The aim of this work is to attach such dyes to a DO3A chelator derivative. This is motivated by the fact that they could aid the ability of the contrast agent to enter the cell, due to the intrinsic properties of the rhodamine and BODIPY dyes.[153 154] As well as their cellular uptake properties, it is hoped that with the gadolinium(III) complexes the resulting dye conjugate would function as a dual modality imaging agent [i.e. detectable by both fluorescence microscopy (optical dye) and MRI contrast properties (paramagnetism of gadolinium(III)]. Alternatively, with a luminescent lanthanide ion, the dye conjugate can potentially act to sensitise the lanthanide metal ion through energy transfer processes. This would be advantageous in optical imaging as lanthanide luminescence is longer lived and allows for gating out of background fluorescence from biological systems.

This chapter contains a discussion of the attempted syntheses to produce rhodamine (sections 3.2-3.4) and BODIPY (sections 3.5-3.8) derivatives that have the potential to be conjugated to the chelators, 1,4,7-tris(carboxymethyl)-10-(4-aminobenzyl)-1,4,7,10-tetraazacyclododecane **(40)** and 1,4,7-tris(carboxymethyl)-10-(1-(4-aminobenzyl)-2-methyl benzimidazole)-1,4,7,10-tetraazacyclododecane **(36)**.

For the rhodamine derivatives, two strategies have been employed. Initially work by Nguyen *et al.* was followed to synthesise a rhodamine B derivative bearing a piperazine ring (this was to prevent the formation of the non-fluorescent lactam derivative) that could then be functionalised with an alkyl

halide.[155] This unit could potentially be directly coupled to the chelator derivatives. The second strategy involved the preparation of a rhodamine derivative bearing an alkyl amine that could either be converted to an isothiocyanate group to facilitate conjugation to an amino bearing chelator, or used without modification for coupling to an isothiocyanate bearing chelator. The target rhodamine molecules are shown in figure 79.

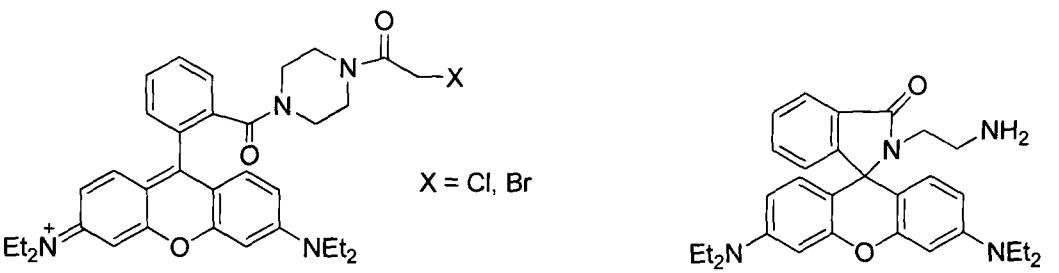

Figure 79 The two target rhodamine derivatives

The synthesis of BODIPY compounds initially involved the formation of a phenyl amine substituted at the 8-position (meso) that could be converted to an isothiocyanate group for conjugation at a later stage. As an alternative route, the addition of an alkyl amine functionality on the phenyl ring at the 8-position was investigated due to possible issues with the reduced nucleophilicity of the aromatic amine in the initial design. The target BODIPY molecules are shown in figure 80.

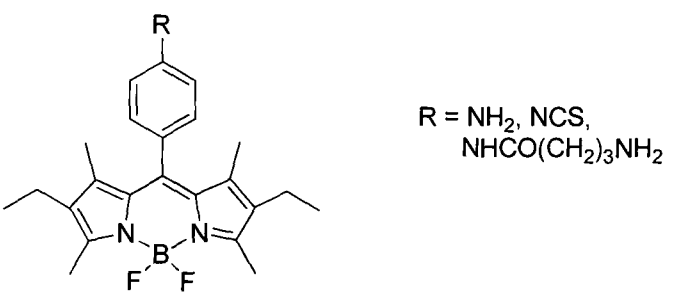

Figure 80 Target molecules for BODIPY derivatives

3.2 Rhodamine optical dyes

The effectiveness of rhodamine as a fluorescent probe to study biological function has encouraged efforts to further functionalise these structures. Currently, purchasing functionalised rhodamine dyes is expensive, for example to purchase rhodamine B isothiocyanate (with the functional group on one of the phenyl ring positions) from Aldrich (2007-2008) will cost £79.20 for 500 mg. When this is compared to the cost of rhodamine B base (£25.40 for 25g), there is a noticeable difference in price and clearly a premium is being charged.

A number of strategies are reported in the literature for synthesising rhodamine derivatives. Methods employed by Minta *et al.* and Lippard and co-workers, involve starting from a xanthone derivative to add functionality at the 12- and 13-positions respectively and a benzophenone derivative to add functionality at the 3-position.[151 156] Here, the functional groups are added by the complete synthesis of a rhodamine derivative from a non-fluorescent precursor, however, this can involve multi step reactions and starting from expensive precursors. Other common approaches utilise a rhodamine compound, such as rhodamine B, and attach other groups on to the carboxylic acid. Therefore, to keep costs down and to allow for synthesis of reasonable amounts of the rhodamine dyes, it was decided to functionalise the rhodamine B base at the carboxylic acid group (figure 81).

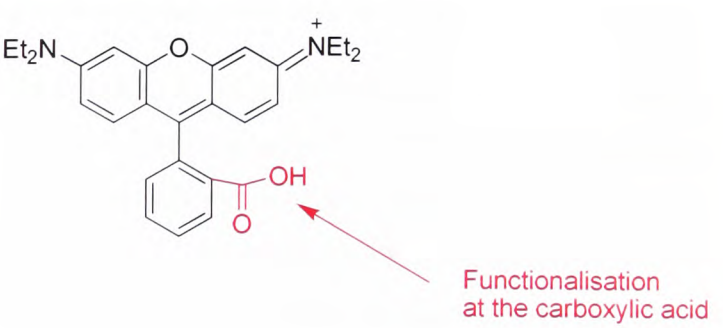

Figure 81 Functionalisation of the rhodamine B base

Analogues of rhodamine have previously been synthesised to act as sensors to measure oxygen concentration, metal ion concentration and temperature. Some examples are described in the following sections along with the synthetic strategies that could be applied to this work.

3.2.1 Rhodamine analogues as oxygen sensors

Ribou and co-workers have reported the synthesis of rhodamine functionalised with a pyrene unit to form (1'-pyrene butyl)-2-rhodamine ester (figure 82).[153] This was prepared by the coupling of 1-pyrenebutanol and rhodamine 110 by a DCC coupling reaction in a 17% yield. This compound was designed to measure oxygen concentrations in the mitochondria of living cells. The oxygen concentrations can be measured by either fluorescence intensity variation or by fluorescence lifetime changes of the pyrene unit, while the rhodamine unit targets the mitochondria.

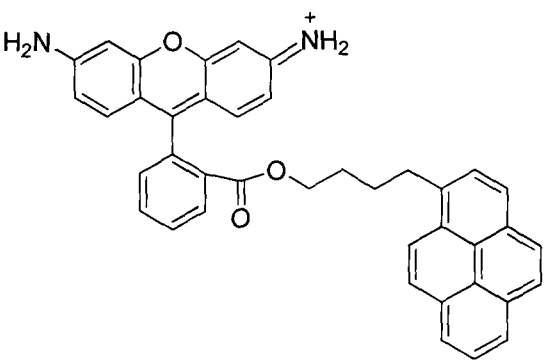

Figure 82 Structure of (1'-pyrene butyl)-2-rhodamine ester

Another example is from the work of Koide *et al.* where they have synthesised a rhodamine derivative bearing either a 4-amino- or 4-hydroxyphenyl ether moiety that can detect highly reactive oxygen species in the mitochondria of living cells (figure 83).[157] Normally this is not fluorescent, but in the presence of reactive oxygen species (peroxide), the phenyl group is cleaved to form a highly fluorescent molecule.

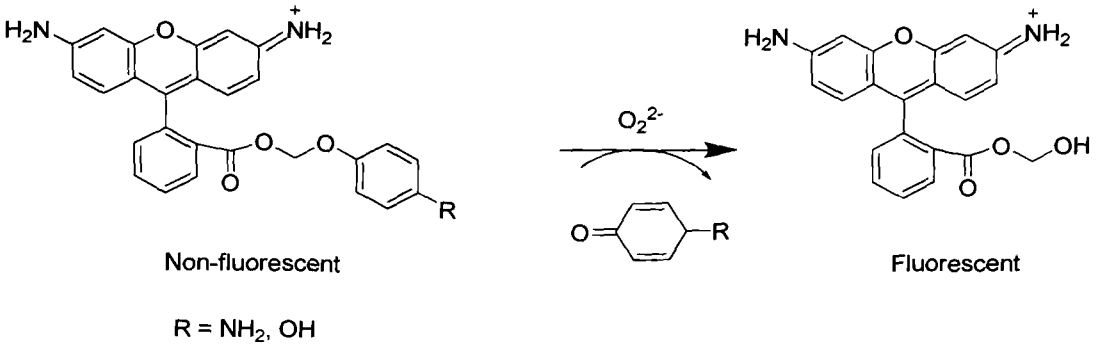

Figure 83 Structure of a reactive oxygen sensor based on rhodamine

3.2.2 Rhodamine analogues as metal ion sensors

Rhodamine derivatives have also been shown to act as sensors for a number of metal ions including iron(III), zinc(II) and mercury(II). Xiang *et al.* have synthesised an iron(III) selective rhodamine derivative based on rhodamine B and diethylenetriamine.[158] The molecule was prepared by the addition of diethylenetriamine to two equivalents of rhodamine 123 to form a lactam derivative that is non-fluorescent. The fluorescence increases in the presence of iron(III) due to the opening of the spirocyclic ring on complexation with iron(III), and the resulting fluorescent complex can then be detected.

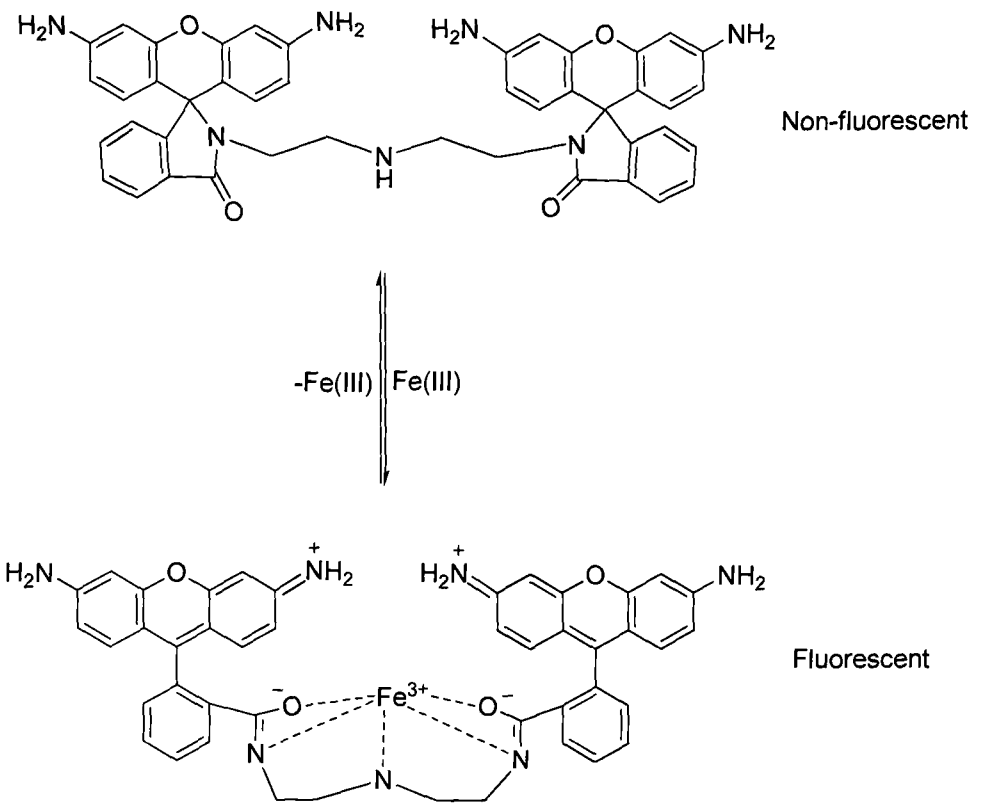

Figure 84 Structure of the iron(III) selective probe synthesised by Xiang *et al.*[158]

Yang *et al.* have reported the synthesis of an optical-electrochemical sensor for mercury(II) based on rhodamine B bearing a ferrocene substituent and an 8-hydroxyquinoline moiety.[159] This compound is synthesised by the coupling of an amine on the ferrocene unit to the carboxylic acid on the rhodamine unit resulting in a lactam derivative that is non-fluorescent. The ferrocenyl group was incorporated to act as a reversible redox-active group, while 8-hydroxyquinoline acts as a coordinating site for the metal ion. Changes in the UV/visible absorption spectrum, fluorescence emission spectrum and electrochemical properties have been observed upon binding with mercury(II), while confocal microscopy has demonstrated the application of this conjugate to monitor mercury(II) levels in living cells.

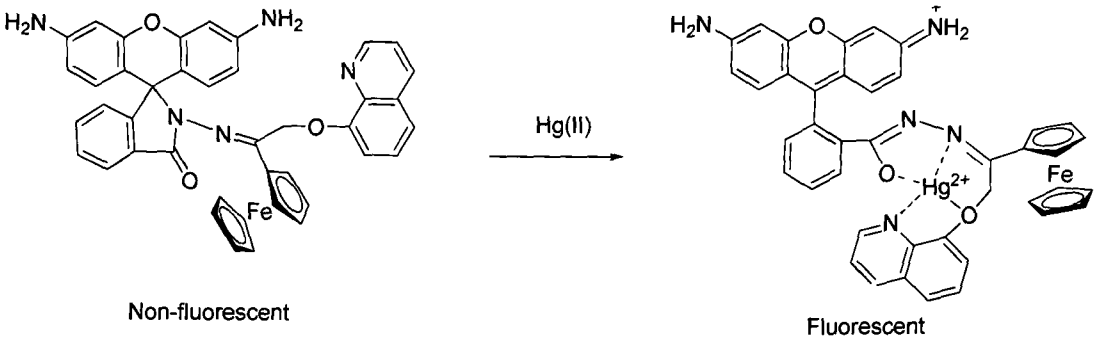

Figure 85 Reaction between a rhodamine B derivative, with a ferrocene unit and 8-hydroxyquinoline, with mercury(II)

3.2.3 Rhodamine analogues as temperature sensors

A polymer based on *N*-isopropylacrylamide and rhodamine that is sensitive to changes in temperature has been prepared (figure 86).[160] The polymer was shown to exhibit a selective emission enhancement in the temperature range of 25 – 33°C in acidic media. This change in optical properties is thought to be caused by polymer aggregation. At temperatures below 25°C, the polymer chain forms a non-fluorescent coil, while an increase in temperature to above 25°C causes the coil to form fluorescent globules of 1 – 200 μm due to polymer aggregation. At temperatures greater than 35°C, the globules become so large (>200 μm) that there is a reduction of fluorescence due to a decrease in the amount of incident light absorbed.

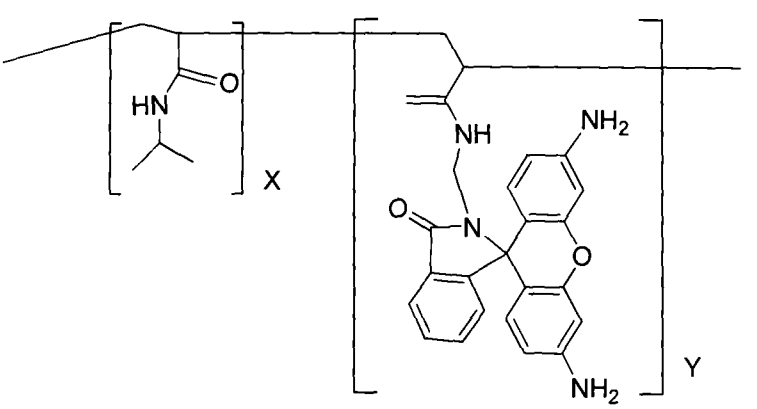

Figure 86 Structure of a temperature sensing polymeric rhodamine derivative

3.3 The attempted synthesis of rhodamine B piperazine amide derivatives

To be able to conjugate these optical dyes to the chelators **(36)** and **(40)** that contain a benzyl amine, the rhodamine molecule needs to have a reactive functional group available. Nguyen *et al.* have reported a practical synthetic route to produce functionalised rhodamine dyes that can be coupled to proteins, providing materials for biomolecule modification.[155] This strategy has been followed here using the routes shown in figure 87.

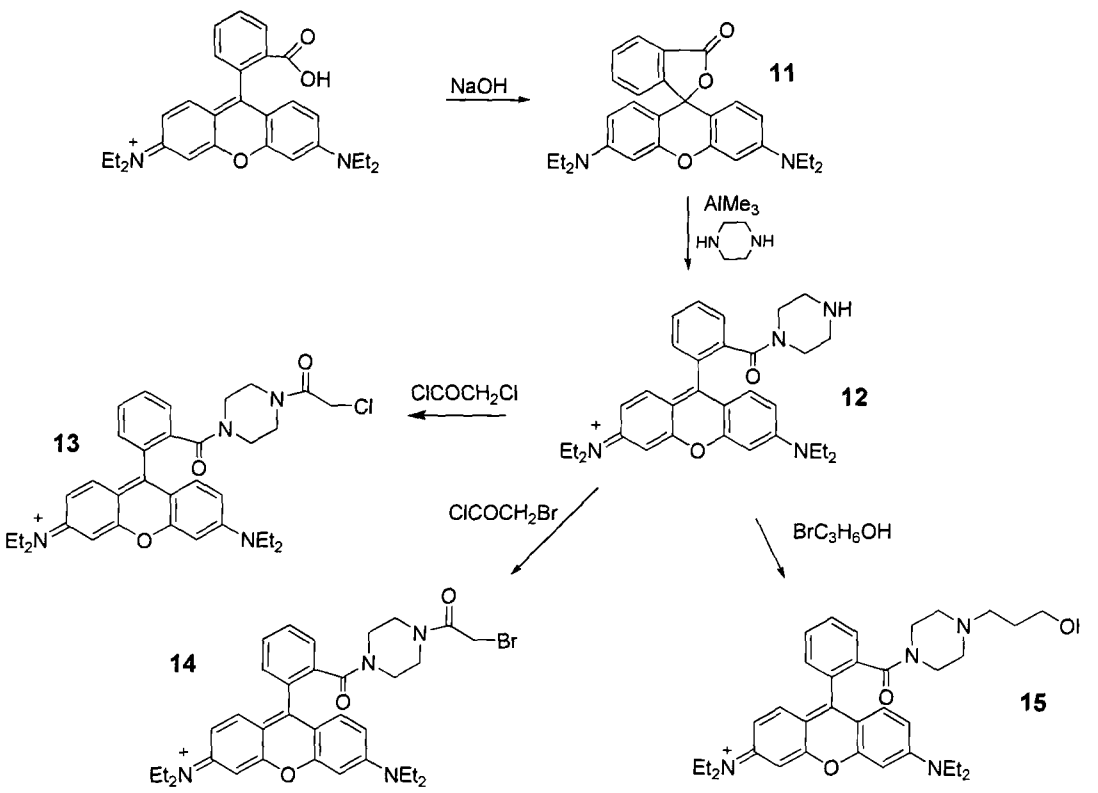

Figure 87 The synthetic scheme used to produce functionalised rhodamine B derivatives

The advantage of this route, apart from the use of the inexpensive rhodamine B starting material, is that the cyclisation to a non-fluorescent species (lactam) is avoided due to the formation of a tertiary amine on addition of the piperazine unit. Generally, functionalising at the carboxylate group to form an amide bond can lead to a rapid cyclization that results in the non-fluorescent lactam (figure 88). The loss of fluorescence means that the rhodamine derivative is no longer useful for biological imaging.

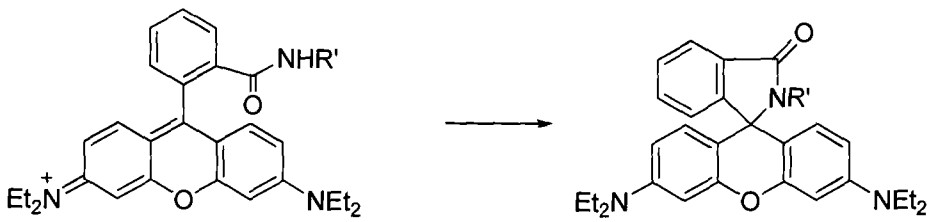

Figure 88 Cyclization of the rhodamine amide (right) to form a lactam (right)

Nguyen *et al.* have reported that the piperazine unit can subsequently be further functionalised at the secondary amine with either an acid chloride or an alkyl halide.[155] This could be coupled onto the secondary amine group on DO3A **(31)** or at the aromatic amine position on **(36)** and **(40)**.

The first step is to convert rhodamine B to the lactam derivative known as rhodamine B base **(11)**. This is readily done by partitioning the compound between aqueous 1M sodium hydroxide solution and ethyl acetate with the organic layer collected. The solvent was then removed from the organic layer to leave a pink foam. The yield achieved was 93%, which was the same as that quoted in the literature method.[155] The synthesis of **(11)** was confirmed by analysis of the ^{1}H NMR spectrum, which corresponded to the published data.

3.3.1. The synthesis of rhodamine B piperazine amide (12)

Rhodamine B piperazine amide **(12)** was synthesised from **(11)**. The first step was the dropwise addition of trimethylaluminium in toluene to a solution of piperazine in dry dichloromethane over 1 hour. A solution of **(11)** in dichloromethane was then added, and the resulting reaction mixture heated at reflux for 24 hours. After allowing the reaction mixture to cool to room temperature, the aluminium reagent was quenched with 0.1 M of hydrochloric acid solution. This was then filtered to remove any solids formed, washed with dichloromethane and methanol, followed by removal of the solvent. The compound was purified by using a simple extraction work up. The de-protonated product **(12)** has a much greater water solubility than **(11)**, and therefore was extracted selectively into the basic aqueous solution when partitioned with ethyl acetate. The aqueous solution was then saturated with

sodium chloride followed by acidification with 1 M hydrochloric acid solution, and **(12)** was extracted from the aqueous layer with propan-2-ol and dichloromethane. The product was isolated as a dark purple solid in 57% yield. From the ^{1}H NMR spectrum, the triplet at 1.32 ppm can be assigned to the CH_3, with the multiplet at 3.69 ppm to the CH_2 on the diethylamine moiety. The key marker is the broad singlet at 3.33 ppm that has an integration of four and can be assigned to the piperazine ring protons. The ^{13}C NMR spectrum contains 17 peaks as expected, and the electrospray mass spectrum has a peak that corresponds to the molecular ion. The literature preparation reports a higher yield than was obtained in this work (70% compared to 57%). This may be due to insufficient extraction in the work up resulting in the loss of product or it is possible that salts could have been retained in the reported procedure that artificially increased their yield.

3.3.2 The synthesis of a rhodamine B piperazine amide derivative containing an alkyl halide

The next step, involves a nucleophilic substitution reaction at the secondary amine position on the piperazine ring to form a functionalised rhodamine B derivative. The literature contains reports of a number of different substitutions, using reagents such as succinic anhydride, chloroacteyl chloride and 3-bromopropanol, see figure 87.[155] In this work, chloroacetyl chloride was initially used. The attempted synthesis of rhodamine B 4-(2-chloroacetyl)piperazine **(13)** was carried out by dissolving **(12)** in dichloromethane and then cooling this solution to 0°C. Chloroacetyl chloride was then added to the reaction mixture, followed by the addition of pyridine (to act as a base). The reaction mixture was warmed to room temperature and then allowed to stir for 4 hours. The literature quotes a yield of 95%, however, the desired product was not isolated.[155] The reaction was repeated using the same procedure but replacing chloroacetyl chloride with bromoacetyl chloride to form rhodamine B 4-(2-bromoacetyl)piperazine **(14)**, but once again the desired product was not isolated. It was initially thought that the acid chloride had been hydrolysed to give the analogous carboxylic acid and hence did not react. Therefore, an alternative route using 3-bromopropanol was investigated.

The attempted synthesis of rhodamine B 4-(propoxy)piperazine **(15)** involved the addition of 3-bromopropanol and diisoethylpropylamine to a solution of **(12)** in dimethylformamide under an atmosphere of nitrogen followed by stirring the reaction mixture for 24 hours. At this point, further amounts of 3-bromopropanol and diisoethylpropylamine were added and the reaction mixture was left to stir for a further 2 hours. The solution was then concentrated and the extraction procedure carried out, however the desired product was not isolated. This suggests that the issue may be with the secondary amine group on **(12)** and that it could be deactivated, preventing the substitution reaction of either the acid chloride/bromide or alkyl bromide. This reaction was not investigated further and alternative routes were pursued.

3.4 The synthesis of rhodamine B ethylenediamine derivatives

Kim and co-workers have reported the synthesis of two different rhodamine based sensors for which the fluorescence is selectively 'turned on' in the presence of mercury(II) (figure 89).[161] The two derivatives have slightly different structures, however they both work on a similar principle where upon binding of mercury(II) the molecule is converted from the non-fluorescent cyclised lactam to the non-cyclised fluorescent structure. One of these compounds is *N*-(rhodamine-6G)lactam-*N'*-phenylthiourea-ethylenediamine where the mercury(II) causes a desulfurization reaction, and the other is based on rhodamine B and bears both a tris(2-aminoethyl)amine and two sulphonamide groups. In the latter compound, the mercury(II) binds to oxygen donor of the rhodamine amide group and the N-donor groups of the two deprotonated sulfonamide groups.[162]

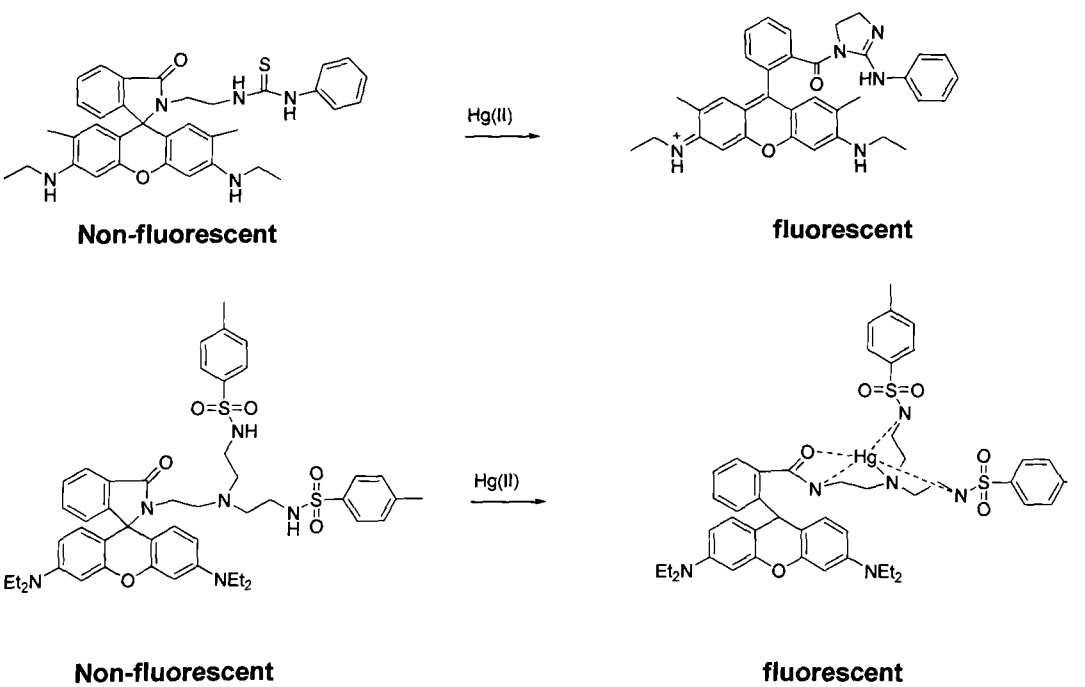

Figure 89 Structures of the two compounds reported by Kim and co-workers *N*-(rhodamine-6G)lactam-*N'*-phenylthiourea-ethylenediamine (top), and a rhodamine B derivative containing both a tris(2-aminoethyl)amine and two sulphonamide groups (bottom)[162] [161]

These compounds were synthesised in a similar fashion from either rhodamine 6G, or rhodamine B by treatment with ethylenediamine. A related approach

was exploited in this work by adopting the ethylenediamine as a linking group to join the dye to the chelator.

3.4.1 The synthesis of rhodamine B base ethylenediamine (16)

The formation of the rhodamine B ethylenediamine complex offers the potential for the ethylenediamine primary amine group to be coupled to an isothiocyanate group. The proposed synthetic scheme is shown in figure 90.

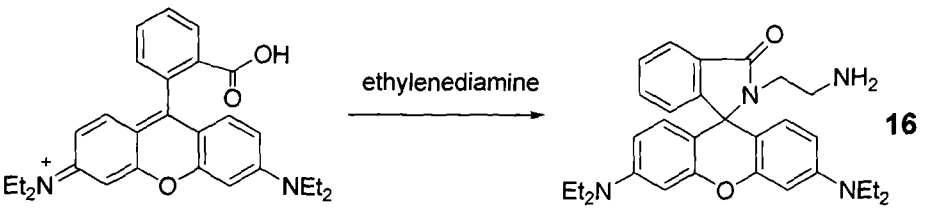

Figure 90 Reaction scheme of the preparation of rhodamine B base ethylenediamine **(16)**

A major issue with this synthetic route is that the rhodamine derivatives produced are not fluorescent due to the lactam formation. However, such molecules do hold the potential to act as mercury(II) sensors.

The synthesis of **(16)** was carried out by dissolving rhodamine B into hot ethanol, adding a 5-fold excess of ethylenediamine, and heating the mixture at reflux for 6 hours. The solution was then concentrated to a volume of around 5 ml and cooled to below 0°C. A precipitate formed that was collected by filtration and then recrystallised from a minimum amount of acetonitrile to give an orange/pink solid in a 38% yield. In the ^{1}H NMR spectrum, the aromatic region is very complex and individual peaks cannot be fully assigned, however in the alkyl region there are peaks at 2.32 ppm that 3.11 ppm that are both triplets representing the 2 CH_2 environments and are characteristic for ethylenediamine. The ^{13}C NMR spectrum shows 17 different carbon environments representing 1 CH_3, 3 CH_2, 7 CH, and 6 C carbons.

3.4.2 The synthesis of rhodamine B base ethylenephenylthiourea (18)

To confirm that the alkyl amine would be reactive towards phenyl isothiocyanates, a test reaction was undertaken to form the thiourea compound **(18)**. The reaction scheme is presented in figure 91.

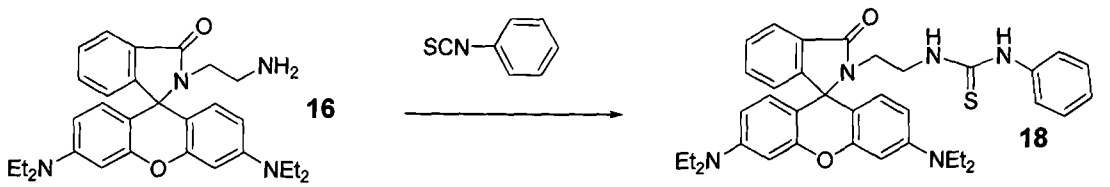

Figure 91 Reaction scheme for the synthesis of rhodamine B ethylenephenylthiourea **(18)**

Phenylisothiocyanate was added to a solution of **(16)** in dry dichloromethane and the resulting mixture was stirred for 48 hours at room temperature under an atmosphere of nitrogen. The solvent was then removed, and the crude material recrystallised from a minimum amount of acetonitrile to give a light pink solid. The peaks in the ^{1}H NMR spectrum overlap and are difficult to fully assign, however the integration values do equate to what is expected, and the ^{13}C NMR spectrum contains peaks representing 22 unique carbon environments. The electrospray mass spectrum contains the expected molecular ion peak. This test reaction confirms that the alkyl amine can undergo reaction with an isothiocyanate moiety.

A rhodamine unit, **(16)**, has been synthesised that can be conjugated to DO3A derivatives containing a phenylisothiocyanate group, however the dye is not in a fluorescent form. There are potential applications of this system, such conjugates could still show promise as mercury(II) sensors and the rhodamine moiety will cause localisation at the mitochondria in cellular systems. Hence, such a conjugate coupled with a luminescent lanthanide ion may still be useful as an optical sensor in biological systems.

3.5 BODIPY derivatives as optical dyes

Boron dipyrromethenes (BODIPY) have been exploited as fluorescent probes in life science applications.[163] This is due to their attractive photophysical properties as characterised by a tunable emission spectral profile in the 500-650 nm range, high fluorescence quantum yields, low rates of intersystem crossing, large molar absorption coefficients, and excellent photostability.[164] The general structure of the BODIPY molecule is shown in figure 92, however, this does have the limitation of small Stokes shifts (around 600 cm^{-1}) and hence requires specific excitation wavelengths. Different approaches have been employed to tune the optical properties including functionalisation at the meso position *i.e.* 8-position, substitutions at the 3- and 5- position and replacement of the fluorine atoms on the boron.[165] [166]

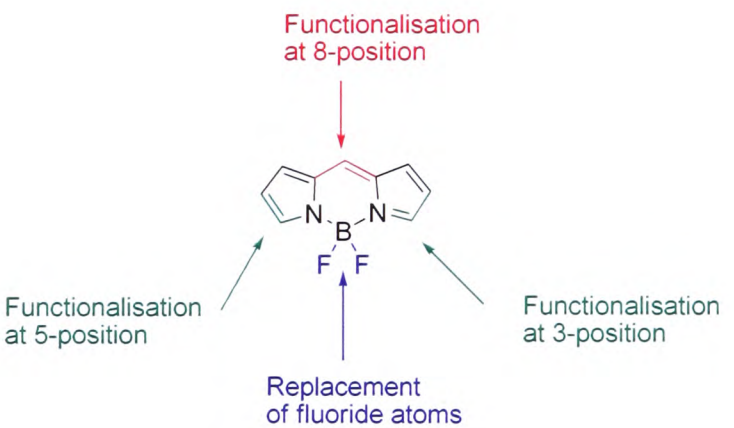

Figure 92 Diagram illustrating the different approaches used to functionalise BODIPY

3.5.1 Synthesis of BODIPY derivatives with substitution at the 3-and 5-position

Rohand *et al.* have investigated substituting BODIPY dyes at the 3 and 5 position to synthesise 3,5-dichloro-BODIPY.[166] The synthesis started from 4-methylbenzaldehyde and pyrrole to form the dipyrromethane. This is followed by chlorination with *N*-chlorosuccinimide, then oxidation with *p*-chloranil and complexation with trifluoroboronetherate giving the product in overall yields of 20% (figure 93).

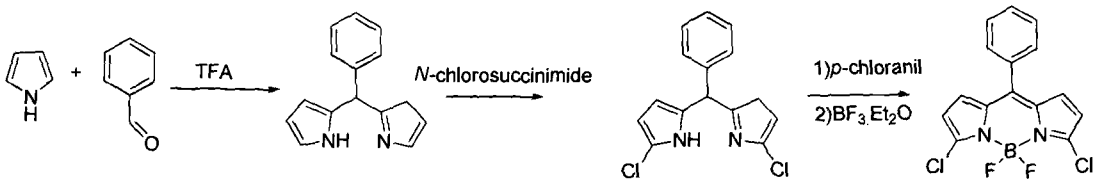

Figure 93 Reaction scheme to synthesise 3,5-dichloro-BODIPY

From the chloro BODIPY derivative, they have prepared a selective potassium binding BODIPY chemosensor via linkage to an azacrown ether.[166] The 3,5-dichloro-BODIPY compound was selectively substituted by a methoxy group upon addition of sodium methoxide, and the second chloride substituted by an aza-18-crown-6 in 40% overall yield (figure 94).

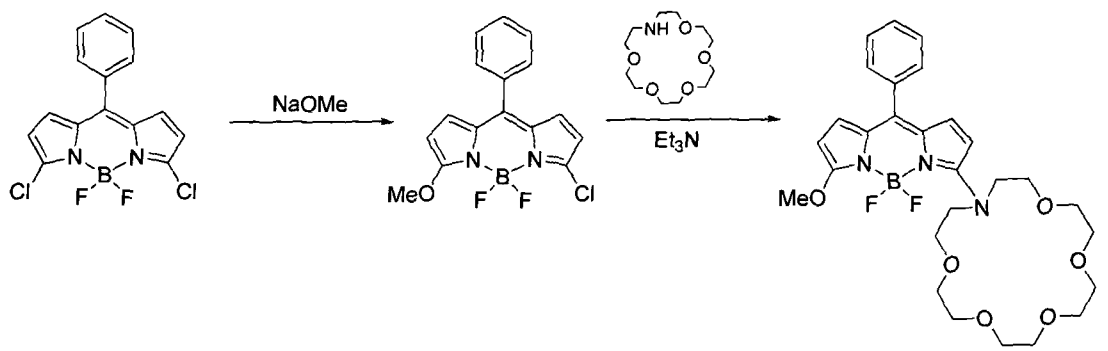

Figure 94 Reaction scheme to synthesise 3-[(4,7,10,13,16)-pentaoxa-1-aza-cyclooctadecane]-3a,4a-diaza-4,4-difluoro-5-methoxy-8-phenyl boron dipyrromethene

3.5.2 Synthesis of fluorine substituted BODIPY derivatives

Ziessel and co-workers have optimised the properties of the BODIPY analogues by replacing the fluoride ions with aryl, ethynaryl, ethynylthienyl or ethynylpolypyridine to form a library of compounds.[164] The synthesis involves the use of organometallic reagents (RLi or RMgBr) to displace the fluoride ion, with yields of around 30 – 40%. The compounds remain strongly fluorescent, with a slight increase in the fluorescence relative to the fluoride substituted analogues (figure 95).

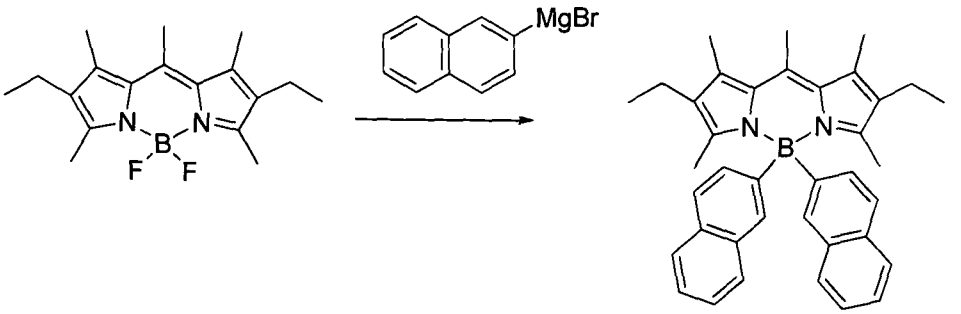

Figure 95 Reaction scheme to synthesise an aryl substituted compound

3.5.3 BODIPY compounds as sensors

BODIPY compounds can be exploited as fluorescent sensors. Baruah *et al.* have synthesised a BODIPY based hydroxyaryl derivative that shows fluorescence enhancement with the decreasing pH (pK_a values ranging from 7.5 to 9.3) (figure 96).[167] While Sunahara *et al.* have reported the synthesis of a switchable fluorescent BODIPY derivative that is sensitive to its environment and can detect local polarity changes in biological samples including proteins, membranes and receptors (figure 96).[168]

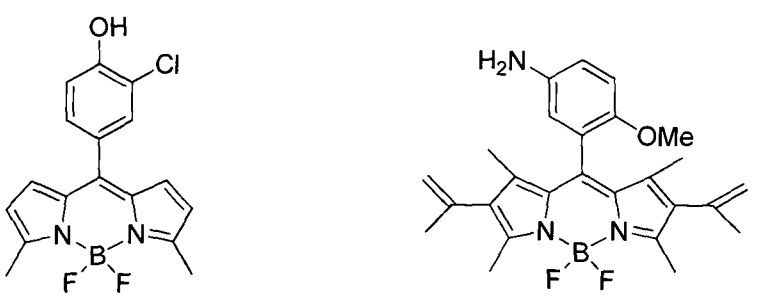

Figure 96 Structures of the pH probe (left), and the polarity probe (right) based on the BODIPY framework

Qi *et al.* have published the synthesis of an interesting tripodal fluorescent system that contains a triazine core and can combine three different functional moieties such as a signalling (BODIPY), a binding and an auxiliary subunit (figure 97).[169] Such a compound has the potential to be used in tagging of biological substrates to give fluorescent chemosensors, and a component of

functionalised nanomaterials. The initial study involved the synthesis of the compound and analysis of its photophysical properties, however, more work is needed to exploit the full potential of this approach.

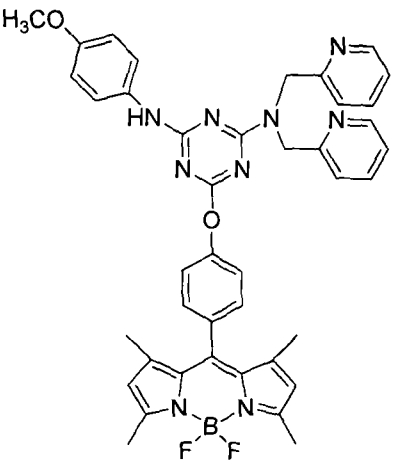

Figure 97 Structure of a novel BODIPY-triazine based tripodal fluorescent compound

3.6 Synthesis of a BODIPY functionalised at the 8-position

The preparation of BODIPY analogues that contain functionality for further conjugation to DO3A derivatives, can be achieved by substituting at the meso position (8-position), with a secondary amine that could be converted to a isothiocyanate group. Numerous research groups have investigated routes to introduce functionality at the 8-position to improve the optical properties of the BODIPY dye.[170] The addition of a further aromatic group e.g. a phenyl ring can lead to improved fluorescence. There are a number of methods to synthesise such BODIPY analogues. A strategy employed by Peña-Cabrera *et al.* involves substitution with a derivatised boronic acid onto 8-thiomethylBODIPY using Pd(0) and Cu(I)-2-thienylcarboxylate in overall yields of greater than 70% (figure 98).[154]

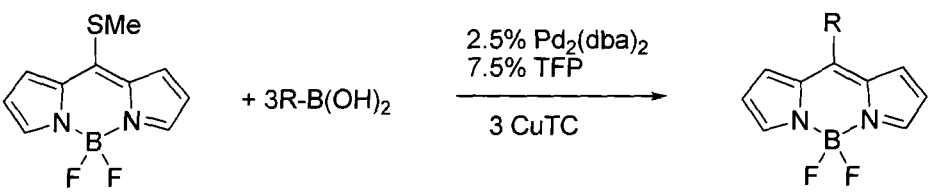

Figure 98 Reaction scheme showing the use of boronic acids to produce 8-substituted BODIPY derivatives

Porres *et al.* reported the reaction of a substituted aldehyde with 2,4-dimethyl-3-ethylpyrrole to form a multichromophoric BODIPY analogue (figure 99)[171] The synthetic strategy employed here involved 2,4-dimethyl-3-ethylpyrrole undergoing a condensation reaction with a substituted benzaldehyde ((1,1'-biphenyl)-4,4'-dicarboxaldehyde). The dipyrromethane was converted to a dipyrromethene using DDQ (dichlorodicyanoquinine) oxidation, and then treated with trifluoroboronetherate, to give the desired product in overall yields of 42%.

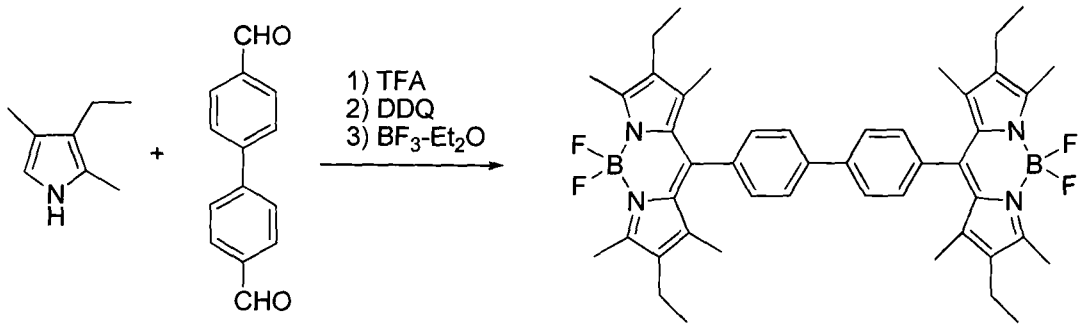

Figure 99 Reaction scheme for the synthesis of a multichromophoric BODIPY analogue

Ulrich and co-workers have reported the synthesis of 4,4-difluoro-4-bora-3a,4a-diaza-*s*-indacene derivatives bearing an isothiocyanate or isocyanate functional group (figure 100).[172] They started from 2,4-dimethyl-3-ethylpyrrole which was treated with nitrobenzoyl chloride, followed by conversion to the boron complex using trifluoroboronetherate, and finally the nitro group was reduced to an amine with 5% Pd/C in yields over 50%. The amine group can then be converted to an isothiocyanate or isocyanate group ready for conjugation to biomolecules.

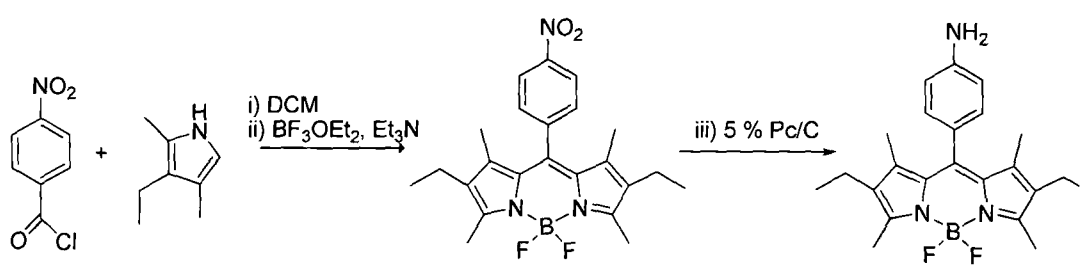

Figure 100 Reaction scheme for the synthesis of an aminophenyl BODIPY.

3.6.1 The synthesis of 5-(4-isothiocyanatophenyl) boron dipyrromethene (21)

The method chosen for the synthesis of 5-(4-isothiocyanatophenyl) boron dipyrromethene **(21)** was developed by Boyle and co-workers.[173] The reason for using this route is that the amide functionalised benzaldehyde reacts

efficiently and the amide group in the resulting product can readily be converted to the desired amine. The synthetic scheme used is shown in figure 101.

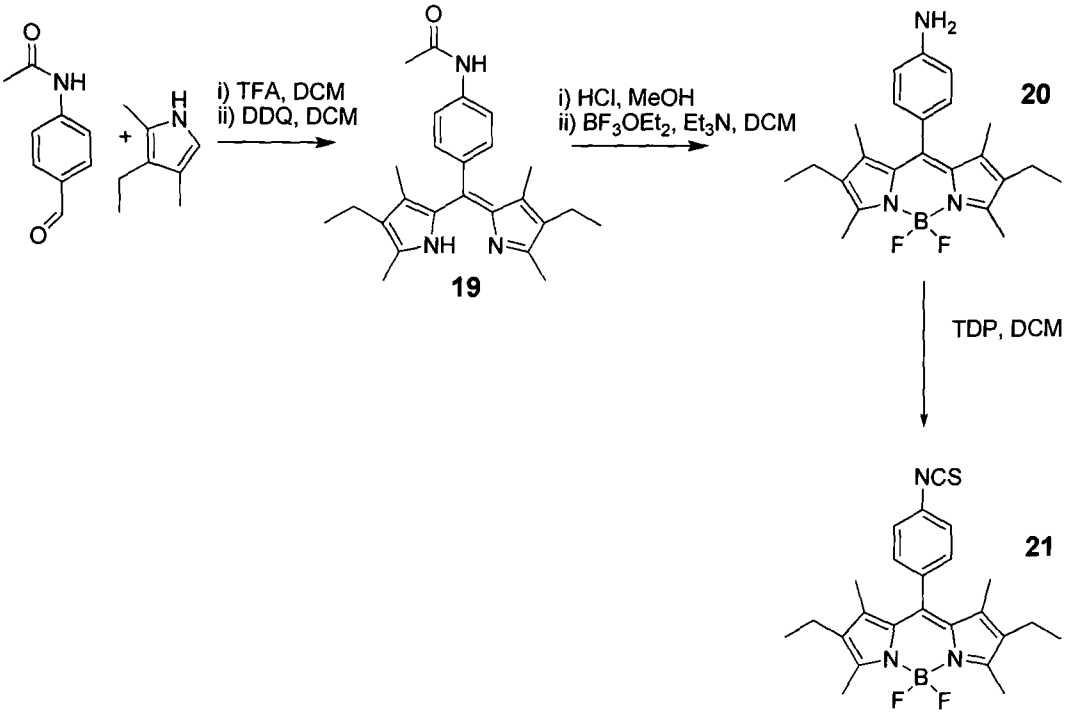

Figure 101 Synthetic scheme used to prepare 5-(4-isothiocyanatophenyl)BODIPY **(21)**

The reason for using the 3-ethyl-2,3-dimethylpyrrole rather than pyrrole is to restrict the rotation of the 5-phenyl ring, which leads to a ten-fold increase in fluorescence quantum yield. The synthesis of **(19)** involved the reaction of 4-acetamidobenzaldehyde and 3-ethyl-2,3-dimethylpyrrole in dry dichloromethane, with the addition of a catalytic amount of trifluoroacetic acid (TFA) and stirring at room temperature overnight. The dipyrromethane derivative was converted to the dipyrromethene by DDQ oxidation (stirred for 1 hour at room temperature). The reaction mixture was washed with water, and then the organic layer was collected and the solvent removed. The mixture was then purified by flash chromatography on silica gel with a solvent gradient from 100% dichloromethane to 10% methanol in dichloromethane. This gave **(19)** as a purple solid in 37% yield, which was higher than the reported yield in the literature.[173] ^{1}H NMR spectroscopy was used to analyse the product, giving a complex spectrum with a number of overlapping peaks. However, the

integration values and peak positions are consistent with the previously reported data.

To convert the amide to the amine, 1 M hydrochloric acid was added to a solution of **(19)** in methanol and the reaction mixture was heated at reflux for 1 hour. It was then cooled to room temperature and neutralised with a solution of 2 M sodium hydroxide, followed by an extraction into dichloromethane. The compound was used crude to form the boron complex. The crude solid was dissolved into dry dichloromethane, triethylamine and trifluoroboronetherate and then stirred at room temperature for 3-4 hours under nitrogen. The reaction mixture was washed with water and brine, and the crude material was purified by flash column chromatography using 2:1 dichloromethane:hexane as the eluent. The product elutes with an r.f. of 0.36, to give **(20)** as a red solid in 36% yield. The ^{1}H NMR spectrum highlights the loss of the amide peak to suggest that the deprotection step had occurred, with the electrospray mass spectrum confirming the identity of the BODIPY complex **(20)**.

To allow for conjugation of **(20)** onto the DO3A derivatives, the primary amine was converted to an isothiocyanate group to form **(21)** by the use of TDP in dry dichloromethane. The solution was stirred under nitrogen for 4 hours and was purified by flash chromatography with a 2:1 mixture of hexane:dichloromethane as eluent to give a red solid in 75% yield. The ^{1}H NMR spectrum highlights the shift in position of the aromatic CH peaks upon conversion to the isothiocyanate from 7.37–7.39 ppm in **(20)** to 7.0-7.02 ppm in **(21)**.

3.6.2 Attempted synthesis of 5-(4-phenyl(thioureaphenyl))borondipyrromethene (22)

Boyle and co-workers have already demonstrated that the isothiocyanate BODIPY **(21)** can be coupled to proteins bearing alkyl amines (lysine side chains).[173] To test the reactivity of the isothiocyanate group towards aromatic

amines, an attempt was made to react **(21)** with phenylamine as shown in figure 102.

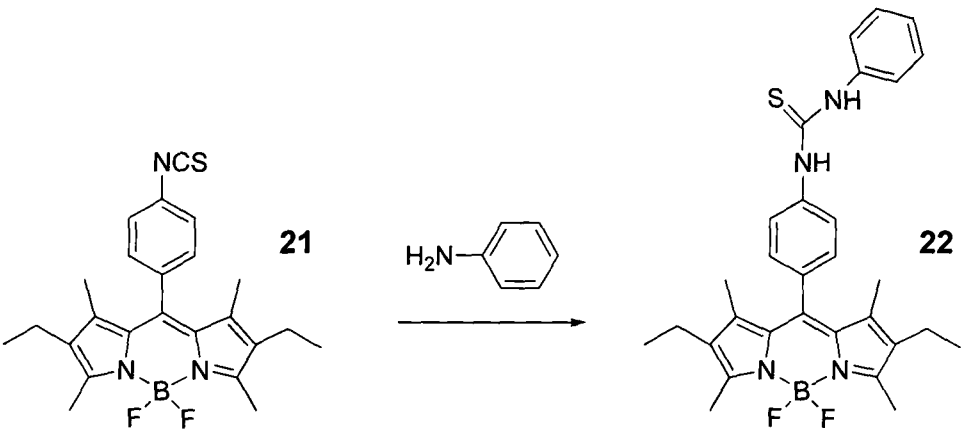

Figure 102 Attempted synthesis of 5-(4-phenyl(thioureaphenyl))borondipyrromethene **(22)**

The reaction mixture was stirred under nitrogen at room temperature for 7 days. The progress of the reaction mixture was monitored by t.l.c., and showed that no reaction had occurred. This suggests that the aminophenyl group is unreactive with the isothiocyanate or the reaction is only proceeding very slowly. A slow reaction would be problematic as hydrolysis of the isothiocyanate may compete. The delocalisation of electron density on the amine group into the aromatic system probably accounts for its reduced reactivity.

3.7 Synthesis of boron dipyrromethane complexes bearing an alkyl amine

There are a number of options available in the synthesis of alkyl amine bearing BODIPY derivatives. These derivatives offer an alternative to the aromatic amine BODIPY analogues, in which the alkyl amine may react with the isothiocyanate group more readily then its aromatic amine counterpart. The target BODIPY analogue is shown in figure 103.

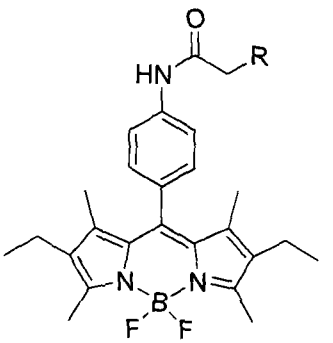

Figure 103 Target BODIPY analogue bearing an alkyl amine, where R = $CH_2NH(CH_2)_2NH_2$, or $(CH_2)_3NH_2$

The three synthetic strategies that have been investigated are depicted in figure 104. Methods 1 and 2 involve the use of a Boc-protected aminobutyric acid with ethyl chloroformate used to activate the carboxylic acid. In method 3, 5-(4-aminophenyl)BODIPY **(20)** is treated with bromoacetyl chloride followed by the reaction with an excess of ethylenediamine.

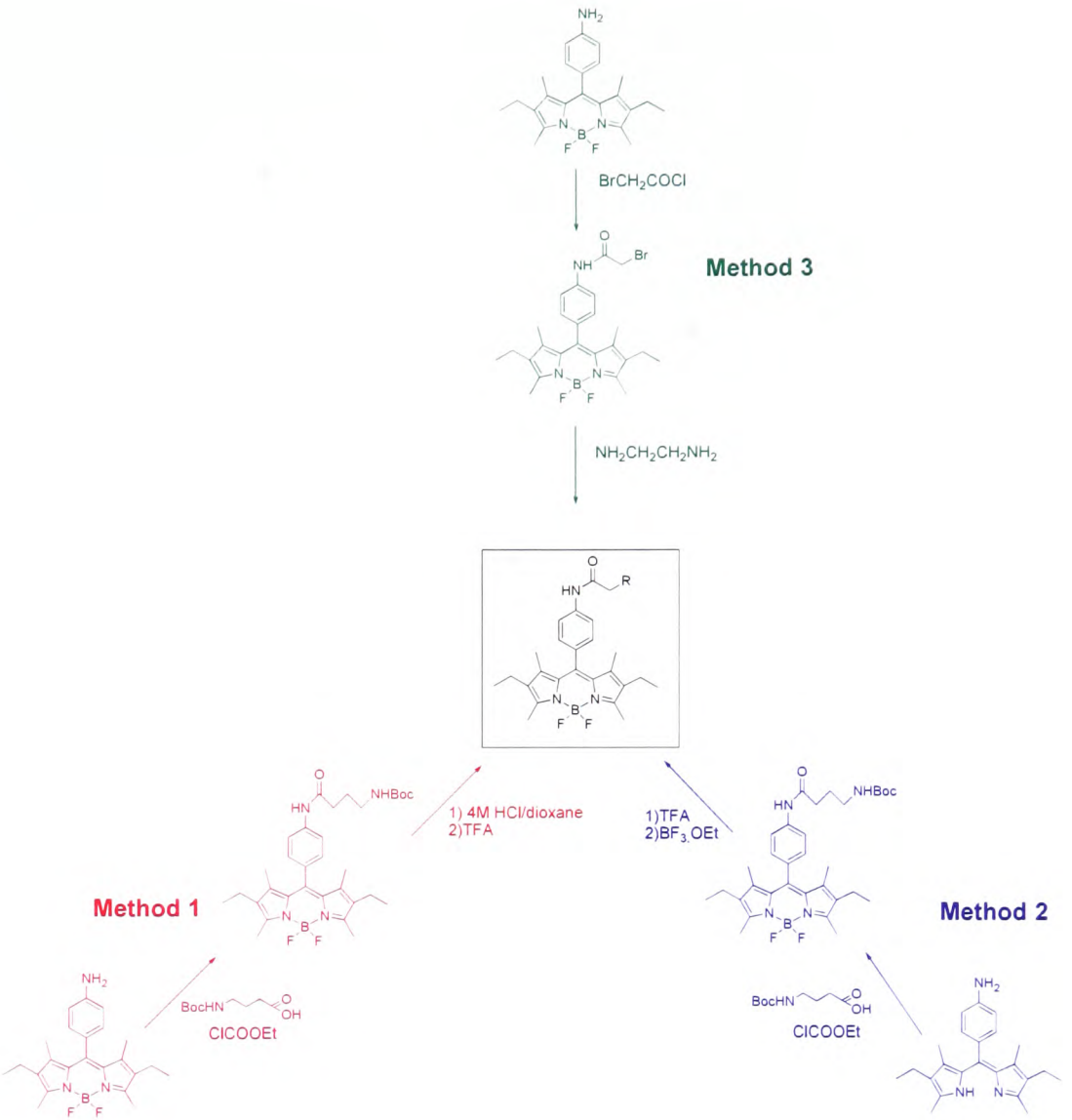

Figure 104 Routes to prepare BODIPY analogue bearing an alkyl amine, where R = $CH_2NH(CH_2)_2NH_2$, or $(CH_2)_3NH_2$

3.7.1 The synthesis of BODIPY derivatives using methods 1 and 2

In the literature, there are a number of examples of the addition of an alkyl amine onto aromatic amine bearing compounds. An example investigated by Perillo *et al.*, involves 2-bromoethylamine hydrobromide being substituted onto an arylamine.[174] This relies on the arylamine being more reactive than the amine on 2-bromoethylamine hydrobromide. Poindexter *et al.* coupled 2-oxazolidinones onto an aromatic amine, which results in an alkyl amine

extending from the phenyl ring.[175] An interesting method investigated by Biron *et al.* involved the preparation of a cationic porphyrin that bears an amino acid derivative (figure 105).[176] This was synthesised by the coupling of a porphyrin to a Boc protected glutamic acid *via* an amide bond through the activation of the carboxylic acid in 80% yield. The removal of the Boc protecting group was performed quantitatively by stirring in a solution of 4 M HCl in dioxane.

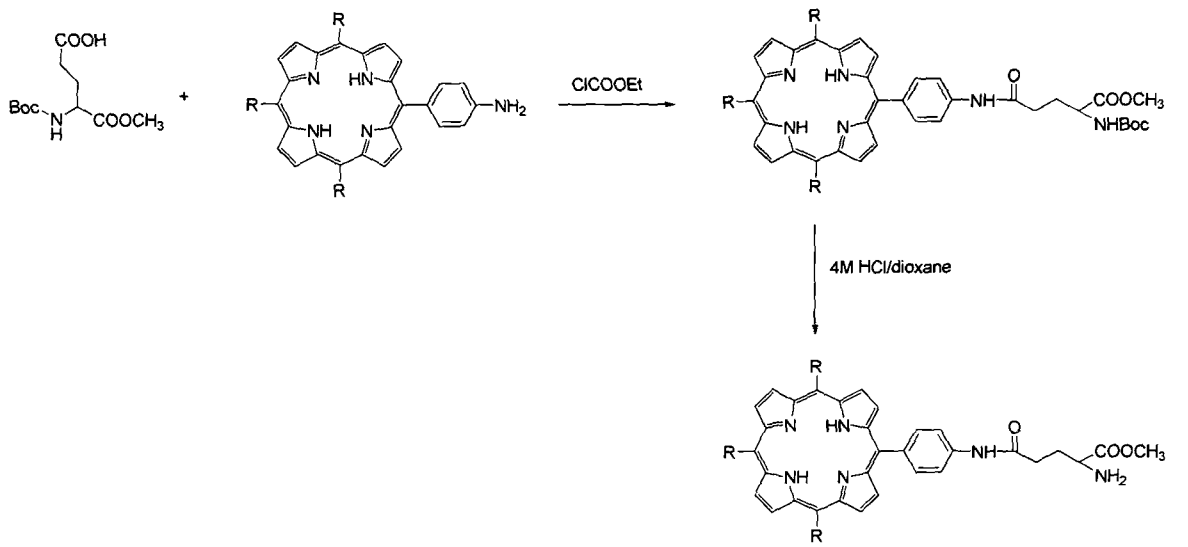

Figure 105 Synthetic scheme to react a porphyrin with a modified amino acid reported by Biron *et al.*

3.7.2 Synthesis of 4-Boc aminobutyric acid (23)

A modified method based on the synthesis reported by Biron *et al.* was followed in the preparation of an alkyl amine bearing BODIPY compound **(25)**. [176]Initially, the Boc protected aminobutyric acid **(23)** was prepared following the method reported by Itoh *et al.*.[177] This involved reacting 4-aminobutyric acid and *tert*-butyloxycarbonyl in a mixture of triethylamine and dioxane, which was stirred for 4 hours at 0°C. The solution was then concentrated to give a white solid, which was dissolved into water and washed with ethyl acetate. Collection of the aqueous layer followed by removal of the solvent gave a clear oil in 49% yield. The ^{1}H NMR spectrum confirmed the presence of the Boc group with a singlet at 1.30 ppm representing the three CH_3 groups, and the

peaks at 1.63, 2.16, and 2.97 ppm representing the three CH_2 groups with the expected splitting pattern of a quintet, triplet and triplet respectively.

3.7.3 Synthesis of 5-(4-aminobutylamidophenyl) boron dipyrromethene (25)

The carboxylic acid group on **(23)** was activated by stirring with ethylchloroformate and triethylamine in dry dichloromethane. The mixture was allowed to stir for 30 minutes at room temperature under nitrogen and the acyl chloride derivative of **(23)** was isolated. The compound was dissolved into dry dichloromethane, the solution was cooled to 0°C, followed by the addition of **(20)** and then the reaction mixture was left to stir for 1 hour under nitrogen. The resulting crude solid was purified by flash column chromatography with a solvent gradient from 100% dichloromethane to 2% methanol in dichloromethane to give a red solid with a yield of 85%. The ^1H NMR spectrum shows two peaks in the aromatic region at 7.21 and 7.78 ppm. In the alkyl region, the triplet at 0.97 ppm is from one of the CH_3 groups on the BODIPY, while the other peaks are overlapping with two broad multiplets between 1.2 – 2 ppm, and 2.3 – 2.5 ppm with a total integration of 21 protons. The electrospray mass spectral data shows the expected molecular ion peak. The reaction scheme is shown in figure 106.

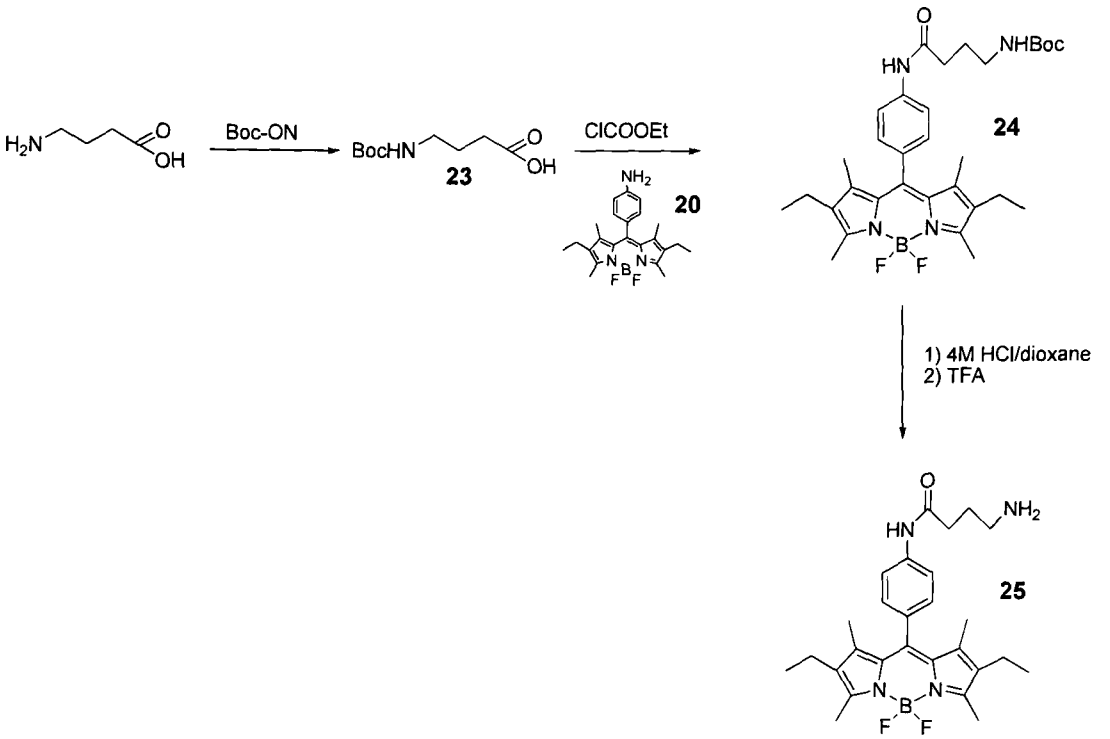

Figure 106 Reaction scheme showing the synthesis of 5-(4-aminobutylamidophenyl) borondipyrromethene **(25)**

Initial efforts to deprotect the boc-protected amine involved following a modified method based on the synthesis reported by Biron *et al.*. [176]This involved dissolving **(24)** into a mixture of 4 M hydrochloric acid and dioxane, and then stirring for 4 hours at room temperature while monitoring by t.l.c. the reaction. After 4 hours, there were no signs of Boc deprotection and so an alternative method was then investigated. This procedure was repeated with dissolving **(24)** in trifluroracetic acid and dichloromethane and stirred for 20 minutes at room temperature. However, the addition of the trifluoroacetic acid caused a colour change of the solution from bright red to purple that is characteristic of the uncomplexed dipyrrin compound. The t.l.c. had a number of spots at r.f values that are not characteristic of the polar boron complexes. This suggests that the trifluoroacetic acid had reacted with the BODIPY unit and possibly caused the decomplexation of the boron.

3.7.4 Synthesis of 5-(4-aminobutylamidophenyl) borondipyrromethene (26) (method 2)

Method 2 involved starting from 5-(4-aminophenyl) dipyrromethene and coupling to the acyl chloride derivative of **(23)** with the reaction scheme shown in figure 107. The activated 4-boc aminobutyric acid **(23)** was dissolved into dry dichloromethane and 5-(4-aminophenyl) dipyrromethene was added. The reaction mixture was stirred for 1 hour at 0°C, followed by 1 hour at room temperature. The resulting solid was purified by flash column chromatography eluting with a solvent gradient of methanol in dichloromethane to form a purple solid **(26)** in 45% yield. The ^1H NMR spectrum was very broad, with two aromatic peaks at 7.24 and 7.88 ppm, and the alkyl region from 0.84 and 2.44 ppm. The broadening of the NMR signals may be due to the restricted molecular rotation of the compound.

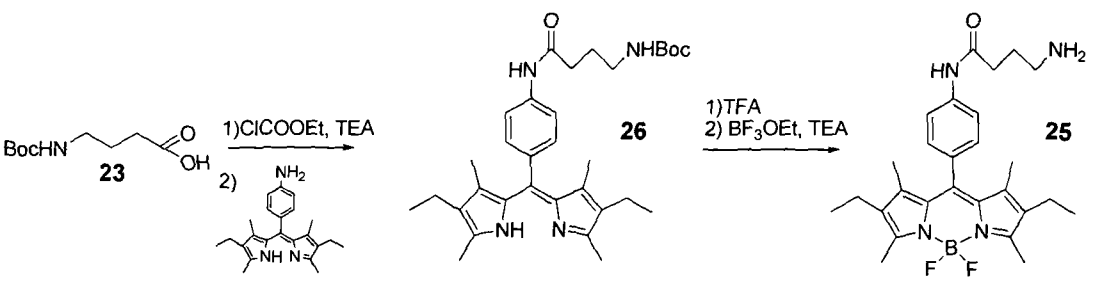

Figure 107 Attempted synthesis of 5-(4-aminobutylamidophenyl) borondipyrromethene **(25)**

3.7.5 The synthesis of 5-(4-aminobutylamidophenyl) borondipyrromethene (25)

Attempts were made to deprotect the amino Boc group on **(26)** to give **(25)**. **(26)** was dissolved in a mixture of trifluoroacetic acid and dichloromethane and allowed to stir for one hour at room temperature. The solvent was removed, and the solid was re-dissolved into ethyl acetate and washed with sodium hydrogen carbonate. The resulting crude solid, isolated from the organic layer, was complexed to boron by the reaction with trifluoroboronetherate in the presence of triethylamine. The reaction mixture was stirred for four hours at room temperature under an atmosphere of nitrogen. After work up, t.l.c. analysis was

performed on the reaction mixture, which indicated the presence of two polar compounds that may contain boron. It was proposed that a mixture of **(25)**, and the starting material **(26)** had been isolated. This was not investigated further due to the small amount of product obtained.

3.7.6 Synthesis of 5-(4-bromomethylamidophenyl) borondipyrromethene (28) (method 3)

An alternative method to form an alkyl amine appended on a BODIPY complex was investigated where bromoacetyl chloride was treated with 5-(4-aminophenyl)borondipyrromethene to form 5-(4-bromomethylamidophenyl) borondipyrromethene **(28)**. Ethylenediamine can be reacted with **(28)** to form 5-(4-ethylenediaminomethylamidophenyl)borondipyrromethene **(29)**. The reaction scheme is shown in figure 108.

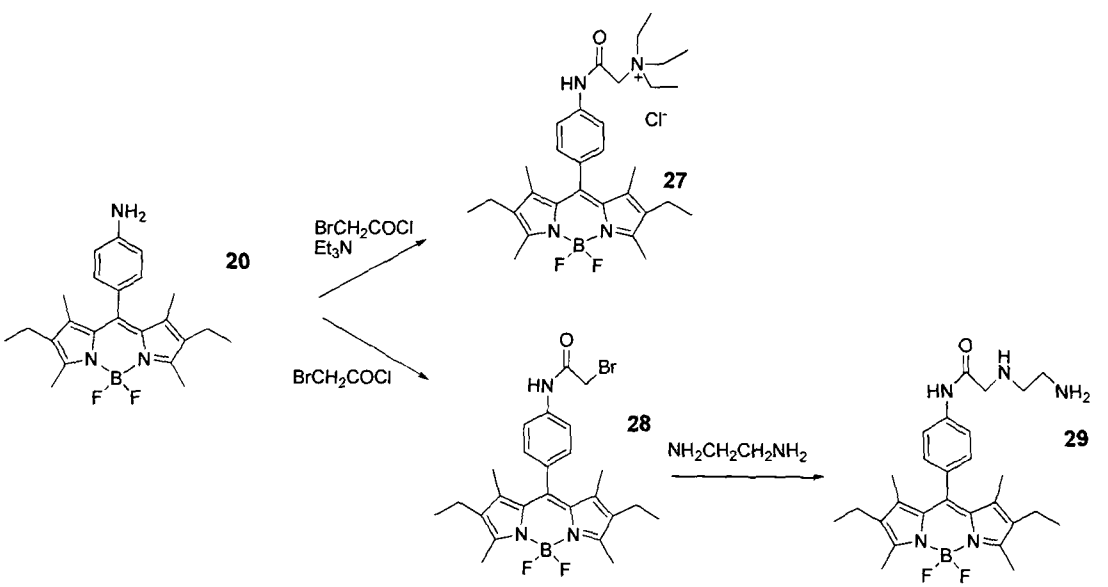

Figure 108 The reaction scheme used to prepare 5-(4-ethylenediaminomethylamidophenyl) borondipyrromethene **(29)**

The first attempt to synthesise **(28)**, involved dissolving 5-(4-aminophenyl) dipyrromethene into dry dichloromethane in the presence of triethylamine and cooling the reaction mixture in an ice bath to 0°C. Bromoacetyl chloride was added and the reaction mixture was stirred for 24 hours. The compound was

purified by preparative t.l.c. using 10% methanol in dichloromethane as eluent to give a red solid in 82% yield. The analytical data from the ^{1}H NMR and ^{13}C NMR spectroscopy and electrospray mass spectrometry showed that instead of **(28)**, the triethylamine BODIPY derivative **(27)** had been formed by reaction with triethylamine. Triethylamine acted as a nucleophile to react with the alkyl bromide group on the BODIPY moiety. The ^{1}H NMR spectrum contains two doublets at 7.21 and 7.85 ppm that represent the two aromatic proton environments, and a triplet at 0.94 ppm, quintet at 2.26 ppm and two singlets at 1.37 and 2.5 ppm that were assigned to BODIPY protons. The singlet at 4.62 ppm represents the CH_2 next to the amide group. The two peaks at 1.44 ppm and 3.74 ppm (triplet and a quintet) represent the CH_2 groups of the triethylamine. The electrospray mass spectral data shows a molecular ion peak that corresponds to **(27)**. While it is not possible to couple this compound to the DO3A chelators, it may have potential as a dye compound for cellular imaging studies. The quaternarised amino group will improve water solubility of the BODIPY derivative and the positive charge may aid cellular uptake of the compound. This route is also generally applicable to the formation of other quaternised amino derivatives of BODIPY and incorporating different alkyl chains or functionality may influence cellular localisation. The cellular uptake of this compound was studied using fluorescence microscopy and the results are presented in chapter 5.

To produce **(28)**, the reaction was repeated and 5-(4-aminophenyl) dipyrromethene was washed with sodium hydrogen carbonate solution to make the phenyl amine more susceptible to undergo nucleophilic substitution by deprotonating the amine. The compound was then re-dissolved in dry dichloromethane and cooled in an ice bath to 0°C under nitrogen. Bromoacetyl chloride was added, and the reaction mixture was allowed to stir for 4 hours, no triethylamine was added. The solvent was removed, and the compound was purified by preparative t.l.c. using dichloromethane as eluent. The product was isolated as a red solid in 77% yield. Analysis by ^{1}H NMR, ^{13}C NMR spectroscopy and electrospray mass spectrometry confirmed the formation of **(28)**.

3.7.7 Synthesis of 5-(4-ethylenediaminemethylamidophenyl) borondipyrromethene (29)

The synthesis of the alkyl amine containing compound **(29)** was achieved by dissolving **(28)** into acetonitrile, adding ethylenediamine and stirring the reaction mixture overnight under nitrogen. The solvent was removed, and work up yielded a red solid. To purify the crude material, a preparative t.l.c was performed to give a red solid in 13% yield. The ^{1}H NMR spectrum, showed the neighbouring CH_2 next to the amide shifted to 2.21 ppm, and two multiplets at 2.72 and 2.83 ppm that represent the two CH_2 groups on the ethylenediamine. The electrospray mass spectrum contained the expected molecular ion peak at 493 for **(29)**.

3.8 Synthesis of zinc(II) (di-5-(4-aminophenyl)) dipyrromethene (30)

The use of transition metal complexes with dipyrromethene ligands in fluorescence imaging applications is limited by quenching processes associated with a metal centre that reduce the quantum yield. However, the combination of a diamagnetic metal centre and restricted internal rotation of the phenyl group can be used to increase these quantum yields.[178] Attempts were made to produce the zinc(II) (di-5-(4-aminophenyl))dipyrromethene complex **(30)**. The two equivalents of ligand form a four coordinate tetrahedral environment around the metal centre. The complex has two primary amine groups available to react with isothiocyanate functionalised DO3A chelators (figure 109). Ultimately this could be used to form a trimetallic species with two gadolinium(III) ions, *e.g.* Gd_2ZnL_2, that could function as a multimodality imaging agent. The quantum yield for the fluorescence process will still be lower than that observed for BODIPY derivatives but an increase in the number of gadolinium(III) ions will improve the properties as an MRI contrast agent relative to the BODIPY analogue.

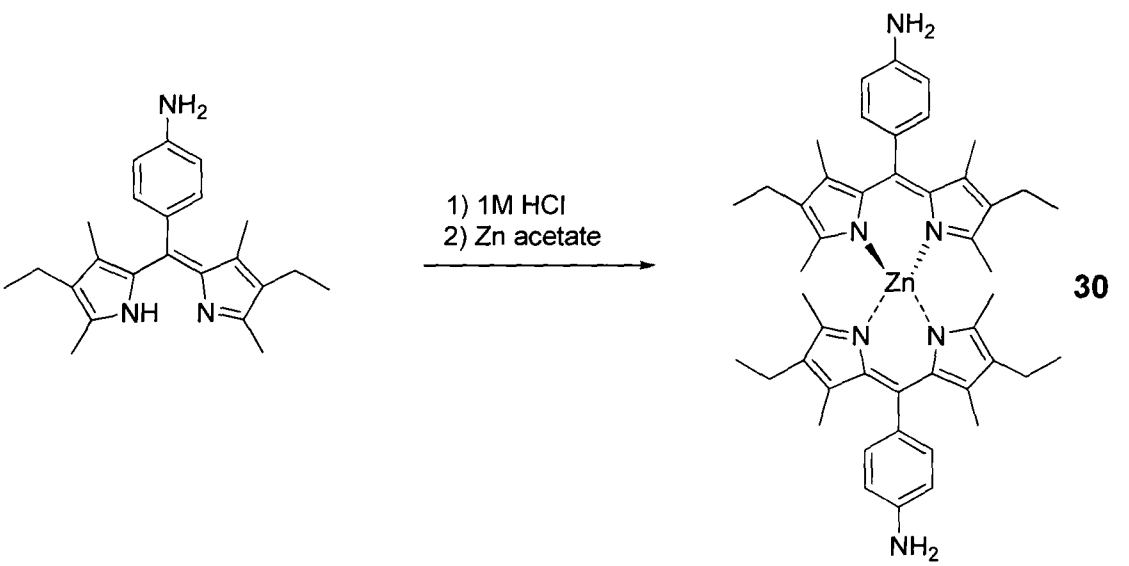

Figure 109 Synthetic scheme to show the preparation of zinc(II) (di-5-(4-aminophenyl)) dipyrromethene **(30)**

The method used to synthesise the zinc(II) complex was a modified version of that reported by Dolphin and co-workers, where zinc(II) acetate in methanol

was added to the solution of 5-(4-aminophenyl) dipyrromethene in methanol under nitrogen, and the reaction mixture heated at reflux overnight.[179] The reaction was worked up and resulted in a green solid in 83% yield. The ^{1}H NMR spectrum was very similar to the dipyrrin starting material and therefore could not be unequivocally assigned to the formation of the zinc(II) complex. High resolution mass spectrometry confirmed the formation of **(30)**. Further evidence was obtained from the UV-vis spectrum, where the mean absorbance peak for the starting material 5-(4-aminophenyl) dipyrromethene was at 461 nm, shifted to 504 nm upon zinc(II) complexation. The zinc(II) complex could theoretically be coupled to a DO3A chelator derivative, but this was not attempted as similar issues with reactivity of the amino group exist as were encounted for the BODIPY derivatives (see chapter 4).

3.9 Conclusions

This chapter contains discussion of the synthesis of optical dyes that contain appropriate functionality for conjugation to a DO3A derivative. The two optical dyes investigated were based on rhodamine and boron dipyrromethene (BODIPY).

The rhodamine synthesis involved following the method reported by Nguyen *et al.* where a piperazine ring was coupled onto rhodamine B base using trimethylaluminium.[155] The piperazine ring will prevent the cyclisation reaction to form a non-fluorescent lactam. Efforts were made to attach appropriate functionality for conjugation to a DO3A chelator by reacting chloroacetyl chloride, bromoacetyl chloride and 3-bromopropanol at the secondary amine on the piperazine unit **(13)**. However, this proved unsuccessful, possibly due to inhibition of the reactivity of the amine on piperazine by protonation.

The preparation of a rhodamine derivative bearing an alkyl amine was investigated, as this would readily undergo nucleophilic substitution with an isothiocyanate group to form a thiourea link. The compound **(16)** was formed by the reaction between rhodamine B and ethylenediamine. However, compound **(16)** forms a non-fluorescent lactam that will limit its use as an optical dye. It may still have cellular uptake and localisation properties that are of interest and could potentially be used as a sensor for mercury(II).

BODIPY analogues have been synthesised using the method developed by Boyle and co-workers.[173] This method involved the reaction between 3-ethyl-2,3-dimethylpyrrole and 4-acetamidobenzaldehyde to form the dipyrromethane, with DDQ oxidation to convert it to the dipyrromethene **(19)**. The amide was then removed using HCl, followed by complexation with boron to form a BODIPY derivative containing an aromatic amine **(20)**. The isothiocyanate derivative **(21)** can then be synthesised by reaction with TDP.

To form a BODIPY molecule containing an alkyl amine, efforts initially involved the coupling reaction between the Boc protected amine group **(23)** with the amino BODIPY **(20)**. The carboxylic acid unit in this compound was activated using ethylchloroformate to form the acyl chloride. While this reaction worked, attempts to deprotect the Boc group with TFA resulted in the decomplexation of the boron. The reaction was repeated using 5-(4-aminophenyl) dipyrromethene to form the compound 5-(4-Bocaminobutylamidophenyl)dipyrromethene **(26)**. Attempts to deprotect the Boc group, and complex the compound to boron without isolating the intermediates led to the formation of a number of side products.

An alternative method was investigated where 5-(4-aminophenyl) dipyrromethene was coupled to bromoacetyl chloride in the presence of triethylamine, however, instead of forming the desired compound **(28)**, the triethylamine reacted with the alkyl halide to form **(27)**. This compound is of interest as a fluorescent probe due to its improved solubility properties and potential for cellular uptake. The reaction was repeated where the 5-(4-aminophenyl) dipyrromethene was washed with base to deprotonate the phenyl amine, and then coupled with bromoacetyl chloride to result in the formation of **(28).** This in turn was treated with ethylenediamine to produce a BODIPY derivative with an alkyl amine **(29)**.

A number of optical dyes that have the potential to be conjugated to a DO3A chelator derivative have been prepared, including a rhodamine derivative containing an alkyl amine**(16)**, and BODIPY analogues with either an aromatic amine **(20)**, an alkyl amine **(29)** or an isothiocyanate group **(21)**.

4. Synthesis of macrocyclic chelators for lanthanides

4.1 Introduction

With the development of biomedical applications for metal ions, such as gadolinium(III) complexes as MRI contrast agents, there has been a growing interest in the synthesis of functionalized polydentate ligands that can complex lanthanide metal ions. For polydentate chelators to be used in biomedical applications, the complexes formed need to have high thermodynamic stability and be kinetically inert. Dissociation of the lanthanide ion is undesirable, as the free lanthanide metal ion is toxic. The equilibrium between the complexed lanthanide ion and other competing endogenous metal ions or anions can lead to dissociation of the metal ion. Common ligands utilised for lanthanide complexation in biological systems include 1,4,7,10-tetraazacyclododecane-1,4,7,10-tetraacetic acid (DOTA), a macrocycle incorporating a cyclen ring and diethylenetriaminepentaacetatic acid (DTPA), a branched acyclic chelator, as shown in figure 2. The DOTA ligand is known to form more thermodynamically stable lanthanide(III) complexes than the DTPA ligand. This is due to the macrocyclic effect. This means that complexes of macrocyclic ligands are more thermodynamically stable than linear polydentate analogues with the same number and type of donor atoms. Macrocyclic ligands are in a preorganised conformation that requires minimal reorganisation on metal ion complexation. The stability constant K_{ML} is defined by the equation below.

$$K_{ML} = \frac{[ML]}{[M][L]}$$

Figure 110 Stability constant

The equilibrium lies towards the lanthanide complex. At physiological pH, the ligand can be protonated, which will lower the stability constant. This is defined as the pH dependent stability constant K^*_{ML}. The table below shows typical stability constants for common lanthanide(III) chelators (see also figure 6 for ligands forming gadolinium(III) complexes).[9]

Ligand	Log K_{ML}	Log K^*_{ML}
DTPA	22.46	17.70
DTPA-BMA	16.85	14.9
DTPA-BMEA	16.84	-
DOTA	25.3	18.6
DO3A	21.0	14.97
HP-DO3A	23.8	17.21
BOPTA	22.59	-

Table 9 Stability constants for selected lanthanide(III) complexes (K^*_{ML} is the stability constant for the protonated complex)

The data shows that DOTA has the highest thermodynamic stability constant. However, there are no simple methods to attach further functional groups to DOTA. Modified chelators *e.g.* HP-DO3A, generally have lower stability than DOTA, but are still sufficiently stable for biological applications.[9 180]

This chapter is split into two parts, the first part (sections 4.1 – 4.5) presents discussion of the synthetic strategy to produce a chelator that has an appropriate functional group for coupling to an optical dye. The second section (4.6) contains discussion of the synthetic strategies used to produce multimodality imaging agents. The chelator unit used in the multi-modal lanthanide contrast agents is based on cyclen, DO3A **(31)**. This allows for attachment of a further chelating arm by reaction with either 1-(4-nitrobenzylmethyl)-2-chloromethyl benzimidazole **(7)** or 4-nitrobenzylbromide, which can be used to conjugate to other molecules. These chelators complex lanthanide ions and after conversion of the nitro group to an amine, an optical dye such as BODIPY or a rhodamine analogue can be attached. A target molecule is depicted in figure 111. Here, the DO3A chelator bears a benzimidazole linker that is coupled to the optical dye BODIPY.

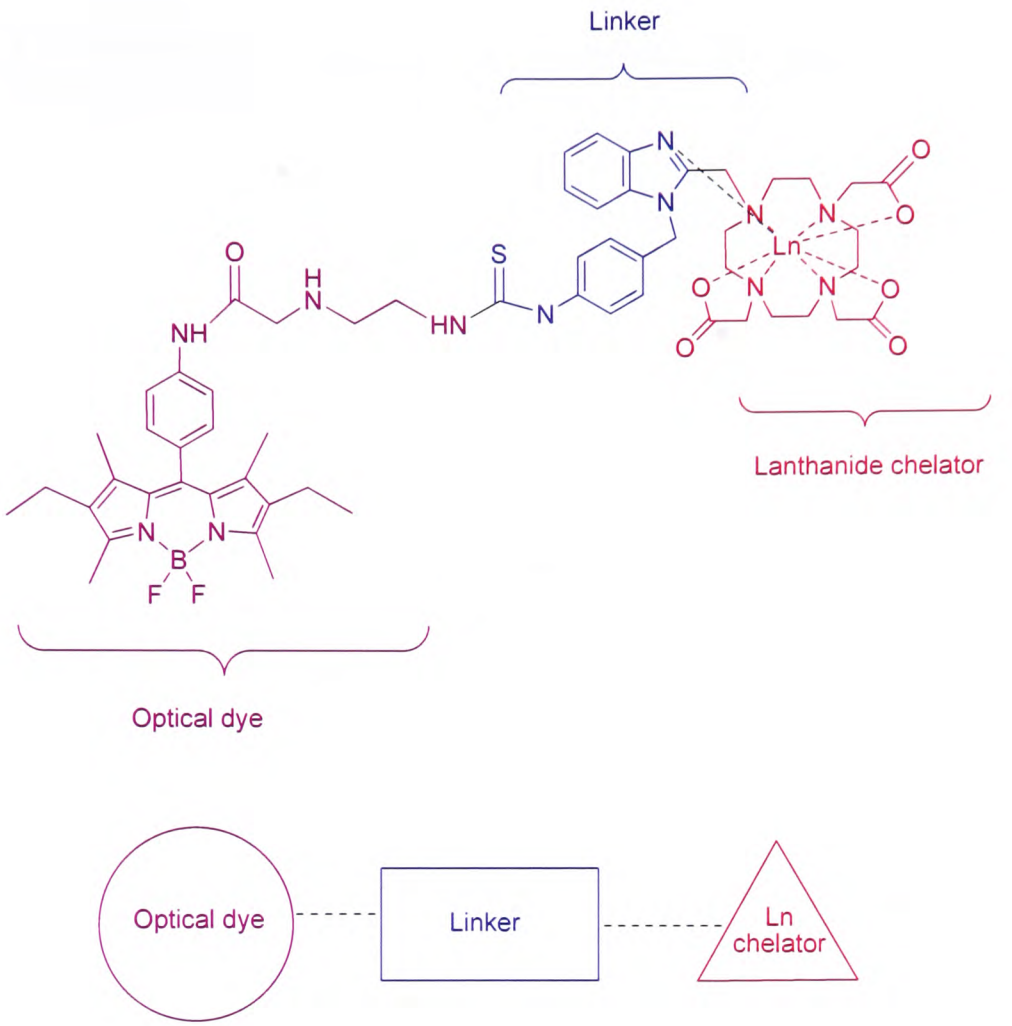

Figure 111 A target multi-modality contrast agent

This chapter focuses on the synthetic strategy and methodology used in the preparation of multi-modality contrast agents that contain a lanthanide(III) chelator (DO3A), a linker group (benzimidazole or benzyl) and an optical dye (BODIPY or rhodamine).

4.2 Synthetic strategy to produce a functionalised chelator bearing an amine

Chelating ligands based on cyclen form thermodynamically stable lanthanide complexes.[2] The desired chelator precursor is based on cyclen, with three acetate arms, and the remaining N-position functionalised with a benzimidazole unit (**7**). The structure of this molecule is shown in figure 112.

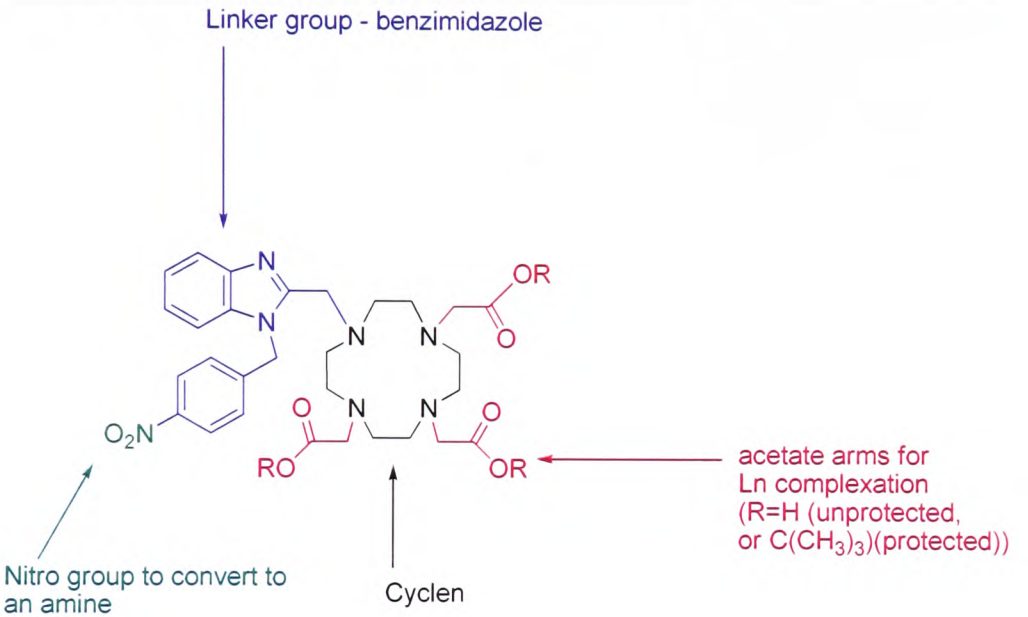

Figure 112 Chelator functionalised with a benzimidazole group

Methods for the synthesis of such functionalised chelators for lanthanide imaging agents include initial coupling of the functionalised arm (*i.e.* with a benzimidazole or benzyl unit), followed by attachment of the three acetate arms (method 1), or performing the two steps in reverse order (method 2)

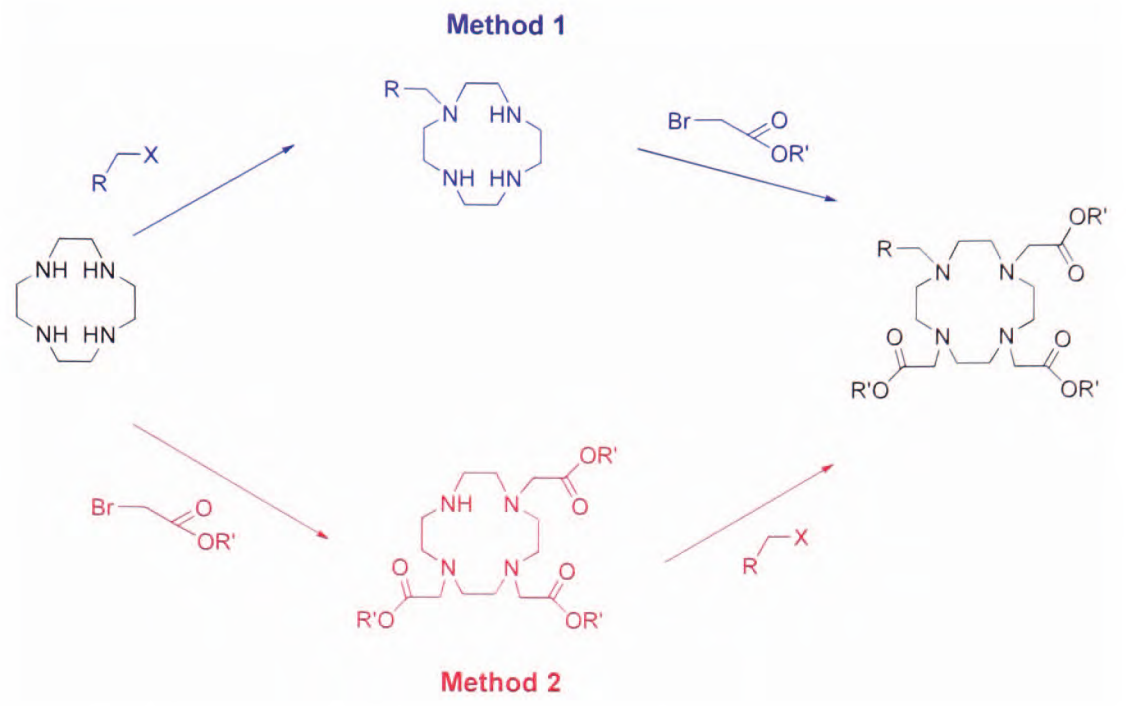

Figure 113 Synthetic method to produce the functionalised chelators, X = Cl, Br, and R' = $C(CH_3)_3$ or H

The preparation of functionalised chelators using method 1 has been investigated by Balogh *et al.* to produce monopropionate analogues of $DOTA^{4-}$ and $DTPA^{5-}$.[181] They investigated and compared two routes to synthesise these analogues. One route involved using an excess of the cyclen to selectively mono-alkylate, while the second route involved bridging the cyclen with glyoxal, that allows controlled mono-alkylation of the cyclen. The glyoxal bridge can be removed using hydrazine. The route is shown in figure 114.

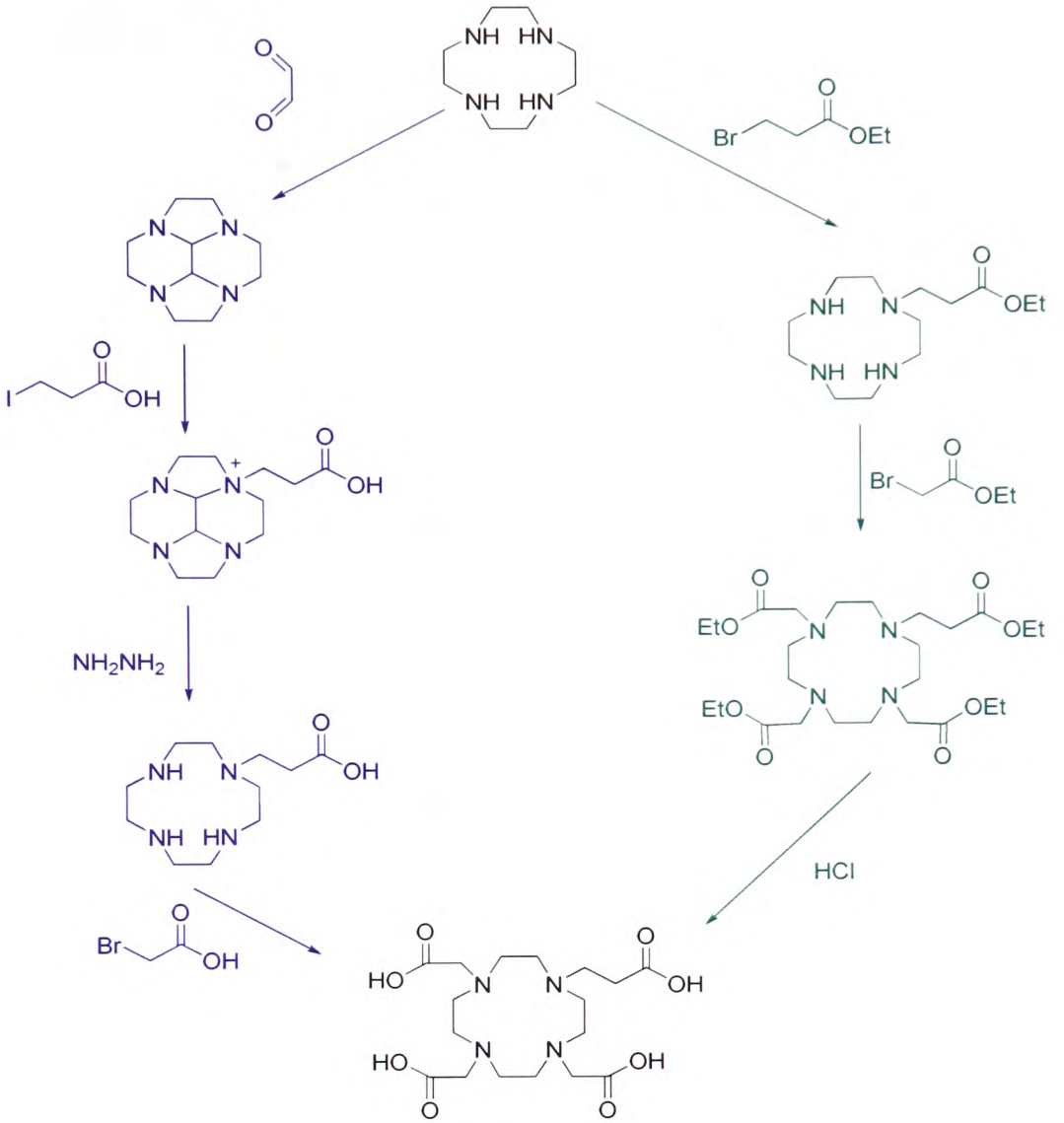

Figure 114 Two routes to produce DO3A chelator derivatives investigated by Balogh *et al.* [181]

To make their target compound via the bis-aminal route, cyclen is bridged using glyoxal and then mono-alkylated with 3-iodopropionic acid. The removal of the glyoxal bridge is performed by refluxing in hydrazine, and this is followed by alkylation at the remaining secondary amine position with chloroacetic acid in overall yields of 80%. The other route involves three steps and includes an initial selective mono-alkylation of cyclen with ethyl-3-bromopropionate, followed by the quantitative alklyation of the three amines with ethylbromoacetate, and then hydrolysis in 6 M HCl to give the product in 85% overall yield. When compared to method 2, these routes will either increase the number of steps, or lead to an excess use of cyclen that cannot be recovered.

Method 2 is therefore more advantageous because the 3-armed chelator (DO3A **(31)**) can be synthesised readily in reasonable yields to give a generally applicable precursor. The synthesis involves the initial preparation of DO3A **(31)** and then the remaining secondary amine is alkylated with the selected alkyl halide benzimidazole **(7)** or 4-nitrobenzyl bromide (figure 115).

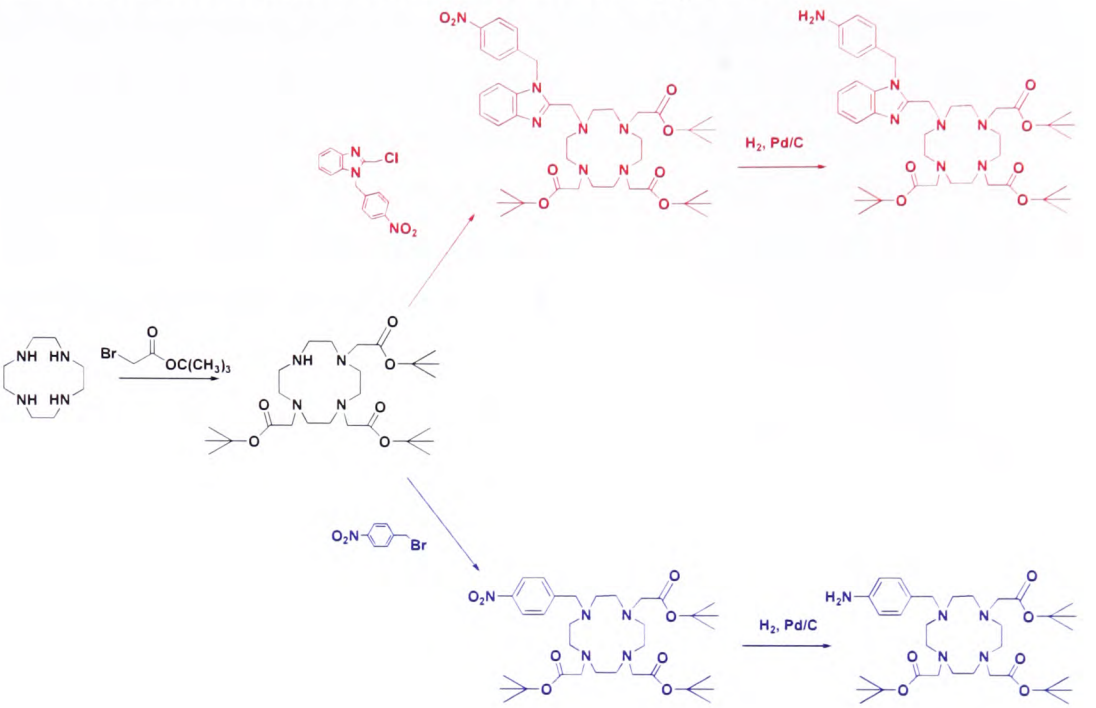

Figure 115 Proposed routes to produce a functionalised chelator with an appended amine moiety

The initial strategy involved the formation of the DO3A ligand by following a literature method using three equivalents of *tert*-butylbromoacetate to one equivalent cyclen.[77] The next step involved the attachment of the functional group, *e.g.* **(7)**, by stirring the two together with base and heating to reflux. Li *et al.* have synthesised a functionalized 1,4,7-triazacyclononane bearing benzimidazole groups, and numerous other groups have also reported the attachment of various alkyl halides to DO3A suggesting such reactions should readily occur.[143] Many literature reports have shown that the nitro group can be converted to an amine by a palladium on carbon catalysed hydrogenation, however there are potential issues with debenzylation of the functional arm.[182] [183] Sections 4.3 - 4.5 contains discussion of the synthesis of benzimidazole or benzyl amine bearing DO3A chelators

4.3 Synthetic strategy to produce chelators bearing a benzimidazole group

The coupling of the chelator DO3A **(31)** to the benzimidazole, 1-(4-nitrobenzyl)-2-bromomethyl benzimidazole **(7)** will form the compound 1,4,7-tris(*tert*-butoxycarbonylmethyl)-10-(1-(4-nitrobenzyl)-2-methylbenzimidazole)-1,4,7,10-tetraazacyclododecane **(32)**. The nitro group can then be converted to the amine by reduction and the lanthanide complexes formed for both the nitro **(34a-d)** and the amine bearing benzimidazole DO3A chelators **(37a-d)**. The routes to form the benzimidazole chelator DO3A derivatives and the lanthanide complexes are shown in figure 116.

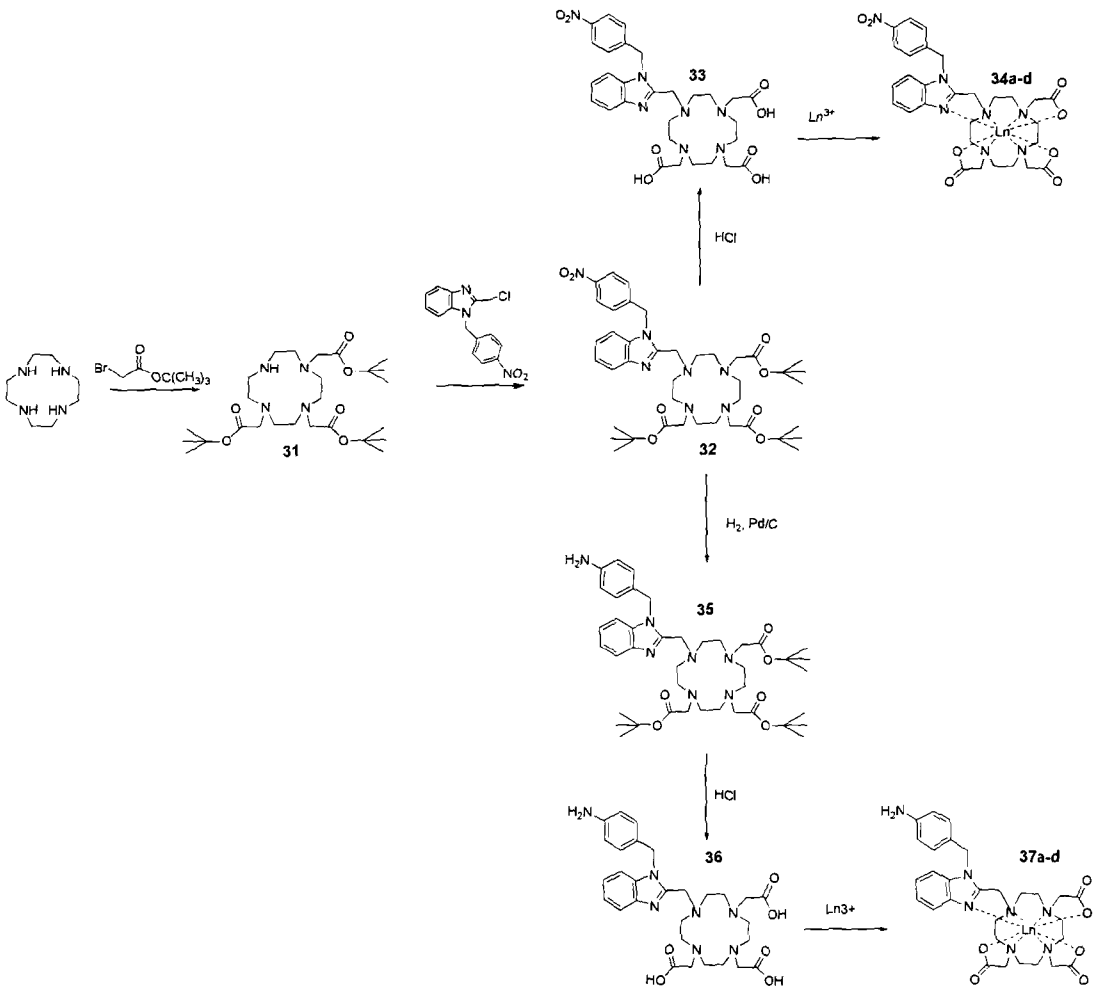

Figure 116 Synthetic scheme to produce the benzimidazole derivatives

4.3.1 Synthesis of 1,4,7-tris(*tert*-butoxycarbonylmethyl)-1,4,7,10-tetraazacyclododecane (31)

The synthesis of the tri-substituted cyclen (**31**) involves the selective alkylation of the cyclen ring. The initial attempt used 3 equivalents of the *tert*-butylbromoacetate dissolved in chloroform, which was added dropwise to a mixture of potassium carbonate and cyclen in chloroform. The solution was stirred for 72 hours and filtered to remove the inorganic material. The filtrate was then concentrated to leave a cream solid, which was purified by flash column chromatography, with a gradient elution of 100% dichloromethane to 5% methanol in dichloromethane. The resulting solid was washed with diethyl ether to yield a white solid in 56% yield. An alternative method was investigated where acetonitrile was used as the solvent instead of chloroform. This led to an increase in the yield to 60%. This compares well with the literature, with reported yields ranging from 42 – 73%.[184]

4.3.2 Synthesis of 1,4,7-tris(*tert*-butoxycarbonylmethyl)-10-(1-(4-nitrobenzyl)-2-methylbenzimidazole)-1,4,7,10-tetraazacyclododecane (32)

1-(4-Nitrobenzyl)-2-chloromethyl benzimidazole (**7**) was substituted onto DO3A (**31**) to form 1,4,7-tris(*tert*-butoxycarbonylmethyl)-10-(1-(4-nitrobenzyl)-2-methylbenzimidazole)-1,4,7,10-tetraazacyclododecane (**32**). A number of reaction conditions were investigated to form (**32**), which are described in this section, the synthetic scheme is shown in figure 117.

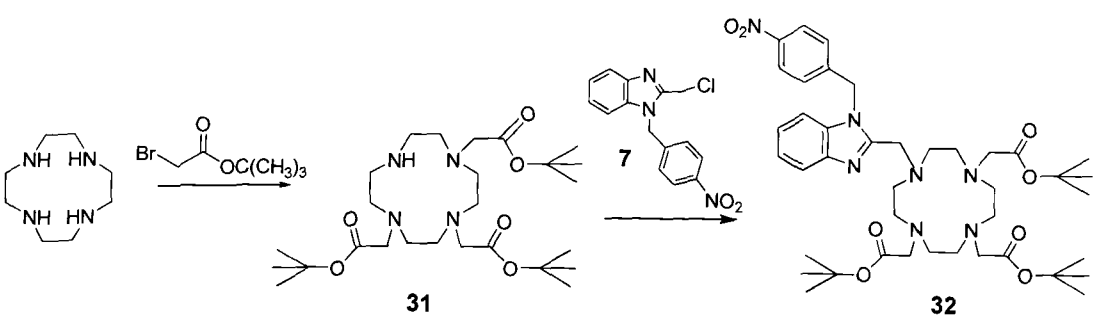

Figure 117 The synthetic route used to form (**32**)

The initial method attempted involved adding **(31)** to a mixture of **(7)** and three equivalents of potassium hydrogen carbonate in dry acetonitrile and then heating to reflux for 3 days. The reaction mixture was concentrated, and the residue purified by flash column chromatography on silica with an increasing gradient of methanol in dichloromethane to give the desired product in a 30% yield. However, attempts to repeat this reaction were unsuccessful. Therefore, efforts turned to improving the reactivity of the benzimidazole unit by the use of potassium iodide to replace the chloro group with an iodo group.

Attempts had been made to isolate the iodo derivative of the benzimidazole [attempted synthesis of **(8)**]. This route involved *in situ* generation of **(8)** by heating a solution of chloro benzmidazole **(7)** and potassium iodide and then performing the coupling reaction in acetonitrile with **(31)**. Analysis of the ^{1}H NMR spectrum, suggested that no reaction occurred, with t.l.c. analysis showing no products formed. The reaction was repeated, with no base and the use of a catalytic amount of potassium iodide in dry tetrahydrofuran. The first attempt resulted in **(32)** as a white solid in 78% yield after purification by flash column chromatography with a solvent gradient of 100% dichloromethane to 2% methanol in dichloromethane for the eluent. However, the reaction was not reproducible.

The issue is most probably with the protonation of the secondary amine on **(31)** and so conditions were altered to deprotonate this amine. Conditions investigated involved using either a two-fold excess of sodium hydride or lithium diisopropylamide. Analysis suggested that both bases caused reaction of the ester groups. Milder reaction conditions using potassium hydrogen carbonate as the base were investigated with dimethylformamide as the solvent. Analysis by ^{1}H NMR spectroscopy and t.l.c. suggested that no reaction had occurred. In a further attempt to deprotonate the amine, **(31)** was washed with a solution of sodium hydrogen carbonate and extracted into dichloromethane. The base wash removed the slight yellow colour to form a white solid. A ^{1}H NMR spectrum was recorded that showed the compound was intact after the base wash. The compound was then re-dissolved into acetonitrile with an eight-fold excess of the base sodium hydrogen carbonate and a slight excess of **(7)**

and was heated to 60°C for 24 hours. The solvent was removed and the product purified by flash column chromatography with an increasing gradient of methanol in dichloromethane to give a white solid in 76% yield. The ^{1}H NMR spectrum shows the typically broad peaks for cyclen based compounds with the CH_3 peaks at 1.42 ppm, and a broad multiplet from 2.2 – 3.5 ppm representing the other protons on the cyclen unit. A characteristic peak at 3.94 ppm represents the CH_2 group on the benzimidazole unit and the peak at 5.43 ppm was assigned to the CH_2 group on the nitro benzyl group. The expected peaks were identified in the ^{13}C NMR spectrum although the CH_2 group on the benzimidazole was masked by broadened CH_2 cyclen peaks. The identity of the compound was confirmed by high resolution mass spectrometry. The X-ray crystal structure of the sodium complex formed with **(32)** was obtained. The crystals were grown by slow evaporation of a dichloromethane solution over a period of two weeks, resulting in the formation of colourless blocks.

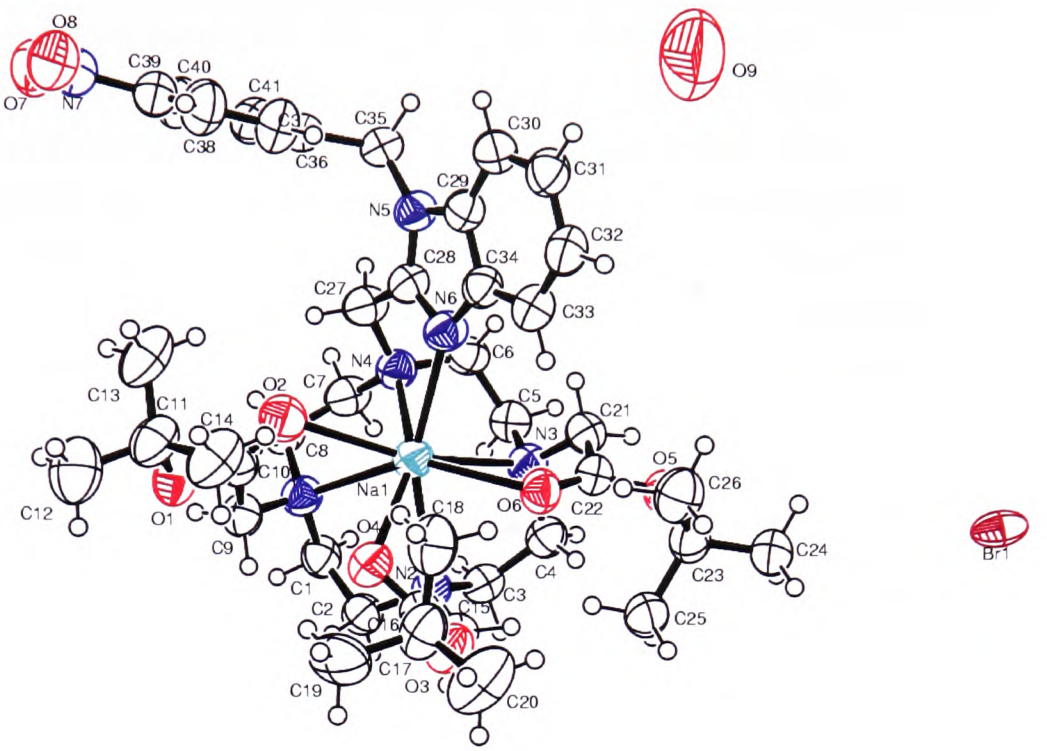

Figure 118 The molecular structure of the sodium bromide complex 1,4,7-tris(*tert*-butoxycarbonylmethyl)-10-(1-(4-nitrobenzyl)-2-methylbenzimidazole)-1,4,7,10-tetraazacyclododecane **(32)** showing the atom labelling and 50% probability ellipsoids for non-H atoms

The X-ray structure revealed a sodium ion coordinated to the neutral ligand with a bromide counter anion to balance the charge and a water molecule also present in the asymmetric unit. As shown in figure 119, the sodium ion is 8-coordinate sitting above the plane of the tetraazamacrocyclic cyclen ring and is encapsulated by the pendant arms, bonding to all four macrocyclic ring N-donors, three pendant ester arm O donors and to the N-3 position of the imidazole ring. The ionic radius of sodium metal (132 pm), is very similar to that of the lanthanides (gadolinium(III) = 119.3 pm, and europium(III) = 120.6 pm) and therefore the structure should be analogous to the lanthanide ion complexes that have not been structurally characterised. A selection of bond lengths and angles describing the coordination environment of the sodium ion are presented in table 10.

The Cambridge crystallographic database was searched to locate some relevant published structures for comparison of bond lengths and angles. Particularly relevant to this structure are the sodium complexes of the 1,4,7,10-tetra(ethoxycarbonylmethyl)-1,4,7,10-tetraazacyclododecane and 1,4,7,10-tetra(*tert*-butoxycarbonylmethyl)-1,4,7,10-tetraazacyclododecane ligands. Each of these structures have four pendant ester arms that are coordinated to form 8 coordinate sodium complexes. A third structure that is highly appropriate for comparison has sodium coordinated to a cyclen ligand with three pendant ester arms and a fourth arm with a coordinating pyridyl group, 1,4,7-tris(*tert*-butoxycarbonylmethyl)-10-(6-(bis(2-pyridylmethyl)aminoethyl)-2-pyridylmethyl)-1,4,7,10-tetraazacyclododecane.[184]

The sodium-cyclen N distances show some variation for $[Na\mathbf{32}]^+$ in the range 2.487(4) to 2.649(4) Å, which is in contrast to the two tetraester structures where the bond lengths were in the ranges, 2.523(2) Å to 2.557(2) Å and 2.532(5) Å to 2.580(6) Å, respectively for the ethoxy and *tert*-butoxy ester complexes. The unsymmetrical nature of the pendant arms may account for this deviation as the triester monopyridyl cyclen sodium complex shows greater variation with Na-N(cyclen) bond lengths in the range 2.551(2) to 2.665(2) Å. The Na-N benzimidazole distance in $[Na\mathbf{32}]^+$ is 2.498(4) Å. This is a longer distance than is observed for the Na-N bond lengths in other less sterically constrained sodium imidazole complexes, ca. 2.36(3) to 2.39(4) Å, but it is shorter than the Na- N(pyridyl) distance of 2.797(4) Å in the related unsymmetric Na cyclen structure, possibly explaining the greater distortion of the other Na-N bond lengths in $[Na\mathbf{32}]^+$.[184 183]

In $[Na\mathbf{32}]^+$ the sodium is bonded to the carbonyl oxygen of all three pendant arms with bond lengths in the range 2.451(4) to 2.681(3) which are consistent with the known structures. The angles N(cyclen)-Na-O/N(attached pendant) are in the range 64.38(13) to 68.41(12)° for $[Na\mathbf{32}]^+$ which is comparable to the other known structures. However, the largest angle in the structure is the N(cyclen)-Na-N(benzimidazole) in$[Na\mathbf{32}]^+$, again suggesting that the chelator is

distorting slightly to optimise the favourable bonding interaction between the sodium and the imidazole.

The space filling diagram, figure 119(b), shows that access to the metal centre is blocked by the *tert*-butyl groups which limits the potential for a further ligand to bind, preventing the formation of species with higher coordination numbers. However, the tetra-ethoxyester cyclen structure still has an 8 coordinate metal centre despite reduced steric bulk. It is also relevant to note that the nitrobenzyl group protrudes in an appropriate orientation for attachment of other molecules without interfering with binding of the chelator to the metal centre. This is important for the formation of functional lanthanide complexes.

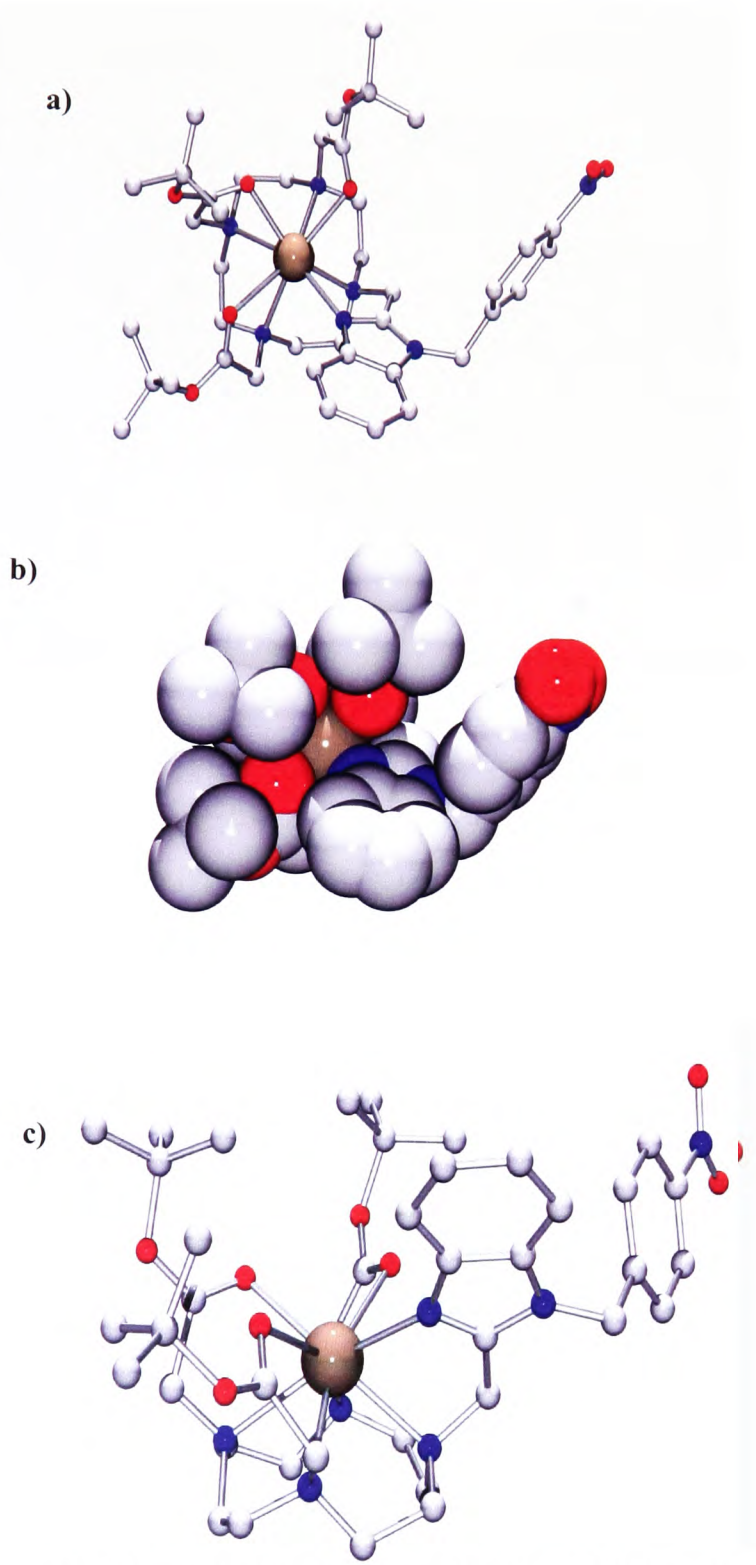

Figure 119 Ball and stick representations of [Na**32**]$^+$ (a) view from above, (b) space filling view from above and (c) view from the side

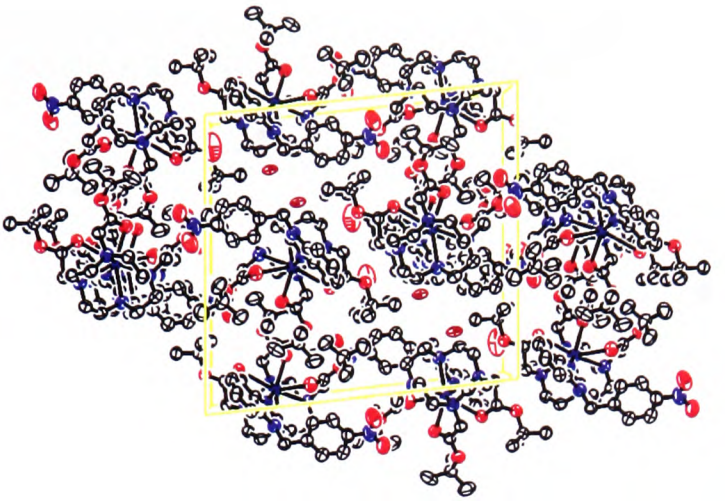

Figure 120 Packing diagram for the X-ray structure of the sodium complex with $[Na32]^+$ (unit cell shown in yellow)

The packing diagram shows layers of bromide anions and layers of complex cations, see figure 120. In contrast to the crystal structures of the benzimidazole precursors **(5)** and **(7)**, no short intermolecular π-stacking or edge to face phenyl interactions are present.

Bond length Å		N(1)-Na(1)-O(6)	151.99(13)
N(1)-Na(1)	2.632(4)	N(4)-Na(1)-N(3)	73.13(12)
N(2)-Na(1)	2.649(4)	N(6)-Na(1)-N(3)	90.55(14)
N(3)-Na(1)	2.596(4)	O(2)-Na(1)-N(3)	160.46(14)
N(4)-Na(1)	2.487(4)	O(4)-Na(1)-N(1)	82.51(12)
N(6)-Na(1)	2.498(4)	N(4)-Na(1)-N(1)	70.93(13)
O(2)-Na(1)	2.594(4)	N(6)-Na(1)-N(1)	127.02(13)
O(4)-Na(1)	2.451(4)	O(2)-Na(1)-N(1)	64.38(12)
O(6)-Na(1)	2.681(3)	N(3)-Na(1)-N(1)	108.58(13)
Bond and torsion angles °		O(4)-Na(1)-N(2)	64.50(12)
O(4)-Na(1)-N(4)	152.64(13)	N(4)-Na(1)-N(2)	109.66(14)
O(4)-Na(1)-N(6)	127.29(14)	N(6)-Na(1)-N(2)	158.37(14)
N(4)-Na(1)-N(6)	68.41(13)	O(2)-Na(1)-N(2)	120.50(13)
O(4)-Na(1)-O(2)	75.01(12)	N(3)-Na(1)-N(2)	68.86(12)
N(4)-Na(1)-O(2)	87.35(13)	N(1)-Na(1)-N(2)	68.60(11)
N(6)-Na(1)-O(2)	81.13(13)	O(4)-Na(1)-O(6)	80.06(11)
O(4)-Na(1)-N(3)	123.40(12)	N(4)-Na(1)-O(6)	126.96(12)
N(6)-Na(1)-O(6)	80.95(11)	O(2)-Na(1)-O(6)	130.31(13)
N(3)-Na(1)-O(6)	64.74(11)	N(2)-Na(1)-O(6)	84.09(11)

Table 10 Selected bond lengths [Å] and angles [°] for sodium complex of $[Na32]^+$

4.3.3 Synthesis of lanthanide complexes of 1,4,7-tris(carboxymethyl)-10-(1-(4-nitrobenzyl)-2-methylbenzimidazole)-1,4,7,10-tetraazacyclododecane (34a-d)

The lanthanide complexes of the nitrobenzyl benzimidazole DO3A chelator **(32)** were synthesised. The gadolinium(III) complex is of interest as these highly paramagnetic compounds can act as MRI contrast agents. The europium(III) and terbium(III) complexes are expected to be luminescent and could have appropriate properties for optical imaging. Lanthanum(III) is diamagnetic and the resulting complex can be analysed by NMR without the paramagnetic shifts that would be observed for the other lanthanide ions.

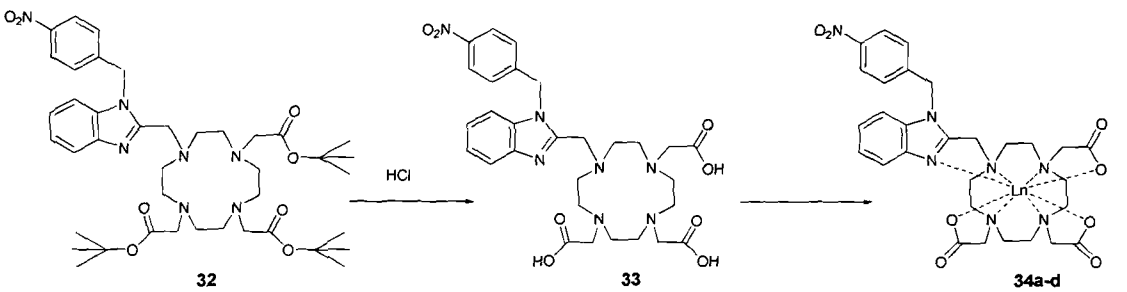

Figure 121 The synthesis of the lanthanide complexes of the ligand (L) 1,4,7-tris(carboxymethyl)-10-(1-(4-nitrobenzyl)-2-methylbenzimidazole)-1,4,7,10-tetraazacyclododecane **(34a - d)** where **(34a)** = EuL, **(34b)** = TbL, **(34c)** = GdL and **(34d)**=LaL

The *tert*-butyl ester groups were removed from the acetate arms using conc. hydrochloric acid. The solution was concentrated, the residue re-dissolved into water and filtered through a 0.2 μm syringe filter to remove any insoluble material. After removal of the solvent, a yellow solid was isolated. The ^{1}H and ^{13}C NMR spectra contain broad peaks making assignment difficult, however the peaks that represented the *tert*-butyl group are no longer present. High resolution mass spectrometry showed the identity of the molecular ion peak.

The lanthanide metal ions used to prepare complexes were europium(III), gadolinium (III), lanthanum(III) and terbium(III). The complexation reactions were carried out in water using either the triflate or chloride metal salts. A base was used to deprotonate the HCl salt of the ligand. Care was taken to avoid formation of lanthanide hydroxide salts, which tend to be less soluble and

precipitate from solution. The reaction mixture was heated at reflux overnight in each case. The solution was concentrated, and the product was purified using size exclusion chromatography on LH-20 sephadex. The europium(III) complex **(34a)** formed as a yellow solid in a yield of 68%. The ^{1}H NMR spectrum was recorded for the paramagnetic europium(III) complex as information about the coordination geometry can be obtained from the shifted spectrum. The peaks were observed in the range of -18 to 30 ppm, the spectrum is shown in figure 122.

It has been shown that two isomers are present for lanthanide(III) DOTA complexes in aqueous solution, a square antiprism and a twisted square antiprism. The exchange process between the two isomers is slow enough to be observed on the NMR timescale, where two sets of six resonances are observed for the diastereotopic CH_2CO and ring NCH_2CH_2N protons. Aime and co-workers have identified these isomers and have shown that the major isomer in solution adopts the square antiprism shape, where there is a shift to higher frequency of the closest axial ring protons, with the minor isomer generally forming less shifted proton resonances.[185, 186] The ratio of these isomers varies depending on the size of the lanthanide, concentration and counterion. Aime and co-workers have also performed NMR structural studies on the lanthanide(III) complexes of 1,4,7,10-tetraazacyclododecane-4,7,10-triacetic-1-(H_4DO3A-P).[187] Here it was shown that there was a higher abundance of the fast-exchanging twisted square antiprism compared to the square antiprism.[185] Using the information from these papers, identification of the isomers present for the europium(III) complex **(34a)** was attempted. The peaks representing the square antiprism can be identified between 30.9 – 28.82 ppm (as these peaks are more shifted), while the exchanging twisted square antiprism is located around 10.62 – 9.5 ppm. The ratio is in favour of the square antiprism at around 2:1.

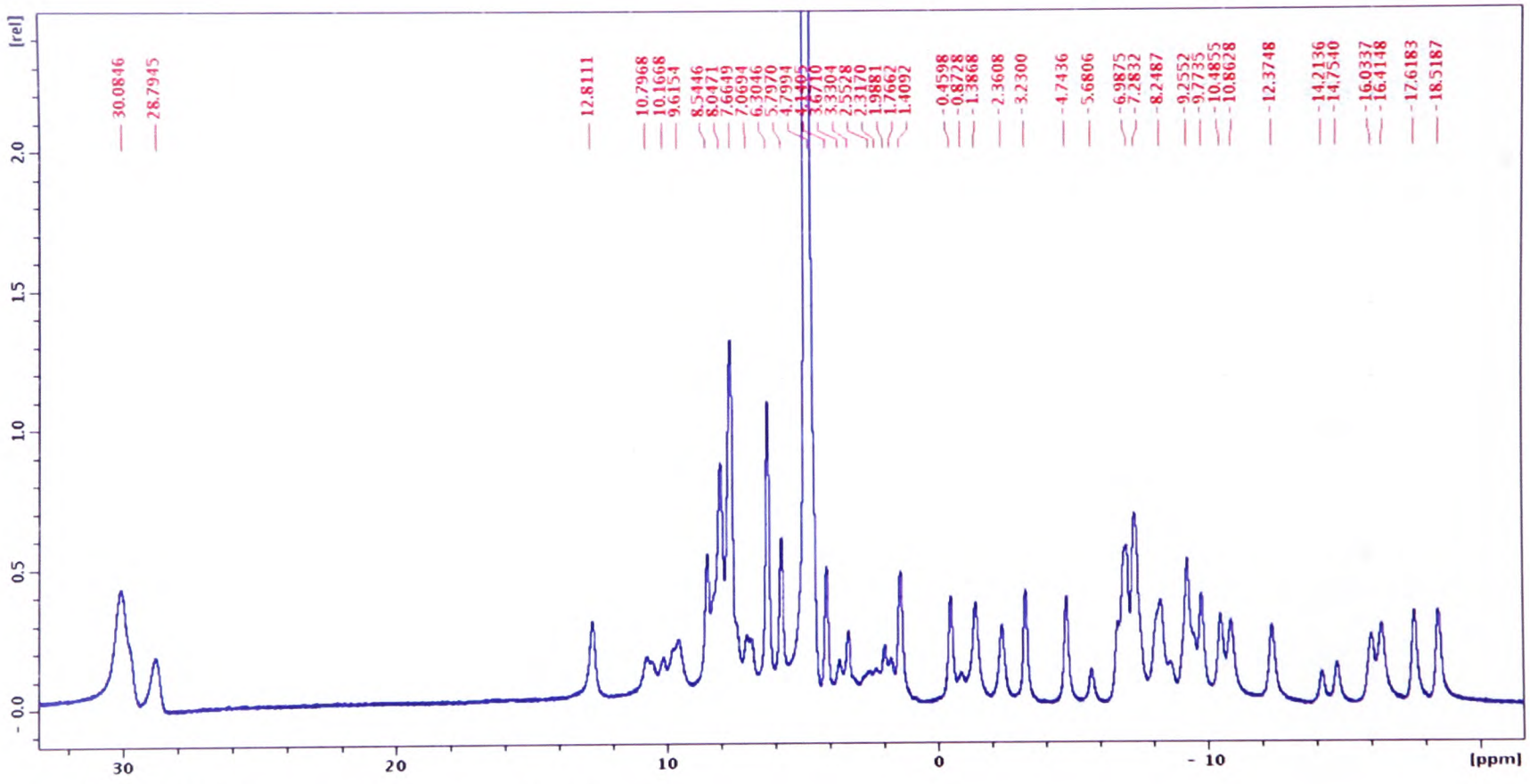

Figure 122 The ^{1}H NMR spectrum of the europium(III) complex (34a)

The terbium(III), gadolinium(III) and lanthanum(III) complexes **(34b-d)** were prepared in yields of greater than 70%. The identity of the compound was confirmed by high resolution mass spectrometry. The ^{1}H NMR spectrum of the lanthanum(III) complex **(34d)** is shown in figure 123.

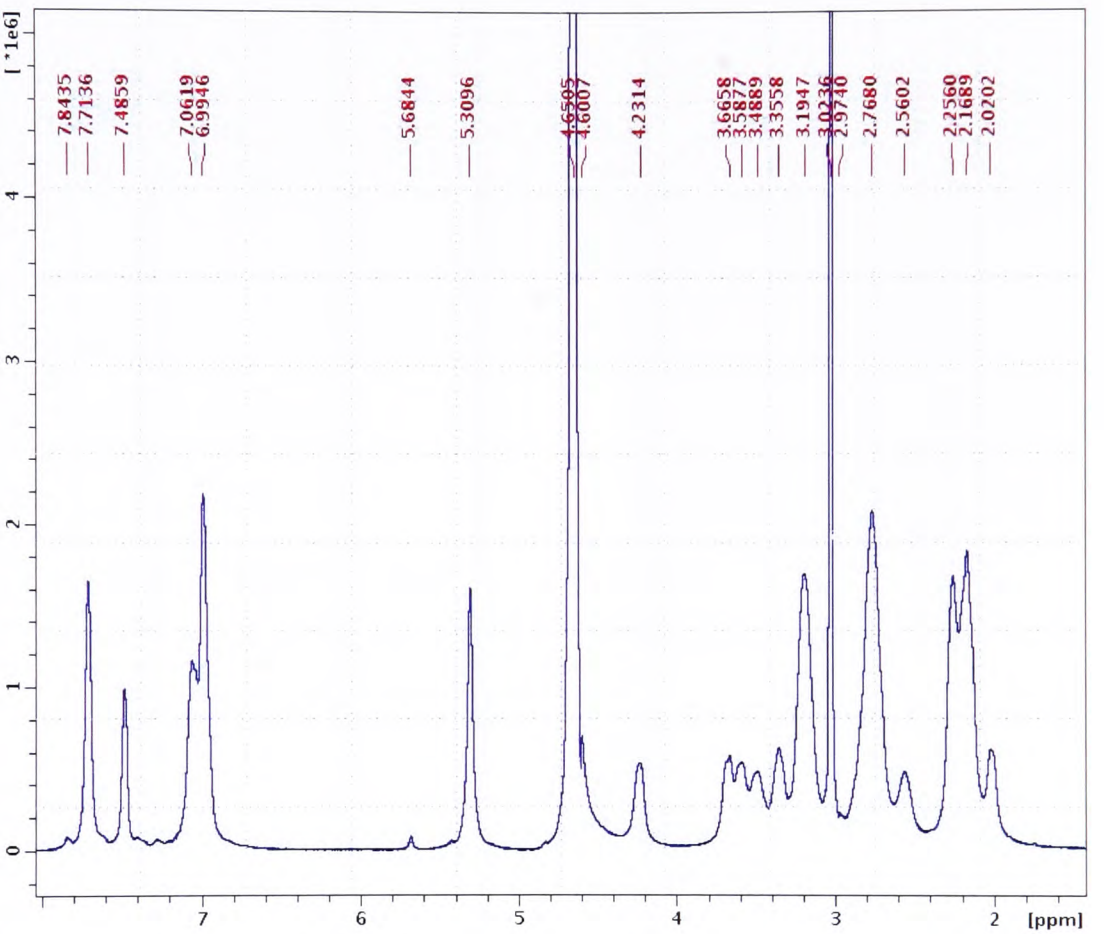

Figure 123 ^{1}H NMR spectrum of the lanthanum(III) complex **(44d)**

Both the alkyl and aromatic regions are broad making complete assignment difficult. However, the peaks at 4.2 and 5.3 ppm can be assigned to the CH_2 on the benzimidazole, and the CH_2 peak on the nitro benzyl group respectively. ^{13}C and DEPT NMR studies were also performed and the spectra are shown in figure 124.

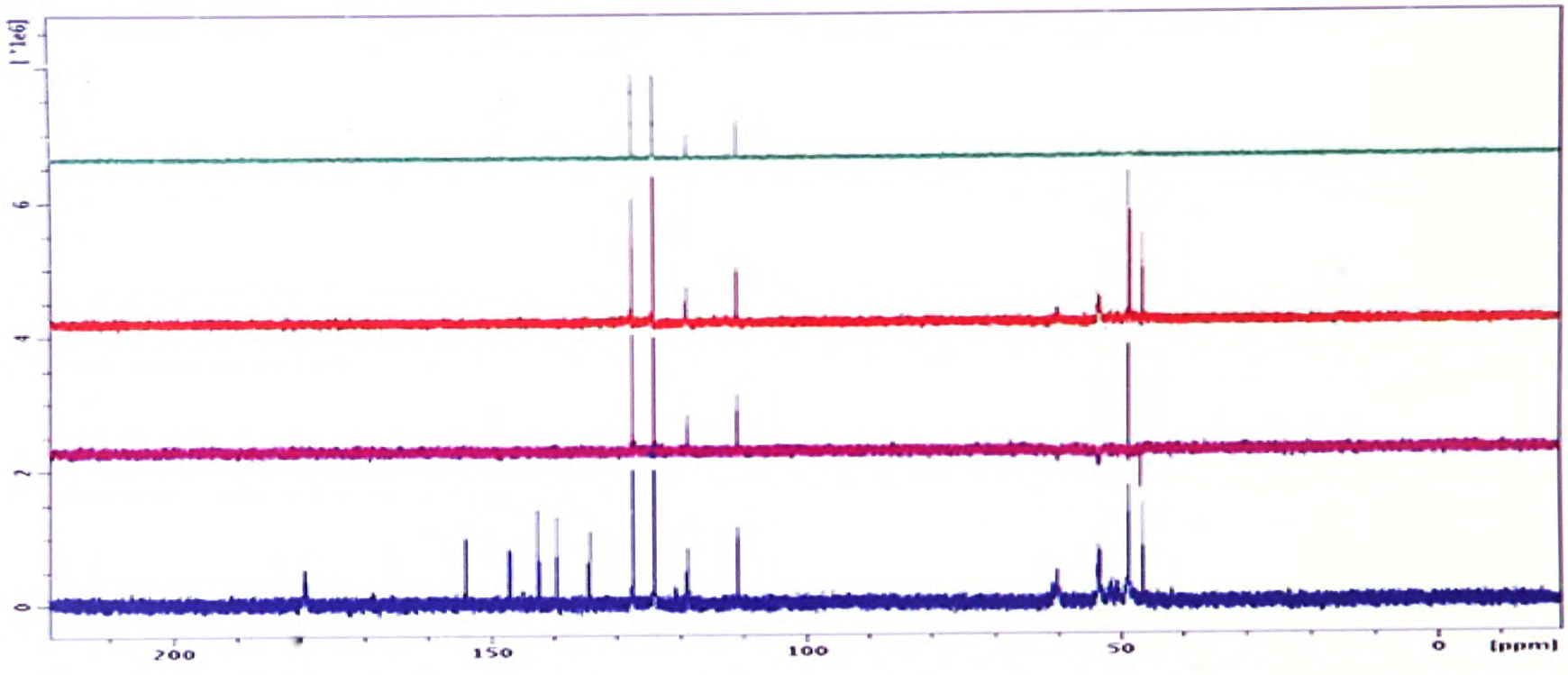

Figure 124 ^{13}C and DEPT NMR spectra of the lanthanum(III) complex **(34d)**. The blue graph represents the 13C NMR spectrum, the purple graph represents the DEPT 135o spectrum, the red graph represents the DEPT 45o spectrum, and the green graph represents the DEPT 90° spectrum

The blue graph represents the ^{13}C NMR spectrum, the purple graph represents the DEPT 135° spectrum, the red graph represents the DEPT 45° spectrum, and the green graph represents the DEPT 90° spectrum. Varying the degree of the pulse will alter the orientation of the peaks on the plot, and allow assignment of the number of directly attached protons on each carbon. The DEPT 135 spectrum can be used to assign the CH and the CH_3 peaks as they point up on the graph, and the CH_2 peaks point down, with the C peaks suppressed. While the DEPT 90 spectrum will only show the CH peaks, and the dept 45 spectrum contains the CH, CH_2 and CH_3 peaks (point up) with the C peaks suppressed. Using this data, the ^{13}C NMR spectrum is shown to contain 6 C peaks, 6 CH peaks and a CH_3 peak. Complete assignment of the CH_2 peaks is challenging because they are broad and overlapping.

The proton-carbon correlation spectrum is shown in figure 125. The alkyl region between 2.02 – 4.23 ppm correlates with the CH_2 region between 46.51 – 60.72 ppm. The aromatic proton peaks at 7.48 and 7.84 ppm correlate with the carbon peaks at 118.79 and 123.99 ppm respectively. These peaks can be assigned to the benzimidazole unit.

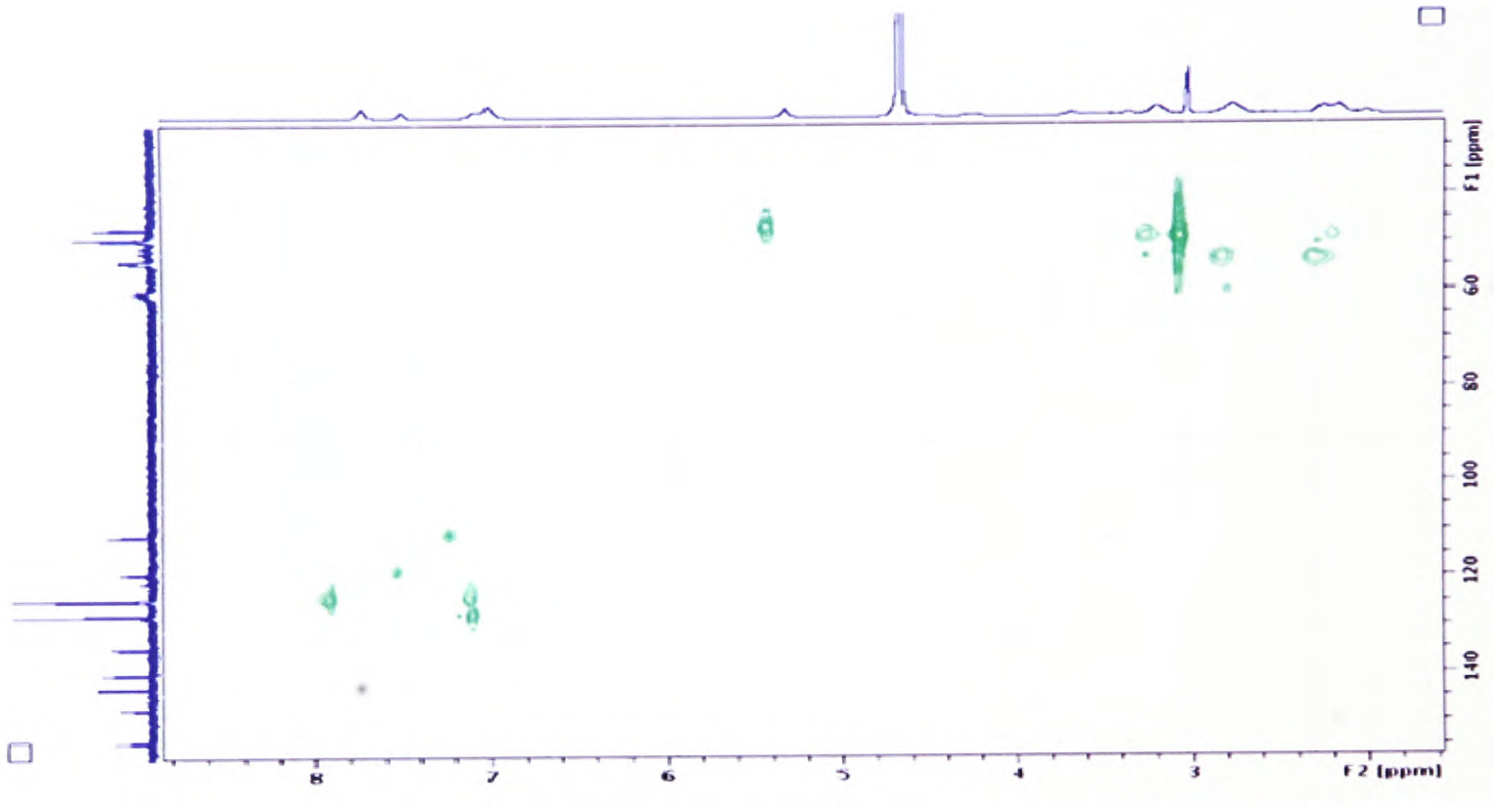

Figure 125 Proton-carbon correlation spectrum of the lanthanum complex (34d)

4.4 Synthesis of a chelator bearing an aminobenzyl benzimidazole

The next stage in the synthesis involves the conversion of the nitro group to a primary amine. An example of this reaction was investigated by Sircar *et al.* where a nitro benzyl substituted imidazole based compound was converted to an amine by the use of a palladium on carbon catalyst under a hydrogen atmosphere in a yield of 78% yields (figure 126).[188]

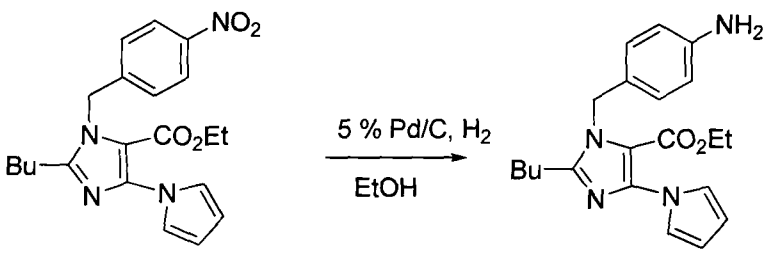

Figure 126 Hydrogenation reaction carried out by Sircar *et al.*[188]

In the literature, palladium on carbon is commonly used to remove benzyl groups from the macrocycle, cyclen and cyclam, and Nwe *et al.* have shown that using it with cyclohexane can remove 4-nitrobenzyl groups from cyclen.[189] However, the nitrobenzyl substituted imidazole compound in figure 126 is similar to the benzimidazole compound (**7**), the first method investigated was the use of palladium on carbon.

4.4.1 Synthesis of 1,4,7-tris(*tert*-butoxycarbonylmethyl)-10-(1-(4-aminobenzyl)-2-methylbenzimidazole)-1,4,7,10-tetraazacyclododecane (35)

The initial method employed, involved a solution of (**32**) dissolved in methanol, to which 5% palladium on carbon was added and the solution stirred for 24 hours under a hydrogen atmosphere. Analysis suggested that a reaction occurred, however, the isolated compound was not the desired product (**35**) or starting material (**32**). This suggested that debenzylation of either the

nitrobenzyl group from the benzimidazole unit, or the benzimidazole unit from DO3A had occurred.

Lalancette *et al.* have reported the use of a selective reducing agent, sulfurated borohydride, that can reduce a nitro group to the corresponding amine, without interfering with halogens, esters, nitriles, olefins or ethers.[190] The proposed synthetic route to convert the nitro compound **(32)** to the corresponding amino compound **(35)** using this sulfurated borohydride is shown in figure 127.

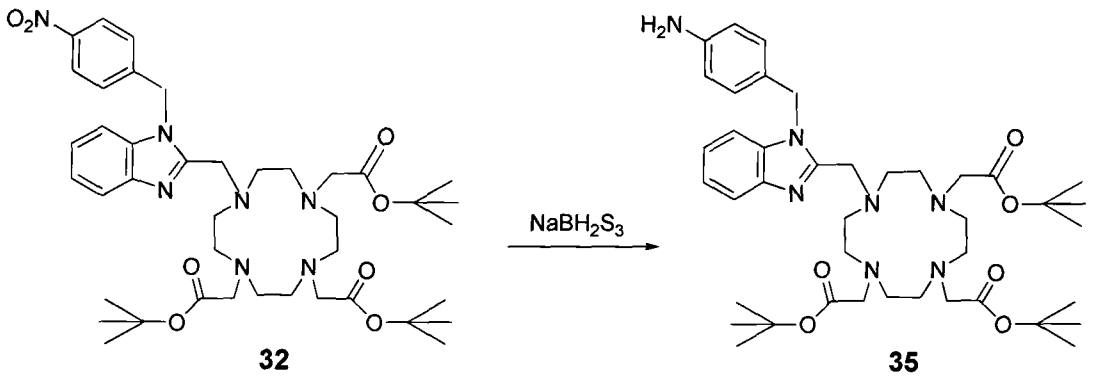

Figure 127 Reaction scheme for the preparation of the aminobenzyl benzimidazole DO3A derivative **(35)**

The sulfurated borohydride was prepared *in situ* by stirring sodium borohydride and sulphur in dry tetrahydrofuran under nitrogen for one hour. During this time, an evolution of hydrogen gas occurs as the sulfurated product forms ($NaBH_2S_3$). The addition of the nitro benzimidazole DO3A chelator **(32)** was added as a solution in dry tetrahydrofuran and the reaction mixture heated at reflux for 24 hours. The product was purified by flash chromatography on alumina with an increasing gradient of methanol in dichloromethane to form a yellow solid in 65% yield. Analysis by ^1H NMR spectroscopy, confirms the formation of the amine product by the shift of the relevant aromatic peaks to 6.52 and 6.75 ppm and a decrease in the coupling constant to 8.0 Hz. In the ^{13}C NMR spectrum, there is a shift in peak position of the carbon coupled to the amine to 115.25 ppm.

4.4.2 Synthesis of the lanthanide(III) complexes of 1,4,7-tris(carboxymethyl)-10-(1-(4-aminobenzyl)-2-methylbenzimidazole)-1,4,7,10-tetraazacyclododecane (37a-d)

The lanthanide(III) complexes of the aminobenzyl benzimidazole DO3A chelator **(35)** were prepared after removal of the *tert*-butyl groups from the acetate arms by reaction with the appropriate metal salt **(37a-d)**. The reaction scheme for the synthesis of the lanthanide(III) complexes **(37a-d)** is shown in figure 128.

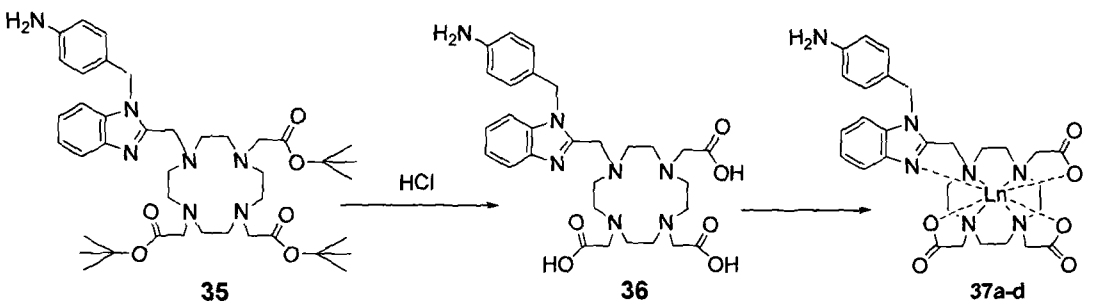

Figure 128 Proposed reaction scheme for the synthesis of the lanthanide complexes **(37a-d)** where **(37a)** = EuL, **(37b)** = TbL, **(37c)** = GdL and **(37d)** = LaL

The deprotection of **(35)** gave a yellow solid in 93% yield with the identity of the compound confirmed by ^{1}H NMR spectroscopy, ^{13}C NMR spectroscopy and high resolution mass spectrometry

The lanthanide complexes **(37a-d)** were prepared in yields of greater than 60%. The identity of the compounds were confirmed by high resolution mass spectrometry. The ^{1}H NMR spectrum for the europium(III) complex is shown in figure 129.

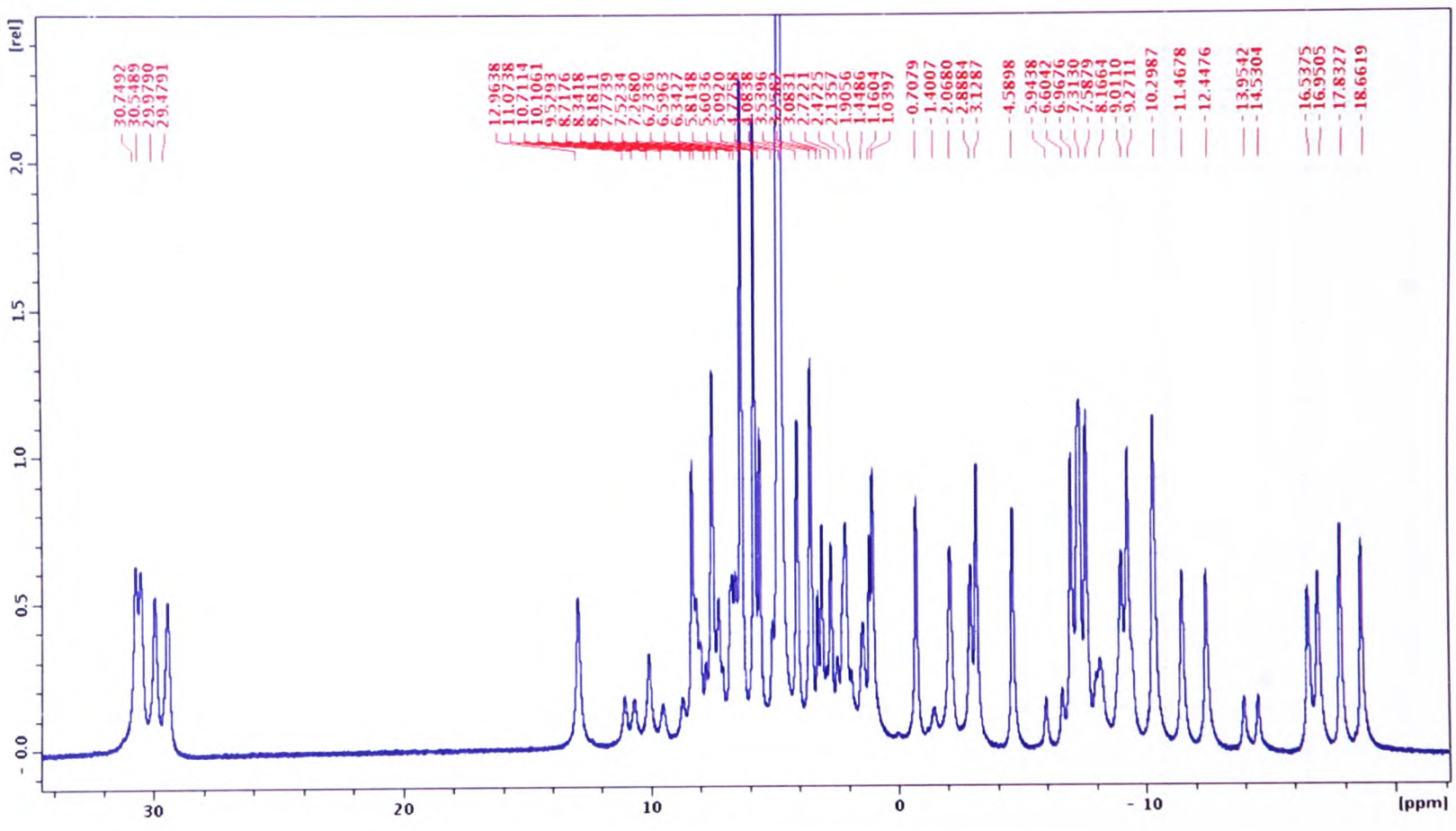

Figure 129 ^{1}H NMR spectrum of the europium(III) complex **(37a)**

The peaks in the ^{1}H NMR spectrum show the typical shifted peaks for the europium(III) metal complex. The spectrum is very similar to that of the nitrobenzyl benzimidazole europium(III) complex **(34a)**. A similar isomer distribution pattern can be seen here with the 4 peaks between 39.75 - 29.48 ppm for the square antiprism and the peaks for the twisted square antiprism between 11.07 – 10.1 ppm in a 2:1 ratio.

The ^{1}H NMR spectrum of the lanthanum(III) complex is shown in figure 130. The ^{1}H NMR spectrum is broad with overlapping CH_2 peaks from the DO3A ring making complete assignment difficult. The two singlet peaks at 4.79 and 5.87 ppm can be assigned to the CH_2 groups on the benzimidazole unit and amino benzyl group respectively. The ^{13}C NMR spectrum in figure 131, shows the shift in the C peak to 125.0 ppm compared to the lanthanum(III) nitrobenzyl benzimidazole DO3A complex **(34d)** due to the conversion of the nitro group to an amine.

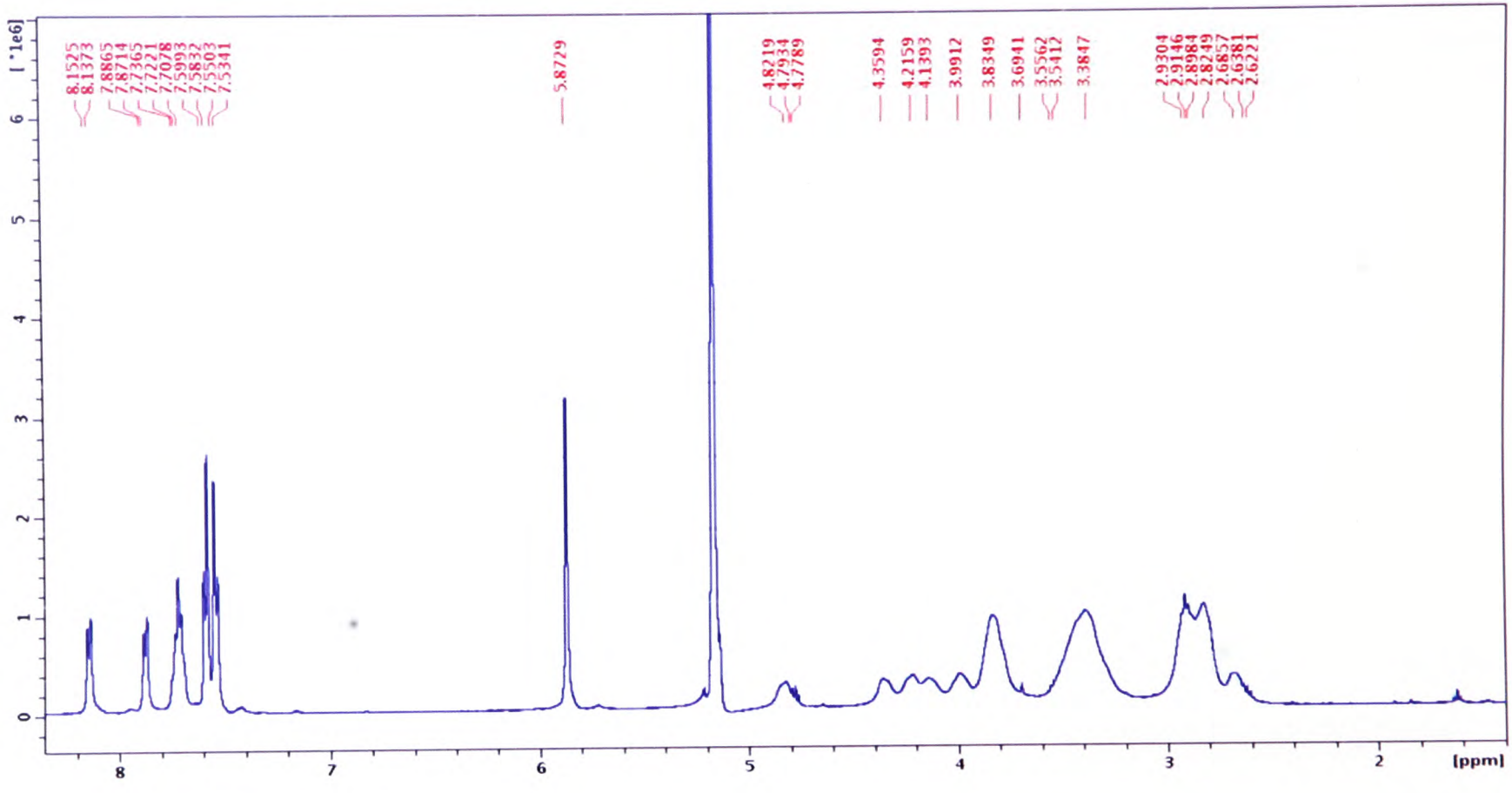

Figure 130 The ^{1}H NMR spectrum of the lanthanum(III) complex **(37d)**

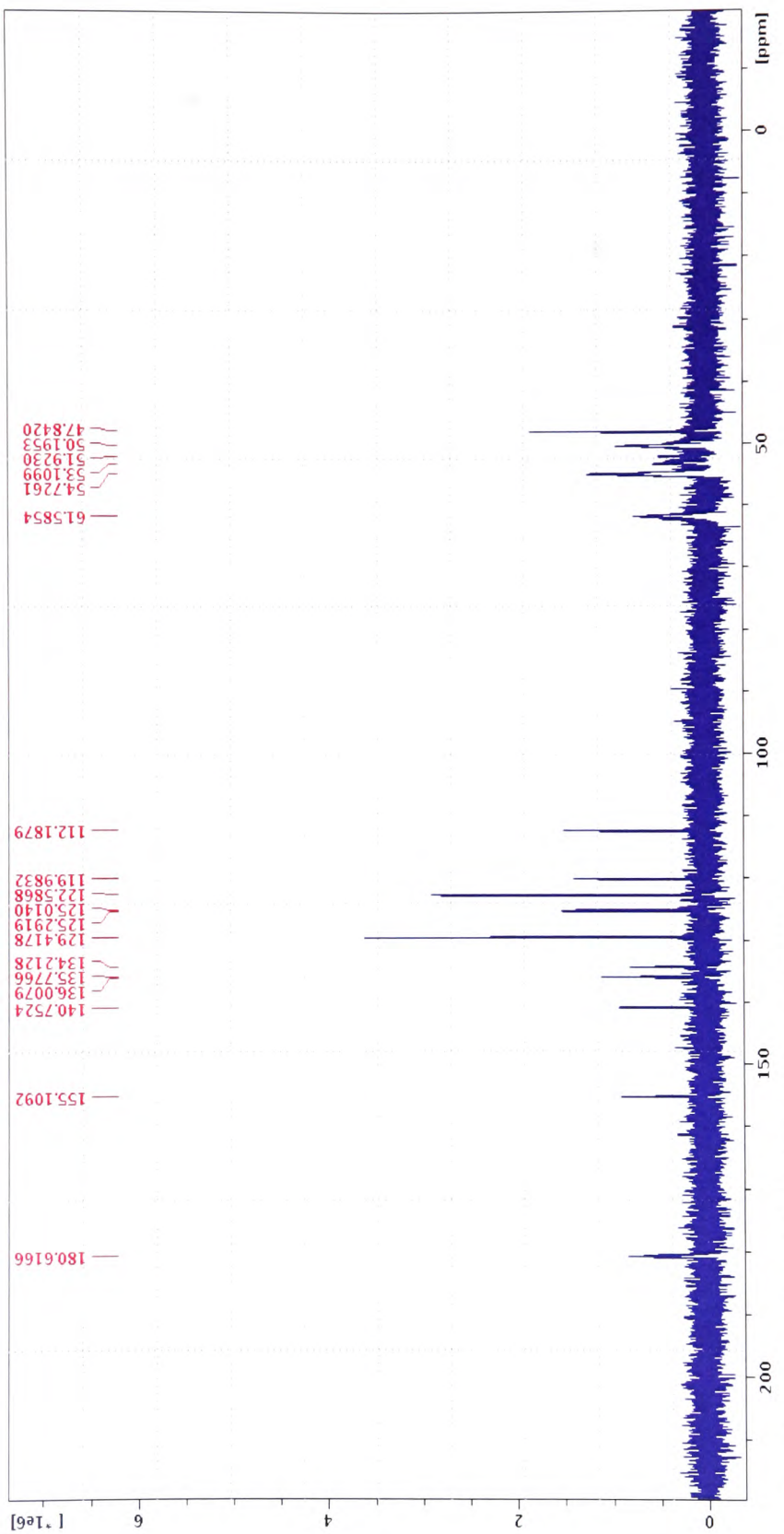

Figure 131 The ^{13}C NMR spectrum of the lanthanum(III) complex **(37d)**

4.5 Synthesis of a chelator bearing an aminobenzyl derivative

As an alternative compound to the nitrobenzyl benzimidazole functionalised chelator (**7**), 4-nitrobenzylbromide was coupled to DO3A (**31**) to form 1,4,7-tris(*tert*-butoxycarbonylmethyl)-10-(4-nitrobenzyl))-1,4,7,10-tetraazacyclododecane (**38**). This synthetic method is well characterised in the literature, Maillet *et al.* have shown that the formation of the nitrobenzyl DO3A derivative can be undertaken by the selective reaction of 4-nitrobenzylbromide with a ten-fold excess of cyclen in the prescence of sodium hydride, followed by treatment with bromoacetate to give the desired product in a yield of 50%.[191] They also investigated an alterative synthetic route, where the tri-substituted cyclen with three ethyl bromoacetate arms was synthesised initially and then substituted with 4-nitrobenzylbromide on the remaining secondary amine position. They reported a lower overall yield of 37% in comparison to other reports which quote yields of greater than 69%.[191] The nitro group can be converted to a primary amine to form 1,4,7-tris(*tert*-butoxycarbonylmethyl)-10-(4-aminobenzyl))-1,4,7,10-tetraazacyclododecane (**39**) using palladium on carbon.[94] As (**31**) had already been prepared in good yields, it was decided to couple 4-nitrobenzylbromide to (**31**), followed by the conversion of the nitro group to an amino group (figure 132).

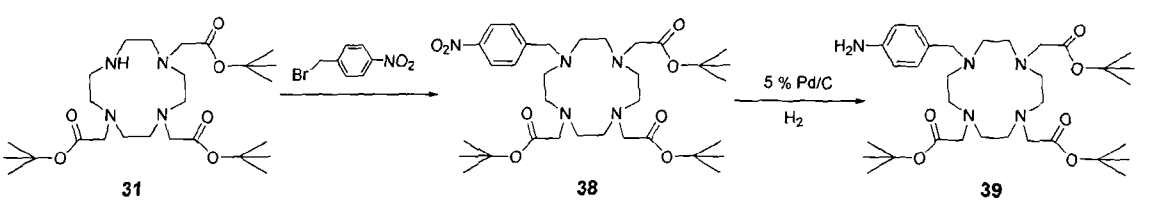

Figure 132 Reaction scheme for the preparation of (**39**)

4.5.1 Synthesis of 1,4,7-tris(*tert*-butoxycarbonylmethyl)-10-(1-(4-aminobenzyl))-1,4,7,10-tetraazacyclododecane (39)

The synthetic procedure used to synthesise **(38)** was the same as that used to synthesise the benzimidazole compound **(32)**. **(31)** was dissolved in dry acetonitrile, with both an eight fold excess of sodium hydrogen carbonate and a slight excess of 4-nitrobenzylbromide added. The reaction mixture was heated to 70°C and stirred for 24 hours under a nitrogen atmosphere. The compound was then purified by flash column chromatography on silica with an increasing gradient of methanol in dichloromethane to yield a white solid. In the ^{1}H NMR spectrum, the *tert*-butyl peak was at 1.23 ppm, with a multiplet between 2.0 – 3.09 ppm with a total integration of 24 protons representing the CH_2 protons. The aromatic region shows two coupled doublets at 7.5 and 8.0 ppm with a total integration of 4 protons, and a splitting constant of 8.44 Hz. The ^{13}C NMR spectrum contains the *tert*-butyl CH_3 peak at 27.9 ppm, with six CH_2 peaks ranging from 50.0 – 65.7 ppm. The $C(CH_3)_3$ peaks appear at 82.5 and 83.0 ppm, with the aromatic CH peaks at 123.6 and 131.1 ppm and the aromatic carbon peaks at 145.3 and 147.2 ppm. The carbonyl peaks are at 172.6 and 173.7 ppm.

To reduce the nitro group on compound **(38)** to give the corresponding amino compound **(39)**, the literature procedure using 5% palladium on carbon was followed. This resulted in a white solid **(39)** in 85% yield. Both the ^{1}H NMR and ^{13}C NMR spectra showed a shift in the aromatic peaks due to the formation of the amino group. The identity of the product was also confirmed by electrospray mass spectrometry

4.5.2 Synthesis of lanthanide complexes of 1,4,7-tris(carboxymethyl)-10-(4-aminobenzyl))-1,4,7,10-tetraazacyclododecane (41a-c)

The lanthanide complexes of the amino benzyl DO3A chelator **(39)** were prepared after removal of the *tert*-butyl groups from the acetate arms with acid.

The reaction scheme detailing the synthesis of the lanthanide complexes **(41a-c)** is shown in figure 133.

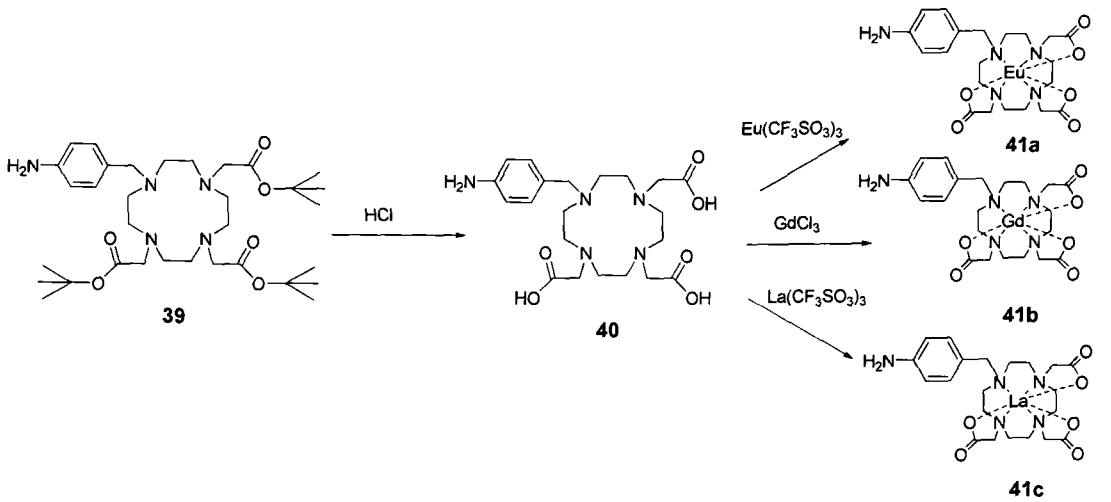

Figure 133 The synthetic scheme for the synthesis of the lanthanide complexes **(41a-c)**

Trifluoroacetic acid has previously been used to remove the *tert*-butyl groups from acetate arms. The method attempted with **(39)** was to suspend the compound in a solution of trifluoroacetic acid in dichloromethane and then stir for 24 hours at room temperature. After 24 hours, t.l.c. analysis was performed but this showed that only starting material **(39)** was present. Thus the deprotection was carried out by stirring in concentrated hydrochloric acid for 3 hours, which resulted in a yellow solid. The ^{1}H NMR spectrum was very broad, however the peaks that represented the *tert*-butyl groups are no longer present.

The europium(III), gadolinium(III) and lanthanum(III) complexes of the aminobenzyl DO3A chelator **(51a-c)** were prepared in yields of greater than 75%. Electrospray mass spectrometry was used to identify the molecular ion peaks of the lanthanide complexes.

4.6 Synthetic strategy for the preparation of multi-modality imaging agents

The synthetic strategy used in the preparation of a multi-modality agent involves coupling an optical dye (rhodamine and BODIPY derivatives) and a DO3A chelator. A number of strategies were investigated and the routes are depicted in figure 135.

4.6.1 The attempted preparation of lanthanide(III) complexes of 1,4,7-tris(carboxymethyl)-10-(4-(5-(4-thioureaphenylene) borondipyrromethane) benzyl)-1,4,7,10-tetraazacyclododecane (42a-c) (route 1)

The initial strategy investigated for the preparation of a multimodality imaging agent involved the reaction between the lanthanide DO3A chelator bearing a benzyl amine group **(41a-c)** with an isothiocyanate functionalised optical dye **(21)** (route 1). Meade and co-workers have reported the conjugation of rhodamine B isothiocyanate to a gadolinium(III) DO3A complex bearing a benzyl amine group, however no yields were given.[2] The proposed synthetic procedure is shown in figure 134.

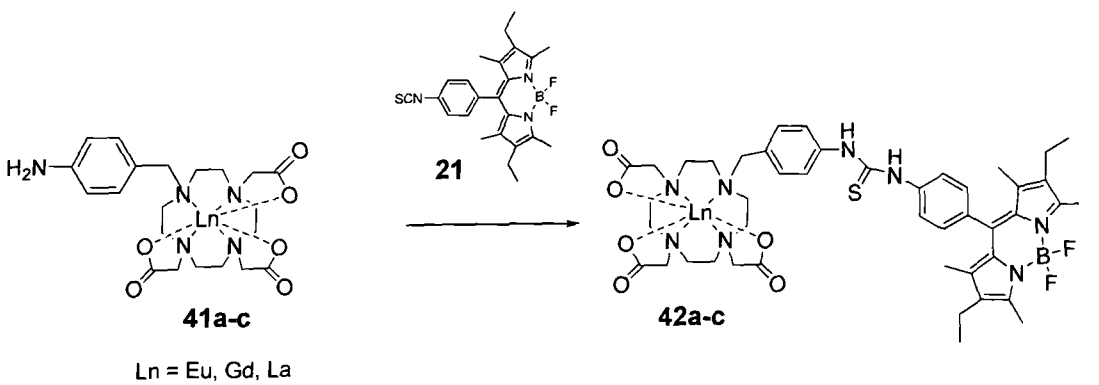

Figure 134 Proposed synthetic strategy for the preparation of a dual functional lanthanide agent **(42a-c)**

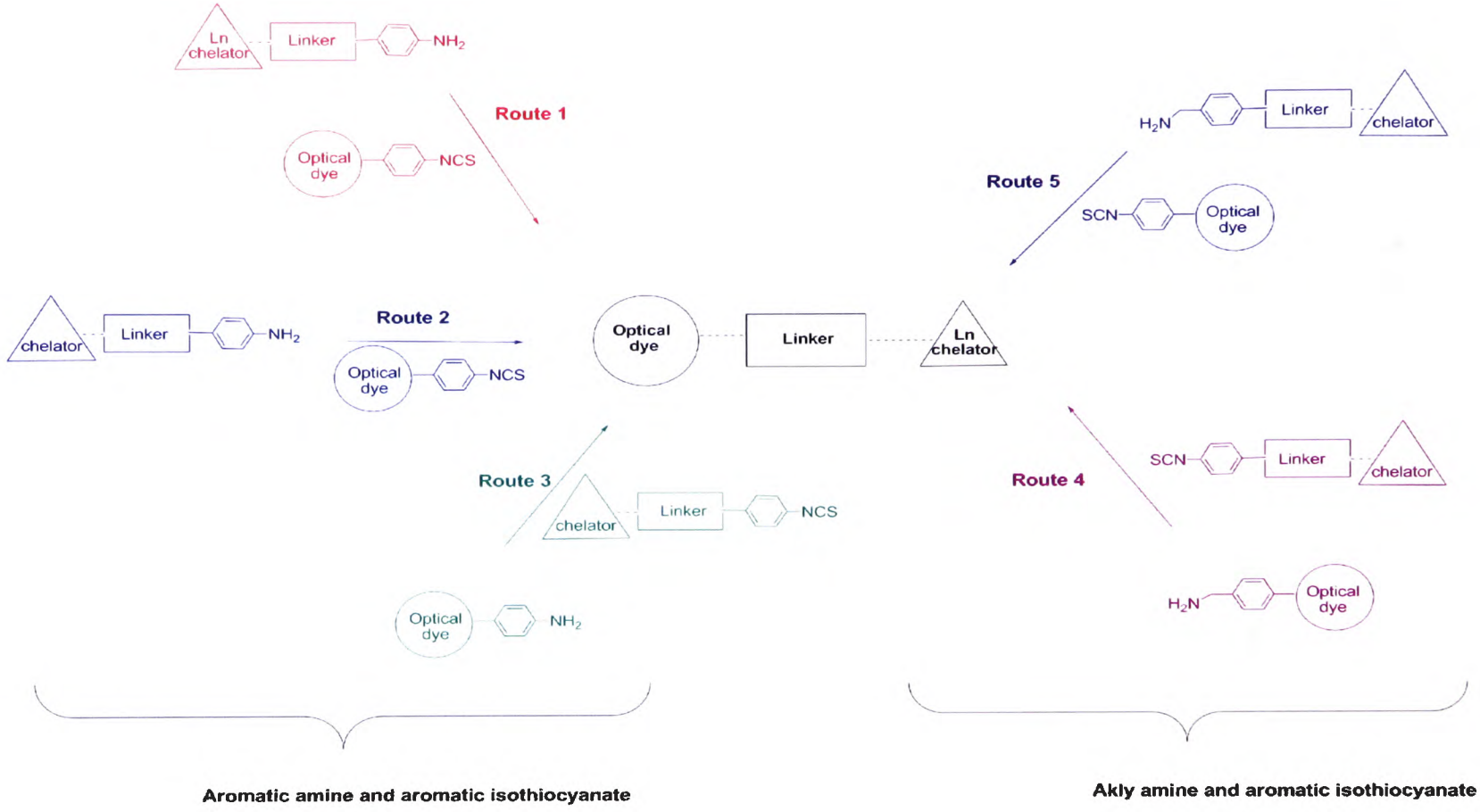

Figure 135 Routes investigated in the preparation of a multimodality imaging agent

The lanthanide complexes **(42a-c)** were dissolved into water with the addition of 1M potassium hydroxide to make a pH 9 solution, followed by the addition of **(21)** in dimethylformamide. The reaction was monitored by t.l.c., but after fourteen days, there was no sign of the formation of the desired product. The reaction was performed in aqueous conditions, which may have hydrolysed the isothiocyanate group and prevented product formation. The reaction was repeated with the amino benzyl DO3A chelator **(40)** in case the presence of the lanthanide metal ion was preventing the formation of the product.

4.6.2 The attempted preparation of 1,4,7-tris(carboxymethyl)-10-(4-(5-(4-thioureaphenylene) borondipyrromethane) benzyl)-1,4,7,10-tetraazacyclododecane (43) (route 2)

The second route investigated (route 2) involved the coupling between the BODIPY isothiocyanate **(21)** and the uncomplexed DO3A derivative bearing an aminobenzyl unit **(40)**. The synthetic scheme is shown in figure 136.

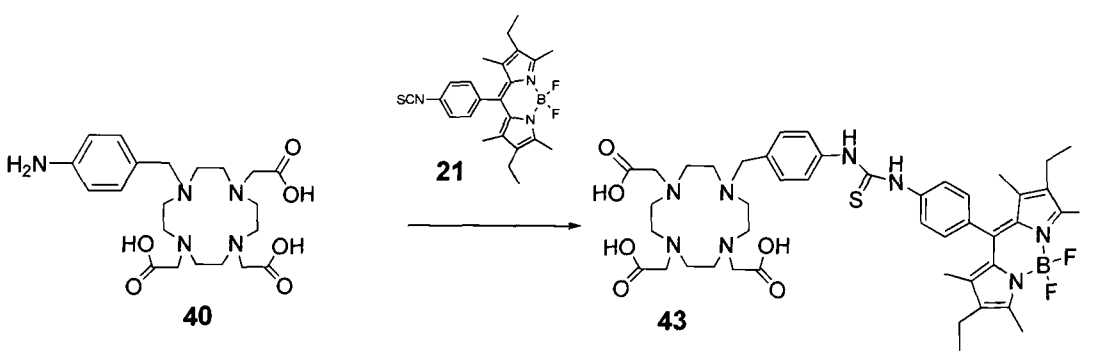

Figure 136 The proposed synthetic scheme for the preparation of **(43)**

The reaction was stirred for 14 days with a mixture dimethylformamide and water at pH 9 as solvent. Analysis by t.l.c. showed that no product was formed. The BODIPY isothiocyanate analogue **(21)** has previously been shown to couple with alkyl amines such as oligodeoxynucleotides by Boyle and co-workers.[173] The attempted coupling reaction of the BODIPY functionalised with an isothiocyanate group **(21)** with a phenylamine did not result in the

formation of the desired product **(22)**. To investigate whether this was an issue with the reaction attempted here, the coupling of phenylisothiocyanate to the DO3A benzylamine chelator **(40)** was investigated (figure 137).

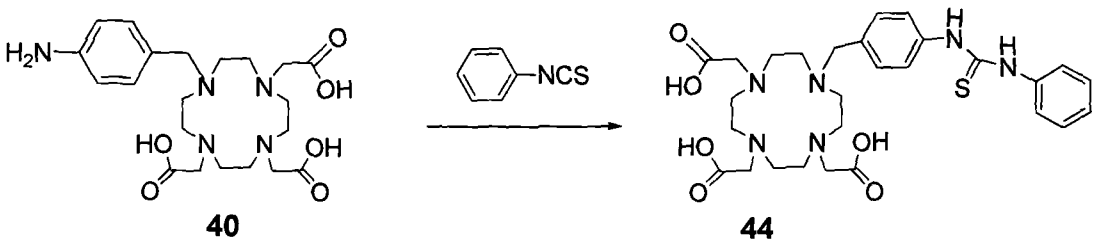

40 **44**

Figure 137 Proposed synthetic scheme for the preparation of **(44)**

The reaction conditions were varied slightly, with the reaction performed in pure dimethylformamide and stirred for 24 hours. An attempt was made to isolate the product **(44)**, however, the ^{1}H NMR spectrum showed that no product was formed. This suggests that the benzyl amine on both **(36)** and **(40)** are insufficiently reactive to couple to an isothiocyanate group under these conditions.

4.6.3 The attempted preparation of 1,4,7-tris(carboxymethyl)-10-(4-(5-(4-thioureaphenyl) borondipyrromethane benzyl)-2-methyl benzimidazole)-1,4,7,10-tetraazacyclododecane (47) (route 3)

Route 3 involves converting the benzyl amine on **(32)** and **(40)** to an isothiocyanate group that can then be coupled to a benzyl amine on the BODIPY optical dye **(20)** as shown in the scheme in figure 138. Thiophosgene was used to convert the benzyl amine to an isothiocyanate, in a biphasic solution of water and a chlorinated solvent.

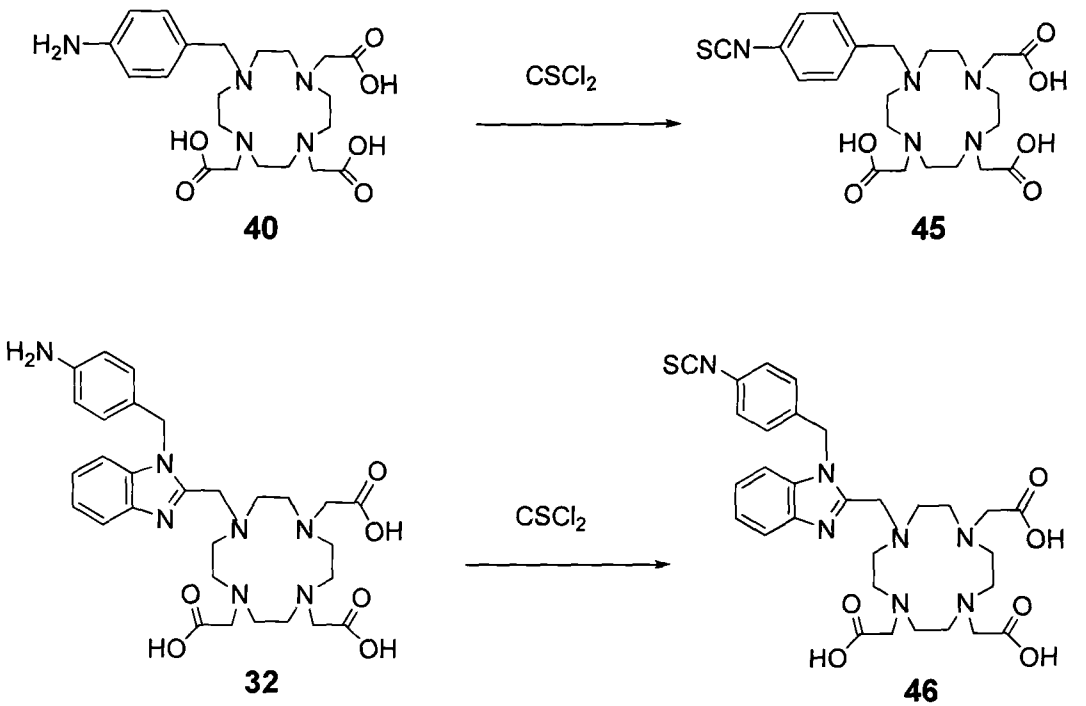

Figure 138 Synthetic scheme for the preparation of the isothiocyanate derivatives **(45)** and **(46)**

In the first method attempted **(40)** was dissolved into water, and the pH adjusted to pH 9 by the addition of 0.05 M sodium hydrogen carbonate solution. The thiophosgene was added as a solution in chloroform and the reaction mixture was stirred overnight. After extraction with chloroform, the aqueous solution was then collected, and the solvent removed to yield a yellow solid. Infra-red analysis did not show the characteristic isothiocyanate stretching frequency at around 2000 cm^{-1}. The literature was searched for alternative methods. Kline *et al.* investigated the conversion of an aromatic amine on a DOTA derivative to the isothiocyanate group, see figure 139.[192] While they still used thiophosgene, here a greater excess of the thiophosgene was used in carbon tetrachloride. They then reacted this with the selected amine compound in acidic conditions and stirred for six hours, isolating the desired product in a reported yield of 99%.

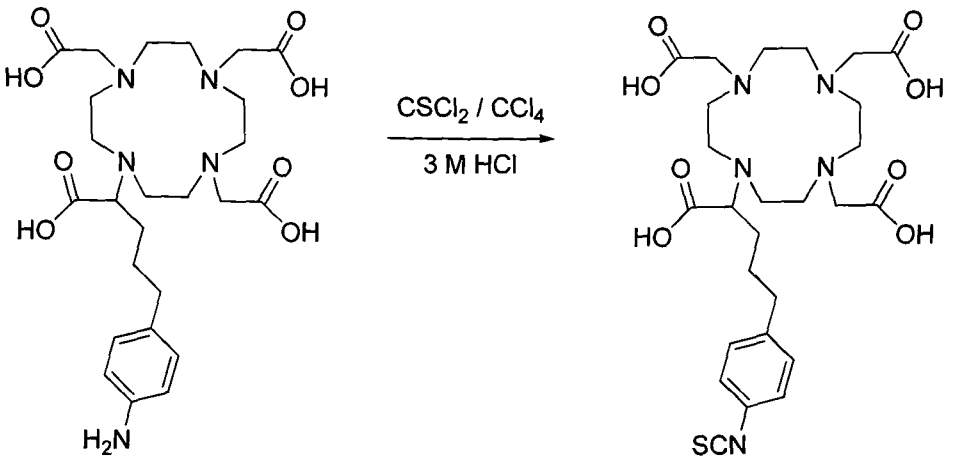

Figure 139 The Kline *et al.* method for the conversion of an amine to a reactive isothiocyanate group[192]

These conditions were repeated with the benzyl amine DO3A chelator (**40**) and the amine benzimidazole DO3A chelator (**32**). The ^{1}H NMR spectrum showed a shift up field in the position of the peaks compared to the amine derivatives. High resolution mass spectrometry and infra-red data confirm that the isothiocyanate compounds have been formed.

Attempts were then made to couple the reactive isothiocyanate group on the benzimidazole DO3A chelator (**46**) with the amine BODIPY analogue (**20**) (figure 140).

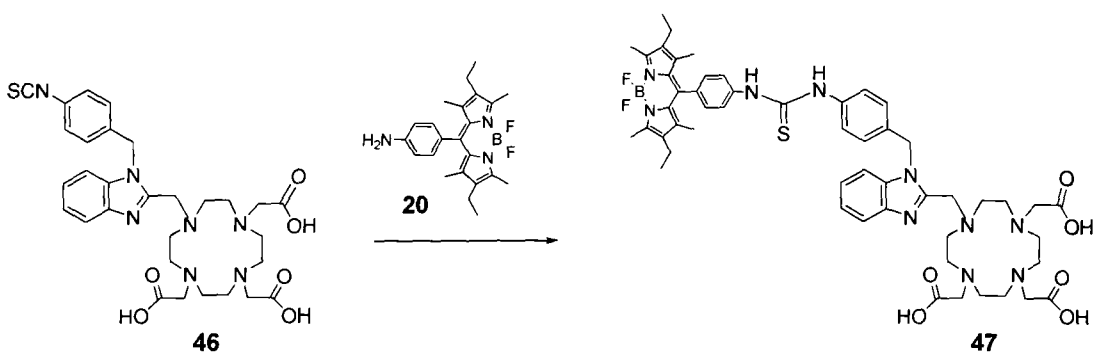

Figure 140 The proposed synthetic scheme for the attempted synthesis of (**47**)

The reaction was performed in a biphasic solution of water and dichloromethane at pH 8. The reaction mixture was monitored by t.l.c. for twenty-one days, with no product formed. The literature data does suggest that there are problems

with the reactivity of aromatic amines, and in many cases the reactions are too slow and do not go to completion.[193] [194]

4.6.4 The preparation of the lanthanum(III) complexes of DO3A chelators bearing a isothiocyanatobenzyl group (route 4)

The literature data suggests that alkyl amines will undergo nucleophilic substitution reactions with an isothiocyanate group more readily.[173] To investigate the feasibility of this reaction, the coupling of an isothiocyanate DO3A chelator to an alkylamine bearing optical dye was attempted initially. The isothiocyanate benzimidazole DO3A chelator **(46)** and the isothiocyanate benzyl DO3A chelator **(45)** were coupled to a benzyl amine, followed by the formation of the lanthanum(III) complex. The proposed synthetic schemes for the preparation of the lanthanum(III) complexes of **(49)** and **(51)** are depicted in figures 141-142.

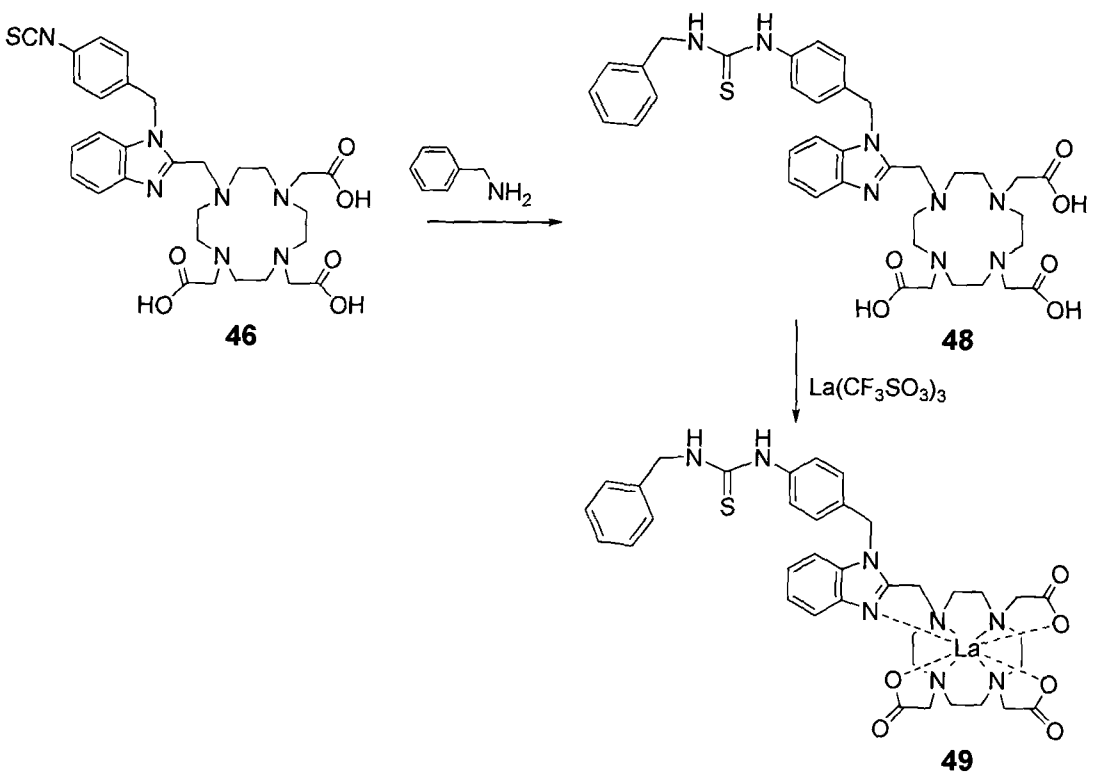

Figure 141 Proposed synthetic scheme for the preparation of the lanthanum(III) complex of **(49)**

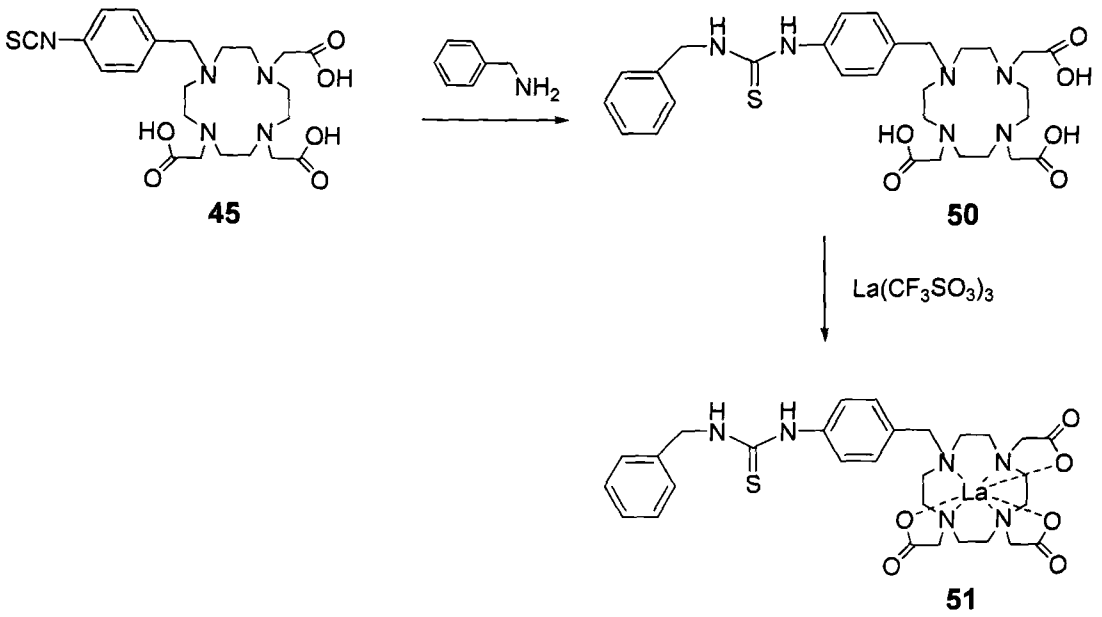

Figure 142 Proposed synthetic scheme for the preparation of the lanthanum(III) complex of **(51)**

The reaction to form the isothiocyanate was performed in water at pH 9 and stirred for 24 hours. The aqueous layer was washed with dichloromethane to remove the starting material. After isolation of a solid, the compound was purified using a sephadex LH-20 column (eluted with methanol) to give a white solid for both **(66)** and **(68)**. The ^{1}H NMR spectra were very broad with overlapping peaks making assignment difficult. The electrospray mass spectral data confirmed the identity of the compounds, while the infra-red spectrum showed the loss of the isothiocyanate group and the formation of the thiourea moiety.

The lanthanum(III) complexes of **(66)** and **(68)** were also prepared, and both isolated as white solids, **(67)** and **(69)**, with the product formation confirmed by electrospray mass spectrometry.

4.6.5 Attempted synthesis of a dual modality MRI agent bearing a rhodamine derivative

The coupling of the ethylamine rhodamine derivative **(16)** to the isothiocyanate cyclen derivatives was investigated (figure 143-144). Initial attempts involved

the benzyl cyclen derivative **(45)** dissolved into water with the pH adjusted to pH 8 by the addition of a 1 M sodium hydrogen carbonate solution. Rhodamine B base ethylamine **(16)** dissolved in dichloromethane was added to the reaction mixture, which was stirred for 48 hours. Analysis of the isolated compound showed that no reaction occurred. The reaction was repeated replacing the dichloromethane/water solvent mixture with either dichloromethane or a dimethylformamide/water mixture. However, no product was isolated in any of these reactions.

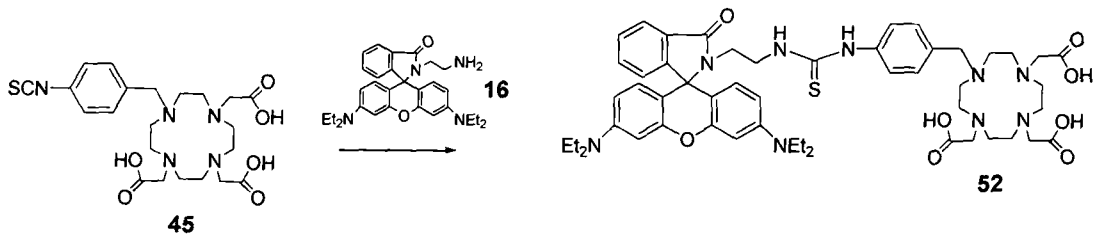

Figure 143 The synthetic scheme for the preparation of an aminobenzyl DO3A compound attached to a rhodamine derivative **(52)**

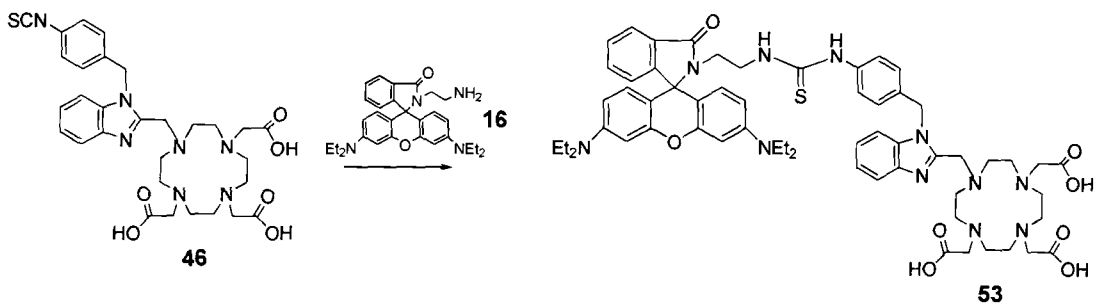

Figure 144 The synthetic scheme for the preparation of a benzimidazole DO3A compound attached to a rhodamine derivative **(53)**

As the alkyl amine rhodamine derivative **(16)** may be forming an unreactive salt, it was washed with sodium hydrogen carbonate solution, and then extracted into dichloromethane. The solvent was removed, and the solid **(16)** went from a pale pink colour to a pure white solid. This was then directly added to a solution of either **(45)** or **(46)** in dimethylformamide and the reactions stirred for 24 hours. The ^{1}H NMR spectra of **(52)** and **(53)** suggested that the desired ligand was formed. T.l.c. was also performed and this showed the formation of a new peak that did not correspond to the starting material. However, electrospray mass spectral data showed that the compound was not formed as no

molecular ion peak was formed. Instead, the data suggested that washing **(16)** with base resulted in the formation of a polymeric species incorporating the rhodamine compound, which prevented the formation of the multimodality imaging agent. This was confirmed by comparing the electrospray mass spectrometry data from this reaction with the spectrum obtained for the rhodamine derivative **(16)**.

4.6.6 Attempted synthesis of a dual modality MRI agents bearing a BODIPY derivative

The reaction to couple the alkyl amine BODIPY analogue **(29)** to the isothiocyanate benzimidazole cyclen derivative **(46)** was also attempted, with the proposed reaction scheme shown in figure 145.

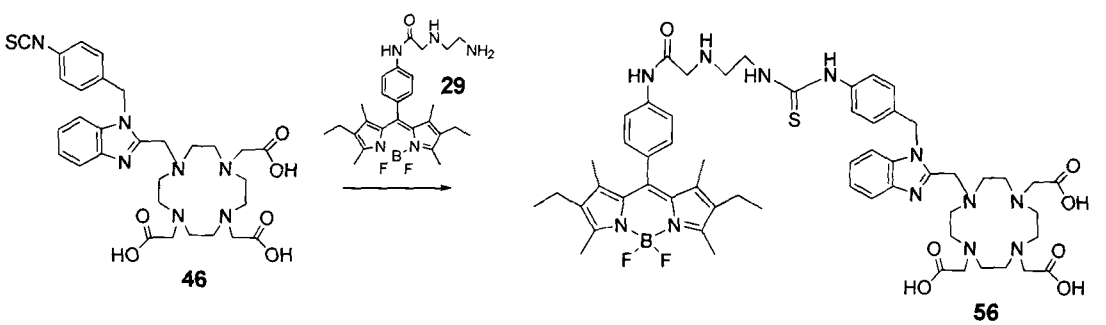

Figure 145 Proposed synthesis to prepare a dual modality MRI agent bearing a BODIPY derivative **(56)**

The alkyl amine bearing BODIPY dye **(39)** was washed with base (sodium hydrogen carbonate solution) and then extracted into dichloromethane. The reaction with **(46)** was carried out in dimethylformamide and the solution was stirred at room temperature for 24 hours. The solvent was removed, and the resulting solid was washed with diethyl ether to remove excess starting material and extracted into water. This gave a red coloured compound that is characteristic of the BODIPY dyes. A t.l.c. analysis was performed that showed the formation of a new compound that did not correspond to the starting material. Electrospray mass spectral data showed that **(56)** was not formed, and only a peak at 993 that may correspond to the formation of a BODIPY polymer.

4.6.7 Attempted preparation of 1,4,7-tris(carboxymethyl)-10-(4-(5-(4-thioureaamidophenyl)borondipyrromethane) methylamidobenzyl)-1,4,7,10-tetraazacyclododecane (58) (route 5)

The attempted preparation of an alkyl amine bearing a DO3A derivative **(58)** was briefly explored, as this compound could then be directly coupled to the BODIPY isothiocyanato compound **(21)**, with the scheme shown in figure 146. An alkyl amine group on the DO3A chelator would offer an appropriate precursor for coupling to a range of optical dyes. The proposed route involves phthaloyl β-alanine chloride being coupled to the aromatic amine on the benzyl DO3A **(40)**. The phthaloyl unit can then be removed to leave an alkyl amine **(58)**, which can be reacted with the BODIPY isothiocyanato compound **(21)** to give **(59)**.

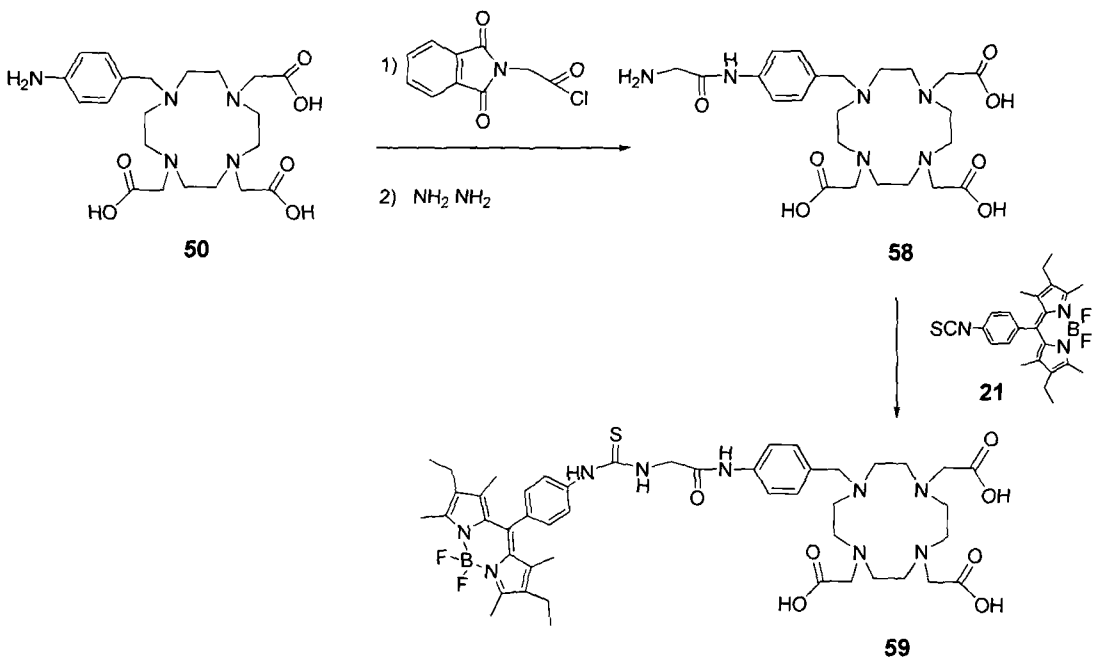

Figure 146 Proposed synthetic strategy for the preparation of **(59)**

There are numerous examples in the literature where phthaloyl β-alanine chloride is used as a protecting group for alkyl amines.[195] Gransey *et al.* refluxed *N*-phtaloylglycine with oxalyl chloride to form the acid chloride that can then be added dropwise to the aromatic amine compound in triethylamine.[196] The reaction mixture was stirred for 3 hours and gave yields of

ca. 70%. A possible problem with this method is that the acid chloride could react with the triethylamine. Yoon *et al.* performed a similar reaction and used magnesium oxide as the base, which is less likely to react with the acid chloride.[197]

Following the second method, gave a compound in which the phthaloyl group could potentially be removed by heating to reflux in hydrazine. [198]The resulting solid containing this alkyl amine was used crude and coupling to the BODIPY isothiocyanate analogue **(29)** attempted. The product **(59)** would be a bright red colour, and this could be readily identified as a red band when purifying using a sephadex column. The coupling reaction was carried out in a biphasic solution of water and dichloromethane at pH 8 and stirred for 24 hours under nitrogen at room temperature. T.l.c. analysis showed that a number of products were formed and isolation of **(59)**, if it is present in the mixture, would be difficult due to the similar r.f. values. The transfer of impurities between steps resulted may have contributed to a complex mixture of products.

4.7 Conclusion

The chapter presented a discussion of the preparation of multi-modality imaging agents that consist of a DO3A chelator with a benzimidazole or benzyl unit that is coupled to an optical dye.

The initial aim was to synthesise a DO3A derivative that can be further functionalised to allow for conjugation to an optical dye. From this, a number of experiments were carried out to determine the best method to attach an optical dye to the lanthanide chelator. The synthesis of a cyclen chelator that contains functionality for the coupling of an optical dye was achieved. Tri-substituted cyclen (DO3A **(31)**) was attached to either 1-(4-nitrobenzyl)-2-chloromethyl benzimidazole **(7)** or 4-nitrobenzylbromide. The optimum conditions for the substitution were determined and applied to the synthesis of the nitrobenzyl benzimidazole DO3A chelators **(32)** and the nitrobenzyl DO3A chelator **(38)**. The nitro group was converted to a secondary amine with sulfurated sodium borohydride for **(32)** and palladium on carbon for **(38)**. The lanthanide complexes were prepared with the nitrobenzyl benzimidazole DO3A ligands **(34a-d)**, the aminobenzyl benzimidazole DO3A ligands **(37a-d)** and the aminobenzyl DO3A ligand **(41a-c)**.

A number of routes were investigated to couple the DO3A chelators to an optical dye to form a multimodality imaging agent. The initial strategy involved the reaction of an aromatic amine on the DO3A chelator with an isothiocyanate group on the optical dye. This was not successful, probably due to the reduced reactivity of the aromatic amine preventing product formation. Investigations then turned to coupling an alkyl amine on the BODIPY **(29)** or rhodamine **(16)** derivatives with an isothiocyanate bearing DO3A chelators **(45)** or **(46)**. Initially, to test the reaction, benzyl amine was successfully coupled to **(45)** and **(46)** and the lanthanum(III) complexes formed. However, when coupling of the optical dyes to DO3A was attempted using the same procedures the reactions were not successful. To make certain that the optical dyes were fully

deprotonated they were washed with base, however this appeared to result in polymer formation.

The preparation of an alkyl amino functionalised chelator from the benzyl amine DO3A chelator **(50)** was also investigated. The route involved the subsitution of phthaloyl β-alanine chloride onto the benzylamine, followed by deprotection of the pthaloyl group by hydrazine. Attempts were made to couple this compound with the isothiocyanate BODIPY **(30)** but the desired product was not isolated.

Overall, suitable component molecules have been synthesised and appropriate reactions to produce multimodality imaging agents have been characterised but further work is required to fully exploit this chemistry.

5. Studies of the physical properties and cellular uptake of lanthanide complexes and novel dye conjugates

5.1 Introduction

Lanthanide complexes of 1,4,7-tris(carboxymethyl)-10-(1-(4-nitrobenzyl)-2-methyl benzimidazole)-1,4,7,10-tetraazacyclododecane [**(34a-c)** europium(III), terbium(III), and gadolinium(III)], 1,4,7-tris(carboxymethyl)-10-(1-(4-aminobenzyl)-2-methyl benzimidazole)-1,4,7,10-tetraazacyclododecane [**(37a-c)** europium(III), terbium(III), and gadolinium(III)] and 1,4,7-tris(carboxymethyl)-10-(4-aminobenzyl)-1,4,7,10-tetraazacyclododecane [**(41b)** gadolinium(III)] have been prepared (chapter 4). These molecules were investigated for their physical properties and interaction with cellular systems, alongside the gadolinium(III) complex 1,4,7-tris(carboxymethyl)-10-(2-methyl benzimidazole)-1,4,7,10-tetraazacyclododecane **(60)**, (supplied by C.Fisher).[199] The structures of these molecules are given in figure 147.

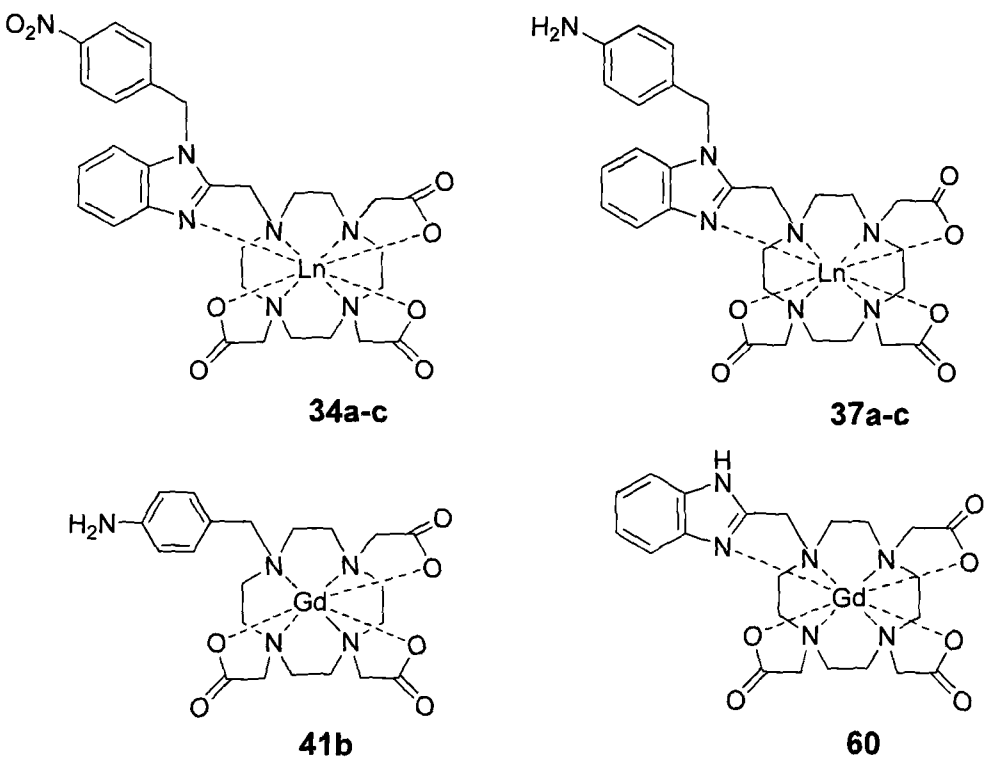

Figure 147 Structures of the lanthanide(III) complexes **(34a-c)** and **(37a-c)**, (where 34/37a = EuL, 34/37b = TbL, 34/37c = GdL), **(41b)** and **(60)**

Initially, the luminescence properties of the europium(III) and terbium(III) complexes of **(34a-b)** and **(37a-b)** were investigated with the excitation and emission spectra recorded and the number of bound water molecules (q)

determined from luminescence lifetime measurements. Other physical measurements performed include NMR studies of the gadolinium(III) complexes that were used to calculate the relaxivity values for **(60)**, **(34c)**, **(37c)** and **(41b)**. MR imaging studies were carried out on samples consisting of a 10mm diameter tube (containing water) with a 5mm tube (containing a gadolinium(III) complex) placed inside. *In vitro* MRI imaging studies were also carried out to investigate the cellular uptake of these four gadolinium(III) complexes. Each contrast agent was incubated with Jurkat cells and cell pellets formed for imaging experiments. Cellular uptake properties were also investigated for the BODIPY compound bearing a triethylamine moiety **(27)**, which was incubated with HT-29 cells and the location tracked using fluorescence microscopy. Fluorescence microscopy was undertaken at the University of Hull by Huguette Savoie.

5.2 Photophysical properties

The excitation and emission spectra were recorded for the europium(III) and terbium(III) complexes of the nitro and amino benzimidazole DO3A chelators **(34a-b)** and **(37a-b)**. The luminescence lifetimes in water and D_2O were measured to allow calculation of the q values (number of bound water molecules) for each complex. Luminescence lifetimes measurements were recorded and analysed at the University of Leicester by Dr Mark Lowe.

5.2.1 Emission spectra of the lanthanide complexes

The emission spectra were recorded for europium(III) and terbium(III) complexes of the nitrobenzyl and aminobenzyl benzimidazole DO3A chelators **(34a-b)** and **(37a-b)**. All of the complexes gave characteristic emission spectra, indicating incorporation of the lanthanide(III) ion within the metal binding site. In the excitation spectra, benzimidazole chromophores generally absorbed at around 272 nm, the structural differences within the chelators did not shift the excitation wavelength significantly. Solutions of concentration 2.5×10^{-5} M were prepared and the luminescence emission spectra recorded at an excitation wavelength of 272 nm. The transitions giving rise to the peaks can be assigned on the basis of the lanthanide energy levels, europium(III) has a $^5D_0$ excited state which results in an emission peak at 17,200 cm^{-1} (λ_{em} = 615 nm) on returning to the $^7F_0$ ground state. Other emission peaks are present for europium(III) at 580, 595, 655 and 700 nm. Terbium(III) has a $^5D_4$ excited state which results in an emission peak at 20,500 cm^{-1} (λ_{em} = 545 nm) on returning to the $^7F_6$ ground state. The emission spectra for the complexes are shown in figures 148-151.

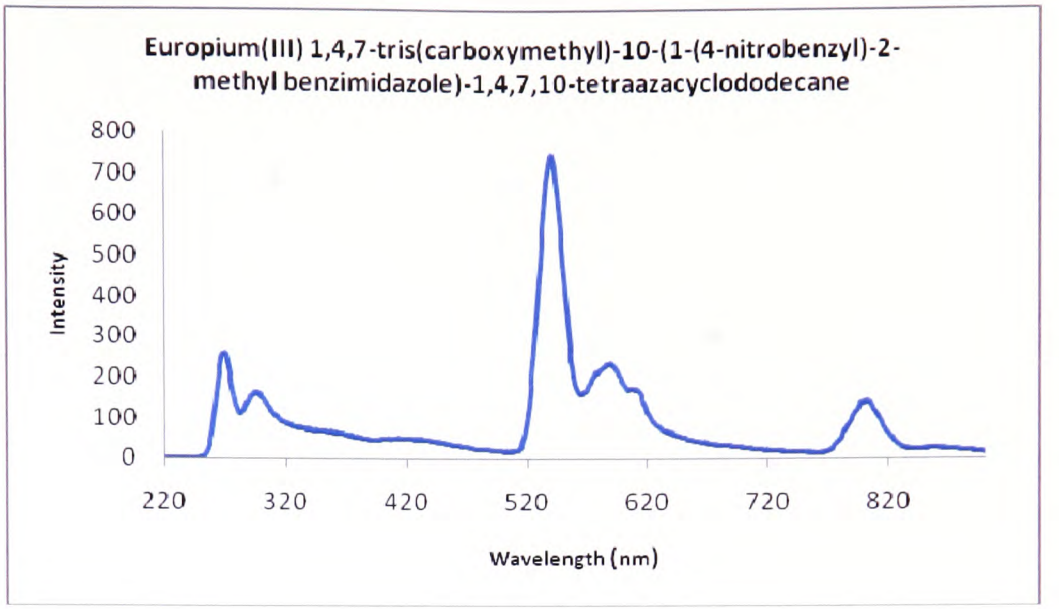

Figure 148 The emission spectrum of the europium(III) complex **(34a)**

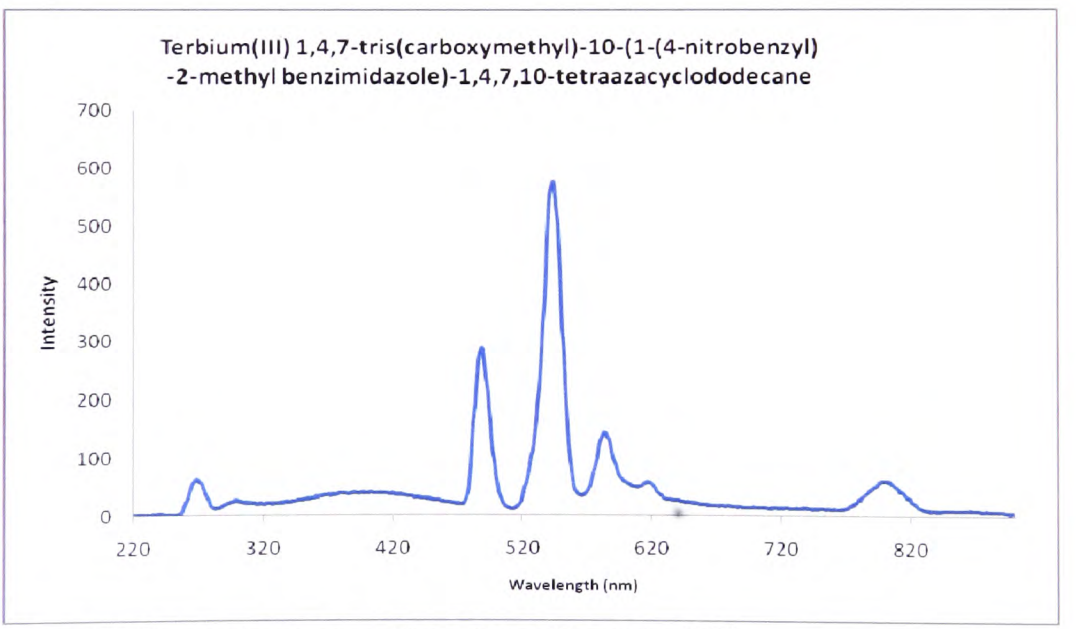

Figure 149 The emission spectrum of the terbium(III) complex **(34b)**

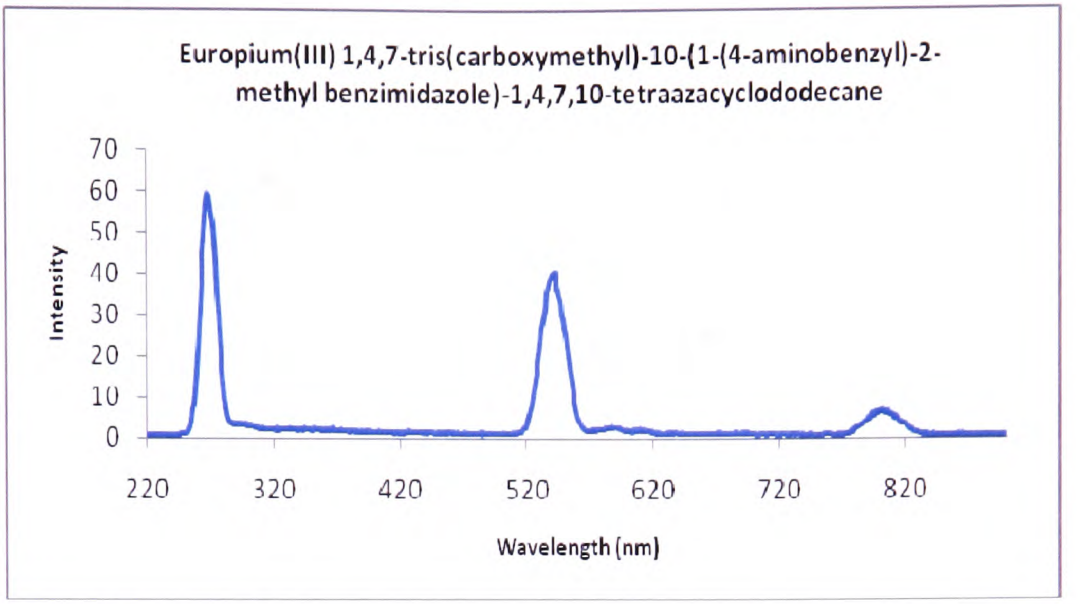

Figure 150 The emission spectrum of the europium(III) complex **(37a)**

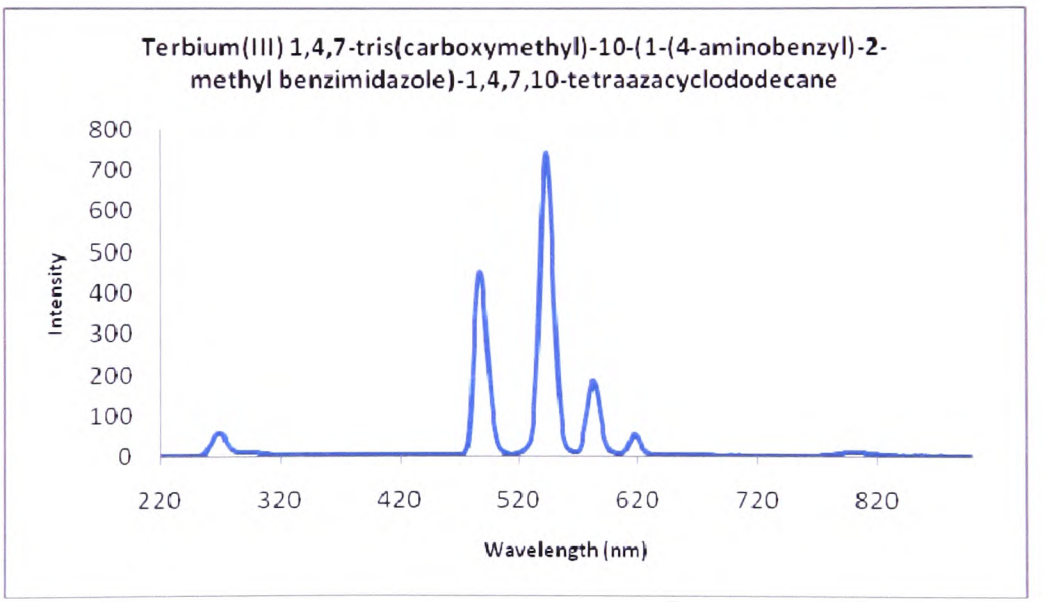

Figure 151 The emission spectrum of the terbium(III) complex **(37b)**

The spectrum of the europium(III) complex with the nitrobenzyl benzimidazole DO3A chelator **(34a)** has emission peaks at 270, 294, 540, 589, 611 and 801 nm. The peaks in the spectrum between 540 – 611 nm can be assigned to the various levels of emission from the lowest lying triplet (T) level. The peak at 540 nm represents the $^5D_0 \rightarrow {}^7F_0$ transition, the peak at 589 nm represents the $^5D_0 \rightarrow {}^7F_1$ transition and the peak at 611 nm represents the $^5D_0 \rightarrow {}^7F_2$ transition. The europium(III) aminobenzyl benzimidazole DO3A chelator **(37a)** shows a

similar spectrum, with the characteristic peaks at 542 nm ($^5D_0 \rightarrow {}^7F_0$), 590 nm ($^5D_0 \rightarrow {}^7F_1$) and 617 nm ($^5D_0 \rightarrow {}^7F_2$).

The terbium(III) complexes have better sensitisation of the lanthanide ion due to a more efficient overlap of the excited states of the benzimidazole and the terbium(III) ion. For the nitrobenzyl benzimidazole DO3A terbium(III) complex **(34a)**, the peak at 488 nm represents the $^5D_4 \rightarrow {}^7F_6$ transition, the peak at 544 nm represents the $^5D_4 \rightarrow {}^7F_5$ transition, the peak at 583 nm represents the $^5D_4 \rightarrow {}^7F_4$ transition and the peak at 616 nm represents the $^5D_4 \rightarrow {}^7F_3$ transition. The aminobenzyl benzimidazole DO3A terbium(III) complex is also similar to the equivalent nitrobenzyl complex, with peaks at 487 nm ($^5D_4 \rightarrow {}^7F_6$), 543 nm ($^5D_4 \rightarrow {}^7F_5$), 585 nm ($^5D_4 \rightarrow {}^7F_4$) and at 617 nm ($^5D_4 \rightarrow {}^7F_3$).

5.2.2 Luminescent lifetimes and q values

From the luminescent lifetimes (τ) of the complexes, it is possible to calculate the number of bound water molecules (q value) by measuring the rate constant for depopulation of the excited state in H_2O and D_2O, provided that a correction is made for the effect of unbound (closely diffusing) H_2O molecules, and for other exchangeable XH oscillators (e.g. amide NH, amine NH). Each amide NH oscillator contributes 0.075 ms^{-1} to quenching of the europium(III) $^5D_0$ excited state but does not contribute to the quenching of the terbium(III) $^5D_4$ excited state. This allows the q values for europium(III) or terbium(III) complexes to be calculated. The decay rates measured in H_2O and D_2O are used to calculate the q value for europium(III) and terbium(III) complexes. The fitted decay emission profiles in D_2O are shown in figures 152 – 156 for the europium(III) and terbium(III) complexes.

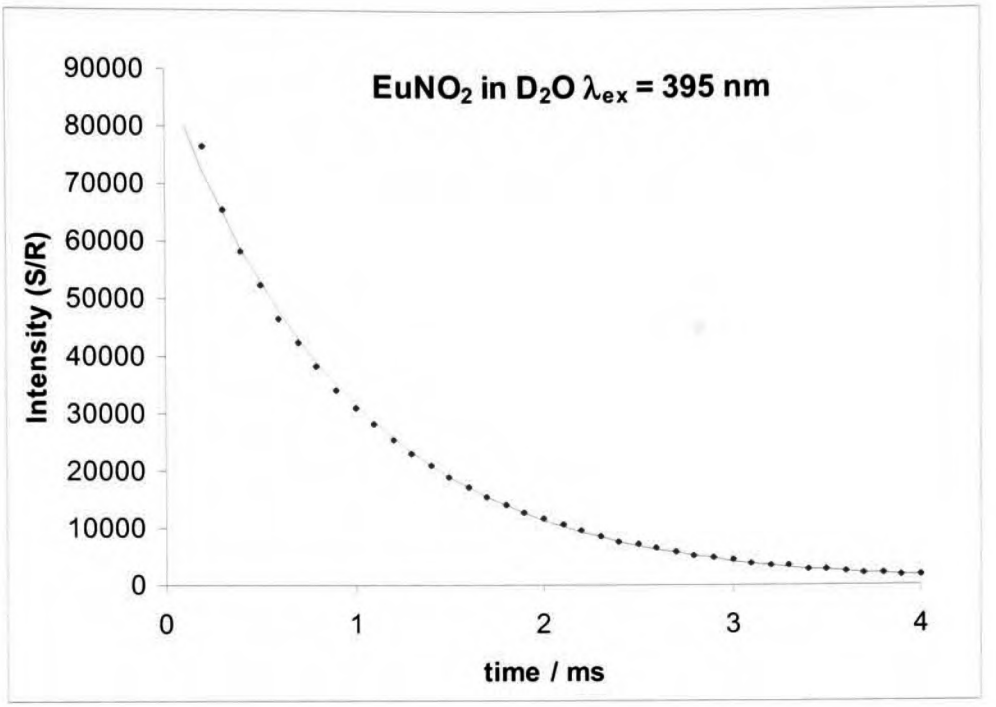

Figure 152 Fitted decay emission spectrum for **(34a)** in D_2O

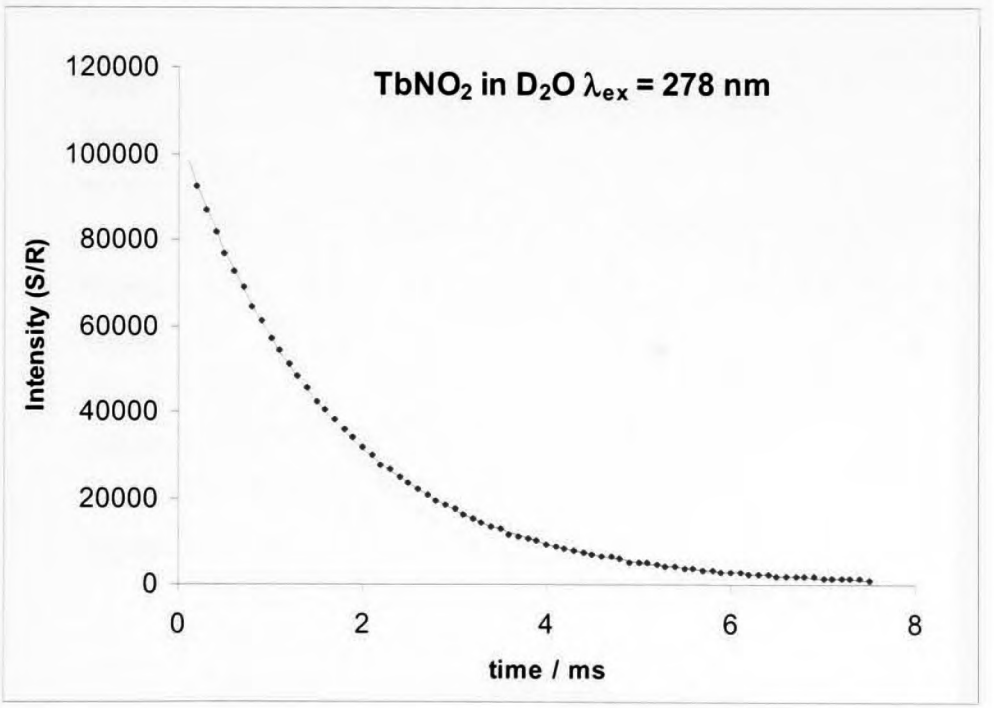

Figure 153 Fitted decay emission spectrum for **(34b)** in D_2O

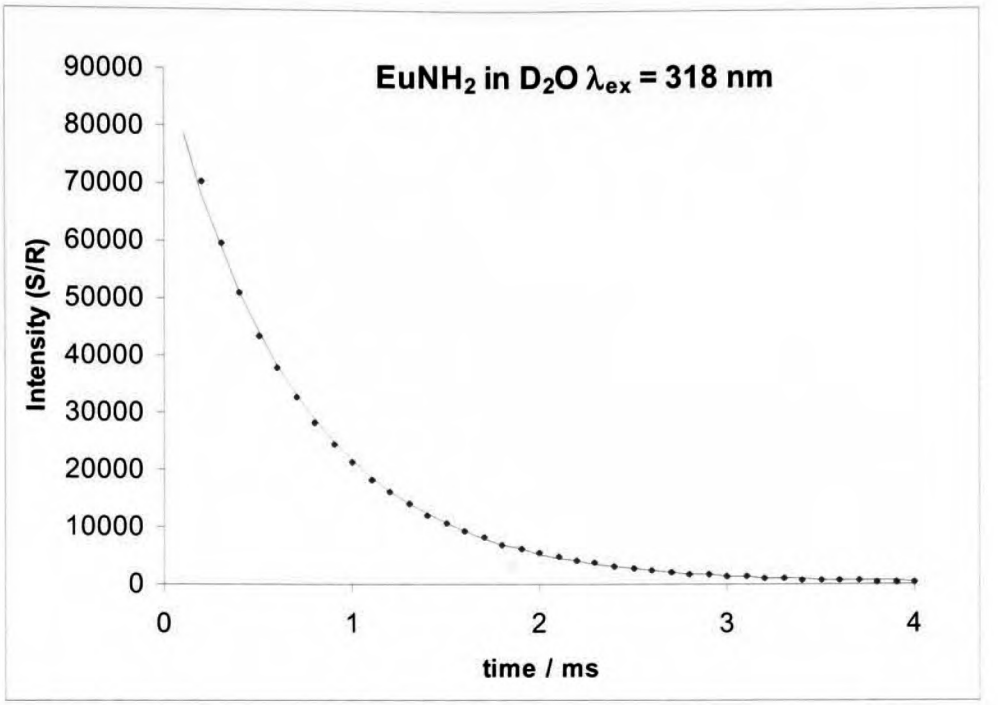

Figure 154 Fitted decay emission spectrum for **(37a)** in D_2O at λ_{ex} = 318 nm

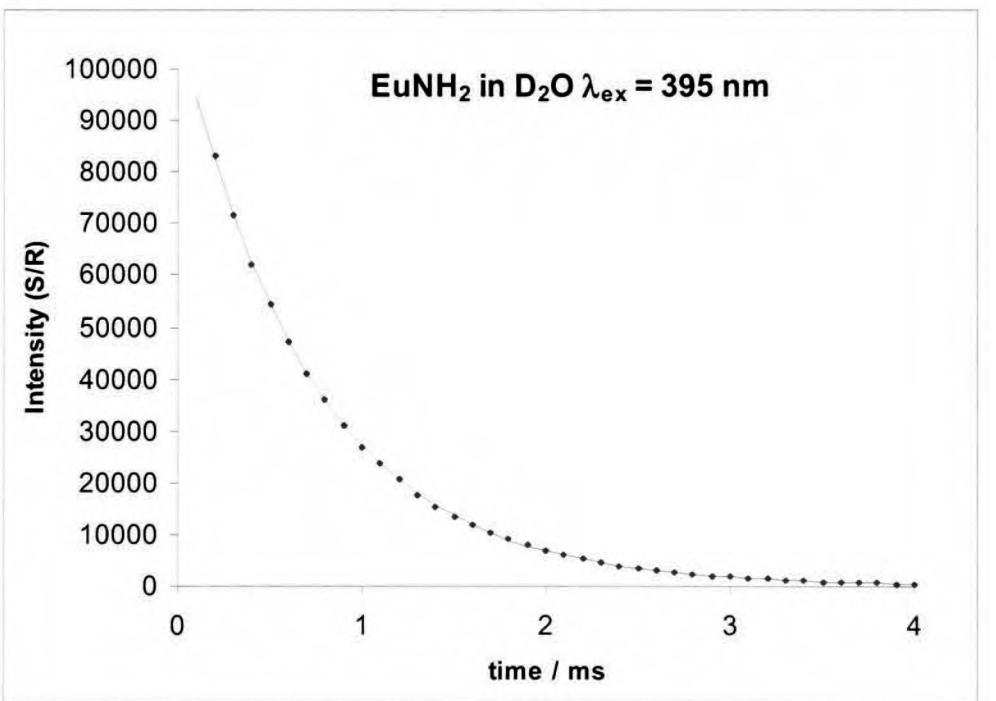

Figure 155 Fitted decay emission spectrum for **(37a)** in D_2O at λ_{ex} = 395 nm

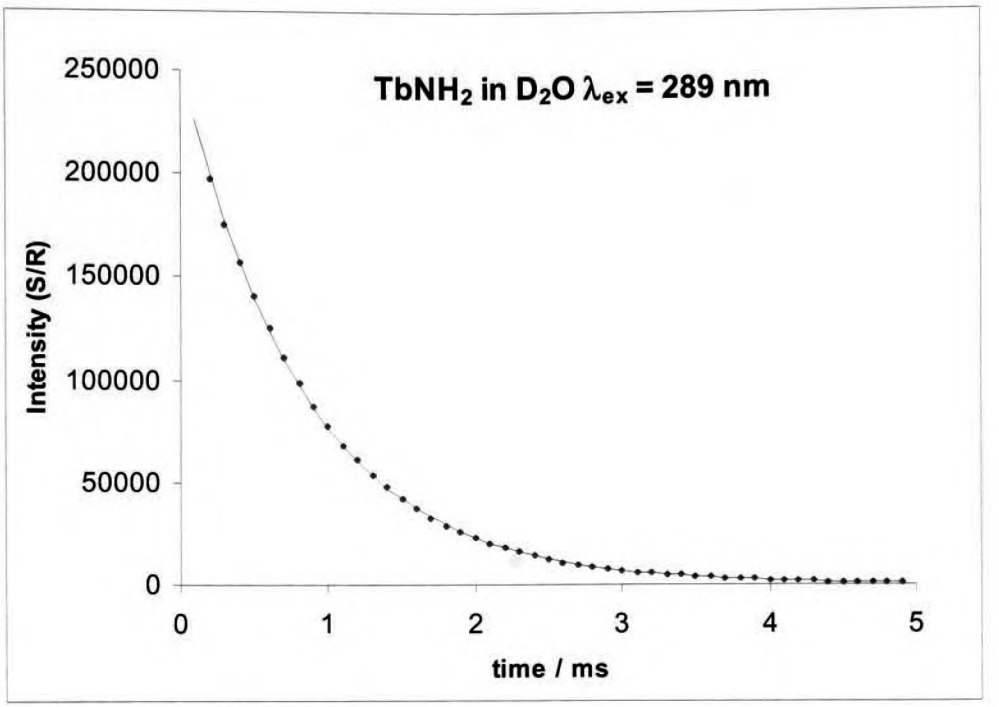

Figure 156 Fitted decay emission spectrum for **(37b)** in D_2O

To compare different methods of calculating the q value for the europium(III) complexes, both the original Horrock's equation and the modified version were used along with Parker's modified equation.[200-202] For the terbium(III) complex, Parker's modified equation was used.[73, 201] These are shown in table 11.

For Eu(III):

Horrocks original equation: $q = 1.05[k_{H_2O} - k_{D_2O}]$

Parker's modification: $q = 1.2[k_{H_2O} - k_{D_2O} - 0.25]$

Horrocks modification: $q = 1.11[k_{H_2O} - k_{D_2O} - 0.31]$

For Tb(III):

Parker's modified equation: $q = 5[k_{H_2O} - k_{D_2O} - 0.06]$

Table 11 Equations used to calculate the q value for europium(III) and terbium(III) complexes using both the Horrocks and Parker equation

Luminescence lifetime measurements were made for the europium(III) and terbium(III) complexes of **(34a-b)** and **(37a-b)**. The luminescence lifetimes in both H_2O and D_2O, and the calculated q values are given in table 12.

	k_{H_2O} (ms^{-1})	k_{D_2O} (ms^{-1})	q (Horrocks original)	q (Parker modification)	q (Horrocks modification)
(34a)(λ_{ex} = 395 nm)	2.28	1.04	1.30	1.19	1.03
(37a)(λ_{ex} = 318 nm)	2.29	1.44	0.89	0.72	0.60
(37a)(λ_{ex} = 395 nm)	2.27	1.39	0.92	0.76	0.63
(34b) (λ_{ex} = 278 nm)	0.91	0.60		1.25	
(37b)(λ_{ex} = 289 nm)	1.14	1.20		-0.6	

Table 12 Rate constants (ms^{-1}) for depopulation of the excited states in H_2O and D_2O with q values

The rate constants for the europium(III) complexes are in the range 2.27 - 2.29 ms^{-1}. For the europium(III) nitro complex **(34a)**, the q value using the Parker modification is 1.19. With the europium(III) amino complex **(37a)**, the q value is lower at 0.7-0.8, which both suggest one inner-sphere water molecule is bound. The terbium(III) complexes have much lower rate constant of 0.91 – 1.14 ms^{-1}. With the terbium(III) nitro complex **(34b)**, the q value of 1.25 indicated one inner sphere water was present, however with the terbium(III) amino complex **(37b)** the calculation gave a negative answer suggesting that there may be an impurity in this sample. Free terbium(III) ions may be present in solution suggesting that the purification of the complex using a sephadex column had not successfully removed all the unreacted metal salts.

5.3 T_1 relaxation studies

The gadolinium(III) contrast agents **(60)**, **(34c)**, **(37c)** and **(41b)** have been investigated for their NMR relaxation properties of water molecules.[203] These compounds **(60)**, **(34c)**, and **(37c)** have been shown to incorporate one bound water molecule, while the aminobenzyl compound **(41b)** contains more than one bound water molecule (q = 2), and hence an improvement in the relaxation properties should be observed.

5.3.1 Longitudinal relaxivity (r_1) of 1,4,7-tris(carboxymethyl)-10-(2-methylbenzimidazole)-1,4,7,10-tetraazacyclododecane (60)

Relaxation measurements was made on the non-functionalised complex **(60)** at three different pH values (6.3, 3.5, and 1.5). At low pH it was expected that the N1-position on the benzimidazole, which was bound to the gadolinium(III) ion, will become protonated, and hence no longer be coordinated. This may allow access for an additional water molecule (increasing q from 1 to 2) that in turn would lead to an improvement in the relaxivity (r_1) (figure 157).

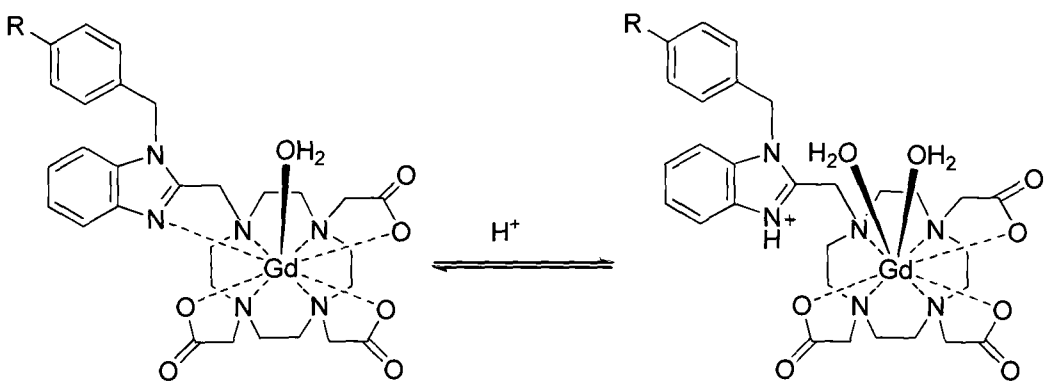

Figure 157 Possible effect of the protonation on the functionalised gadolinium(III) benzimidazole DO3A complex (where R= NO_2 and NH_2)

To measure the longitudual relaxivity (r_1) for a contrast agent interacting with water, the relaxation time (T_1) needs to be recorded in aqueous solutions at a range of concentrations (1 mM, 0.75 mM, 0.5 mM, 0.25 mM and 0.125 mM were selected). A graph can be plotted of 1/ T_1 vs. concentration with the

gradient equating to the relaxivity rate (r_1). The graph for **(60)** at pH 6.8 is shown in figure 158.

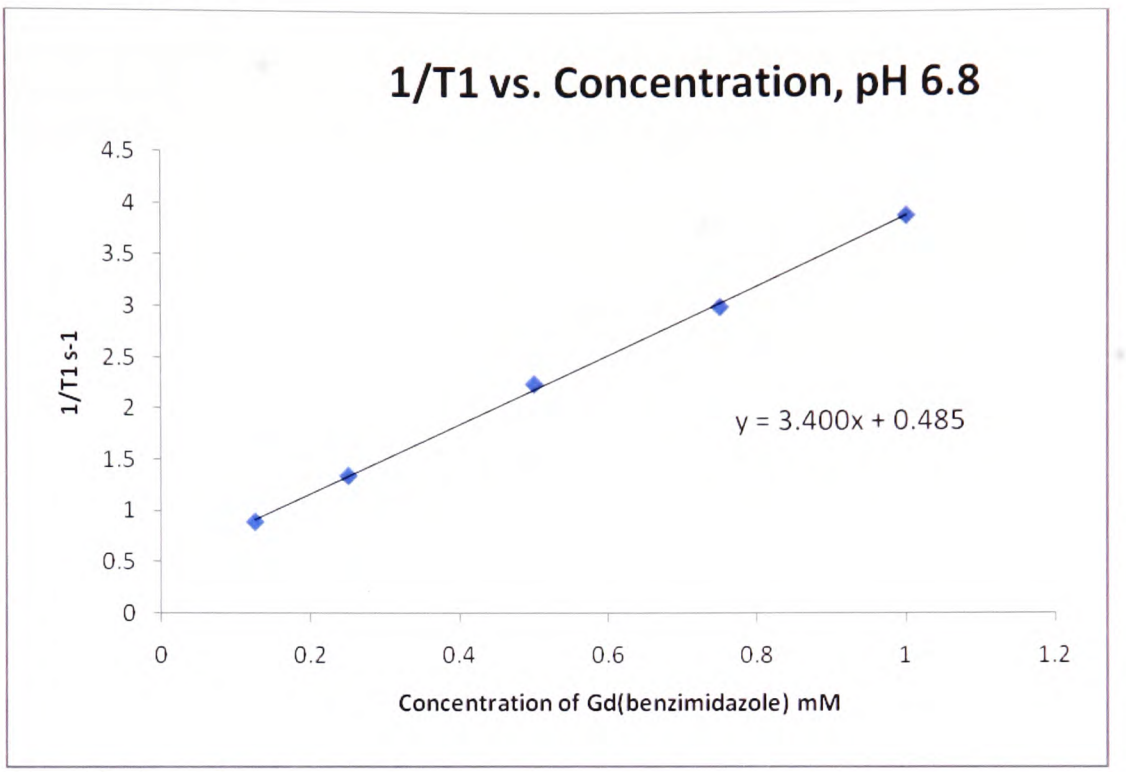

Figure 158 Graph to show $1/T_1$ vs. Concentration at pH 6.8 for **(60)**

From this plot, the relaxivity (r_1) was found to be 3.4 $s^{-1}mM^{-1}$ at pH 6.8. This was repeated at pH 3.5 and 1.5, with the results shown in table 13.

pH	Relaxivity ($s^{-1}mM^{-1}$)
6.8	3.40
3.5	2.90
1.5	3.33

Table 13 The relaxivity of **(60)** at different pH values

The relaxivity of **(60)** at pH 3.5 was found to be 2.90 $s^{-1}mM^{-1}$, while at pH 1.5 it was found to be at 3.33 $s^{-1}mM^{-1}$. These results show that pH does not have an effect on the relaxivity. Protonation of the N1-position does not lead to an increase in the relaxivity and so the number of bound water molecules is unchanged. Typically, lanthanide complexes can be 9-coordinate, however, it may be that in this case, instead of the free coordination site being occupied by

a water molecule, structural rearrangement occurs to give an 8-coordinate complex that still has only one bound water molecule.

5.3.2 Longitudinal relaxivity (r_1) of gadolinium(III) 1,4,7-tris(carboxymethyl)-10-(1-(4-nitrobenzyl)-2-methyl benzimidazole)-1,4,7,10-tetraazacyclododecane (34c)

The relaxivity rate was recorded for the gadolinium(III) nitrobenzylbenzimidazole DO3A compound **(34c)**. It was recorded at three different pH values, 4.6 3.5 and 1.5. The graph is shown for **(34c)** at pH 4.6 in figure 159.

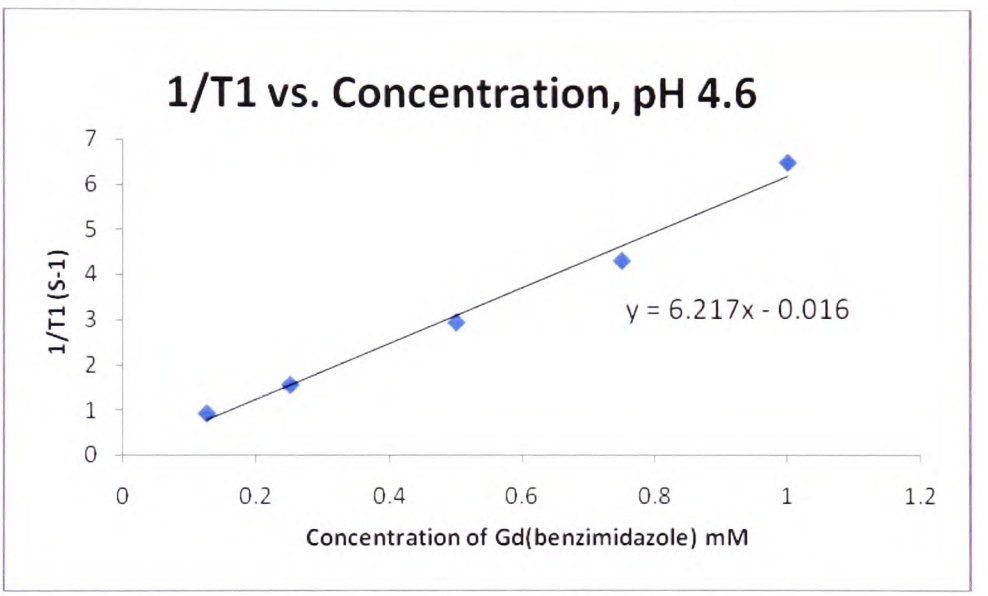

Figure 159 Graph to show $1/T_1$ vs. concentration at pH 4.6 for **(34c)**

pH	Relaxivity ($s^{-1}mM^{-1}$)
6.8	6.22
3.5	5.96
1.5	6.22

Table 14 Relaxation rates of **(34c)** at varying pH

The data shows that the relaxivity is not affected by pH, as was observed for the benzimidazole complex **(60)**, once again a decrease in pH which should protonate the benzimidazole at the N1-position did not change the relaxivity properties. The relaxivity values observed are greater than those measured for the non-functionalised benzimidazole complex **(60)**. A similar relaxivity rate might be expected because they both contain one bound water molecule. The

slight increase in the relaxivity maybe due to the increase in the molecular weight of the gadolinium(III) complex **(34c)** resulting in a decrease in the tumbling rate (τ_R).

5.3.3 Comparison of the longitudinal relaxivity (r_1) for the gadolinium(III) complexes

The relaxivity values were also recorded for the gadolinium(III) complex of aminobenzyl benzimidazole DO3A chelator compound **(37c)**, and aminobenzyl DO3A chelator **(41b)** and for comparison, the commercial DTPA contrast agent Omniscan, with the results shown in table 15.

Compound	Relaxivity ($s^{-1}mM^{-1}$)
60	3.40
34c	6.22
37c	4.51
41b	7.86
Omniscan	5.52

Table 15 Relaxivity values of the gadolinium(III) contrast agents

The relaxivity values were found to be 4.5 $s^{-1}mM^{-1}$ for **(37c)**, 7.86 $s^{-1}mM^{-1}$ for **(41b)** and 5.52 $s^{-1}mM^{-1}$ for Omniscan. The relaxivity values for the aminobenzyl and nitrobenzyl benzimidazole compounds are comparable to the commercially available contrast agent omniscan. The nitrobenzyl benzimidazole derivative **(34c)** has a higher relaxivity than both the aminobenzyl benzimidazole compound **(37c)** and the non-functionalised benzimidazole complex **(60)**. The nitro complex **(34c)** has a higher relaxivity than **(37c)**, this is possibly due to the more favourable environment of **(34c)** for water exchange [increase in residency time (τ_m)]. Both **(34c)** and **(37c)** have a higher relaxivity than **(60)**, perhaps due to a decrease in the tumbling rate (τ_R) that occurs due to the increase in the molecular weight of the gadolinium(III) complexes **(34c)** and **(37c)**. The aminobenzyl DO3A complex **(41b)**, has the highest relaxivity out of all the complexes studied in this work, which can be attributed to the higher number of bound water molecules (q value) relative to the other complexes.

5.4 Imaging with contrast agents

The T_1 (spin-lattice relaxation time) and T_2 (spin-spin relaxation time) are important properties in creating signal contrast. By controlling the repetition time (time between successive 90° pulses) and echo time (time from the 90° pulse to the received signal from the sample), can favour whether a T_1 or a T_2-weighted image is produced. To record a T_1-weighted image, short repetition (<750 ms) and echo times (<40 ms) are required. While for T_2-weighted images, long repetition (>1500 ms) and echo times (>75 ms) are required.

5.4.1 Tube within a tube images

T_1-weighted images were performed with the gadolinium(III) contrast agents **(60)**, **(34c)**, **(37c)** and **(41b)**. The images show a 10 mm NMR tube containing water, with a 5 mm NMR tube inside of it containing the contrast agent. The image intensity values cannot be compared between experiments as they depend on the parameters of the individual measurement. Therefore, the variation in image intensity due to the contrast agents (1 mMol) was compared to an internal standard (distilled water). The images are shown in figure 160. A 'region of interest' was selected containing over 1000 voxels in both the inner and outer tubes allowing a percentage increase in contrast to be calculated relative to the water. The results showing the percentage increase in image intensity due to the gadolinium(III) contrast agents are shown in table 16.

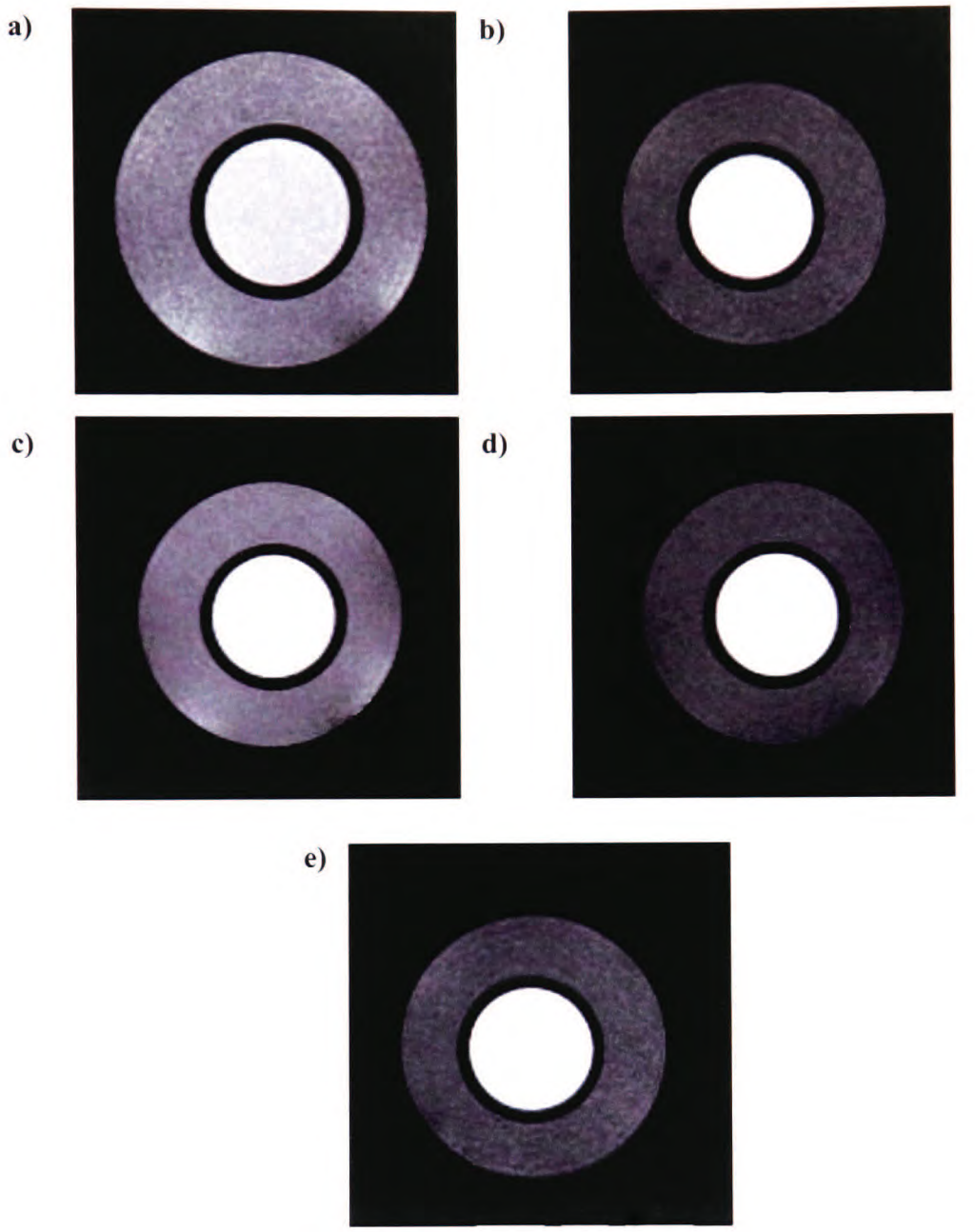

Figure 160 Images showing the contrast enhancement due to the gadolinium(III) contrast agents (internal tube) relative to water, a) **(60)**, b) **(34c)**, c) **(37c)**, d) **(41b)** and e) Omniscan

Sample	% increase in intensity from water
60	51
34c	124
37c	64
41b	148
Omniscan	71

Table 16 Relative image intensity increase due to the gadolinium(III) contrast agents

The results show the expected increase in image intensity due to the gadolinium(III) contrast agent when compared to water using a T_1-weighted pulse sequence. This data is consistent with the results for the relaxivity rates (r_1) reported in section 5.2 showing that the aminobenzyl DO3A complex **(41b)** has the largest relative intensity increase, with the benzimidazole complex **(60)** giving the smallest contrast enhancement.

5.4.2 *In vitro* MR cellular studies

In vitro MR studies to show whether cellular uptake of the complexes occurred were carried out with **(60)**, **(34c)**, **(37c)** and Omniscan, at a field strength of 11.7 T. These studies were performed with Jurkat cells and the aim was to investigate whether these compounds penetrated into the cells. Figure 161 contains the images recorded in the MR study using Jurkat cells with both T_1 and T_2- weighted images shown. In this case the medium above the cell pellet was used as the internal standard, the cells had been exposed to the contrast agents at a high concentration and then this solution was washed away and replaced by growth medium.

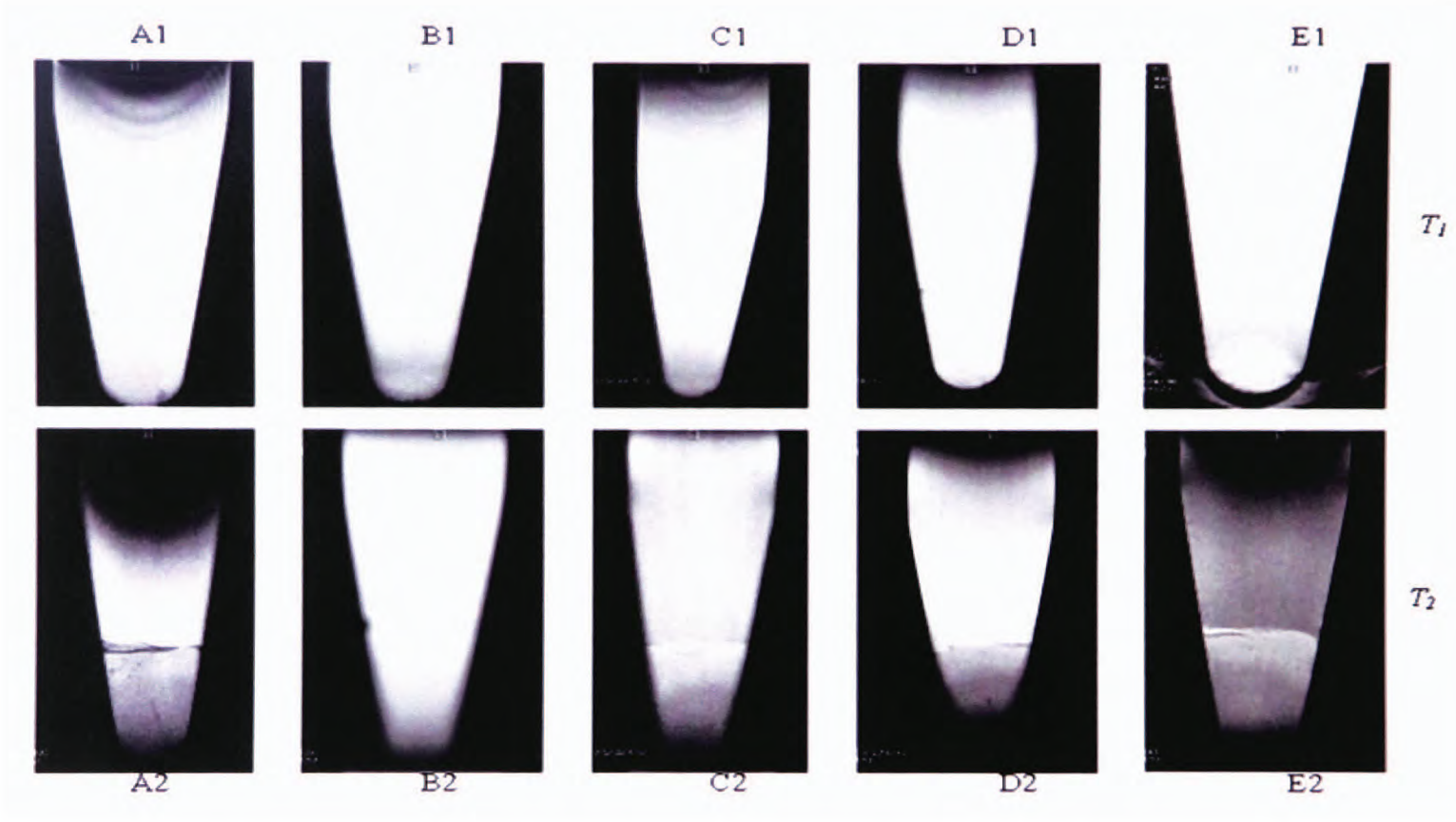

Figure 161 T_1 (A1-E1) and T_2 (A2-E2) weighted images of cell pellets. [(A1-2) pelleted cells in medium, (B1-2) pelleted cells labelled with 300 μM **(60)** in medium, (C1-2) pelleted cells labelled with 300 μM **(34c)** in medium, (D1-2) pelleted cells labelled with 300 μM **(37c)** in medium, (D1-2) pelleted cells labelled with 300 μM **(51b)** in medium and (E1-2) pelleted cells labelled with *300 μM of Omniscan* in medium]

Sample	% difference in intensity from medium
control	20.4
60	23.2
34c	4.8
37c	0
Omniscan	28.3

Table 17 Intensity variation in the T_2-weighted images of cell pellets in medium

The T_1- weighted images showed no difference in intensity when compared to the medium. In the T_2- weighted images, the cell pellet is generally seen to be darker, showing the negative effect on the image intensity that is consistent with a T_2 contrast agent. The contrast variation in the T_2- weighted images was found to be larger than in the T_1- weighted images. This is consistent with work reported by Mishra *et al.*, where they suggest that the T_2 effect is due to the accumulation of the compound in intracellular vesicles that induces local magnetic field inhomogenities due to compartmentalization.[107] However, the control also shows a contrast variation in the T_2- weighted image, which is comparable to the samples containing contrast agents, suggesting that the compound is not being taken up into the cells. The aminobenzyl benzimidazole DO3A complex **(37c)** shows little difference in contrast between the cell pellet and the medium in both T_1 and T_2-weighted images. It may be the case that the contrast agents were taken up into the cells, but by the time the image was taken, the complex had diffused or been transported back out of the cells. The conditions need to be optimised for all of these experiments. Ideally, to assist uptake of the contrast agents by the cells, a further functional group could be attached to the molecule that will enhance the cellular uptake pathways and result in a greater contrast difference between the medium and the cell pellet.

5.5 Cellular studies of 5-(4-triethylammoniummethylamidophenyl) borondipyrromethene chloride (27)

A number of groups have reported the preparation of BODIPY analogues as probes for optical imaging. Sunahara *et al.* have reported the synthesis of a library of meso substituted BODIPY derivatives with ON/OFF switching capabilities in the presence of changes in solvent polarity that have been employed to establish the polarity at the surface of a protein and at the membrane in living cells.[168] Hall *et al.* have reported the preparation of BODIPY dyes that are based on a tetraarylazadipyrromethene fluorophores that employs a receptor-methylene spacer-fluorophore architecture.[204] This molecule has also been used as a sensing molecule to detect polarity and pH changes. *In vivo* cellular imaging has been performed to show that the complex locates within the cytoplasm.

The BODIPY dye 5-(4-triethylammoniummethylamidophenyl) borondipyrromethene chloride **(27)** has been prepared. The compound has the potential to be used as an optical dye in biological imaging experiments, and the quaternary amine group, will impart greater aqueous solubility that may improve cellular uptake properties and may also influence localisation within the cells. The fluorescence emission spectrum was recorded, see figure 162, showing the emission peak at 537 nm.

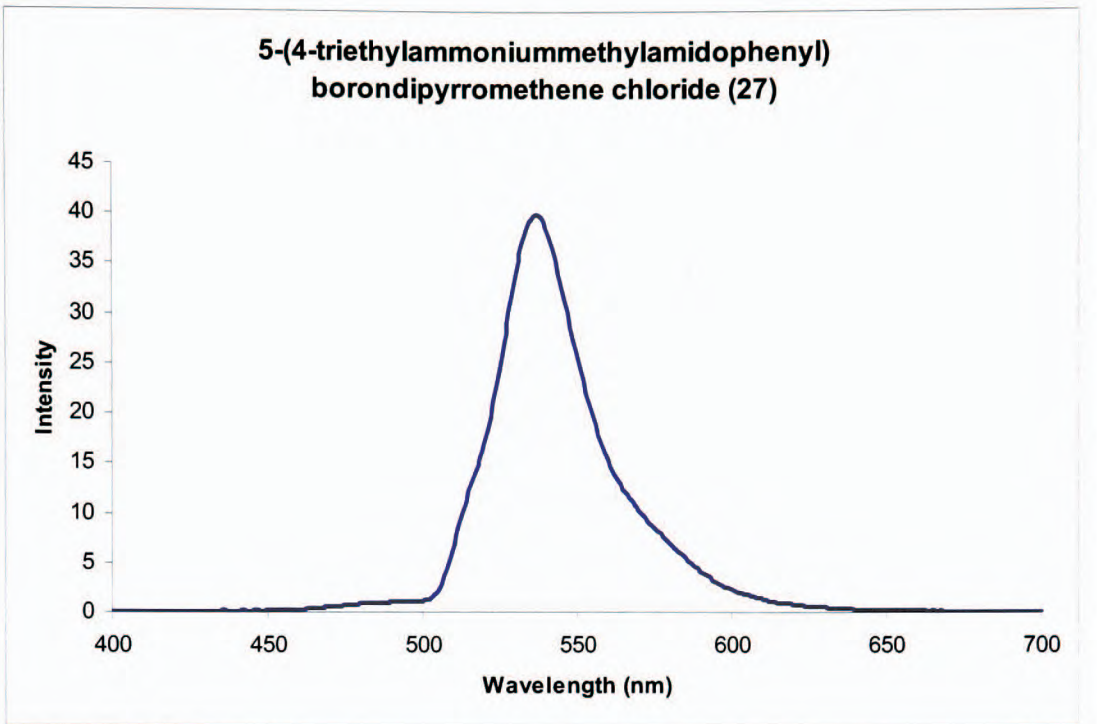

Figure 162 Emission spectrum of the compound 5-(4-triethylammoniummethylamidophenyl) borondipyrromethene chloride **(27)**

The BODIPY dye **(27)** was incubated with HT-29 cells for 1 hour, and after 22 hours of plating, fluorescence microscopy was performed. The images in figure 163 show the localisation of the BODIPY dye in the cell.

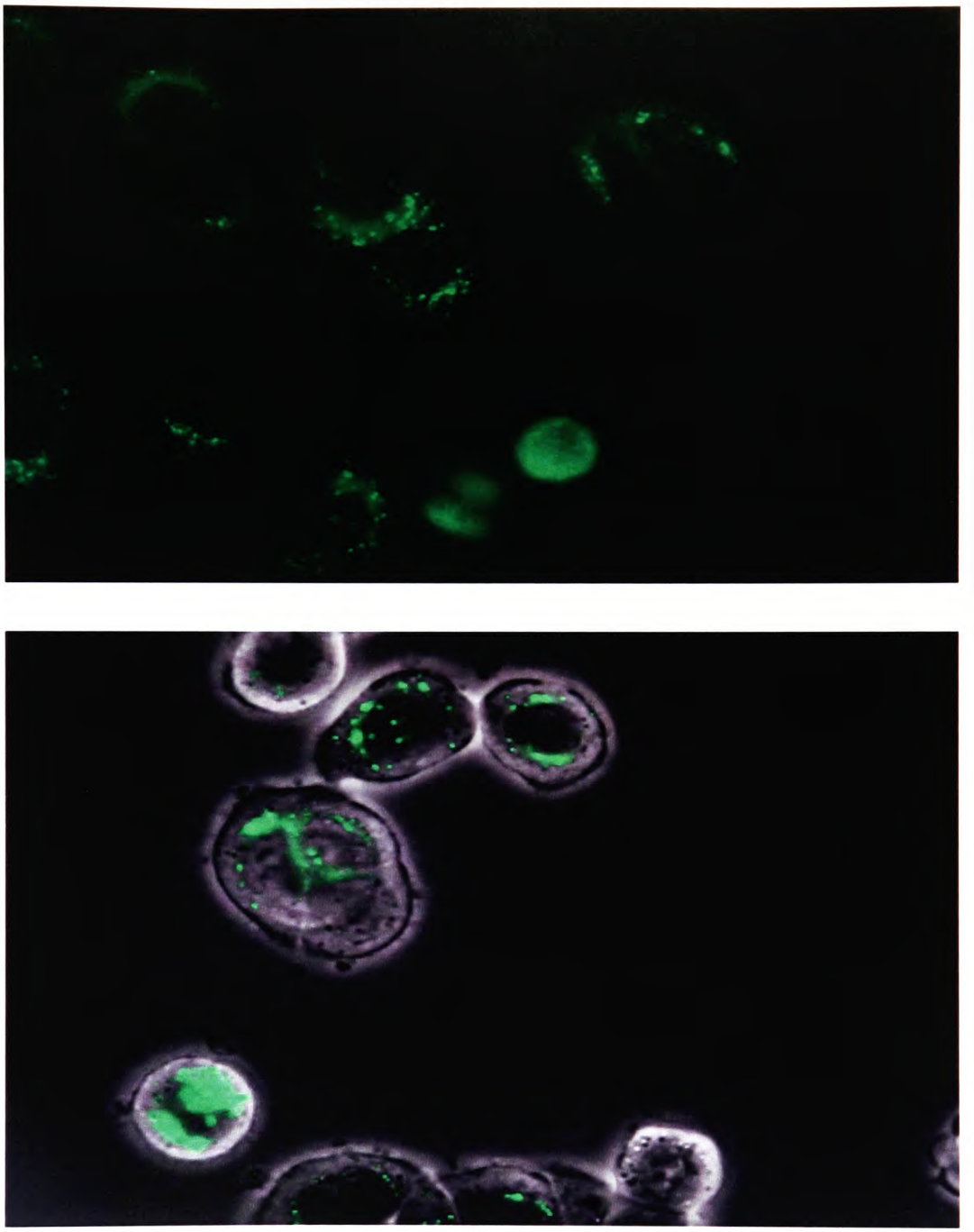

Figure 163 Fluorescence microscopy of the BODIPY dye into HT-29 cells. The top image is of a fluorescence scan detecting the BODIPY dye (green); the bottom image is an overlay of a fluorescence image and a phase contrast image to show localisation within the cells

The images show that the BODIPY optical dye is taken up by the cell, while there is a faint diffused fluorescence, the localised brighter fluorescence is likely to be due to uptake of the dye into lysosomes. To confirm this, co-localisation studies can be undertaken with a known dye that locates within the lysosomes.

5.6 Conclusions

This chapter contains a discussion of the physical properties and cellular uptake of the lanthanide contrast agents synthesised and the BODIPY dye **(27)**. The photophysical properties of the europium(III) and terbium(III) complexes of the nitrobenzyl and aminobenzyl benzimidazole ligands **(34a-b)** and **(37a-b)** were investigated. The benzimidazole component can act as a weak sensitizer for lanthanide ion based emission. The luminescence emission spectrum of the terbium(III) complex contained more defined peaks, suggesting that the benzimidazole ligand provides better sensitisation for this metal ion. The complexes were shown to each have one bound inner sphere water molecule.

Relaxivity studies were undertaken on the gadolinium(III) contrast agents **(60)**, **(34c)**, **(37c)** and **(41b)**. Initially, pH variation effects were investigated using compounds **(60)** and **(34c)**, as it was believed that at low pH, the N1-position would become protonated and dissociate from the gadolinium(III) ion leading to an increase in the bound water molecules and therefore an improvement in relaxivity properties. However, varying the pH did not change the relaxivity, which suggests that the protonation of the N1-position on the benzimidazole leads to a structural rearrangement from a 9 coordinate compound to an 8 coordinate compound with no net change in the number of inner sphere water molecules. The gadolinium(III) contrast agents **(60)**, **(34c)**, **(37c)** and Omniscan all have one bound water molecule, while **(41b)** contains two bound water molecules and therefore, it was expected that the latter will have the greatest relaxivity value. This trend was observed and the results also showed that **(60)** had the lowest relaxivity in comparison to the functionalised benzimidazoles **(34c)** and **(37c)**. This is possibly due to the increase in molecular weight and a decrease in the tumbling rate (τ_R). The aminobenzyl benzimidazole complex **(37c)** had a lower relaxivity than the nitrobenzyl benzimidazole complex **(34c)**. An explanation could be that the nitro benzimidazole complex **(34c)** had a more favourable environment for water exchange that may effect the residency time (τ_m).

The T_1-weighted images of a 5 mm NMR tube containing the gadolinium(III) contrast agent located inside a 10 mm NMR tube containing distilled water were produced. The image intensity variation of the contrast agent solutions was scaled to an internal standard and the increases in intensity were in the same order that was observed for the longitudinal relaxation rates. The next step was to investigate their cellular uptake properties. This was undertaken by incubating the contrast agent with Jurkat cells and forming cell pellets. T_1-weighted images showed no difference in contrast between the medium and the cell pellet. However, with the T_2-weighted images, there was some negative contrast differences *i.e.* darker cell pellet [except for **(37c)**]. This may suggest that the contrast agent is accumulating in the intracellular vesicles. However, the control sample of the cell pellet and medium also had a similar intensity differences, which may suggest that the agent is not being taken up into the cell under these experimental conditions. The aminobenzyl benzimidazole complex **(37c)**, had no effect on the image intensity in either the T_1 or the T_2-weighted image highlighting that there may have been issues with the contrast agent either diffusing or being transported out of the cells prior to collection of the images.

Fluorescence microscopy was performed with the BODIPY dye **(27)** to investigate whether it was taken up into HT-29 cells. The images show that the dye was taken up into the cells and appeared to localise in the lysosomes.

6. Conclusion and Further Work

6.1 Introduction

This thesis reported the research into the synthesis of dual modality imaging agents that have the potential to act as both MRI and optical contrast agents, and could also target cellular function. The initial aim of this research was to synthesise a compound that has the capability to encapsulate a lanthanide metal ion and has further functionality for the attachment of an optical dye. The physical properties and cellular uptake/ localisation where then investigated for the resulting multi-modality imaging agents.

To achieve this, there are three main components that are required, the chelator (DO3A), the chromophore/linker (benzimidazole) and the optical dye (rhodamine B or BODIPY) (figure 3). Chapter 2 presented the synthesis of the chromophore/linker group benzimidazole that contains a reactive alkyl halide for coupling to the secondary amine position on the chelator and a nitro group to convert to an amine at a later stage for the attachment of an optical dye. Chapter 3 discussed the preparation of fluorescent dyes based on rhodamine and BODIPY backbones that have isothiocyanate or amine groups for coupling to the DO3A chelator derivative. Chapter 4 reported the synthesis of DO3A chelators that contain a chromophore/linker group with an appropriate functional group for coupling to the optical dye and proposed methodologies for the preparation of multimodality agents. Studies of the physical properties and cellular uptake of lanthanide complexes and novel dye conjugates were investigated and detailed in chapter 5, with the lanthanide complexes of the nitrobenzyl and aminobenzyl benzimidazole DO3A chelators **(34a-c)**, and **(37a-c)**, benzylamineDO3A chelators **(41a-c)**, Gd(III) benzimidazole DO3A chelator **(60)**, and the BODIPY triethylamine compound **(27)** studied.

6.2 Concluding remarks on the synthesis of benzimidazole derivatives

The synthesis of the chromophore unit was based on the compound benzimidazole. The benzimidazole derivative has to contain the functionality for attachment to both the cyclen unit DO3A **(31)** and a fluorescent dye (rhodamine B or BODIPY). The initial strategy involved the functionalisation of 1,2-phenylenediamine with 4-acetamidobenzaldehyde to form 1-(4-acetamidomethylene)phenylenediamine **(1)**, with the imine group reduced by sodium borohydride to form 1-(4-acetamidomethyl)phenylenediamine **(2)**. Efforts to form the benzimidazole **(3)** involved using methyl chloroacetimidate hydrochloride with **(2)**, however the desired product was not formed. The use of an amide protecting group on the benzimidazole unit was deemed initially to be a better approach than the use of a nitro functionality due to the ease of conversion to an amine (acid hydrolysis). However, due to the difficulties in forming the amide derivative benzimidazole, the route to the nitro containing compound was investigated.

The phenylenediamine derivative 1-(4-nitrobenzyl)phenylenediamine **(5)**, was readily formed by the coupling of 1,2-phenylenediamine and 4-nitrobenzyl bromide. Efforts to prepare 1-(4-nitrobenzyl)-2-chloromethyl benzimidazole **(7)** using chloroacetic acid resulted in the displacement of the chloro substiutent with either hydroxide or ammonia during work up. An alternative method involved using glycolic acid to yield 1-(4-nitrobenzyl)-2-hydroxymethyl benzimidazole **(6)**, followed by the conversion of the hydroxo to the chloro substituent, to give the desired molecule, 1-(4-nitrobenzyl)-2-chloromethyl benzimidazole **(7)**.

6.3 Concluding remarks on the synthesis of optical dyes

The development of functionalised rhodamine B and BODIPY optical dye derivatives is reported in chapter 3 of this thesis. The optical dyes need to contain a reactive group that can be coupled to the chromophore/linker compound. The initial route for the synthesis of rhodamine derivatives involved following the method reported by Nguyen *et al.* where a piperazine was coupled to the rhodamine B base to form a fluorescent rhodamine B piperazine amide **(12)**.[155] According to the reported research, this can undergo reactions with acid chlorides (chloroacetyl chloride and bomoacetyl chloride) and alkyl halides (3-bromopropanol). These reactions were attempted herein, but proved unsuccessful.

As an alternative, the rhodamine B derivative with an ethylenediamine moiety was also prepared **(16)**. This was synthesised by coupling rhodamine B and hydrazine to yield a non-fluorescent rhodamine compound, due to the formation of a lactam. Due to the lack of fluorescent properties this derivative is of limited use and further compounds must be synthesised to meet the requirements of a multi-modality imaging agent. The molecule does however have potential as a mercury(II) sensor, as other research groups have reported an increase in fluorescence of similar molecules occurring due to lactam cleavage upon complexation of mercury(II).

BODIPY analogues that contain an isothiocyanate or an amine function have been synthesised. The method involved the condensation reaction between 4-acetamidobenzaldehyde and 3-ethyl-2,3-dimethylpyrrole to form the dipyrromethane, that can then be converted to the dipyrromethene (2,8-diethyl-1,3,7,9-5-(4-acetamidophenyl)dipyrromethene **(19)** by DDQ oxidation. The amide protecting group was then cleaved to give an amine by acid hydrolysis, and the dipyrromethene complexed with boron to form 5-(4-aminophenyl) borondipyrromethene **(20)**. The amine was converted to an isothiocyanate group using of TDP to form **(21)**.

An alkyl amine bearing BODIPY dye was prepared due to the reduced reactivity of the aromatic amine with isothiocyanate groups. The initial method used was based on a modified version of the synthesis reported by Biron *et al.* where a molecule with a Boc protected amine and an activated carboxylic acid group **(23)** was coupled to the amino BODIPY **(20)**.[176] This formed the Boc-protected BODIPY, 5-(4-Boc-aminobutylamidophenyl) borondipyrromethene **(24)**. Unfortunately, the deprotection step resulted in the decomplexation of the boron. This reaction was repeated with 5-(4-aminophenyl) dipyrromethene, using the activated carboxylic acid containing compound **(23)**,which resulted in the formation of 5-(4-bocaminobutylamidophenyl)-dipyrromethene **(24)**. Attempts to deprotect the Boc group, and then complex with boron in one continuous process were unsuccessful.

A further method to synthesise alkyl amine containing dye derivatives was then investigated. 5-(4-aminophenyl) dipyrromethene was reacted with bromoacetyl chloride in the presence of triethylamine. Instead of forming the desired compound **(28)**, the triethylamine acted as a nucleophile and formed 5-(4-triethylammoniummethylamidophenyl) borondipyrromethene chloride **(27)**. To prepare **(28)**, 5-(4-aminophenyl) dipyrromethene was washed with base to deprotect the phenyl amine, and then coupled to bromoacetyl chloride to give the desired compound, 5-(bromomethylamidophenyl) borondipyrromethene **(28),** which was then treated with ethylenediamine to form 5-(ethylenediaminemethylamidophenyl) borondipyrromethene **(29)**

6.4 Concluding remarks on the synthesis of macrocyclic ligands for lanthanides

The coupling reaction between DO3A **(31)** and either the benzimidazole **(7)** or 4-nitrobenzyl bromide was found to be problematic. After numerous attempts, the optimal conditions were found to require an initial wash of **(31)** with base and then the use of an excess of sodium hydrogen carbonate in the presence of the desired chromopore/linker unit while heating at reflux for 24 hours.

The nitro group on the chromophore/linker attached to the DO3A chelalor was reduced to an amine with either sulfurated sodium borohydride for the benzimidazole DO3A chelator, or using a palladium on carbon catalyst in the presence of hydrogen for the nitrobenzyl DO3A chelator. The lanthanide complexes were formed with the nitrobenzyl and aminobenzyl benzimidazole DO3A chelators **(34a-d)** and **(37a-d)**, and for the aminobenzyl DO3A chelators **(51a-c)**.

A number of strategies were investigated in order to couple the optical dye to the benzimidazole/benzyl DO3A chelators. This involved the reaction of an isothiocyanate function with the phenylamine group on either the DO3A chelator or on the optical dye. However, these reactions did not proceed at all or were extremely slow and so an alternative approach was required.

An alkyl amine bearing BODIPY dye was prepared due to the reduced reactivity of the aromatic amine with isothiocyanate groups. The initial method was based on a modified version by Biron *et al.* where a Boc protecting amine with an activated carboxylic acid group **(23)** was coupled to the amino BODIPY **(20)**.[176] This was confirmed, by the formation of **(48)** and **(50)**, the DO3A chelator derivative bearing an isothiocyanate group **(46)** and **(45)** was reacted with benzylamine. The lanthanum complexes were then formed to demonstrate

that this was a valid route to produce multi-modality imaging agents incorporating lanthanide ions.

Continuing with this approach, an attempt was made to couple the two optical dyes with alkyl amine groups, ethylenediamine rhodamine **(16)** or the BODIPY analogue **(29)**, to the isothiocyanate group on the DO3A chelator derivatives. Initially, the alkyl amine optical dye was stirred with the DO3A chelator, which did not give the desired compound. The alkyl amine optical dye was then washed with base before attempting the coupling reaction with the DO3A chelator, unfortunately this resulted in the polymerisation of the optical dye prior to reaction. This route appears to be the best approach to the production of multi-modality contrast agents but requires further optimisation of the conditions.

Attempts were made to attach an alkyl amine onto the DO3A chelator derivative **(50)**. Phthaloyl β-alanine chloride was reacted with the phenylamine, followed by the deprotection of the phthaloyl group using hydrazine. Attempts were made to couple this to the isothiocyanate BODIPY **(21)**, but t.l.c. analysis showed formation of multiple products. This again appears to be a viable route to synthesise multi-modality imaging agents but also requires further optimisation of the reaction conditions.

6.5 Concluding remarks on the studies of the physical properties and cellular uptake of lanthanide complexes and novel dye conjugates

The emission and the luminescence lifetime spectra were recorded for the europium(III) and terbium(III) nitrobenzyl and aminobenzyl benzimidazole complexes **(34a-b)** and **(37a-b)**. The emission spectra showed typical spectra for lanthanide complexes, with the terbium(III) complex containing more defined peaks, which suggests that the benzimidazole ligand provides better sensitisation onto the terbium(III) metal ion. The luminescence lifetime data of the complexes allows for determination of the number of inner sphere water molecules, which gave values approximating to one bound water for each of the complexes.

Relaxivity measurements on the gadolinium(III) contrast agents **(60)**, **(34c)**, **(37c)** and **(41b)** were made. Variable pH studies were performed on **(60)** and **(34c)**, showing that alterations in pH did not result in changes in relaxivity. This was proposed to be due to structural changes on protonation resulting in the formation of an 8-coordinate complex from a 9-coordinate complex. The gadolinium(III) aminobenzyl contrast agent **(41b)** contains two bound water molecules which, as expected, gave the highest relaxivity value of the compounds studied. The relaxivity of **(34c)** and **(37c)** was comparable to the known contrast agent Omniscan, with the nitrobenzyl benzimidazole complex **(34c)** having a higher relaxivity than the aminobenzyl benzimidazole complex **(37c)**. The non-functionalised benzimidazole complex **(60)** has lower relavitiy in comparison to the functionalised benzimidazoles **(34c)** and **(37c)**.

T_1-weighted images were produced of a 10 mm NMR tube containing distilled water that contained a 5 mm NMR tube containing a solution of gadolinium(III) contrast agent. The image intensity of all the contrast agents was shown to be much greater than water, with the image intensity difference greatest for the aminobenzyl gadolinium(III) complex **(41b)**, and the non-functionalised benzimidazole **(60)** showing the smallest difference. The cellular uptake

properties of the contrast agents were investigated by incubating the contrast agent with Jurkat cells and forming cell pellets. Both the T_1 and T_2-weighted images showed little difference in contrast between the medium and the cell pellet suggesting that the agent may not be accumulating in the cell.

Fluorescence microscopy was undertaken on the BODIPY dye **(27)** to investigate the optical dyes ability to be taken into HT-29 cells. The quaternary triethylamine group allowed for uptake into the cells, as confirmed by the optical images with the evidence suggesting that the dye was taken up into the lysosomes. Co-localisation studies can now be carried out on this potentially useful bio-compatible dye molecule.

6.6 Further work

The individual components of the multi-modality agent have been prepared successfully but problems arose when trying to couple the DO3A chelator groups with the optical dye. The main issue is the low reactivity of the aromatic amines. The initial point for further work would be to investigate this coupling reaction again. The most promising route involved the coupling of an alkyl amine containing optical dye to an isothiocyanate DO3A chelator. The reaction could be repeated, with the starting material prepared and used straight away without a base wash of the alkyl amine optical dye to avoid issues of polymer formation.

The other promising route was to form the alkyl amine from the DO3A chelator **(58)**. An alternative procedure could involve starting from the *tert*-butyl protected DO3A chelator with a benzyl amine group [**(35)** or **(39)**] and coupling this to the phthaloyl β-alanine chloride, followed by the deprotection of the phthaloyl group by hydrazine. Purification could then carried out using column chromatography on silica, followed by the deprotection of the acetate arms, and coupling to the optical dye.

Once a multi-modality agent has been prepared, a number of studies can be undertaken. The starting point would be an investigation of the cellular uptake properties to identify the localisation of the compounds within the cell (via co-localisation studies with a known optical dye). From this, the properties can be modified to optimise where the compound locates within the cell. An area of specific interest is the localisation of the contrast agent into the mitochondria, with particular reference to the mitochondria in the heart. Dysfunction in the mitochondria in the heart is known to have a key role in apoptosis, which is associated with heart disease. Agents such as the polyamines spermine and spermidine, are known to target the mitochondria. They could be coupled to the DO3A chelator to provide a target specific agent to localise in the mitochondria. From this, the next step would be to generate a switchable/responsive probe that

would be able to identify the events occurring in the cell, and in particular to detect the first signs of heart disease.

7. Experimental

7.1 General Procedures

7.1.1 NMR Spectroscopy

^{1}H NMR, ^{13}C NMR, and DEPT experiments were performed using a JEOL JNM-LA400 FT NMR spectrometer and a Bruker 500 Biospin NMR spectrometer. Chemical shifts for ^{1}H and ^{13}C NMR spectra are reported in parts per million relative to internal standards arising from the partially deuterated solvent. Coupling constants are reported in Hertz (Hz). Spectral splitting patterns are designated as follows: s = singlet, d = doublet, t = triplet, q = quartet, qu = quintet, m = mulitplet, dd = doublet of doublets and br = broad.

7.1.2 Mass Spectrometry

Electrospray mass spectra were recorded at the University of Hull using a Thermo Finnigan LCQ Classic-Electrospray LC-MS. Both low resolution and high resolution mass spectra were recorded at the EPSRC National Mass Spectrometry Service Centre at the University of Swansea using a Finnigan MAT 900 XLT.

7.1.3 X-ray crystallography

Single crystal X-ray diffraction data sets were collected on a Stöe IPDS-II imaging plate diffractometer, using a 0.5 mm monochromated X-ray beam of wavelength 0.71073 Å produced by a molybdenum K_{α} X-ray generator. Crystals were maintained at 150 K during data collection, with the temperature controlled using an Oxford Systems Cryostream Cooler. Diffraction data were solved using direct methods or Patterson syntheses (ShelXS), and the refinement was performed using the full-matrix least squares against F^2 (ShelXL-97) method. Hydrogen atoms were fixed in idealised positions and refined against a riding model, with C-H distances of 0.97 Å, N-H distances of 0.91 Å, and U_{iso} 1.2 times U_{eq} of the carrier atom, except where it is stated that the hydrogen atoms had been located on the difference map. Data reduction,

structure solution and refinement carried out by Dr Steve Archibald, Dr Jon Silversides and Ryan Mewis.

7.1.4 Solvents

Solvents were supplied by Fisher Scientific. When necessary, solvents were dried according to published procedures, but otherwise were used as received.[205] Dichloromethane (DCM), and acetonitrile (CH_3CN) were distilled from calcium hydride. Methanol (MeOH) was dried by distilling from magnesium turnings/iodine. Diethyl ether (Et_2O), and tetrahydrofuran (THF) were distilled from sodium metal using benzophenone as an indicator.

Deuterated solvents were supplied by Goss Scientific Instruments Ltd.

7.1.5 Chemical Reagents

Reagents were purchased from Sigma Aldrich, Fluka, Lancaster Chemicals, and Strem Chemicals. All reagents were used as supplied unless otherwise stated.

7.1.6 Photophysical studies

Photophysical measurements on europium(III) and terbium(III) complexes were carried out at the University of Hull using an Agilent 8453E UV-visible spectroscopy system, a SLM AB2 Luminescence Spectrometer and an Aminco Bowman Series 2 Luminescence Spectrometer SLM (Aminco Spectronic Instruments). Samples were prepared as aqueous solutions of concentration 2.5 $x10^{-5}$ M.

Excited-state lifetime measurements were made at the University of Leicester by Dr Mark Lowe on a Jobin Yvon Horiba Fluoromax-P spectrometer (using DataMax for Windows v2.2). Lifetimes were measured by excitation (395 nm direct) of the sample with a short 40 ms pulse of light (500 pulses per point) followed by monitoring of the integrated intensity of light (615 nm) emitted

during a fixed gate time of 0.1 ms, at a delay time later. Delay times were set at 0.1 ms intervals, covering four or more lifetimes. Excitation and emission slits were set to 15 and 5 nm bandpasses, respectively. The obtained decay curves were fitted to a simple mono exponential first-order decay curve using Microsoft Excel.

7.1.7 T_1 measurements

The longitudinal relaxivity of the gadolinium(III) complexes was determined from the spin-lattice relaxation time, T_1. The T_1 measurements were carried out using a Bruker 500 Biospin NMR spectrometer operating at 500 MHz. The aqueous solutions of gadolinium(III) complexes were made up using distilled water and transferred to 5 mm diameter NMR tubes. The T_1 measurements were made using the standard inversion-recovery pulse sequence (180°-τ-90°) with phase-sensitive detection and varying the τ values ranging from 50 μs to 6 s for each concentration of the complex. The computer programme Topspin was used to plot the time versus the signal intensity to get an exponential plot, and the T_1 values were calculated from the plot. A delay of at least 5 T_1 was maintained between successive pulses to allow for complete return of the spin system to equilibrium. The T_1 values of five different concentrations of the complex was measured. A plot of $1/T_1$ versus the concentration of the complex gave a straight line, and the slope was taken as the longitudinal relaxivity (r_1). Five different concentrations of the complex (1, 0.75, 0.5, 0.25 and 1.25 mM) in distilled water were used. The longitudinal relaxivity (r_1) at different pH values were recorded, by adjusting the pH with 0.1 M hydrochloric acid and varying the concentration accordingly.

7.1.8 MRI studies (tube within a tube)

A 1 mM solution of a gadolinium(III) complex was placed into the inner 5 mm NMR tube, with distilled water in outer 10 mm tube. MR imaging of the 10 mm NMR tubes was performed at 500 MHz using T_1 weighted spin-echo

sequences at room temperature (~ 21°C). The axial slice of interest was positioned through the NMR tube. Experimental parameters for T_1 were: 0.9 x 0.9 cm^2, matrix 256 x 128, slice thickness 1.0 mm, *TE* 2.0 ms, *TR* 100.0 ms and 6 averages.

7.1.9 In vitro MR studies

For MR imaging of cells, exponentially growing Jurkat cells were labelled with 300 μM of the gadolinium(III) contrast agent in 175 cm^2 tissue culture flasks for 18 h. After repeated washings with Hanks' buffered saline, cells were trypsinized, centrifuged and resuspended in 0.5 ml Eppendorf tubes at 1 x 10^7 cells in 500 μL of complete DMEM. Cells were allowed to settle before making MR measurements. Tubes with medium only, cells without gadolinium(III) contrast agent, and cells resuspended in medium containing the extracellular contrast agent Omniscan at 300 μM were used as a control sample.

MR imaging of the cell pellets was performed at 500 MHz using T_1 and T_2 weighted spin-echo sequences at room temperature (~ 21°C). The axial slice of interest was positioned through the cell pellet. Experimental parameters for T_1 were: 0.9 x 0.9 cm^2, matrix 256 x 128, slice thickness 1.0 mm, *TE* 2.0 ms, *TR* 100.0 ms and 6 averages. For T_2 were: 1.2 x 0.8 cm^2, matrix 256 x 256, slice thickness 1.0 mm, *TE* 90.0 ms, *TR* 8000.0 ms and 2 averages.

7.1.10 Cellular uptake assay

For the cellular uptake assay, a frozen culture of HT-29 cells (Human Caucasian colon adenocarcinoma) was obtained from ECACC and sub-cultured in McCoy's 5a medium (Sigma M8403) supplemented with 2mM Glutamine (invitrogen GIBCO 25030) and 10% heat inactivated Fœtal Bovine Serum (Biosera S1910). Adherent cells in the growing log phase were detached from the flask with 1 ml 0.25% Trypsin-EDTA (Invitrogen GIBCO 25200), counted and re-suspended at a concentration of 1 x 10^6 cells/ml in culture medium without serum.

To 800 µl of prepared cells, 200 µl of stock solution (8.9 mg compound dissolved into 1 ml DMSO (Sigma D2650 DIMETHYL SULFOXIDE (DMSO) HYBRI-MAX) giving a concentration of 1.44 x 10^{-2}M) diluted in culture medium without serum was added to give a final concentration of $1x10^{-4}$ M. The cells were returned to the incubator (5% CO_2 and 37 degrees C) for a period of 1 hour. After the incubation period, a further 3 ml of culture medium without serum was added to the cells to wash away any unbound compound and the cells were centrifuged at 550 x g for 10 minutes; the supernatant was decanted and the pellet re-suspended into 1 ml of McCoy's medium with serum; the suspension was then put into 35 mm, glass bottom culture dishes (Mat Tek Corporation P35G-0-10-C) and returned to the incubator overnight to allow the cells to attach.

22 hours after plating, the cells were imaged using a Leica DM-IRB inverted fluorescence microscope, and an ORCA-ER digital camera (Hamamatsu C4742-80) with HC Image imaging software. The excitation light was supplied by a xenon arc lamp housed in a monochromator (Optoscan Monochromator, Cairn Research). The excitation wavelength was set at 480 nm with the input and exit slits set at 15 nm; a FITC filter cube was used (Exciter HQ 480/40 nm, dichroic Q 505 lp, Emitter HQ 535/50, Chroma Corporation C34302) and the images collected with a 63x Pl Fluotar phase objective (Leica) and an acquisition time of 1 sec.

7.2 Synthetic Procedures

7.2.1 Chromatography

Column chromatography was performed using either MP silica 32-63, 60 Å, or Aldrich activated neutral aluminium oxide Brockman type I, standard grade, *ca.* 150 mesh.

Reactions were monitored using either Merck silica gel 60F 254 or aluminium oxide 60F 254 neutral thin layer chromatography (t.l.c) plates and the mobile phase indicated.

7.2.2 Air/Moisture Sensitive Reactions

Air and/or moisture sensitive reactions were carried out using Schlenk techniques under a nitrogen or argon atmosphere. Glassware was flame-dried when required.

7.3 Experimental procedures

7.3.1 Synthesis of *N*-(4-((2-aminophenylimino)methyl)phenyl) acetamide (1)

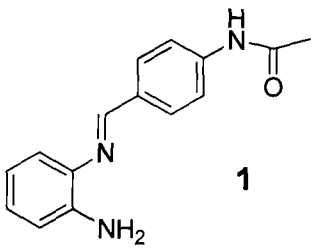

1

Method 1 - (Preferred Route)

4-Acetamidobenzaldehyde (1 g, 6.1 mmol) in methanol (200 ml), was added dropwise to a methanolic solution (250 ml) of 1,2-phenylenediamine (1.95 g, 18.3 mmol) over 3 Å molecular sieves and the resulting mixture was stirred for 72 h. The solvent was removed under reduced pressure. The solid was re-dissolved into a minimum amount of ethanol, the product was allowed to precipitate out and was collected by filtration to give a yellow solid (1.06 g, 69%). δ_H (DMSO): δ 2.09 (s, 3H, CH_3), 6.86 (s, 1H, CH), 7.17 (m, 2H, arCH), 7.58 (m, 2H, arCH), 7.74 (d, 2H, arCH, J = 8.68 Hz), 8.08 (d, 2H, arCH, J = 8.68 Hz), 10.18 (bs, 1H, NCH).

Method 2

4-Acetamidobenzaldehyde (1 g, 6.1 mmol) in methanol (200 ml), was added dropwise to a methanolic solution (250 ml) of 1,2-phenylenediamine (1.95 g, 18.3 mmol) then stirred for 4 h at room temperature and heated at reflux for 20 min. The solvent was removed under reduced pressure. The solid was re-dissolved into a minimum amount of ethanol, a solid was allowed to precipitate out was collected by filtration to give a red solid. The desired product was not isolated using this synthetic procedure.

7.3.2 Synthesis of *N*-(4-((2-aminophenylamino)methyl)phenyl) acetamide (2)

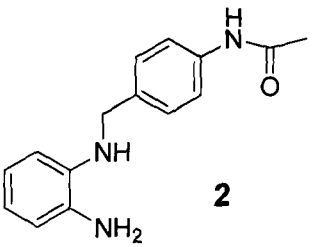

2

To a stirred solution of *N*-(4-((2-aminophenylimino)methyl)phenyl) acetamide (7.0 g, 2.8 mmol) in ethanol (200 ml), sodium borohydride (4.69 g, 0.124 mol) was added in small portions over 20 min. The reaction mixture was heated at reflux for 4 h. The solvent was then removed under reduced pressure to give an orange solid, which was dissolved in water and extracted into dichloromethane (2 x 100 ml). The combined extracts were dried over magnesium sulphate, and the solvent removed under reduced pressure to yield an orange solid, (3.74 g, 53%). δ_H (DMSO): δ 2.09 (s, 3H, CH_3), 4.51 (s, 2H, CH_2), 7.17 (m, 2H, arCH), 7.49 (m, 1H, arCH), 7.62 (m, 1H, arCH), 7.74 (d, 2H, arCH, J = 8.68 Hz), 8.08 (d, 2H, arCH, J = 8.68 Hz), 10.18 (s, 1H, NH).

7.3.3 Attempted synthesis of 1-(4-acetamidobenzyl)-2-chloromethyl benzimidazole (3)

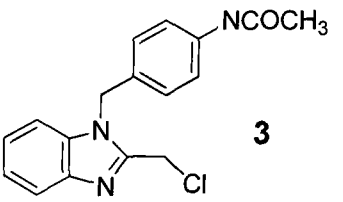

3

Method 1

Hydrogen chloride gas was bubbled into a solution of chloroacetonitrile (5 ml, 0.079 mol) in dry ethanol (3 ml) and dry diethyl ether (10 ml) for 5 mins, and the reaction mixture was then stirred for 24 h under nitrogen. *N*-(4-((2-aminophenylamino)methyl)phenyl) acetamide (0.5 g, 0.002 mol) was added and the resulting mixture was heated at reflux for 24 h. The solvent was then removed under reduced pressure to give a red solid. The desired product was not isolated using this synthetic procedure.

Method 2

Dry methanol (3.7 ml) and sodium (0.0036 g, 0.16 mmol) were stirred under nitrogen for 1 h to form sodium methoxide. Chloroacetonitrile (0.59 ml, 1 mmol) was then added and the reaction mixture was left to stir overnight. *N*-(4-((2-aminophenylamino)methyl)phenyl) acetamide (0.25 g, 1 mmol) dissolved in dry methanol (5 ml) was added to the reaction mixture which was then heated at reflux overnight. The solvent was removed under reduced pressure to give a yellow solid. The desired product was not isolated using this synthetic procedure.

.

7.3.4 Synthesis of 1-(4-nitrobenzylidene)benzene-1,2-diamine (4)

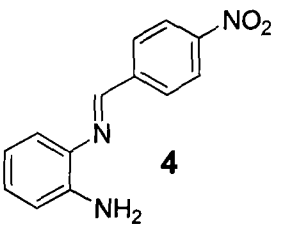

4

4-Nitrobenzaldehyde (5 g, 0.023 mol) dissolved in methanol (300 ml) was added dropwise over 30 min, to a stirred solution of 1,2-phenylenediamine (12.51 g, 0.12 mol) in methanol (400 ml) over 3 Å molecular sieves. The reaction mixture was then stirred at room temperature for 72 h. The solution was filtered, and the solvent removed under reduced pressure to give a red solid, which was then re-crystallised from ethanol to yield red crystals, (2.35 g, 71%). δ_H ($CDCl_3$): δ 6.81 (m, 2H, CH_2), 7.15 (m, 2H, CH_2), 8.07 (m, 2H, CH_2), 8.32 (m, 2H, CH_2), 8.63 (s, 1H, NCH).

7.3.5 Synthesis of 1-(4-nitrobenzyl)phenylenediamine (5)

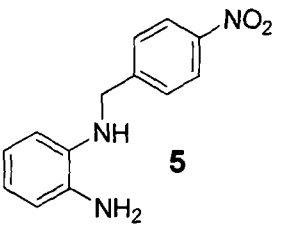

5

Method 1 - (Preferred Route)

4-Nitrobenzylbromide (5 g, 0.023 mol) dissolved in methanol (300 ml) was added dropwise to a stirred solution of 1,2-phenylenediamine (12.51 g, 0.12 mol) in methanol (400 ml) over 30 min. The reaction was stirred at room temperature for 4 h. Evaporation of the solvent under reduced pressure gave a red solid, which was dissolved in ethanol (250 ml) with heat, and allowed to cool. The orange precipitate was collected by filtration. The product was purified by column chromatography using dichloromethane as eluent (r.f. = 0.37) to yield a red/orange solid, (3.56 g, 60%). δ_H (CD_2Cl_2): δ 3.34 (s, 2H, NH_2), 3.91 (s, 1H, NH), 4.38 (s, 2H, CH_2), 6.39 (dd, 1H, CH_2, J = 7.3 Hz, J = 1.68 Hz), 6.65 (m, 3H, CH_2), 7.49 (dt, 2H, CH_2, J = 8.7 Hz, J = 1.97 Hz), 8.0 (dt, 2H, CH_2, J = 8.7 Hz, J = 1.97 Hz). *m/z*: 244.1 (100 $(M-H)^+$).

Method 2

Sodium borohydride (1,62 g, 40 mmol) was added in small portions over 20 mins to a stirred solution of 1-(4-nitrophenylmethylene)phenylenediamine (1.09 g, 4 mmol) in ethanol (200 ml). The reaction mixture was then heated at reflux for 4 h. The solvent was removed under reduced pressure to give an orange solid, which was dissolved in dichloromethane (2 x 100 ml) and washed with water. The organic layer was extracted and dried over magnesium sulphate, and the solvent removed under reduced pressure to yield a red/orange solid, (0.52 g, 48%). δ_H ($CDCl_3$): δ 4.46 (s, 2H, CH_2), 6.46 (dd, 2H, CH_2, J = 7.3 Hz), 6.71 (m, 2H, CH_2), 7.56 (d, 2H, CH_2, J = 8.7 Hz), 8.19 (m, 2H, CH_2), 8.69 (s, 1H, NH).

7.3.6 Synthesis of 1-(4-nitrobenzyl)-2-hydroxymethyl benzimidazole (6)

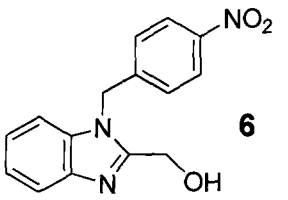

6

1-(4-Nitrobenzyl)phenylenediamine (0.2 g, 2 mmol) and glycolic acid (0.07 g, 2.9 mmol) were dissolved in 5 N hydrochloric acid (10 ml) and the reaction mixture was heated at reflux for 48 h to form a dark brown solution. The solution was cooled to 0°C, and then the pH adjusted with 5% sodium hydroxide solution resulting in a yellow precipitate. The yellow precipitate was collected by filtration, and washed with water (20 ml), followed by diethyl ether (2 x 20 ml) to give a light brown solid, (0.23 g, 77%). δ_H (CD_3OD): δ 4.83 (s, 2H,CH_2), 5.69 (s, 2H, CH_2), 7.29 (m, 5H,arCH), 7.60 (d, 1H, J = 8.14), 8.1 (dt, 2H, J = 8.7, J = 1.97). δ_C (CD_3OD): δ 46.89 (CH_2), 56.99 (CH_2), 110.05 (CH), 119.25 (CH), 122.92 (CH), 123.64 (CH), 124.08 (CH), 127.54 (CH), 135.0 (C), 141.28 (C), 143.23 (C), 147.68 (C), 154.17 (C). *m/z*: 283.8 (100 $(M-H)^+$).

7.3.7 Synthesis of 1-(4-nitrobenzyl)-2-chloromethyl benzimidazole (7)

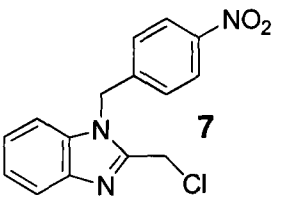

7

Method 1 – (Preferred route)

Thionyl chloride (10 ml) was added to 1-(4-nitrobenzyl)-2-hydroxymethyl benzimidazole (0.5 g, 1.7 mmol) under nitrogen and stirred for 24 h. The thionyl chloride was removed under reduced pressure to leave a brown solid. The product was then dissolved into the minimum amount of methanol and excess diethyl ether was added to precipitate a cream solid, (0.36 g, 68%). δ_H (CD_3OD): δ 5.74 (s, 2H,CH_2), 6.32 (s, 2H, CH_2), 7.68(m, 2H, arCH), 7.82(m, 3H, arCH), 8.01 (d, 1H, J = 8.14), 8.1 (dt, 2H, J = 8.7, J = 1.97). δ_C (CD_3OD): δ 32.87 (CH_2), 48.93 (CH_2), 114.08(CH), 116.28 (CH), 124.76 (CH), 127.81 (CH), 127.03 (CH), 129.44 (CH), 131.60 (C), 133.19 (C), 142.07 (C), 148.85 (C), 149.53 (C). *m/z*: 301.8 (100 $(M-H)^+$).

Method 2

1-(4-Nitrobenzyl)phenylenediamine (0.5 g, 2 mmol) and chloroacetic acid (0.25 g, 2.9 mmol) were dissolved in 5 N hydrochloric acid (50 ml) and refluxed for 18 h. The solution was cooled to 0°C, and the pH adjusted with ammonia hydroxide solution to cause the formation of a precipitate. The resulting oily brown solid was collected by filtration, and dissolved in methanol, the solvent was then removed under reduced pressure to give a brown solid. The desired product was not isolated using this synthetic procedure.

Method 3

A mixture of 1-(4-nitrobenzyl)phenylenediamine (0.5 g, 2 mmol) and chloroacetic acid (0.25 g, 2.9 mmol) were dissolved in 5 N hydrochloric acid (50 ml) and heated at reflux for 18 h. The solution was then cooled to 0°C, and the pH adjusted with 5 % sodium hydroxide solution to cause the formation of a precipitate. The resulting oily brown solid was collected by filtration, and dissolved in methanol, with the solvent removed under reduced pressure. The product was allowed to air dry forming a brown solid. The desired product was not isolated using this synthetic procedure.

Method 4

A solution of 4-nitrobenzylbromide (0.75 g, 3.5 mmol) dissolved in dichloromethane (50 ml) was added dropwise over 30 min to a solution of 2-chloromethyl benzimidazole (0.5 g, 3 mmol) in dichloromethane (100 ml) with a drop of triethylamine. The reaction mixture was left to stir for 24 h at room temperature. The solvent was removed under reduced pressure. The desired product was not isolated using this synthetic procedure.

Method 5

4-Nitrobenzylbromide (1.29 g, 6 mmol) and 2-chloromethyl benzimidazole (1 g, 6 mmol) were dissolved in tetrahydrofuran (100 ml) with a drop of triethylamine and stirred for 24 h at room temperature. The reaction was then heated at reflux for 3 h. The solvent was removed under reduced pressure. An attempt to purify by flash chromatography (dichloromethane with an increasing gradient of methanol from 0 % to 10 %) did not isolate any of the desired product.

Method 6

4-Nitrobenzylbromide (1.43 g, 6.6 mmol), 2-chloromethyl benzimidazole (1 g, 6 mmol) and potassium carbonate (0.62 g, 4.5 mmol) were dissolved in dimethylformamide (40 ml) and the mixture was brought to reflux for 3 h. Dichloromethane (100 ml) was added to the reaction mixture causing the formation of a precipitate. This was collected by filtration and the solvent removed under reduced pressure. The desired product was not isolated using this synthetic procedure.

Method 7

4-Nitrobenzylbromide (1.77 g, 8 mmol), 2-chloromethyl benzimidazole (1 g, 6 mmol) and sodium hydroxide (0.28 g, 6 mmol) were dissolved in acetonitrile (100 ml) and the mixture was heated at reflux for 24 h. The reaction mixture was filtered and the solvent removed from the filtrate under reduced pressure to produce a brown/orange oil. The oil was dissolved into minimum acetonitrile and left to recrystallise at 0°C. The desired product was not isolated using this synthetic procedure.

Method 8

Sodium hydride (0.086 g, 3.6 mmol) was added in small portions to a mixture of 4-nitrobenzylbromide (0.65 g, 3 mmol) and 2-chloromethyl benzimidazole (0.5 g, 3 mmol) dissolved in dimethylformamide (40 ml) over 30 min. The reaction was then stirred at room temperature for 1 week, followed by heating to reflux for 3 h. Dichloromethane (100 ml) was added to the reaction mixture causing the formation of a precipitate to occur. The solid was removed by filtration and then the solvent was removed from the filtrate under reduced pressure. The solid was dissolved into dichloromethane (100 ml) and washed with water (100 ml). The organic layer was extracted and dried over sodium sulphate. This solution was then filtered and the solvent removed under vacuum. The desired product was not isolated using this synthetic procedure.

Method 9

4-Nitrobenzylbromide (0.97 g, 4.5 mmol), 2-chloromethyl benzimidazole (0.5 g, 3 mmol) and potassium carbonate (0.83 g, 6 mmol) were dissolved in acetone (100 ml) and the resulting mixture brought to reflux for 24 h. The reaction mixture was filtered and the solvent removed from the filtrate under reduced pressure. The desired product was not isolated using this synthetic procedure.

Method 10

2-Chloromethyl benzimidazole (1 g, 6 mmol) dissolved in dry tetrahydrofuran (50 ml) was stirred at −30°C under nitrogen, followed by the dropwise addition of lithium diisopropylamide (0.86 g, 4.8 mmol) over 5 min. The reaction mixture was allowed to stir at −30°C for 15 min. After 15 min 4-nitrobenzylbromide (1.29 g, 6 mmol) in dry tetrahydrofuran (50 ml) was added. The reaction mixture was allowed to warm up to room temperature and then left to stir overnight under nitrogen. The solvent was removed under reduced pressure but the desired product was not isolated.

Method 11

2-Chloromethyl benzimidazole (1 g, 6 mmol) in tetrahydrofuran (50 ml) was stirred at −30°C under nitrogen, followed by the dropwise addition of lithium diisopropylamide (0.86 g, 4.8 mmol) over 5 min. The reaction was allowed to stir for 2 h. After this period, 4-nitrobenzylbromide (1.29 g, 6 mmol) in tetrahydrofuran (50 ml) was added. The reaction mixture was allowed to stir overnight under nitrogen. The solvent was removed under reduced pressure but the desired product was not isolated.

7.3.8 Attempted synthesis of 1-(4-nitrobenzyl)-2-iodomethyl benzimidazole (8)

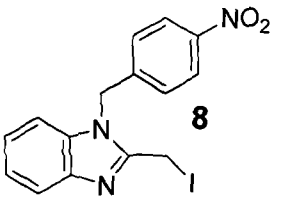

8

1-(4-Nitrobenzyl)-2-chloromethyl benzimidazole (0.5 g, 1.7 mmol) was added to a solution of sodium iodide (0.37 g, 2.5 mmol) in acetone (50 ml) and heated at reflux for 6 h. The organic layer was washed with water (50 ml), dried over magnesium sulphate, filtered, and then the solvent was removed under reduced pressure. The desired product was not isolated using this synthetic procedure.

7.3.9 Synthesis of 1-(4-nitrobenzyl)-2-methylpyridinium benzimidazole bromide (9)

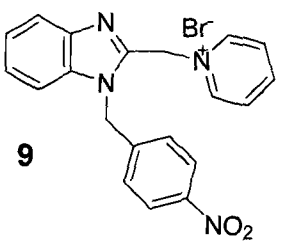

9

1-(4-Nitrobenzyl)-2-chloromethyl benzimidazole (0.1 g, 3.3 mmol) in pyridine (2.68 ml, 33 mmol) was heated at reflux for 30 min. The solvent was removed and the resulting solid was recrystallised from methanol to yield a white solid, (0.89 g, 52.4%). δ_H ($CDCl_3$): δ 6.14 (s, 2H, CH_2), 6.97 (s, 2H, CH_2), 7.30 (m, 5H, arCH), 7.65 (d, 1H, arCH, J = 8.14 Hz), 7.93 (m, 4H, arCH), 8.35 (t, 1H, arCH, J = 8.7 Hz), 9.67 (d, 2H, arCH, J = 6.6 Hz). δ_C ($CDCl_3$): δ 46.83 (CH_2), 56.03 (CH_2), 110.33 (CH), 120.28 (CH), 124.05 (CH), 124.70 (CH), 127.73 (CH), 127.93 (CH), 142.06 (C), 143.34 (C), 145.74 (C), 146.12 (C), 146.65 (C). *m/z*: 345.8 (100 $(M-H)^+$).

7.3.10 Attempted synthesis of 2-chloromethyl benzimidazole (10)

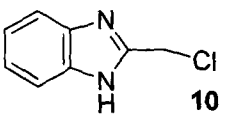

10

Method 1

1,2-Phenylenediamine (2 g, 0.018 mol) and chloroacetic acid (2 g, 0.0029 mol) were dissolved in 5 N hydrochloric acid (50 ml) and heated at reflux for 18 h. The solution was cooled to 0°C, and the pH adjusted with aqueous ammonia solution to cause the formation of a precipitate to occur. The solid was collected by filtration, dissolved into methanol and the solvent removed under reduced pressure. The product was allowed to air dry to give a brown solid. The desired product was not isolated using this synthetic procedure.

Method 2

Hydrogen chloride gas was bubbled into a solution of chloroacetonitrile (0.25 ml, 4 mmol) in a mixture of dry ethanol (2 ml) and dry diethyl ether (8 ml) for 5 min, and then the reaction mixture was stirred for 24 h under nitrogen. 1,2-Phenylenediamine (0.38 g, 3.5 mmol) dissolved in dry dichloromethane was added at 0°C and the mixture was then left to stir for 24 h at room temperature. The solvent was then removed under reduced pressure to give a white solid. The desired product was not isolated using this synthetic procedure.

7.3.11 Synthesis of rhodamine B base (11)

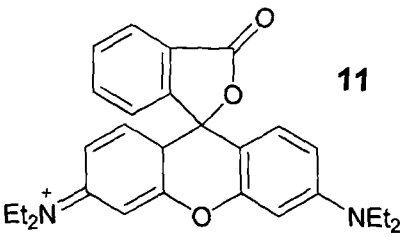

Rhodamine B (5 g, 0.001 mol) was partitioned between aqueous 1 M NaOH and ethyl acetate. After separation of the organic layer, the aqueous layer was extracted with two additional portions of ethyl acetate. The combined organic layers were washed with NaOH and then with brine. The resulting organic solution was dried over Na_2SO_4, filtered, and concentrated under reduced pressure to yield a bright pink solid, (4.39 g , 93%). δ_H (CD_3OD): δ 1.19 (t, 12H, J = 7.16 Hz), 3.56 (q, 8H, J = 7.16 Hz), 6.81 (d, 2H, J = 2.56 Hz), 6.89 (m, 2H), 7.16 (m, 3H), 7.52 (m, 2H), 7.97 (m, 1H).

7.3.12 Synthesis of rhodamine B piperazine amide (12)

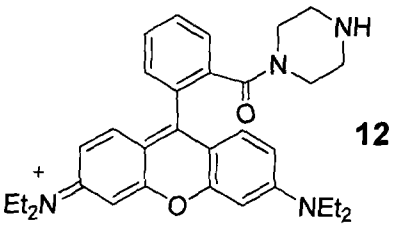

A 2.0 M solution of trimethyl aluminium in toluene (1.13 ml, 2.26 mmol) was added dropwise to a solution of piperazine (0.4 g, 4.5 mmol) in dry dichloromethane (35 ml) at room temperature for 1 h. A solution of rhodamine B base (0.5 g, 1.13 mmol) in dry dichloromethane (20 ml) was then added dropwise. After heating at reflux for 24 h the reaction mixture was then allowed to cool to room temperature at which point a 0.1 M aqueous solution of HCl was added dropwise until gas evolution ceased. The solution was filtered and washed in turn with dichloromethane followed by a 4:1 dichloromethane/methanol solution. The solvent was removed under reduced pressure, and the resulting solid was then partitioned between dilute aqueous $NaHCO_3$ and ethyl acetate. The aqueous layer was separated and washed with 3 additional portions of ethyl acetate to remove residual starting material. The aqueous layer was saturated with NaCl, acidified with 1 M aqueous HCl and then extracted with multiple portions of 2:1 propan-2-ol/dichloromethane, until only a faint colour persisted. The combined organic layers were then dried over Na_2SO_4, filtered, and concentrated under reduced pressure. The resulting purple solid was dissolved into a minimum amount of methanol and precipitated out by the addition of a large volume of diethyl ether. The product was collected by filtration as a dark purple solid, (0.33 g, 57%). δ_H (CD_3OD): δ 1.32 (t, 12H, J=7.12), 3.33 (brs, 4H), 3.69 (m, 12H), 6.97 (d, 2H, J = 2.4 Hz), 7.1 (d, 2H, J = 2.4 Hz, 9.52 Hz), 7.27 (d, 2H, J = 9.52 Hz), 7.51 (m, 1H), 7.78 (m, 3H). δ_C (CD_3OD): δ 14.93 (CH_3), 49.08 (CH_2), 51.09 (CH_2), 51.3 (CH_2), 51.9 (CH_2), 99.46, 116.91, 117.58, 130.97, 133.49, 133.69, 133.96, 135.13, 158.80, 159.32, 161.34, 171.58 (C=O). *m/z*: 511 (100 $(M-H)^+$).

7.3.13 Attempted synthesis of rhodamine B 4-(2-chloroacetyl)piperazine amide (13)

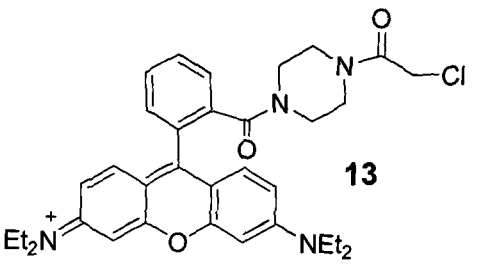

Rhodamine B piperazine amide (0.5 g, 0.9 mmol) was dissolved in dichloromethane (2 ml) and cooled to 0°C. Chloroacetyl chloride (0.229 g, 1.96 mmol) and pyridine (0.186 g, 2.35 mmol) were added in turn, and the reaction mixture was allowed to warm to ambient temperature over a period of 4 h. The dark red solution was concentrated under reduced pressure and partitioned between diethyl ether and aqueous 1 M K_2CO_3. After washing with 3 portions of 1:4 isopropanol/dichlromethane, the combined organic layers were separated, dried over Na_2SO_4, filtered, and concentrated. The desired product was not isolated using this synthetic procedure.

7.3.14 Attempted synthesis of rhodamine B 4-(2-bromoacetyl)piperazine amide (14)

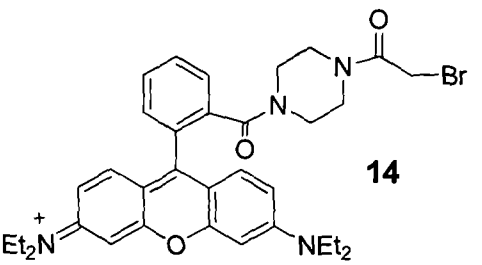

Rhodamine B piperazine amide (0.5 g, 0.9 mmol) was dissolved in dichloromethane (2 ml) and then cooled to 0°C. Bromoacetyl chloride (0.3 g, 1.96 mmol) and pyridine (0.186 g, 2.35 mmol) were added and the reaction mixture was allowed to warm to ambient temperature over a period of 4 h. The dark red solution was concentrated under reduced pressure and partitioned between diethyl ether and aqueous 1 M K_2CO_3. After washing with 3 portions of 1:4 isopropanol/dichloromethane, the combined organic layers were separated, dried over Na_2SO_4, filtered, and concentrated. The desired product was not isolated using this synthetic procedure.

7.3.15 Attempted synthesis of rhodamine B 4-(propoxy)piperazine amide (15)

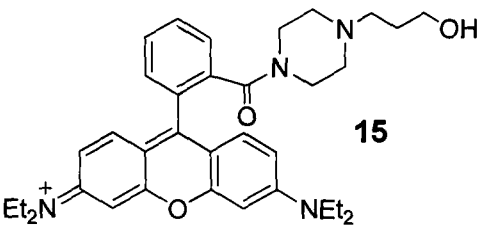

A mixture of 3-bromopropanol (0.105 ml, 1.22 mmol) and diisoethylpropylamine (0.29 ml, 1.7 mol) was added to rhodamine B piperazine amide (0.5 g, 0.9 mmol) in dimethylformamide (2 ml) under nitrogen and stirred for 24 h. After 24 h, a further portion of 3-bromopropanol (0.105ml, 1.22mmol) and diisoethylpropylamine (0.29 ml, 1.7 mol) were added and the solution stirred for a further 2 h. The dark red solution was concentrated under reduced pressure and partitioned between diethyl ether and aqueous 1 M K_2CO_3. After washing with 3 portions of 1:4 isopropanol/dichlromethane, the combined organic layers were separated and dried over Na_2SO_4, filtered, and concentrated. The desired product was not isolated using this synthetic procedure.

7.3.16 Synthesis of rhodamine B base ethylamine (16)

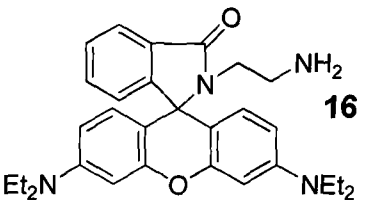

Rhodamine B (1 g, 2.09 mmol) was dissolved into hot ethanol (20 ml), followed by the addition of ethylene diamine (0.7 ml, 10 mmol). The mixture was heated at reflux for 6 h, and then the volume was reduced to 5ml by evaporation under reduced pressure, followed by the cooling to below 0°C. This resulted in a precipitate that was collected by filteration and recrystallised from minimum acetonitrile, to produce an orange/pink solid, (0.41 g, 38%). δ_H ($CDCl_3$): δ 1.08 (t, 12H, CH_3, J = 67 Hz), 2.32 (t, 2H, CH_2, J = 6.7 Hz), 3.11 (t, 2H, CH_2, J = 6.7 Hz), 3.34 (m, 4H,CH_2), 6.18 (m, 2H, arCH), 6.35 (m, 4H, arCH), 7.09 (m, 1H, arCH), 7.36 (m, 2H, arCH), 7.83 (m, 1H, arCH). δ_C ($CDCl_3$): δ 12.67 (CH_3), 40.92 (CH_2), 44.01 (CH_2), 44.42 (CH_2), 97.78 (CH), 105.79 (C), 108.22 (CH), 122.82 (CH), 123.90 (CH), 128.10 (CH), 128.77 (CH), 131.96 (C), 132.45 (CH), 148.87 (C), 153.35 (C), 153.55 (C), 168.66 (CO).

7.3.17 Synthesis of rhodamine B base ethylaminethioureamethylbenzyl (18)

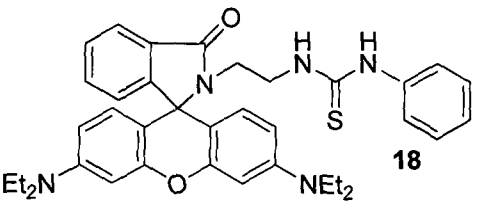

18

Rhodamine B base ethylamine (0.05 g, 0.01 mmol) was dissolved in dry dichloromethane (50 ml) followed by the addition of phenylisothiocyanate (0.014 ml, 0.01 mmol) under nitrogen. The reaction mixture was stirred under nitrogen at room temperature for 48 h while protected from light. The solvent was then removed under reduced pressure. The crude product was recrystallised from the minimum amount of acetonitrile to yield a light pink solid (0.064 g, 79%). δ_H ($CDCl_3$): δ 1.08 (m, 12H, CH_2), 3.2 (m, 12H, CH_2), 6.16 (m, 2H, CH), 6.28 (d, 4H, CH, J = 9.72), 6.97 (m, 1H, CH), 7.2-7.37 (m, 6H, CH), 7.74 (m, 1H, CH). δ_C ($CDCl_3$): δ, 12.69 (CH_3), 39.77 (CH_2), 44.53 (CH_2), 48.22(CH_2), 97.87, 104.42, 108.43, 122.88, 123.99, 127.61, 127.96, 128.26, 128.44, 128.70, 130.27, 133.0, 137.41, 149.6, 153.35, 153.95, 170.14 (C=O), 181.60 (C=S). *m/z*: 635.4 (100 $(M-H)^+$).

7.3.18 Synthesis of 2,8-diethyl-1,3,7,9-tetramethyl-5-(4-acetamidophenyl) dipyrromethene (19)

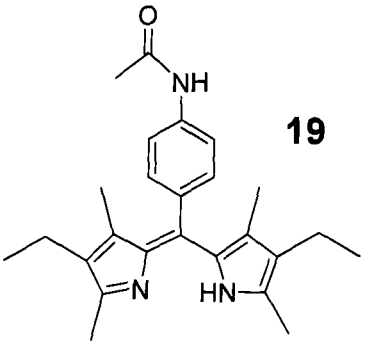

19

1-Acetamidobenzaldehyde (1.32 g, 8.1 mmol) and 2-kryptopyrrole (2 g, 16.2 mmol) were dissolved in anhydrous dichloromethane under an atmosphere of nitrogen. A drop of TFA was added and the mixture was left stirring at RT overnight. DDQ (1.83 g, 8.1 mmol) was added and then the reaction mixture was allowed to stir for 1h at RT. It was then washed with water and dried over Na_2SO_4. After filtering and removing the solvent under reduced pressure, the crude mixture was purified by column chromatography on silica gel (9:1 dichlromethane/methanol, r.f. = 0.25) to give a purple solid, (1.16 g, 37%). δ_H ($CDCl_3$): δ 1.04-1.17 (m, 6H), 1.87 (s, 6H), 2.15 (m, 4H), 2.37-2.52 (m, 6H), 7.0-7.02 (d, 2H, J = 8.16), 7.7-7.78 (b, 2H).

7.3.19 Synthesis of 5-(4-aminophenyl) borondipyrromethene (20)

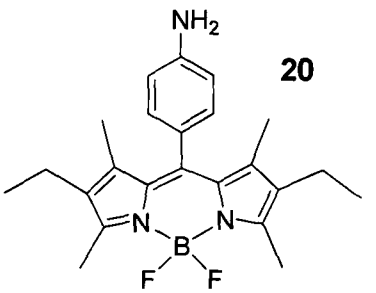

20

2,8-Diethyl-1,3,7,9-tetramethyl-5-(4-acetamidophenyl) dipyrromethane (0.33 g, 0.84 mmol) was dissolved in a mixture of methanol (20 ml) and 1 M HCl (20 ml), and then heated at reflux for 1 h. The reaction mixture was cooled and neutralised with 2 M NaOH. The aqueous solution was extracted with dichloromethane, and the combined organic extracts dried over Na_2SO_4. The solvent was removed under reduced pressure. The crude product was dissolved in anhydrous dichloromethane (50 ml), containing triethylamine (1 ml), and $BF_3.OEt_2$ (1 ml) and stirred under nitrogen, at room temperature for 3-4 h while protected from light. The reaction mixture was washed with water, brine, and dried over Na_2SO_4. The solvent was removed, and the crude product was purified by column chromatography on flash silica (2:1 dichloromethane:hexane, (r.f. = 0.36)) to give a red solid, (0.12 g, 36%). δ_H ($CDCl_3$): δ 0.79-0.83 (m, 6H), 0.89-0.91 (m, 6H), 2.22 (m, 4H), 2.4 (s, 6H), 7.37-7.39 (d, 2H, J = 8.44 Hz), 7.68-7.7 (d, 2H, J = 8.44 Hz). *m/z*: 395 (100 $(M-H)^+$).

7.3.20 Synthesis of 5-(4-isothiocyanatophenyl) borondipyrromethene (21)

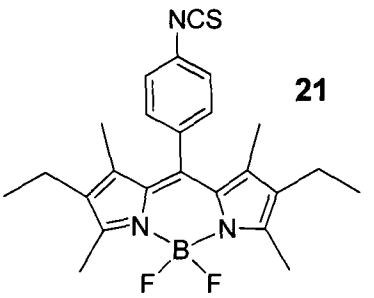

21

5-(4-Aminophenyl) borondipyrromethene (0.229 g, 0.51 mmol) was dissolved in dry dichloromethane (50 ml) followed by the addition of 1,1-thiocarbonyldi-2(1H)-pyridone (0.24g, 1.0 mmol) while under an atmosphere of nitrogen. The reaction mixture was stirred under nitrogen, at room temperature for 4 h while protected from light. The solvent was removed under reduced pressure. The crude product was purified by column chromatography on silica gel with hexane-dichloromethane 1:2 as eluent. (r.f. = 0.65 in hexane-dichloromethane 1:2). The fractions containing the product were combined and the solvent was removed under reduced pressure to yield a red solid, (0.24 g, 75%). δ_H ($CDCl_3$): δ 0.89 (m, 6H, CH_3), 1.21 (s, 6H, CH_3), 2.21 (m, 4H, CH_2), 2.44 (s, 6H, CH_3), 7.2 (d, 2H, CH, J = 8.08 Hz), 7.27 (d, 2H, CH, J = 8.08 Hz).

7.3.21 Attempted synthesis of 5-(4-phenylthiourephenyl) borondipyrromethene (22)

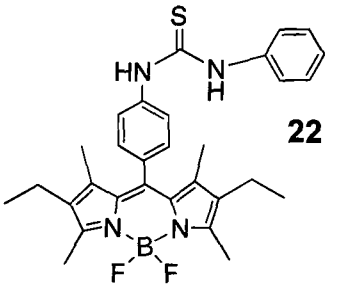

22

5-(4-aminophenyl) borondipyrromethane (0.01 g, 0.025 mmol) was dissolved in dry dichloromethane (50 ml) followed by the addition of phenylisothiocyanate (0.003 ml, 0.025 mmol) under nitrogen. The reaction mixture was then stirred under nitrogen at RT for 7 days while protected from light. The solvent was removed under reduced pressure. The desired product was not isolated using this synthetic procedure.

7.3.22 Synthesis of Boc-aminobutyric acid (23)

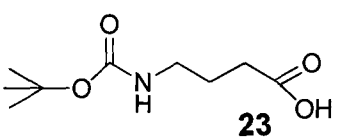

23

A mixture of 4-aminobutyric acid (2 g, 0.019 mol), Boc-ON (5.25 g, 0.021 mol) and triethylamine (4 ml, 0.029 mol) in dioxane (20 ml) was stirred for 4 h at 0 °C under an atmosphere of nitrogen. The solvent was then removed under reduced pressure. The resulting white solid was dissolved in water (50 ml) and washed with ethyl acetate (2 x 50 ml). The aqueous layer was separated and the solvent was removed under reduced pressure to yield a clear oil, (1.94 g, 49%). δ_H (CD_3OD): δ 1.30 (s, 9H, CH_3), 1.63 (qu, 2H, CH_2, J = 7.0 Hz), 2.16 (t, 2H, CH_2, J = 7.28 Hz), 2.97 (t, 2H, CH_2, J = 7.0 Hz). *m/z*: 204 $(100(M-H)^+)$.

7.3.23 Synthesis of 5-(4-*Boc*-aminobutylamidophenyl) borondipyrromethene (24)

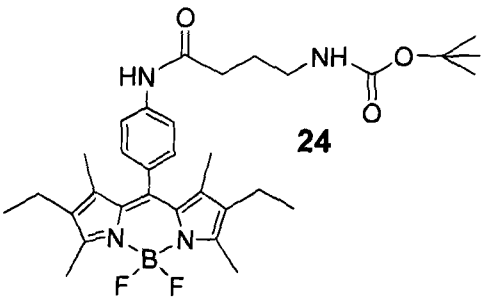

24

Triethylamine (0.04 ml, 0.29 mmol) and ethylchloroformate (0.024 ml, 0.24 mmol) were added to Boc-aminobutyric acid (0.05 g, 0.24 mmol) in dry dichloromethane (50 ml) under an atmosphere of nitrogen the resulting mixture stirred for 30 min at RT. The solvent was removed under reduced pressure. The solid was then re-dissolved into dry dichloromethane (50 ml) followed by the addition of 5-(4-aminophenyl) borondipyrromethene (0.032 g, 0.086 mmol). The reaction mixture was then stirred under nitrogen for 1 h at 0 °C followed by 1 h at RT. The solvent was removed under reduced pressure and the residue purified by column chromatography (using an increasing gradient of 100% dichloromethane to 2% methanol in dichloromethane, r.f. = 0.22 in 2% methanol in dichloromethane). The fractions containing the product were combined and the solvent was removed under reduced pressure to yield a red solid (0.04 g, 85%). δ_H ($CDCl_3$): δ 0.97 (t, 6H, CH_3, J = 7.72 Hz), 1.2 - 2.0 (br, 15H, CH_3/CH_2), 2.3 - 2.5 (m, 6H, CH_2), 7.21 (d, 2H, CH, J = 8.16 Hz), 7.78 (d, 2H, CH_2, J = 8.16 Hz). *m/z*: 581.4 ($100(M-H)^+$).

7.3.24 Attempted synthesis of 5-(4-aminobutylamidophenyl) borondipyrromethene (25)

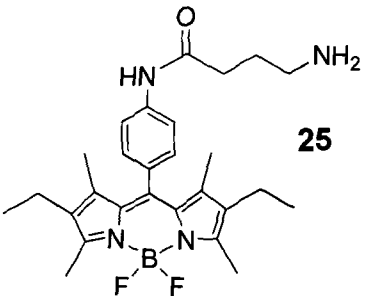

25

Method 1

5-(4-Boc-aminobutylamidophenyl) borondipyrromethene (0.04 g, 0.07 mmol) was dissolved in a mixture of 4 M hydrochloric acid (0.3 ml) and dioxane (1 ml) which was then stirred for 4 h at RT. The solvent was removed under reduced pressure. The desired product was not isolated using this synthetic procedure.

Method 2

5-(4-Boc-aminobutylamidophenyl) borondipyrromethene (0.04 g, 0.07 mmol) was dissolved in a mixture of trifluoroacetic acid (3 ml) and dichloromethane (3 ml) which was then stirred for 20 min at RT. The solvent was removed under reduced pressure. The desired product was not isolated using this synthetic procedure.

Method 3

5-(4-Boc-aminobutylamidophenyl) dipyrromethene (0.018 g, 0.03 mmol) dissolved in trifluoroacetic acid (3 ml) and dichloromethane (3 ml) was stirred for 1 h at RT. The solvent was then removed under reduced pressure. The resulting purple solid was re-dissolved into ethyl acetate and washed with aqueous sodium hydrogen carbonate (2 x 50 ml). The organic layer was collected and dried over sodium sulphate, filtered and the solvent removed under reduced pressure. The crude product was dissolved in anhydrous dichloromethane (50 ml), containing dry triethylamine (0.5 ml), and $BF_3.OEt_2$ (0.5 ml) and the reaction mixture stirred under nitrogen, at room temperature for 3-4 h, while protected from light. The reaction mixture was washed with water,

brine, and dried over Na_2SO_4. The solvent was removed under reduced pressure. The desired product was not isolated using this synthetic procedure.

7.3.25 Synthesis of 5-(4-Boc-aminobutylamidophenyl) dipyrromethene (26)

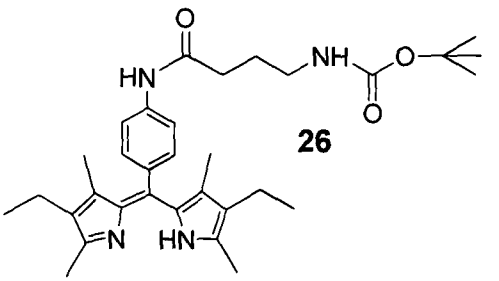

26

Triethylamine (0.04 ml, 0.29 mmol) and ethylchloroformate (0.024 ml, 0.24 mmol) were added to a solution of Boc-aminobutyric acid (0.05 g, 0.24 mmol) in dry dichloromethane (50 ml) under nitrogen and stirred for 30 min. The solvent was removed under reduced pressure. The solid was re-dissolved into dry dichloromethane (50 ml) followed by the addition of 5-(4-aminophenyl) dipyrromethane (0.028 g, 0.082 mmol) under nitrogen. The reaction misxture was then stirred at 0 °C for 1 h followed by RT for 1 h. The solvent was removed under reduced pressure and the residue purified by column chromatography (increasing gradient of 100 % dichloromethane to 10 % methanol in dichloromethane, r.f. = 0.22 in 10 % methanol in dichloromethane) to yield a purple solid, (0.018 g, 45%). δ_H ($CDCl_3$): δ 0.84 – 2.44 (br, 37H), 7.24 (m, 2H, CH), 7.88 (m, 2H, CH).

7.3.26 Synthesis of 5-(4-triethylammoniummethylamidophenyl) borondipyrromethene chloride (27)

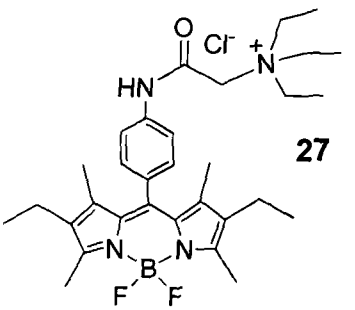

27

5-(4-Boc-aminobutylamidophenyl) borondipyrromethene (0.04 g, 0.1 mmol) was dissolved in a mixture of dry dichloromethane (10 ml) and triethylamine (0.5 ml). The mixture was then cooled in an ice bath at 0 °C under an atmosphere of nitrogen. Bromoacetylchloride (0.013 ml, 0.15) was then added and the solution stirred for 24 h while protected from the light. The solvent was removed under reduced pressure, and the residue was purified by preparative tlc using 10% methanol in dichloromethane as the eluent, (r.f. = 0.08 in 10% methanol in dichloromethane) to yield a red solid, (0.045 g, 82%). δ_H ($CDCl_3$): δ 0.94 (t, 6H, CH_3, J = 7.6), 1.37 (s, 6H, CH_3), 1.44 (t, 9H, CH_3), 2.26 (q, 4H, CH_2, J = 7.28 Hz), 2.50 (s, 6H, CH_3), 3.74 (q, 6H, CH_2, J = 7.28 Hz), 4.62 (s, 2H, CH_2), 7.21 (d, 2H, CH, J = 8.44 Hz), 7.85 (d, 2H, CH, J = 8.44 Hz). δ_C ($CDCl_3$): δ 12.08 (CH_3), 12.55 (CH_3), 14.69 (CH_3), 17.13 (CH_3), 50.87 (CH_2), 54.68 (CH_2), 56.96 (CH_2), 120.77 (CH), 128.95 (CH), 130.95 (C), 132.19 (C), 132.86 (C), 138.08 (C), 138.53 (C), 139.76 (C), 153.78 (C), 161.91 (C=O). *m/z*: 538.4 (100 $(M\text{-}H)^+$). HRMS: calcd. for $C_{31}H_{44}O_1N_4{}^{10}B_1F_2$: 536.3607 found 536.3600.

7.3.27 Synthesis of 5-(4-bromomethylamidophenyl) borondipyrromethene (28)

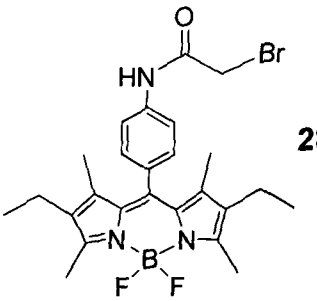

28

5-(4-Boc-aminobutylamidophenyl) borondipyrromethene (0.02 g, 0.05 mmol) was dissolved in dichloromethane and washed with sodium hydrogen carbonate solution. The organic layer was then separated and dried over sodium sulphate. The solvent was removed under reduced pressure. The residue was then re-dissolved into dry dichloromethane (25 ml) and the resulting solution cooled in an ice bath at 0°C under nitrogen. Bromoacetylchloride (0.002 ml, 0.034) was added and the reaction mixture stirred for 4 h protected from the light. The solvent was removed under reduced pressure, and the compound purified by preparative tlc using 100% dichloromethane as eluent (r.f. = 0.44 in 100% dichloromethane) to yield a red solid, (0.02 g, 77%). δ_H ($CDCl_3$): δ 0.98 (t, 6H, CH_3, J = 7.6 Hz), 1.32 (s, 6H, CH_3), 2.31 (q, 4H, CH_2, J = 7.6 Hz), 4.06 (s, 2H, CH_2), 7.26 (d, 2H, CH, J = 8.4 Hz), 7.71 (d, 2H, CH, J = 8.4 Hz). δ_C ($CDCl_3$): δ 11.89 (CH_3), 12.50 (CH_3), 14.59 (CH_3), 17.05 (CH_3), 29.43(CH_2), 120.03 (CH), 129.19 (CH), 132.13 (C), 132.87 (C), 137.59 (C), 138.24 (C), 139.31 (C), 158.87 (C), 163.39 (C=O). δ_B ($CDCl_3$) δ -0.98. *m/z*: 514.4 (100 $(M-H)^+$).

7.3.28 Synthesis of 5-(4-ethylenediaminemethylamidophenyl) borndipyrromethene (29)

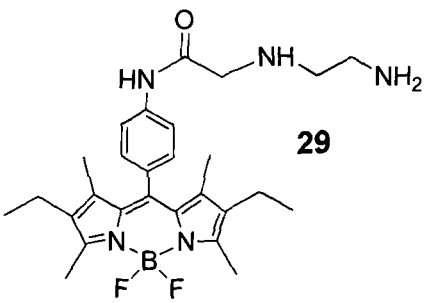

29

5-(4-Bromomethylamidophenyl) borondipyrromethene (0.16 g, 0.3 mmol) and ethylenediamine (0.41 ml, 4.3 mmol) were dissolved in acetonitrile (50 ml) and the reaction mixture was stirred overnight under nitrogen protected from the light. The solvent was then removed under reduced pressure, the resulting residue was re-dissolved into dichloromethane and it was washed with aqueous sodium hydrogen carbonate solution (2 x 100 ml). The organic layer was collected, dried over sodium sulphate, filtered and the solvent removed under reduced pressure. The compound was then purified by preparative tlc using 100% dichloromethane as the eluent, (r.f. = 0.12 in 100% dichloromethane) to yield a red solid, (0.02 g, 13%). δ_H ($CDCl_3$): δ 0.91 (t, 6H, CH_3, J = 7.28 Hz), 1.22 (s, 6H, CH_3), 2.21 (s, 2H, CH_2) 2.34 (q, 4H, CH_2, J = 7.28 Hz), 2.45 (s, 6H, CH_3), 2.72 (m, 2H, CH_2), 2.83 (m, 2H, CH_2), 7.14 (d, 2H, CH, J = 8.4 Hz), 7.72 (d, 2H, CH, J = 8.4 Hz). *m/z*: 496.3 (100 $(M-H)^+$).

7.3.29 Synthesis of di-5-(4-aminophenyl) zincdipyrromethene (30)

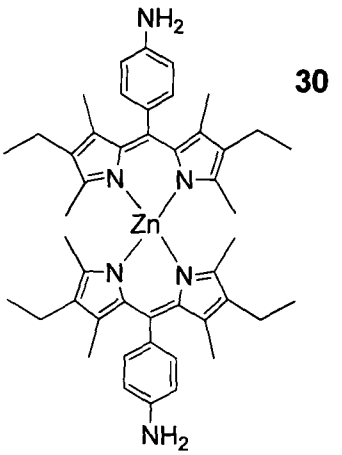

30

Zinc acetate (0.13 g, 0.7 mmol) dissolved in dry methanol (10 ml) was added to a solution of 5-(4-aminophenyl) borondipyrromethene (0.5 g, 1.4 mmol) in dry methanol (40 ml) under nitrogen and the mixture was heated at reflux for 24 h. The solvent was removed under reduced pressure, the resulting solid was then re-dissolved into dichloromethane (50 ml) and washed with water (2 x 50 ml). The organic layer was collected, dried over sodium sulphate, filtered, and the solvent removed under reduced pressure to yield a green solid, (0.44 g, 83%). δ_H (CD_3OD): δ 0.8 (s, 12H, CH_3), 1.25 (s, 12H, CH_3), 1.84 (s, 12H, CH_3), 2.18 (s, 8H, CH_2), 6.67 (s, 4H, CH), 7.00 (s, 4H, CH). *m/z*: 756 (100 $(M\text{-}H)^+$). HRMS: calcd. for $C_{46}H_{56}N_6Zn$: 756.3852 found 756.3859.

7.3.30 Synthesis of 1,4,7-tris(*tert*-butoxycarbonylmethyl)-1,4,7,10-tetraazacyclododecane (31)

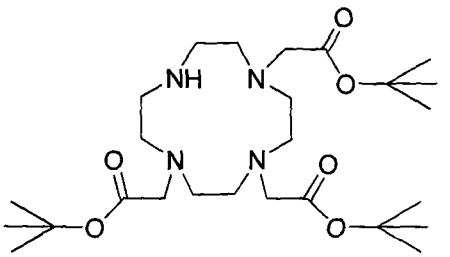

31

Method 1 – (Preferred route)

A solution of *tert*-butylbromoacetate (10.01 g, 0.052 mol) in acetonitrile (300 ml) was added dropwise to a mixture of sodium hydrogen carbonate (4.39 g, 0.052 mol) and 1,4,7,10-tetraazacyclododecane (3 g, 0.018 mol) in acetonitrile (900 ml). The solution was stirred at room temperature for 72 h and the undissolved material was then removed by filtration. The solvent was removed from the filtrate under reduced pressure and the residue purified by column chromatography over silica gel, with gradient elution from pure dichloromethane to 2% methanol in dichloromethane (r.f. = 0.63 in 5% MeOH in DCM) to yield an off-white solid. The product was then washed with diethyl ether, and collected by filtration to yield a white solid, (5.4 g, 60%). δ_H(DMSO): δ 1.42 (s, 9H, CH_3), 1.42 (s, 18H, CH_3), 2.65 – 2.84 (brs, 16H, CH_2), 2.98 (brs, 4H, CH_2), 3.34 (s, 2H, CH_2), 8.75 (s, 1H, NH). δ_C (DMSO): δ 27.8 (CH_3), 45.4 (CH_2), 48.4 (CH_2), 49.6 (CH_2), 51.3 (CH_2), 52.2 (CH_2), 55.9 (CH_2), 80.57 ($C(CH_3)_3$), 170.5 (C=O). *m/z*: 514 (100, $(M-H)^+$).

Method 2

A solution of *tert*-butylbromoacetate (9.99 g, 0.051 mol) in chloroform (300 ml) was added dropwise to a mixture of potassium carbonate (7.08 g, 0.051 mol) and 1,4,7,10-tetraazacyclododecane (2.94 g, 0.017 mol) in chloroform (900 ml). The resulting solution was stirred at room temperature for 72 h and any undissolved material was then removed by filtration. The solvent was evaporated under reduced pressure and the residue purified by column

chromatography over silica gel, with gradient elution from pure dichloromethane to 5% methanol in dichloromethane (r.f. = 0.625 in 5% MeOH in DCM) to yield a white solid, (4.9 g, 56%). δH(DMSO): δ 1.40 (s, 9H, CH_3), 1.41 (s, 18H, CH_3), 2.63 – 2.84 (brs, 16H, CH_2), 3.01 (brs, 4H, CH_2), 3.33 (s, 2H, CH_2), 8.7 (s, 1H, NH). δC (DMSO): δ 27.1 (CH_3), 45.6 (CH_2), 48.1 (CH_2), 49.6 (CH_2), 51.6 (CH_2), 52.2 (CH_2), 56.01 (CH_2), 80.60 ($C(CH_3)_3$), 170.8 (C=O). m/z: 514 (100, (M-H)+).

7.3.31 Synthesis of 1,4,7-tris(*tert*-butoxycarbonylmethyl)-10-(1-(4-nitrobenzyl)-2-methyl benzimidazole)-1,4,7,10-tetraazacyclododecane (32)

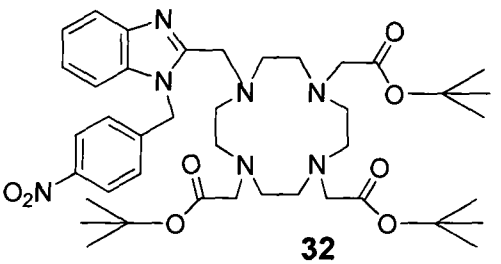

32

Method 1 – (preferred route)

1,4,7-Tris(*tert*-butoxycarbonylmethyl)-1,4,7,10-tetraazacyclododecane hydrobromide salt (0.5 g, 0.97 mmol) was dissolved in dichloromethane and the solution was then washed with saturated sodium hydrogen carbonate solution. The organic layer was separated and dried over sodium sulphate, filtered and then the solvent removed under reduced pressure. The resulting white solid was dissolved in dry acetonitrile followed by the addition of 1-(4-nitrobenzyl)-2-chloromethyl benzimidazole (0.32 g, 1.1 mmol) and sodium hydrogen carbonate (0.8 g, 7.8 mmol). The reaction mixture was then stirred under an atmosphere of nitrogen, heated to 60°C and left to react for 24 h. The solvent was removed under reduced pressure. The resulting residue was dissolved in a minimum volume of dichloromethane and then purified by flash chromatography (SiO_2, dichloromethane with an increasing gradient of methanol from 0% to 2%), (r.f. = 0.56 in 10% MeOH in DCM). The eluted fractions containing the product were combined and the solvent was removed under reduced pressure to give an off white solid, (0.58 g, 76%). δ_H ($CDCl_3$): δ 1.42 (m, 27H, CH_3), 2.2-3.5 (brm, 22H,CH_2), 3.94 (brs, 2H,CH_2), 5.43 (brs, 2H, CH_2), 7.09 (dt, 1H, CH, J = 6.96 Hz, J = 1.08 Hz), 7.15 (dt, 1H, CH, J = 6.96 Hz, J = 1.08 Hz), 7.23 (d, 1H, CH, J = 7.8 Hz), 7.33 (d, 2H, CH, J = 8.8 Hz), 7.42 (d, 1H, CH, J = 7.8 Hz), 8.01(dt, 2H, CH, J = 8.8 Hz, J = 2.0 Hz). δ_C ($CDCl_3$): δ 27.9 (CH_3), 46.3 (CH_2), 50.75(CH_2), 55.52 (CH_2), 56.4 (CH_2), (CH_2), 80.57 ($C(CH_3)_3$), 81.88 ($C(CH_3)_3$), 109.34 (CH), 119.31 (CH), 121.91 v, 122.73 (CH), 124.04 (CH), 127.40 (CH), 135.53 (C), 142.42 (C), 144.02 (C),

147.43 (C), 153.82 (C), 172.4 (C=O), 172.7 (C=O). *m/z*: 780.5 (100 $(M-H)^+$). HRMS: calcd. For $C_{41}H_{62}O_8N_7$: 780.46564 found 780.4645.

Method 2

1,4,7-Tris(*tert*-butoxycarbonylmethyl)-1,4,7,10-tetraazacyclododecane hydrobromide salt (0.5 g, 0.97 mmol) was dissolved in dry acetonitrile and stirred under an atmosphere of nitrogen with 1-(4-nitrobenzyl)-2-chloromethyl benzimidazole (0.29 g, 0.97 mmol) and potassium hydrogen carbonate (0.29 g, 2.9 mmol) added as solid. The resulting mixture was heated to 60°C and stirred for 96 h. The solvent was then removed under reduced pressure. The residue was dissolved in a minimum volume of dichloromethane and then purified by flash chromatography (SiO_2, dichloromethane with an increasing gradient of methanol from 0% to 2%), (r.f. = 0.56 in 10% MeOH in DCM). The fractions containing the product were combined and the solvent was removed under reduced pressure yielding an off white solid, (0.23 g, 30%). δ_H ($CDCl_3$): δ 1.42 (m, 27H, CH_3), 2.2-3.5 (brm, 22H, CH_2), 3.94 (brs, 2H, CH_2), 5.43 (brs, 2H, CH_2), 7.09 (dt, 1H, CH, J = 6.96 Hz, J = 1.08 Hz), 7.15 (dt, 1H, CH, J = 6.96 Hz, J = 1.08 Hz), 7.23 (d, 1H, CH, J = 7.88 Hz), 7.33 (d, 2H, CH, J = 8.8 Hz), 7.42 (d, 1H, CH, J = 7.88 Hz), 8.01(dt, 2H, CH, J = 8.8 Hz, J = 2.0 Hz). δ_C ($CDCl_3$): δ 27.9 (CH_3), 46.3 (CH_2), 50.75(CH_2), 55.52 (CH_2), 56.4 (CH_2), (CH_2), 80.57 ($C(CH_3)_3$), 81.88 ($C(CH_3)_3$), 109.34 (CH), 119.31 (CH), 121.91 v, 122.73 (CH), 124.04 (CH), 127.40 (CH), 135.53 (C), 142.42 (C), 144.02 (C), 147.43 (C), 153.82 (C), 172.4 (C=O), 172.7 (C=O).

Method 3

1,4,7-Tris(*tert*-butoxycarbonylmethyl)-1,4,7,10-tetraazacyclododecane, hydrobromide salt (0.5 g, 0.97 mmol) was dissolved in dry tetrahydrofuran (50 ml) and stirred under nitrogen. 1-(4-Nitrobenzyl)-2-chloromethyl benzimidazole (0.29 g, 0.97 mmol) and a catalytic amount of potassium iodide were added, The mixture was then heated to 60°C and stirred for 96 h. The solvent was removed under reduced pressure after cooling to RT. The resulting residue was dissolved in a minimum volume of dichloromethane and purified by flash chromatography (SiO_2, dichloromethane with an increasing gradient of methanol from 0% to 2%), (r.f. = 0.56 in 10% MeOH in DCM). The fractions containing the product were combined and the solvent was evaporated yielding an off white solid, (0.76 g, 78%). δ_H ($CDCl_3$): δ 1.42 (m, 27H, CH_3), 2.2-3.5 (brm, 22H, CH_2), 3.94 (brs, 2H, CH_2), 5.43 (brs, 2H, CH_2), 7.09 (dt, 1H, CH, J = 6.96 Hz, J = 1.08 Hz), 7.15 (dt, 1H, CH, J = 6.96 Hz, J = 1.08 Hz), 7.23 (d, 1H, CH, J = 7.88 Hz), 7.33 (d, 2H, CH, J = 8.8 Hz), 7.42 (d, 1H, CH, J = 7.88 Hz), 8.01(dt, 2H, CH, J = 8.8 Hz, J = 2.0 Hz).

Method 4

1-(4-Nitrobenzyl)-2-chloromethyl benzimidazole (0.29 g, 0.97 mmol) was added to a solution of potassium iodide (0.16 g, 0.97 mmol) in acetone (50 ml) and heated at reflux for 6 h. The organic layer was washed with water (50 ml), dried over magnesium sulphate, filtered, and the solvent removed from the filtrate under reduced pressure. The resulting solid was dissolved in acetonitrile and 1,4,7-tris(*tert*-butoxycarbonylmethyl)-1,4,7,10-tetraazacyclododecane hydrobromide salt (0.5 g, 0.97 mmol) was added as solid. The reaction mixture was heated at reflux for 24 h. The solvent was then removed under reduced pressure. The desired product was not isolated using this synthetic procedure.

Method 5

Sodium hydride (0.05 g, 1.9 mmol) and 1,4,7-tris(*tert*-butoxycarbonylmethyl)-1,4,7,10-tetraazacyclododecane hydrobromide salt (0.5 g, 0.97 mmol) were added to dry tetrahydrofuran (100 ml) and the mixture was stirred under nitrogen for 1 h. 1-(4-Nitrobenzyl)-2-chloromethyl benzimidazole (0.29 g, 0.97 mmol) dissolved in dry tetrahydrofuran (50 ml) was then added and the mixture was heated to 60°C and stirred for 24 h. The solvent was removed under reduced pressure. The resulting solid was redissolved into dichloromethane (100 ml) and washed with water (100 ml). The organic layer was separated, dried over sodium sulphate, filtered and the solvent removed under reduced pressure. The desired product was not isolated using this synthetic procedure.

Method 6

A mixture of lithium diisopropylamide (0.123 ml, 0.58 mmol) and 1,4,7-tris(*tert*-butoxycarbonylmethyl)-1,4,7,10-tetraazacyclododecane hydrobromide salt (0.1 g, 0.19 mmol) in dry tetrahydrofuran (100 ml) was stirred under nitrogen for 2 h. 1-(4-Nitrobenzyl)-2-chloromethyl benzimidazole (0.059 g, 0.19 mmol) dissolved in dry tetrahydrofuran (50 ml) was then added and the mixture was stirred for 24 h. The solvent was removed under reduced pressure. The resulting solid was then redissolved into dichloromethane (100 ml) and the solution washed with water (100 ml). The organic layer was separated, dried over sodium sulphate, filtered and the solvent removed under reduced pressure. The desired product was not isolated using this synthetic procedure.

Method 7

1,4,7-Tris(*tert*-butoxycarbonylmethyl)-1,4,7,10-tetraazacyclododecane hydrobromide salt (0.5 g, 0.97 mmol) dissolved in dry dimethylformamide and stirred under nitrogen. 1-(4-nitrobenzyl)-2-chloromethyl benzimidazole (0.29 g, 0.97 mmol) and potassium hydrogen carbonate (0.52 g, 3.9 mmol) were then added as solids. The resulting mixture was heated to 60°C and stirred for 24 h. The solvent was then removed under reduced pressure. The desired product was not isolated using this synthetic procedure.

7.3.32 Synthesis of 1,4,7-tris(carboxymethyl)-10-(1-(4-nitrobenzyl)-2-methyl benzimidazole)-1,4,7,10-tetraazacyclododecane (33)

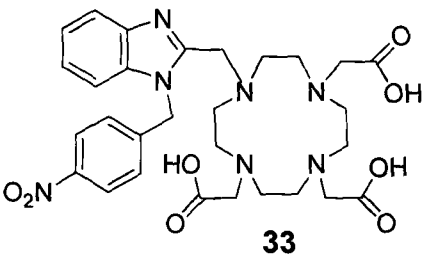

33

1,4,7-Tris(*tert*-butoxycarbonylmethyl)-10-(1-(4-nitrobenzyl)-2-methyl benzimidazole)-1,4,7,10-tetraazacyclododecane (0.23 g, 0.29 mmol) was dissolved in 37% aqueous HCl (30 ml) and the solution was stirred at room temperature for 3 h. The solvent was then removed under reduced pressure, the residue was redissolved into water (5 ml) and filtered through a 0.2 μm syringe filter. The solvent was removed under reduced pressure to give a yellow solid, (0.18 g, 100%). δ_H (D_2O): δ 2.94-3.68 (brm, 18H,CH_2), 3.99 (s, 2H, CH_2), 4.12 (s, 2H, CH_2), 4.54 (s, 2H, CH_2), 5.95 (s, 2H, CH_2), 7.41 (d, 2H, CH, J = 8.8 Hz), 7.54-7.70 (m, 3H, CH), 7.79 (d, 1H, CH, J = 8.16 Hz), 8.10 (d, 2H, CH, J = 8.8 Hz). δ_C (D_2O): δ 48.3 (CH_2), 48.55 (CH_2), 48.17 (CH_2), 51.16 (CH_2), 53.07 (CH_2), 53.67 (CH_2), 55.07 (CH_2), 113.28 (CH), 115.5 (CH), 124.72 (CH), 127.77 (CH), 128.02 (CH), 128.29 (CH), 130.18 (C), 132.12 (C), 140.74 (C), 148.01 (C), 149.23 (C), 169.7 (C=O), 177.63 (C=O). *m/z*: 612.3 (100$(M-H)^+$). HRMS: calcd. For $C_{29}H_{35}O_8N_7$: 612.2776 found 612.2774.

7.3.33 Synthesis of europium(III) 1,4,7-tris(carboxymethyl)-10-(1-(4-nitrobenzyl)-2-methyl benzimidazole)-1,4,7,10-tetraazacyclododecane (34a)

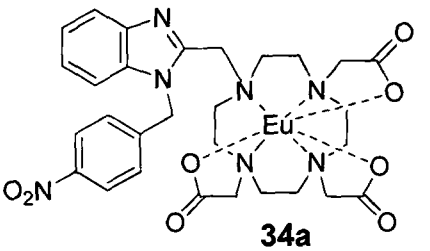

34a

1,4,7-Tris(carboxymethyl)-10-(1-(4-nitrobenzyl)-2-methyl benzimidazole)-1,4,7,10-tetraazacyclododecane (0.19 g, 0.26 mmol) and europium(III) trifluoromethanesulfonate (0.2 g, 0.26 mmol) were dissolved in water (10 ml) and stirred. A solution of potassium carbonate (0.21 g, 1.53 mmol) in water (10 ml) was added dropwise. The solution was heated at reflux for 18 h. The solvent was then evaporated under reduced pressure. The resulting solid was dissolved in a minimum of MeOH and purified using a sephadex column LH-20 (MeOH as eluent). The fractions containing the product were combined and evaporated under reduced pressure to give a yellow solid, (0.16 g, 68%). δ_H (D_2O): δ -18.83, -17.96, -16.78, -16.38, -15.25, -14.56, -12.58, -10.87, -9.97, -9.76, -9.46, -8.52, -7.58, -7.46, -7.27, -7.12, -6.86, -5.87, -4.99, -3.44, -2.58, -1.56, -0.59, 1.25, 2.38, 2.19, 3.16, 3.19, 3.97, 5.63, 6.13, 6.74, 6.93, 7.31, 7.48, 7.58, 7.90, 8.18, 8.36, 9.50, 10.01, 10.62, 12.57, 28.82, 29.95, 30.09. *m/z*: 760.1 (100 $(M-H)^+$). HRMS: calcd. For $C_{29}H_{35}O_8N_7{}^{151}Eu$: 760.1740 found 760.1739.

7.3.34 Synthesis of terbium(III) 1,4,7-tris(carboxymethyl)-10-(1-(4-nitrobenzyl)-2-methyl benzimidazole)-1,4,7,10-tetraazacyclododecane (34b)

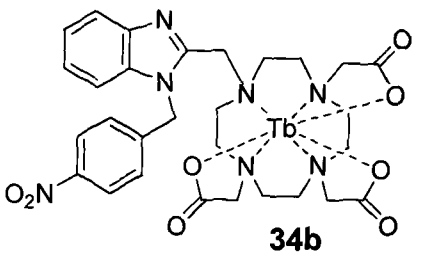

34b

1,4,7-Tris(carboxymethyl)-10-(1-(4-nitrobenzyl)-2-methylbenzimidazole)-1,4,7,10-tetraazacyclododecane (0.039 g, 0.064 mmol), and terbium(III) trifluoromethanesulfonate (0.039 g, 0.064 mmol) were dissolved in water (10 ml) and stirred. A solution of potassium carbonate (0.044 g, 0.32 mmol) in water (10 ml) was added dropwise. The solution was heated at reflux for 18 h. The solvent was then evaporated under reduced pressure. The resulting solid was dissolved in a minimum of MeOH and purified using a sephadex column LH-20 (MeOH as eluent). The fractions containing the product were combined and evaporated under reduced pressure to give a yellow solid, (0.038 g, 79%). m/z: 768.2 (100(M-H)+). HRMS: calcd. for $C_{29}H_{35}O_8N_7Tb$: 768.1795 found 768.1792.

7.3.35 Synthesis of gadolinium(III) 1,4,7-tris(carboxymethyl)-10-(1-(4-nitrobenzyl)-2-methylbenzimidazole)-1,4,7,10-tetraazacyclododecane (34c)

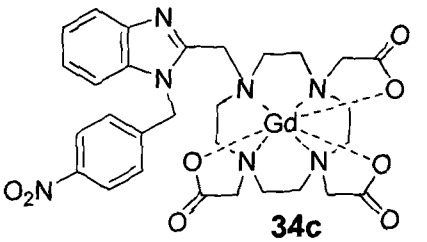

1,4,7-Tris(carboxymethyl)-10-(1-(4-nitrobenzyl)-2-methyl benzimidazole)-1,4,7,10-tetraazacyclododecane (0.25 g, 0.35 mmol), and gadolinium(III) trichloride (0.1 g, 0.35 mmol) were dissolved water (10 ml) and stirred. Potassium carbonate (0.24 g, 1.75 mmol) in water (10 ml) was added dropwise. The solution was heated at reflux for 18 h. The solvent was then evaporated under reduced pressure. The resulting solid was dissolved in a minimum of MeOH and purified using a sephadex column LH-20 (MeOH as eluent). The fractions containing the product were combined and evaporated under reduced pressure to give a yellow solid, (0.21 g, 71%). *m/z:* 763.2 (100 $(M\text{-}H)^+$). HRMS: calcd. for $C_{29}H_{35}O_8N_7{}^{154}Gd$: 763.1750 found 763.1756.

7.3.36 Synthesis of lanthanum(III) 1,4,7-tris(carboxymethyl)-10-(1-(4-nitrobenzyl)-2-methyl benzimidazole)-1,4,7,10-tetraazacyclododecane (34d)

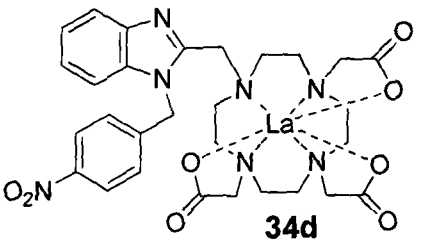

34d

1,4,7-Tris(carboxymethyl)-10-(1-(4-nitrobenzyl)-2-methyl benzimidazole)-1,4,7,10-tetraazacyclododecane (0.2 g, 0.27 mmol), and lanthanum(III) trifluoromethanesulfonate (0.2 g, 0.27 mmol) were dissolved in water (10 ml) and stirred. A solution of potassium carbonate (0.19 g, 1.35 mmol) in water (10 ml) was added dropwise. The solution was heated at reflux for 18 h. The solvent was then evaporated under reduced pressure. The resulting solid was dissolved in a minimum of MeOH and purified using a sephadex column LH-20 (MeOH as eluent). The fractions containing the product were combined and evaporated under reduced pressure to give a yellow solid, (0.18 g, 77%). δ_H (D_2O): δ 2.02-3.66 (brm, 22H,CH_2), 4.23 (s, 2H,CH_2), 5.31 (s, 2H,CH_2,), 6.99-7.06 (m, 6H, CH,), 7.48 (s, 1H, CH), 7.84 (s, 1H, CH). δ_C (D_2O): δ 46.51 (CH_2), 48.62 (CH_2), 50.51 (CH_2), 51.49 (CH_2), 53.37 (CH_2), 59.98 (CH_2), 60.72 (CH_2), 110.7 (CH), 118.79 (CH), 120.67 (CH), 123.99 (CH), 127.35 (CH), 134.38 (C), 139.48 (C), 142.45 (C), 146.97 (C), 153.84(C), 178.95 (C=O), 179.30 (C=O). *m/z*: 748.2 (100$(M-H)^+$). HRMS: calcd. for $C_{29}H_{35}O_8N_7La$: 748.1605 found 748.1601.

7.3.37 Synthesis of 1,4,7-tris(*tert*-butoxycarbonylmethyl)-10-(1-(4-aminobenzyl)-2-methyl benzimidazole)-1,4,7,10-tetraazacyclododecane (35)

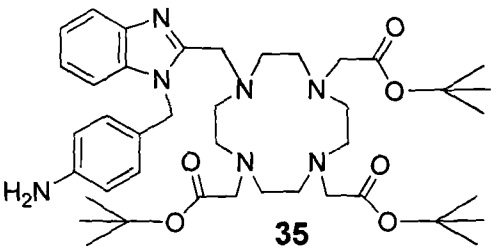

35

Method 1 – (preferred route)

Sodium borohydride (0.015 g, 0.19 mmol) and sulphur (0.037 g, 0.38 mmol) were suspended in dry tetrahydrofuran (50 ml) and stirred under nitrogen for 1 hour. 1,4,7-Tris(*tert*-butoxycarbonylmethyl)-10-(1-(4-nitrobenzyl)-2-methyl benzimidazole)-1,4,7,10-tetraazacyclododecane (0.15 g, 0.19 mmol) dissolved in tetrahydrofuran (20 ml) was added and the reaction mixture was heated at reflux overnight under nitrogen. The resulting solution was then cooled and washed with 5% sodium hydroxide solution (4 x 50 ml), the organic layer was separated, dried over sodium sulphate, filtered and the solvent removed from the filtrate under reduced pressure. The solid product was purified by flash chromatography on alumina (the eluent was dichloromethane with an increasing gradient of methanol from 0 to 5%), (r.f. = 0.28 in 10% MeOH in DCM) to give a yellow solid, (0.09 g, 65%). δ_H ($CDCl_3$): δ 1.42 (m, 27H, CH_3), 2.2-3.6 (brm, 24H,CH_2), 5.14 (s, 2H, CH_2), 6.52 (d, 2H, CH, J = 8.0 Hz), 6.75 (d, 2H, CH, J = 8.0 Hz), 7.04 (t, 1H, CH, J = 7.16 Hz), 7.14 (t, 1H, CH, J = 7.16 Hz), 7.25 (d, 1H, CH, J = 8.1 Hz), 7.37 (d, 1H, CH, J = 8.1 Hz). δ_C ($CDCl_3$): δ 28.07 (CH_3) 48.3 (CH_2), 48.55 (CH_2), 48.17 (CH_2), 51.16 (CH_2), 53.07 (CH_2), 53.67 (CH_2), 55.07(CH_2), 46.61 (CH_2), 51.03 (CH_2), 55.55 (CH_2), 56.43 (CH_2), 81.88 ($C(CH_3)_3$), 82.11 ($C(CH_3)_3$), 109.57 (CH), 115.48 (CH), 119.21 (CH), 121.58 (CH), 122.45 (CH), 124.81 (C), 127.52 (CH), 135.74 (C), 142.29 (C), 14.82 (C), 153.13(C), 171.13 (C=O), 172.77 (C=O). *m/z*: 750.5 (100 $(M-H)^+$). HRMS: calcd. for $C_{41}H_{64}O_6N_7$: 750.4913 found 750.4913.

Method 2

1,4,7-Tris(*tert*-butoxycarbonylmethyl)-10-(1-(4-nitrobenzyl)-2-methyl benzimidazole)-1,4,7,10-tetraazacyclododecane (0.2 g, 0.2 mmol) was dissolved in methanol (50 ml) followed by the addition of palladium on carbon (0.05 g). The suspension was stirred for 24 h with hydrogen bubbling into the reaction mixture. The reaction mixture was then filtered through hyflo to remove the Pd/C and the solvent removed from the filtrate under reduced pressure. The desired product was not isolated using this synthetic procedure.

7.3.38 Synthesis of 1,4,7-tris(carboxymethyl)-10-(1-(4-aminobenzyl)-2-methyl benzimidazole)-1,4,7,10-tetraazacyclododecane (36)

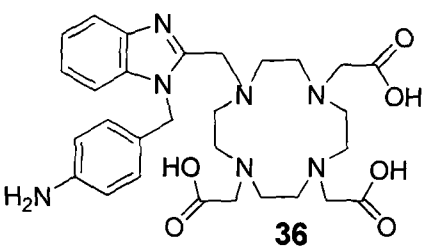

36

1,4,7-Tris(*tert*-butoxycarbonylmethyl)-10-(1-(4-aminobenzyl)-2-methyl benzimidazole)-1,4,7,10-tetraazacyclododecane (0.18 g, 0.24 mmol) was dissolved in aqueous 37% HCl (30 ml) and stirred at RT for 3 h. The solvent was removed under reduced pressure, the residue was redissolved into water (5 ml) and filtered through a 0.2 μm syringe filter. The solvent was again removed under reduced pressure to give a yellow solid, (0.13 g, 93%). δ_H (D_2O): δ2.91 (m, 2H, CH_2), 3.01 (m, 2H, CH_2), 3.23 (m, 2H, CH_2), 3.27 (m, 2H, CH_2), 3.50 (m, 2H, CH_2), 3.57 (s, 2H, CH_2), 3.68 (m, 6H, CH_2), 4.03 (s, 2H, CH_2), 4.24 (s, 2H, CH_2), 4.56 (s, 2H, CH_2), 5.71 (s, 2H, CH_2), 7.43 (m, 4H, arCH), 7.61 (m, 4H, arCH). δ_C ($CDCl_3$): δ 48.38 (CH_2), 48.55 (CH_2), 49.07 (CH_2), 51.17 (CH_2), 53.09 (CH_2), 53.42 (CH_2), 54.81 (CH_2), 113.37 (CH), 115.23 (CH), 124.43 (CH), 127.72 (CH), 128.04 (CH), 128.16 (CH), 129.09 (CH), 130.01 (C), 130.52 (C), 134.78 (C), 148.99 (C), 168.58 (C=O). *m/z*: 582.3 (100 $(M-H)^+$). HRMS: calcd. for $C_{43}H_{40}O_6N_7$: 582.3035 found 582.3030.

7.3.39 Synthesis of europium(III) 1,4,7-tris(carboxymethyl)-10-(1-(4-aminobenzyl)-2-methyl benzimidazole)-1,4,7,10-tetraazacyclododecane (37a)

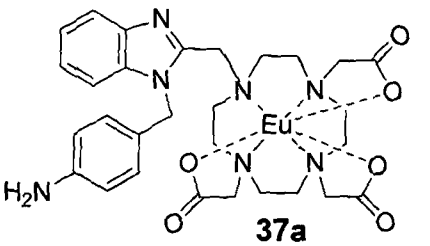

1,4,7-Tris(carboxymethyl)-10-(1-(4-aminobenzyl)-2-methyl benzimidazole)-1,4,7,10-tetraazacyclododecane (0.05 g, 0.089 mmol), and europium(III) trifluoromethanesulfonate (0.05 g, 0.089 mmol) were dissolved in water (10 ml) and stirred. A solution of potassium carbonate (0.06 g, 0.43 mmol) in water (10 ml) was added dropwise. The solution was heated at reflux for 18 h. The solvent was then evaporated under reduced pressure. The resulting solid was dissolved in a minimum of MeOH and purified using a sephadex column LH-20 (MeOH as eluent). The fractions containing the product were combined and evaporated under reduced pressure to give a yellow solid, (0.06 g, 96%). δ_H (D_2O): δ -18.66, -17.83, -16.95, -16.54, -14.53, -13.95, -12.45, -11.47, -10.30, -9.27, -9.01, -8.17, -7.59, -7.31, -6.97, -6.60, -5.94, -4.59, -3.21, -2.89, -2.07, -1.10, -0.71, 1.04, 1.16, 1.45, 1.90, 2.14, 2.47, 2.72, 3.08, 3.26, 3.54, 4.08, 4.78, 5.09, 5.60, 5.81, 6.34, 6.60, 6.73, 7.27, 7.52, 7.77, 8.18, 8.34, 8.72, 9.53, 10.11, 10.71, 11.07, 12.96, 29.48, 29.98, 30.55, 30.75. *m/z*: 730.2 (100(M-H)$^+$).HRMS: calcd. For $^{151}EuC_{29}H_{37}O_6N_7$: 730.1998 found 730.1993.

7.3.40 Synthesis of terbium(III) 1,4,7-tris(carboxymethyl)-10-(1-(4-aminobenzyl)-2-methyl benzimidazole)-1,4,7,10-tetraazacyclododecane (37b)

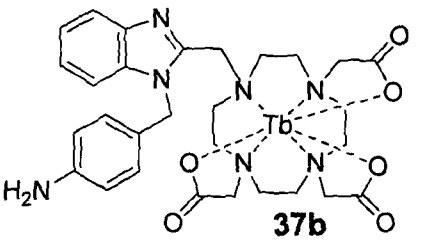

37b

1,4,7-Tris(carboxymethyl)-10-(1-(4-aminobenzyl)-2-methyl benzimidazole)-1,4,7,10-tetraazacyclododecane (0.05 g, 0.089 mmol), and terbium(III) trifluoromethanesulfonate (0.052 g, 0.089 mmol) was dissolved in water (10 ml) and stirred. A solution of potassium carbonate (0.06 g, 0.43 mmol) in water (10 ml) was added dropwise. The solution was heated at reflux for 18 h. The solvent was then evaporated under reduced pressure. The resulting solid was dissolved in a minimum of MeOH and purified using a sephadex column LH-20 (MeOH as eluent). The fractions containing the product were combined and evaporated under reduced pressure to give a yellow solid, (0.039 g, 62%). *m/z*: 738.2(100$(M-H)^+$). HRMS: calcd. for $TbC_{29}H_{37}O_6N_7$: 738.2053 found 738.2053.

7.3.41 Synthesis of gadolinium(III) 1,4,7-tris(carboxymethyl)-10-(1-(4-aminobenzyl)-2-methyl benzimidazole)-1,4,7,10-tetraazacyclododecane (37c)

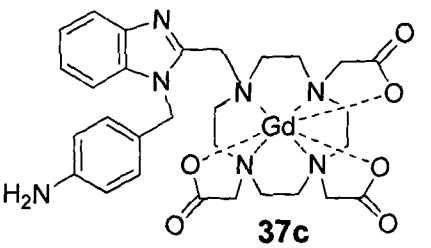

1,4,7-Tris(carboxymethyl)-10-(1-(4-aminobenzyl)-2-methyl benzimidazole)-1,4,7,10-tetraazacyclododecane (0.05 g, 0.089 mmol), and gadolinium(III) trifluoromethanesulfonate (0.039 g, 0.089 mmol) were dissolved in water (10 ml) and stirred. A solution of potassium carbonate (0.05 g, 0.43 mmol) in water (10 ml) was added dropwise. The solution was heated at reflux for 18 h. The solvent was then evaporated under reduced pressure. The resulting solid was dissolved in a minimum of MeOH and purified using a sephadex column LH-20 (MeOH as eluent). The fractions containing the product were combined and evaporated under reduced pressure to give a yellow solid, (0.05 g, 79%). *m/z*: 733.2 (100(M-H)$^+$). HRMS: calcd. for $^{154}GdC_{29}H_{37}O_6N_7$: 733.2008 found 733.2012.

7.3.42 Synthesis of lanthanum(III) 1,4,7-tris(carboxymethyl)-10-(1-(4-aminobenzyl)-2-methyl benzimidazole)-1,4,7,10-tetraazacyclododecane (37d)

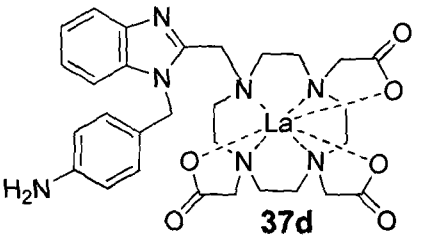

37d

1,4,7-Tris(carboxymethyl)-10-(1-(4-aminobenzyl)-2-methyl benzimidazole)-1,4,7,10-tetraazacyclododecane (0.05 g, 0.089 mmol), and lanthanum(III) trifluoromethanesulfonate (0.05 g, 0.089 mmol) were dissolved in water (10 ml) and stirred. A solution of potassium carbonate (0.06 g, 0.43 mmol in water (10 ml) was added dropwise. The solution was heated at reflux for 18 h. The solvent was then evaporated under reduced pressure. The resulting solid was dissolved in a minimum of MeOH and purified using a sephadex column LH-20 (MeOH as eluent). The fractions containing the product were combined and evaporated under reduced pressure to give a yellow solid, (0.05 g, 81%). δ_H (D_2O): δ 2.62 – 2.93 (m, 8H, CH_2), 3.39 – 3.69 (br, 4H CH_2), 3.83 – 4.36 (m, 10H, CH_2), 4.79 (br, 2H, CH_2), 5.87 (s, 2H, CH_2), 7.53 – 7.60 (m, 2H, CH), 7.71 (m, 2H, CH), 7.87 (m, 2H, CH), 8.14 (m, 2H, CH). δ_C (D_2O): δ 47.84 (CH_2), 50.20 (CH_2), 51.93 (CH_2), 53.10 (CH_2), 54.72 (CH_2), 61.59 (CH_2), 112.19 (CH), 119.98 (CH), 112.59 (CH), 125.21 (CH), 129.42 (CH), 134.21 (C), 135.78 (C), 140.75 (C), 155.11 (C), 180.62 (C=O). *m/z*: 728.2 (100(M-H)$^+$). HRMS: calcd. for $LaC_{29}H_{37}O_6N_7$: 718.1863 found 728.1859.

7.3.43 Synthesis of 1,4,7-tris(*tert*-butoxycarbonylmethyl)-10-(1-(4-nitrobenzyl))-1,4,7,10-tetraazacyclododecane (38)

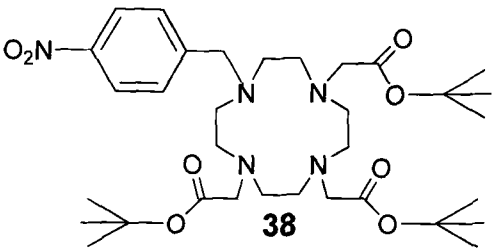

38

1,4,7-Tris(*tert*-butoxycarbonylmethyl)-1,4,7,10-tetraazacyclododecane hydrobromide salt (1 g, 1.9 mmol) was dissolved in dry acetonitrile and the solution stirred under nitrogen. 4-Nitrobenzylbromide (0.46 g, 2 mmol) and sodium hydrogen carbonate (1.66 g, 15.2 mmol) were added as solid. The reaction mixture was heated to 70°C and stirred for 24 h. The solvent was then evaporated under reduced pressure. The resulting residue was dissolved in a minimum volume of dichloromethane and purified by flash chromatography (SiO_2, dichloromethane with an increasing gradient of methanol from 0% to 5%, product (r.f. = 0.21 in 5% MeOH in DCM). The fractions containing the product were combined and the solvent was removed under reduced pressure to give an off-white solid, (1.15 g, 87%). δ_H ($CDCl_3$): δ 1.23 (s, 27H, CH_3), 2.0-3.09 (br, 24H, CH_2), 7.52 (d, 2H, ar CH, J = 8.44 Hz), 7.95 (d, 2H, arCH, J = 8.44 Hz). δ_C ($CDCl_3$): δ 27.89 (CH_3), 50.0 (CH_2), 50.56 (CH_2), 55.72 (CH_2), 56.06 (CH_2), 58.78 (CH_2), 65.68 (CH_2), 82.49 (C), 83.05 (C), 123.57 (CH), 131.123, (CH), 145.25 (C), 147.21 (C), 172.58 (C=O), 173.65 (C=O). *m/z*: 650.3 (100 $(M-H)^+$).

7.3.44 Synthesis of 1,4,7-tris(*tert*-butoxycarbonylmethyl)-10-(4-aminobenzyl)-1,4,7,10-tetraazacyclododecane (39)

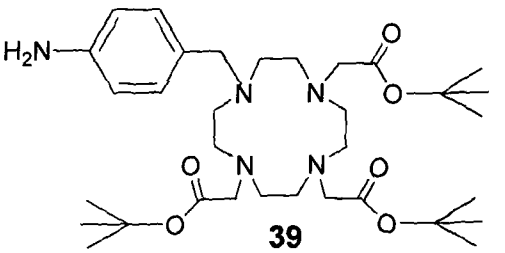

39

Palladium on carbon (0.1 g) was added to a solution of 1,4,7-tris(tert-butoxymethyl)-10-(1-(4-nitrobenzyl)-1,4,7,10-tetraazacyclododecane (2 g, 3.2 mmol) in methanol (50 ml) and the reaction mixture was stirred for 18 h with hydrogen bubbling through the solution. The reaction mixture was then filtered through hyflo and the solvent removed under reduced pressure to leave a white solid, (1.61 g, 85%). δ_H ($CDCl_3$): δ 1.39 (s, 27H, CH_3), 1.98 – 3.03 (br, 24H, CH_2), 6.56 (d, 2H, arCH, J = 8.4 Hz), 7.14 (d, 2H, arCH, J = 8.4 Hz). δ_C ($CDCl_3$): δ 28.07, 28.27 (CH_3), 50.81 (CH_2), 50.3 (CH_2), 59.01 (CH_2), 82.30 (CH_2), 82.74 (C), 115.17 (CH), 126.91 (C), 131.10 (CH), 146.03 (C), 172.58 (C=O), 173.52, (C=O). *m/z*: 634.5 (100 $(M-H)^+$).

7.3.45 Synthesis of 1,4,7-tris(carboxymethyl)-10-(4-aminobenzyl)-1,4,7,10-tetraazacyclododecane (40)

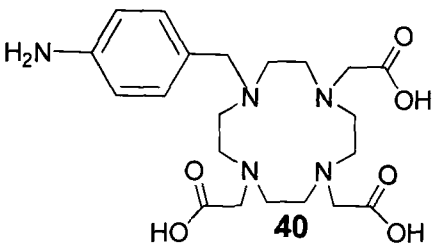

40

Method 1 – (preferred route)

1,4,7-Tris(*tert*-butoxycarbonylmethyl)-10-(4-aminobenzyl)-1,4,7,10-tetraazacyclododecane (0.2 g, 0.3 mmol) was dissolved in 37% aqueous HCl (30 ml) and the resulting solution stirred at RT for 3 h. The solvent was then evaporated under reduced pressure, the remaining residue was redissolved into water (5 ml) and this solution was filtered through a 0.2 μm syringe filter. The solvent was removed under reduced pressure to leave a yellow solid, (0.15 g, quantitative). δ_H (D_2O): δ 2.03 – 3.59 (br, 24H, CH_2), 6.78 (d, 2H, arCH, J = 7.56 Hz), 7.08 (d, 2H, arCH, J = 7.56 Hz). *m/z*: 453.1. (100 $(M-H)^+$).

Method 2

1,4,7-Tris(*tert*-butoxycarbonylmethyl)-10-(1-(4-aminobenzyl)-1,4,7,10-tetraazacyclododecane (0.2 g, 0.3 mmol) was suspended in a mixture of trifluoroacetic acid (5 ml) and dichloromethane (5 ml) and the resulting solution stirred at RT for 24 h. The solvent was removed under reduced pressure to leave a solid. The desired product was not isolated using this synthetic procedure.

7.3.46 Synthesis of europium(III) 1,4,7-tris(carboxymethyl)-10-(4-aminobenzyl)-1,4,7,10-tetraazacyclododecane (41a)

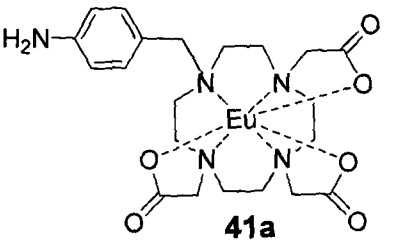

41a

1,4,7-Tris(carboxymethyl)-10-(4-aminobenzyl)-1,4,7,10-tetraazacyclododecane (0.18 g, 0.4 mmol), and europium(III) trimethanesulfonate (0.24 g, 0.4 mmol) were dissolved in water (10 ml). A solution of potassium carbonate (0.24 g, 2 mmol) in water (10 ml) was added dropwise. The solution was heated at reflux for 18 h. The solvent was then evaporated under reduced pressure. The resulting solid was dissolved in a minimum of MeOH and purified using a sephadex column LH-20 (MeOH as eluent). The fractions containing the product were combined and evaporated under reduced pressure to give a yellow solid, (0.19 g, 81%). *m/z*: 602.0 (100 $(M\text{-}H)^+$).

7.3.47 Synthesis of gadolinium(III) 1,4,7-tris(carboxymethyl)-10-(4-aminobenzyl)-1,4,7,10-tetraazacyclododecane (41b)

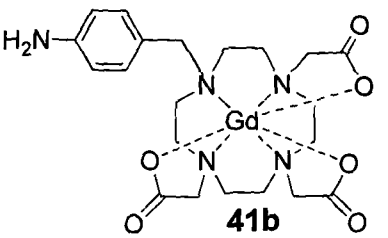

41b

1,4,7-Tris(carboxymethyl)-10-(1-(4-aminobenzyl)-1,4,7,10-tetraazacyclododecane (0.15 g, 0.33 mmol), and gadolinium(III) trichloride (0.2 g, 0.33 mmol) were dissolved in water (10 ml) and the resulting solution was stirred. A solution of potassium carbonate (0.23 g, 1.7 mmol) in water (10 ml) was added dropwise. The solution was heated at reflux for 18 h. The solvent was then evaporated under reduced pressure. The resulting solid was dissolved in a minimum of MeOH and purified using a sephadex column LH-20 (MeOH as eluent). The fractions containing the product were combined and evaporated under reduced pressure to give a yellow solid, (0.15 g, 76%). *m/z*: 607.1 (100 $(M-H)^+$).

7.3.48 Synthesis of lanthanum(III) 1,4,7-tris(carboxymethyl)-10-(4-aminobenzyl)-1,4,7,10-tetraazacyclododecane (41c)

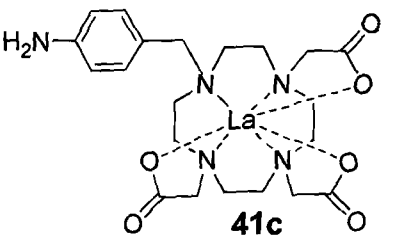

41c

1,4,7-Tris(carboxymethyl)-10-(1-(4-aminobenzyl)-1,4,7,10-tetraazacyclodecane (0.12 g, 0.26 mmol), and lanthanum(III) trimethanesulfonate (0.15 g, 0.26 mmol) were dissolved in water (10 ml) and the resulting solution was stirred. A solution of potassium carbonate (0.23 g, 1.7 mmol) in water (10 ml) was added dropwise. The solution was heated at reflux for 18 h. The solvent was then evaporated under reduced pressure. The resulting solid was dissolved in a minimum of MeOH and purified using a sephadex column LH-20 (MeOH as eluent). The fractions containing the product were combined and evaporated under reduced pressure to give a yellow solid, (0.19 g, 81%). *m/z*: 588.2 (100 $(M-H)^+$).

7.3.49 Attempted synthesis of europium(III) 1,4,7-tris(carboxymethyl)-10-(4-(5-(4-thioureaphenylene) borondipyrromethane) benzyl)-1,4,7,10-tetraazacyclododecane (42a)

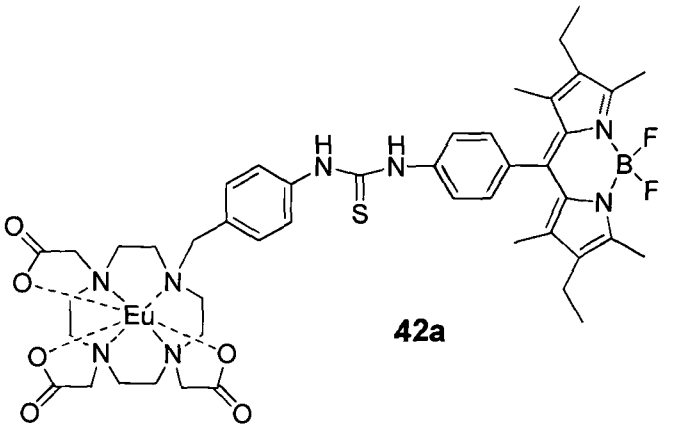

42a

Europium(III)1,4,7-tris(carboxymethyl)-10-(4-aminobenzyl)-1,4,7,10-tetraazacyclododecane (0.07 g, 0.013 mmol) was dissolved in water (1 ml) and 1 M potassium hydroxide solution was added until the pH reached 9. A solution of 5-(4-isothiocyanatophenyl) borondipyrromethene (0.072 g, 0.165 mmol) dissolved in dimethylformamide (2 ml) was added dropwise, the flask was covered in aluminium foil and the reaction mixture was stirred for 14 days. The solvent was then removed under reduced pressure to give a solid. The desired product was not isolated using this synthetic procedure.

7.3.50 Attempted synthesis of gadolinium(III) 1,4,7-tris(carboxymethyl)-10-(4-(5-(4-thioureaphenylene) borondipyrromethane)benzyl)-1,4,7,10-tetraazacyclododecane (42b)

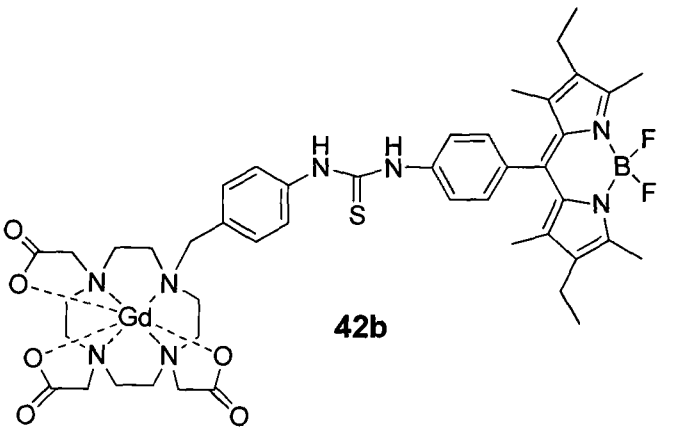

42b

Gadolinium(III)1,4,7-tris(carboxymethyl)-10-(4-aminobenzyl)-1,4,7,10-tetraazacyclododecane (0.1 g, 0.165 mmol) was dissolved in water (1 ml) and 1 M potassium hydroxide solution was added until the pH reached 9. A solution of 5-(4-isothiocyanatophenyl) borondipyrromethene (0.072 g, 0.165 mmol) dissolved in dimethylformamide (2 ml) was added, the flask was covered in aluminium foil and the reaction mixture was stirred for 14 days. The solvent was then removed under reduced pressure to give a solid. The desired product was not isolated using this synthetic procedure.

7.3.51 Attempted synthesis of lanthanum(III) 1,4,7-tris(carboxymethyl)-10-(4-(5-(4-thioureaphenyenel) borondipyrromethane)benzyl)-1,4,7,10-tetraazacyclododecane (42c)

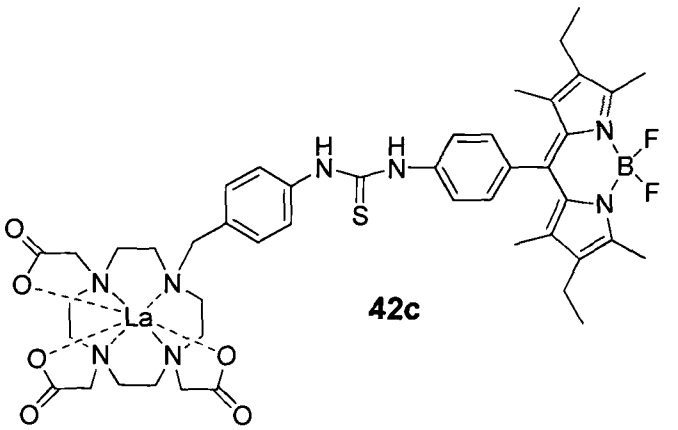

42c

Lanthanum(III)1,4,7-tris(carboxymethyl)-10-(4-aminobenzyl)-1,4,7,10-tetraazacyclodecane (0.05 g, 0.0085 mmol) was dissolved in water (1 ml) and 1 M potassium hydroxide solution was added until the pH reached 9. A solution of 5-(4-isothiocyanatophenyl) borondipyrromethene (0.072 g, 0.165 mmol) dissolved in dimethylformamide (2 ml) was then added, the flask was covered in aluminium foil and the reaction mixture was stirred for 14 days. The solvent was then removed under reduced pressure to give a solid. The desired product was not isolated using this synthetic procedure.

7.3.52 Attempted synthesis of 1,4,7-tris(carboxymethyl)-10-(4-(5-(4-thioureaphenylene) borondipyrromethane) benzyl)-1,4,7,10-tetraazacyclododecane (43)

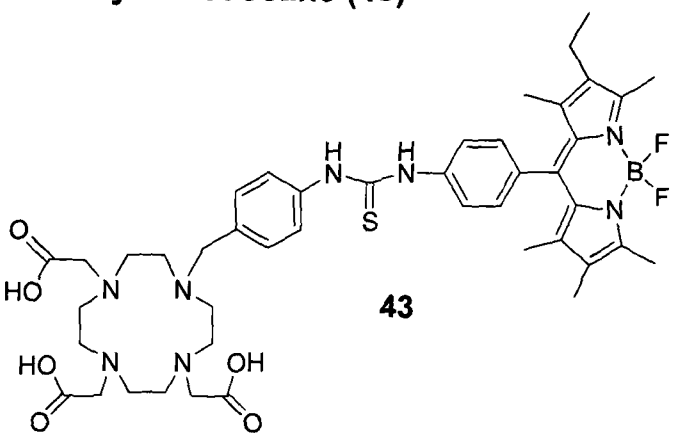

43

1,4,7-Tris(carboxymethyl)-10-(4-aminobenzyl)-1,4,7,10-tetraazacyclododecane (0.01 g, 0.023 mmol) was dissolved into water (1 ml) followed by the addition of 1 M potassium hydroxide to adjust the pH to 9. 5-(4-Isothiocyanatophenyl) borondipyrromethane (0.01 g, 0.023 mmol) was dissolved in dimethylformamide (2 ml) and was added dropwise to the reaction mixture. The resulting solution was stirred at RT for 14 days. The solvent was removed under reduced pressure to give a solid. The desired product was not isolated using this synthetic procedure.

7.3.53 Attempted synthesis of 1,4,7-tris(carboxymethyl)-10-(benzyl-4-(phenylthiourea))-1,4,7,10-tetraazacyclododecane (44)

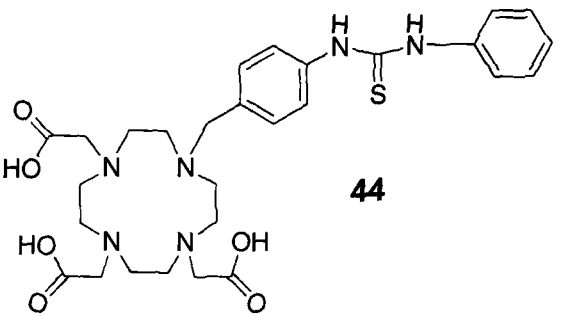

44

A mixture of 1,4,7-tris(carboxymethyl)-10-(4-aminobenzylmethyl)-1,4,7,10-tetraazacyclododecane (0.01 g, 0.022 mmol) and phenyl isothiocyanate (0.0026 ml 0.0022 mmol) was dissolved in dimethylformamide (20 ml) and left to stir for 24 h. The solvent was then removed under reduced pressure. The desired product was not isolated using this synthetic procedure.

7.3.54 Synthesis of 1,4,7-tris(carboxymethyl)-10-(4-isothiocyanatobenzyl)-1,4,7,10-tetraazacyclododecane (45)

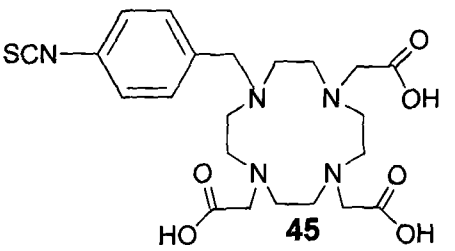

45

Method 1 – (preferred route)

1,4,7-Tris(carboxymethyl)-10-(1-(4-aminobenzyl)-1,4,7,10-tetraazacyclododecane (0.1 g, 0.22 mmol) was dissolved in 3 M aqueous hydrochloric acid (3.5 ml) and then a solution of thiophosgene (0.17 ml, 2.2 mmol) in carbon tetrachloride (0.17 ml) was added dropwise. The biphasic reaction mixture was stirred for 24 h. The solvent was then removed under reduced pressure, and the residue dried under vacuum to give a yellow solid, (0.087g, 80 %). δ_H (D_2O): δ 2.71 – 4.71 (m, 24H, CH_2), 7.2 (s, 2H, CH), 7.4 (s, 2H, CH). *m/z*: 494.2 (100 ($M-H^+$). HRMS: calcd. for $C_{22}H_{32}O_6N_5S_1$ 494.2068 found 494.2068. I.R. (KBr) 2108.8 cm^{-1} υ (NCS).

Method 2

1,4,7-Tris(carboxymethyl)-10-(1-(4-aminobenzyl)-1,4,7,10-tetraazacyclododecane (0.25 g, 0.5 mmol) was dissolved in water (2 ml), and the pH adjusted to 9 by the addition of 0.05 M sodium hydrogen carbonate solution. A 0.025 M solution of thiophosgene in chloroform (10 ml) was added, the flask was then covered in aluminium foil and the reaction stirred for 24 h at RT. Water (10 ml) was added and the aqueous layer was separated and washed with chloroform (2 x 10 ml). The solvent was then removed under reduced pressure. The desired product was not isolated using this synthetic procedure.

7.3.55 Synthesis of 1,4,7-tris(carboxymethyl)-10-(1-(4-isothiocyanatobenzyl)-2-methyl benzimidazole)-1,4,7,10-tetraazacyclododecane (46)

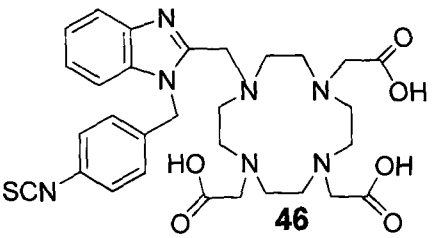

46

1,4,7-Tris(carboxymethyl)-10-(1-(4-aminobenzyll)-2-methyl benzimidazole)-1,4,7,10-tetraazacyclododecane (0.066 g, 0.11 mmol) was dissolved in 3 M hydrochloric acid solution (3.5 ml), followed by the addition of thiophosgene (0.087 ml, 2.2 mmol) in carbon tetrachloride (0.013 ml) and the biphasic mixture stirred for 24 h. The solvent was removed under reduced pressure, and the residue dried under vacuum to give a yellow solid, (0.07, 83 %). δ_H (D_2O): δ 2.8 (m, 4H, CH_2), 3.00 (m, 4H, CH_2), 3.1-3.3 (m, 4H, CH_2), 3.39-3.91 (m, 8H, CH_2), 4.07, (m, 2H, CH_2), 4.83 (s, 2H, CH_2), 5.78 (S, 2H, CH_2), 7.2 (s, 4H, CH), 7.56 (m, 2H, CH), 7.73 (m, 2H, CH). *m/z*: 623 (100$(M-H)^+$). I.R. (KBr) 2106.5 cm^{-1} υ (NCS).

7.3.56 Attempted synthesis of 1,4,7-tris(carboxymethyl)-10-(4-(5-(4-thioureaphenyl) borondipyrromethane benzyl)-2-methyl benzimidazole)-1,4,7,10-tetraazacyclododecane (47)

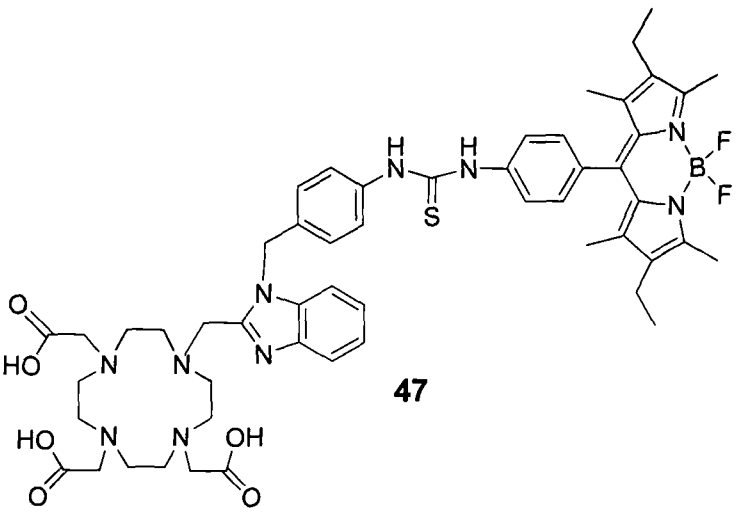

47

1,4,7-Tris(carboxymethyl)-10-((4-isothiocyanatobenzyl)-2-methyl benzimidazole)-1,4,7,10-tetraazacyclododecane (0.06 g, 0.094 mmol) was dissolved in water (50 ml) and the pH adjusted to 8 by the addition of 1 M potassium hydroxide solution. A solution of 5-(4-aminophenyl) borondipyrromethene (0.037 g, 0.094 mmol) in dichloromethane (50 ml) was added, the reaction was vessel covered in foil and the solution allowed to stir for 21 days. The desired product was not isolated using this synthetic procedure.

7.3.57 Synthesis of 1,4,7-tris(carboxymethyl)-10-(1-(4-(N-benzyl)thiourea)benzyl-2-methylbenzimidazole)-1,4,7,10-tetraazacyclododecane (48)

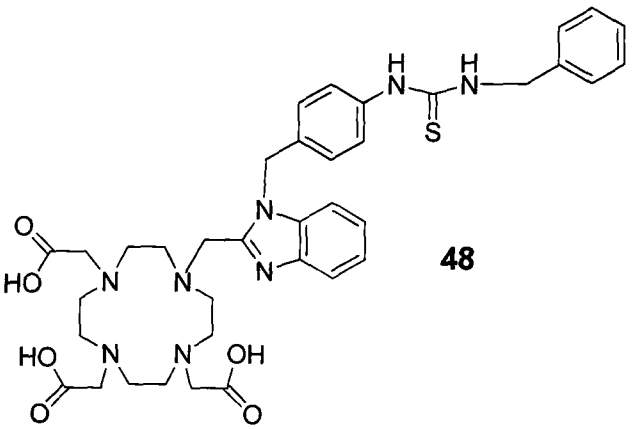

48

1,4,7-Tris(carboxymethyl)-10-(1-(4-isothiocyanatobenzyl)-2-methylbenzimidazole)-1,4,7,10-tetraazacyclododecane (0.01 g, 0.017 mmol) was dissolved in water (1 ml) and the pH adjusted to 9 by the addition of 1 M sodium hydrogen carbonate solution. Benzyl amine (0.001 ml, 0.017 mmol) was added and the reaction mixture left to stir for 24 h. The aqueous layer was washed with dichloromethane (4 x 20 ml), and the solvent removed under reduced pressure. The resulting solid was re-dissolved into water (2 ml) and the salts removed using a sephadex LH-20 column with methanol as the eluent. The fractions containing the product were combined and the solvent was removed under reduced pressure to yield a white solid. δ_H (D_2O): δ 2.2-4.8 (m, 28H, CH_2), 6.85-7.8 (m, 13H, CH). *m/z*: 769.3 (100 $(M+K)^+$). I.R. (KBr) 2925.0 cm^{-1} υ (NCSN), 2962.4 cm^{-1} υ (NCSN).

7.3.58 Synthesis of lanthanum(III) 1,4,7-tris(carboxymethyl)-10-(1-(4-(N-benzyl)thiourea)benzyl-2-methylbenzimidazole)-1,4,7,10-tetraazacyclododecane (49)

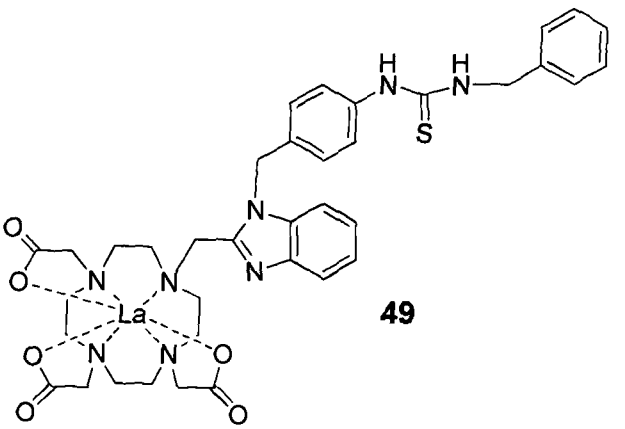

49

1,4,7-tris(carboxymethyl)-10-(1-(4-(N-benzyl)thiourea)benzyl-2-methylbenzimidazole)-1,4,7,10-tetraazacyclododecane (0.009 g, 0.01 mmol), and lanthanum(III) trifluoromethanesulfonate (0.0017 g, 0.001 mmol) were dissolved in a solution of water (10ml) and the resulting mixture was stirred at RT. A solution of potassium carbonate (0.0007 g, 0.005 mmol) in water (5 ml) was added dropwise. The solution was then heated at reflux for 18 h. The solvent was evaporated under reduced pressure and the product was purified using a sephadex LH-20 column (MeOH as eluent). The fractions containing the product were combined and the solvent was evaporated under reduced pressure to give a yellow solid. δ_H (D_2O): δ 2.12 – 4.7 (m, 28H, CH_2), 6.8 - 7.51 (m, 13H, CH). *m/z*: 769.3 (100 $(M+K)^+$).

7.3.59 Synthesis of 1,4,7-tris(carboxymethyl)-10-(4-benzylthiourea)benzyl-1,4,7,10-tetraazacyclododecane (50)

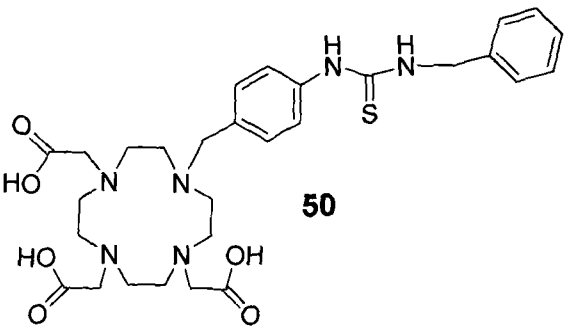

50

1,4,7-Tris(carboxymethyl)-10-(4-isothiocyanateobenzyl)-1,4,7,10-tetraazacyclodecane (0.03 g, 0.06 mmol) was dissolved in water (1 ml) and the pH was adjusted to 9 by the addition of 1 M potassium hydroxide solution. Benzyl amine (0.0066 ml 0.006 mmol) was added and the resulting solution was left to stir for 24 h. The aqueous layer was washed with dichloromethane (4 x 20 ml), separated and the solvent was removed under reduced pressure. The resulting solid was re-dissolved in water (2 ml) and the salts removed using a sephadex LH-20 column using methanol as eluent. The collected fractions were combined and the solvent was removed under reduced pressure to give a white solid. δ_H (D_2O): δ 2.25 - 3.5 (m, 24H, CH_2), 6.9 - 7.51 (m, 11H, arCH). *m/z:* 568 (100 $(M-H)^+$). I.R. (KBr) 2924.0 cm^{-1} υ (NCSC), 2961.9 cm^{-1} υ (NCSN).

7.3.60 Synthesis of lanthanum(III) 1,4,7-tris(carboxymethyl)-10-(4-benzylthiourea)benzyl-1,4,7,10-tetraazacyclododecane (51)

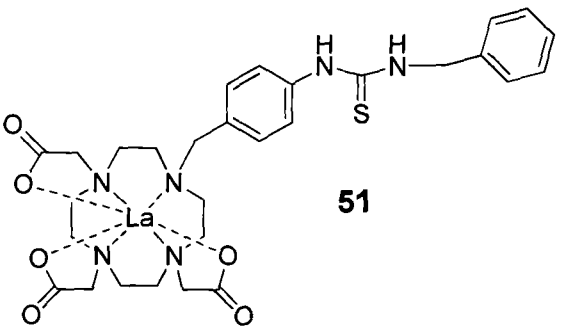

51

1,4,7-tris(carboxymethyl)-10-(4-benzylthiourea)benzyl-1,4,7,10-tetraazacyclododecane (0.036 g, 0.06 mmol), and lanthanum(III) trifluoromethanesulfonate (0.035 g, 0.06 mmol) were dissolved in water (10 ml) and the recation mixture was stirred at RT. Potassium carbonate (0.041 g, 0.3 mmol) in water (5 ml) was added dropwise. The solution was then heated at reflux for 18 h. The solvent was evaporated under reduced pressure and the residue was purified using a sephadex LH-20 column (MeOH as eluent). The fractions containing the product were combined and the solvent was evaporated under reduced pressure to leave a white solid. δ_H (D2O): δ 2.2 - 3.6 (m, 24H, CH2), 6.8 - 7.46 (m, 11H, arCH). m/z: 704(100(M-H)+).

7.3.61 Attempted synthesis of 1,4,7-tris(carboxymethyl)-10-(4-(rhodamine B ethylamine) thiourea)benzyl-1,4,7,10-tetraazacyclododecane (52)

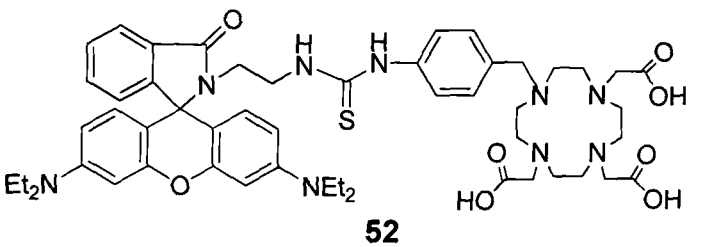

52

Method 1

Rhodamine B ethylamine (0.019 g, 0.036 mmol) was dissolved in dichloromethane and the solution was washed with an aqueous sodium hydrogen carbonate solution. The organic layer was then separated, dried over sodium sulphate and the solvent was removed under reduced pressure. 1,4,7-Tris(carboxymethyl)-10-(4-isothiocyanatobenzyl)-1,4,7,10-tetraazacyclododecane (0.015 g, 0.033 mmol) was added as a solution in dimethylformamide (20 ml), the flask was covered in foil and the reaction mixture left to stir for 24 h. The solvent was then removed under reduced pressure. The pink solid was re-dissolved into water (20 ml) and the aqueous solution washed with diethyl ether (2 x 20 ml). The aqueous layer was separated and the solvent removed under reduced pressure to give a purple solid. The desired product was not isolated using this synthetic procedure.

Method 2

1,4,7-Tris(carboxymethyl)-10-(4-isothiocyanatobenzyl)-1,4,7,10-tetraazacyclododecane (0.06 g, 0.13 mmol) was dissolved in water (5 ml) and the pH adjusted to 8 by the addition of 1 M sodium hydrogen carbonate solution. A solution of rhodamine B ethylamine (0.069 g, 0.13 mmol) dissolved in dichloromethane (5 ml) was added, the flask was covered in foil and the reaction mixture left to stir for 48 h. The aqueous layer was washed with dichloromethane (4 x 20 ml), separated and then the solvent was removed under reduced pressure. The desired product was not isolated using this synthetic procedure.

Method 3

1,4,7-Tris(carboxymethyl)-10-(4-isothiocyanatobenzyl)-1,4,7,10-tetraazacyclododecane (0.05 g, 0.1 mmol) and rhodamine B ethylamine (0.069 g, 0.13 mmol) were dissolved in dichloromethane (10 ml), the flask was covered in aluminium foil and the reaction mixture left to stir for 72 h. The solvent was then removed under reduced pressure. The desired product was not isolated using this synthetic procedure.

Method 4

1,4,7-Tris(carboxymethyl)-10-(4-isothiocyanatobenzylmethyl)-1,4,7,10-tetraazacyclododecane (0.08 g, 0.2 mmol) was dissolved in water (5 ml) and the pH was adjusted to 8 by the addition of 1 M sodium hydrogen carbonate solution, followed by the addition of a solution of rhodamine B base ethylamine (0.092 g, 0.2 mmol) in dimethylformamide (5 ml). The flask was covered in aluminium foil and the reaction mixture was left to stir for 48 h. The solvent was removed under reduced pressure. The desired product was not isolated using this synthetic procedure.

7.3.62 Attempted synthesis of 1,4,7-tris(carboxymethyl)-10-(1-(4-(rhodamine B base ethylamine thiourea)benzyl)-2-methyl benzimidazole)-1,4,7,10-tetraazacyclodecane (53)

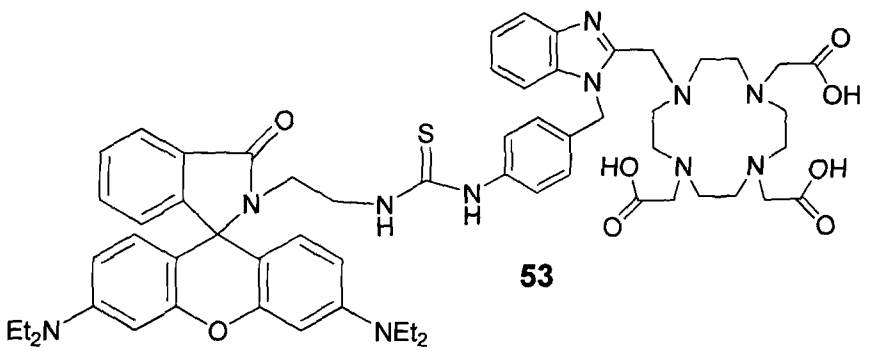

53

Method 1

Rhodamine B base ethylamine (0.016 g, 0.03 mmol) was dissolved in dichloromethane and the resulting solution was washed with aqueous sodium hydrogen carbonate solution. The organic layer was then separated, dried over sodium sulphate and the solvent removed under reduced pressure. 1,4,7-Tris(carboxymethyl)-10-(1-(4-isothiocyanatobenzyl)-2-methylbenzimidazole)-1,4,7,10-tetraazacyclododecane (0.017 g, 0.023 mmol) was added as a solution in dimethylformamide (20 ml), the flask was covered in foil and the reaction mixture left to stir for 24 h at RT. The solvent was then removed under reduced pressure. The pink solid was re-dissolved into water (20 ml) and washed with diethyl ether (2 x 20 ml). The aqueous layer was separated and the solvent removed under reduced pressure to give a purple solid. The desired product was not isolated using this synthetic procedure.

Method 2

1,4,7-Tris(carboxymethyl)-10-(1-(4-isothiocyanatobenzyl)-2-methylbenzimidazole)-1,4,7,10-tetraazacyclododecane (0.066 g, 0.11 mmol) was dissolved in water (5 ml) and the pH adjusted to 8 by the addition of 1 M sodium hydrogen carbonate solution. Rhodamine B base ethylamine (0.059 g, 0.11 mmol) dissolved in dichloromethane (5 ml) was added, the reaction flask was covered in foil and the mixture left to stir for 48 h. The aqueous layer was washed with dichloromethane (4 x 20 ml), and the solvent removed under reduced pressure. The desired product was not isolated using this synthetic procedure.

7.3.63 Synthesis of 1,4,7-tris(carboxymethyl)-10-(4-(5-(4-thioureaethylamidephenyl) borondipyrromethene benzyl)-2-methyl benzimidazole)-1,4,7,10-tetraazacyclododecane (56)

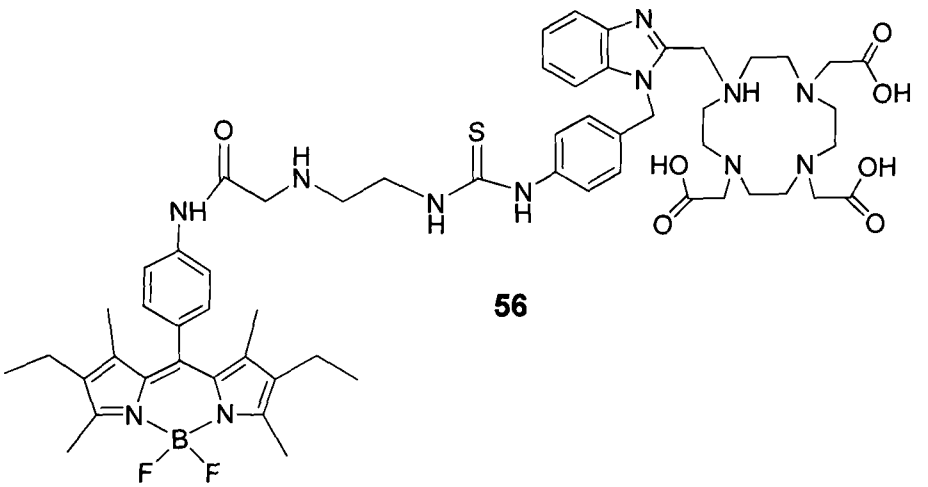

56

5-(4-Ethylenediaminemethylamidophenyl)borondipyrromethene (0.02 g, 0.04 mmol) was dissolved in dichloromethane and the solution was washed with an aqueous sodium hydrogen carbonate solution. The organic layer was then dried over sodium sulphate and the solvent was removed under reduced pressure. 1,4,7-Tris(carboxymethyl)-10-(1-(4-isothiocyanatobenzyl)-2-methyl benzimidazole)-1,4,7,10-tetraazacyclododecane (0.02 g, 0.037 mmol) dissolved in dimethylformamide (20 ml) was added dropwise and the solution was then left to stir for 24 h at RT protected from the light. The solvent was removed under reduced pressure. The resulting red solid was re-dissolved into water (20 ml) and washed with diethyl ether (4 x 50 ml). The aqueous layer was separated and the solvent removed under reduced pressure to give a red solid. The desired product was not isolated using this synthetic procedure.

7.3.64 Synthesis of 1,4,7-tris(carboxymethyl)-10-(aminomethylamidobenzyl)-1,4,7,10-tetraazacyclododecane (58)

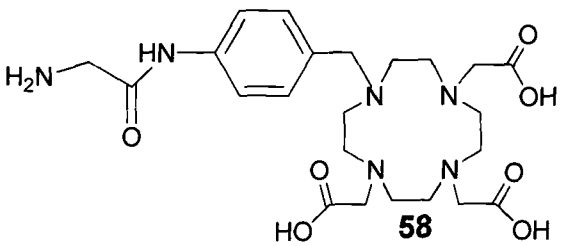

58

N-Pthaloylglycine (0.025 g, 0.12 mmol) was dissolved in thionyl chloride (10 ml) and the mixture heated at reflux for 3 h. The solvent was removed under reduced pressure and the solid used without further purification. 1,4,7-Tris(carboxymethyl)-10-(4-aminobenzyl)-1,4,7,10-tetraazacyclododecane (0.05 g, 0.1 mmol) and magnesium oxide (0.007 g, 0.016 mmol) were dissolved in water (10 ml) and left to stir at room temperature for 4 h. The reaction mixture was allowed to cool to 0°C followed by the addition of phthaloyl β-alanine chloride, prepared in the first step. The reaction micxture was stirred for 30 min at RT and then stirred for a further 4 h at 50°C. The solvent was removed under reduced pressure, the residue was re-dissolved into water (50 ml) and washed with dichloromethane (2 x 50 ml). The aqueous layer was separated and the solvent removed under reduced pressure to yield a yellow solid. The solid was dissolved into a mixture of hydrazine hydrate (5 ml) and ethanol (20 ml). This mixture was heated at reflux for 4 h and was then cooled to 0°C. The precipitate that appeared upon cooling was removed by filtration. The solvent was then removed from the filtrate under reduced pressure to yield a crude product. The solid was used crude for the next step.

7.3.65 Attempted synthesis of 1,4,7-tris(carboxymethyl)-10-(4-(5-(4-thioureaamidophenyl)borondipyrromethane) methylamidobenzyl)-1,4,7,10-tetraazacyclododecane (59)

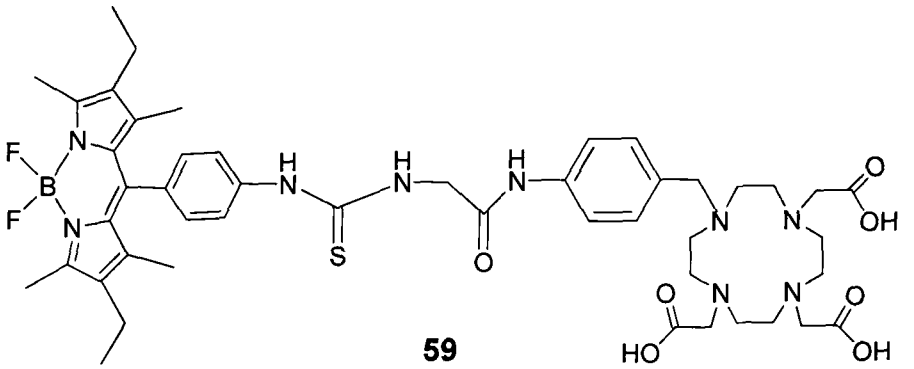

59

1,4,7-tris(carboxymethyl)-10-(aminomethylamidobenzyl)-1,4,7,10-tetraazacyclododecane (0.05 g, 0.098 mmol) was dissolved in water (10 ml) followed by the addition of 1 M aqueous sodium hydrogen carbonate solution to adjust the pH of the solution to 8. 5-(4-Isothiocyanatophenyl) borondipyrromethene (0.04 g, 0.098 mmol) dissolved in dichloromethane (10 ml) was added and the resulting reaction mixture left to stir for 24 h at RT under an atmosphere of nitrogen. The solvent was then removed under reduced pressure. The desired product was not isolated using this synthetic procedure.

8. Appendix

8.1 Crystallographic data for 1-(4-nitrobenzyl)phenylenediamine (5)

Crystals were grown by slow evaporation of a dichloromethane solution over a period of two weeks. Colourless blocks were separated from the solvent and a suitable crystal was selected and mounted on a glass fibre using perfluoropolyether oil.

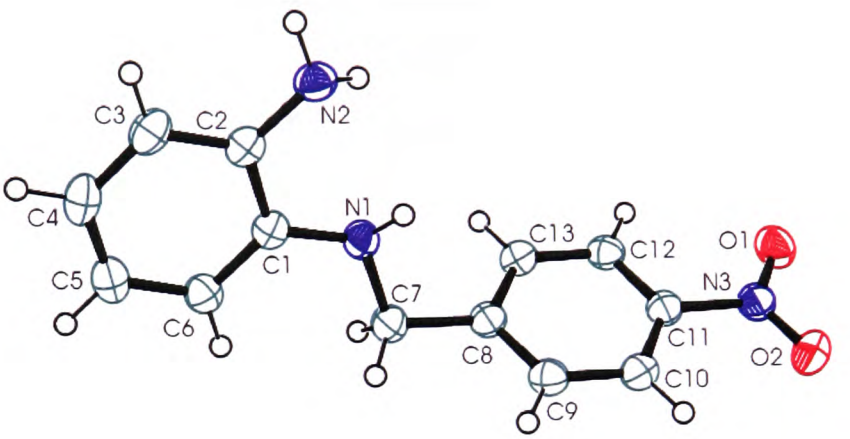

Identification code	sja88_06	
Empirical formula	C13 H13 N3 O2	
Formula weight	243.26	
Temperature	150(2) K	
Wavelength	0.71073 Å	
Crystal system	monoclinic	
Space group	P21/c	
Unit cell dimensions	a = 10.503(2) Å	α= 90°.
	b = 6.7427(9) Å	β= 94.032(15)°.
	c = 16.452(3) Å	γ= 90°.
Volume	1162.3(4) $Å^3$	
Z	4	
Density (calculated)	1.390 Mg/m^3	
Absorption coefficient	0.097 mm^{-1}	
F(000)	512	
Crystal size	0.50 x 0.46 x 0.44 mm^3	
Theta range for data collection	2.48 to 34.75°.	
Index ranges	-16<=h<=16, -10<=k<=8, -26<=l<=26	
Reflections collected	19826	
Independent reflections	4980 [R(int) = 0.0533]	
Completeness to theta = 34.75°	99.1 %	
Refinement method	Full-matrix least-squares on F^2	
Data / restraints / parameters	4980 / 0 / 176	
Goodness-of-fit on F^2	1.028	
Final R indices [I>2sigma(I)]	R1 = 0.0593, wR2 = 0.1582	
R indices (all data)	R1 = 0.1089, wR2 = 0.1941	
Extinction coefficient	0.065(8)	
Largest diff. peak and hole	0.385 and -0.342 $e.Å^{-3}$	

Table 18 Crystal data and structure refinement for 1-(4-nitrobenzyl)phenylenediamine (7)

C(1)-C(6)	1.391(2)
C(1)-N(1)	1.3961(18)
C(1)-C(2)	1.412(2)
C(2)-C(3)	1.394(2)
C(2)-N(2)	1.3998(19)
C(3)-C(4)	1.394(2)
C(3)-H(3)	0.9500
C(4)-C(5)	1.378(2)
C(4)-H(4)	0.9500
C(5)-C(6)	1.395(2)
C(5)-H(5)	0.9500
C(6)-H(6)	0.9500
C(7)-N(1)	1.4570(19)
C(7)-C(8)	1.5085(19)
C(7)-H(7A)	0.9900
C(7)-H(7B)	0.9900
C(8)-C(9)	1.391(2)
C(8)-C(13)	1.3984(19)
C(9)-C(10)	1.387(2)
C(9)-H(9)	0.9500
C(10)-C(11)	1.3858(19)
C(10)-H(10)	0.9500
C(11)-C(12)	1.381(2)
C(11)-N(3)	1.4678(18)
C(12)-C(13)	1.384(2)
C(12)-H(12)	0.9500
C(13)-H(13)	0.9500
N(1)-H(14)	0.92(2)
N(2)-H(16)	0.91(2)
N(2)-H(15)	0.91(2)
N(3)-O(2)	1.2242(18)
N(3)-O(1)	1.2268(17)

Table 19 Bond lengths [Å] for **(5)**

C(6)-C(1)-N(1)	122.91(13)	C(10)-C(9)-C(8)	120.62(13)
C(6)-C(1)-C(2)	119.50(13)	C(10)-C(9)-H(9)	119.7
N(1)-C(1)-C(2)	117.54(12)	C(8)-C(9)-H(9)	119.7
C(3)-C(2)-N(2)	121.72(13)	C(11)-C(10)-C(9)	118.10(13)
C(3)-C(2)-C(1)	118.86(13)	C(11)-C(10)-H(10)	120.9
N(2)-C(2)-C(1)	119.32(12)	C(9)-C(10)-H(10)	120.9
C(4)-C(3)-C(2)	121.04(14)	C(12)-C(11)-C(10)	122.91(13)
C(4)-C(3)-H(3)	119.5	C(12)-C(11)-N(3)	118.51(12)
C(2)-C(3)-H(3)	119.5	C(10)-C(11)-N(3)	118.58(13)
C(5)-C(4)-C(3)	119.88(13)	C(11)-C(12)-C(13)	118.17(12)
C(5)-C(4)-H(4)	120.1	C(11)-C(12)-H(12)	120.9
C(3)-C(4)-H(4)	120.1	C(13)-C(12)-H(12)	120.9
C(4)-C(5)-C(6)	120.00(14)	C(12)-C(13)-C(8)	120.60(13)
C(4)-C(5)-H(5)	120.0	C(12)-C(13)-H(13)	119.7
C(6)-C(5)-H(5)	120.0	C(8)-C(13)-H(13)	119.7
C(1)-C(6)-C(5)	120.71(14)	C(1)-N(1)-C(7)	119.22(11)
C(1)-C(6)-H(6)	119.6	C(1)-N(1)-H(14)	112.9(11)
C(5)-C(6)-H(6)	119.6	C(7)-N(1)-H(14)	113.9(12)
N(1)-C(7)-C(8)	108.98(12)	C(2)-N(2)-H(16)	111.6(14)
N(1)-C(7)-H(7A)	109.9	C(2)-N(2)-H(15)	115.6(13)
C(8)-C(7)-H(7A)	109.9	H(16)-N(2)-H(15)	110.2(18)
N(1)-C(7)-H(7B)	109.9	O(2)-N(3)-O(1)	123.16(13)
C(8)-C(7)-H(7B)	109.9	O(2)-N(3)-C(11)	118.63(12)
H(7A)-C(7)-H(7B)	108.3	O(1)-N(3)-C(11)	118.22(13)
C(9)-C(8)-C(13)	119.59(13)		
C(9)-C(8)-C(7)	120.70(12)		
C(13)-C(8)-C(7)	119.69(13)		

Symmetry transformations used to generate equivalent atoms:

Table 20 Bond angles [°] for **(5)**

8.2 Crystallographic data for 1-(4-nitrobenzylmethyl)-2-chloromethyl benzimidazolium chloride (7).HCl

Crystals were grown by slow evaporation of a dichloromethane solution over a period of two weeks. Colourless blocks were separated from the solvent and a suitable crystal was selected and mounted on a glass fibre using perfluoropolyether oil.

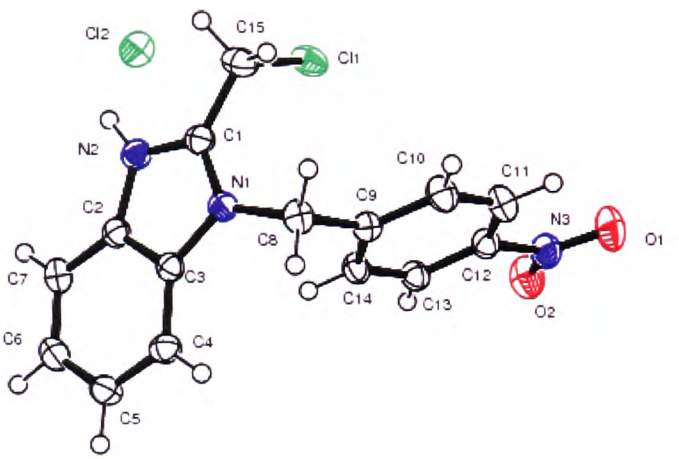

Identification code	sja10_07	
Empirical formula	C15 H13 Cl2 N3 O2	
Formula weight	338.18	
Temperature	150(2) K	
Wavelength	0.71073 Å	
Crystal system	Monoclinic	
Space group	P21/n	
Unit cell dimensions	a = 5.4863(4) Å	α= 90°.
	b = 13.4457(15) Å	β= 92.358(6)°.
	c = 20.1533(16) Å	γ = 90°.
Volume	1485.4(2) $Å^3$	
Z	4	
Density (calculated)	1.508 Mg/m^3	
Absorption coefficient	0.447 mm^{-1}	
F(000)	692	
Crystal size	0.51 x 0.33 x 0.05 mm^3	
Theta range for data collection	2.53 to 34.85°.	
Index ranges	-8<=h<=8, -21<=k<=21, -31<=l<=32	
Reflections collected	39664	
Independent reflections	6409 [R(int) = 0.1507]	
Completeness to theta = 34.85°	99.1 %	
Absorption correction	None	
Refinement method	Full-matrix least-squares on F^2	
Data / restraints / parameters	6409 / 1 / 202	
Goodness-of-fit on F^2	0.823	
Final R indices [I>2sigma(I)]	R1 = 0.0769, wR2 = 0.1788	
R indices (all data)	R1 = 0.1077, wR2 = 0.1944	
Largest diff. peak and hole	0.657 and -0.690 $e.Å^{-3}$	

Table 21 Crystal data and structure refinement for **(7)**.HCl

C(1)-N(2)	1.328(4)	N(2)-C(2)-C(3)	106.8(2)
C(1)-N(1)	1.345(3)	C(7)-C(2)-C(3)	122.3(2)
C(1)-C(15)	1.481(4)	N(1)-C(3)-C(2)	106.3(2)
C(2)-N(2)	1.384(3)	N(1)-C(3)-C(4)	132.6(2)
C(2)-C(7)	1.389(4)	C(2)-C(3)-C(4)	121.1(2)
C(2)-C(3)	1.397(3)	C(5)-C(4)-C(3)	116.7(2)
C(3)-N(1)	1.390(3)	C(4)-C(5)-C(6)	121.9(3)
C(3)-C(4)	1.397(3)	C(7)-C(6)-C(5)	121.8(3)
C(4)-C(5)	1.369(4)	C(6)-C(7)-C(2)	116.1(3)
C(5)-C(6)	1.409(4)	N(1)-C(8)-C(9)	111.5(2)
C(6)-C(7)	1.378(4)	C(14)-C(9)-C(10)	119.1(2)
C(8)-N(1)	1.466(3)	C(14)-C(9)-C(8)	120.3(2)
C(8)-C(9)	1.512(4)	C(10)-C(9)-C(8)	120.5(2)
C(9)-C(14)	1.388(3)	C(11)-C(10)-C(9)	120.6(2)
C(9)-C(10)	1.391(4)	C(12)-C(11)-C(10)	118.5(3)
C(10)-C(11)	1.386(4)	C(11)-C(12)-C(13)	122.5(2)
C(11)-C(12)	1.373(4)	C(11)-C(12)-N(3)	118.7(2)
C(12)-C(13)	1.376(4)	C(13)-C(12)-N(3)	118.8(2)
C(12)-N(3)	1.474(4)	C(12)-C(13)-C(14)	118.4(2)
C(13)-C(14)	1.384(4)	C(13)-C(14)-C(9)	120.8(2)
C(15)-Cl(1)	1.801(3)	C(1)-C(15)-Cl(1)	110.15(18)
N(3)-O(1)	1.217(4)	C(1)-N(1)-C(3)	108.3(2)
N(3)-O(2)	1.230(4)	C(1)-N(1)-C(8)	125.5(2)
		C(3)-N(1)-C(8)	125.8(2)
N(2)-C(1)-N(1)	109.8(2)	C(1)-N(2)-C(2)	108.8(2)
N(2)-C(1)-C(15)	123.3(3)	O(1)-N(3)-O(2)	124.2(3)
N(1)-C(1)-C(15)	126.8(3)	O(1)-N(3)-C(12)	118.5(3)
N(2)-C(2)-C(7)	130.9(2)	O(2)-N(3)-C(12)	117.3(3)

Table 22 Bond lengths [Å] and angles [°] for **(7)**.HCl

8.3 Crystalographic data for 1-(4-nitrobenzylmethyl)-2-methylpyridine benzimidazole (9)

Crystals were grown by slow evaporation of a dichloromethane solution over a period of two weeks. Colourless blocks were separated from the solvent and a suitable crystal was selected and mounted on a glass fibre using perfluoropolyether oil.

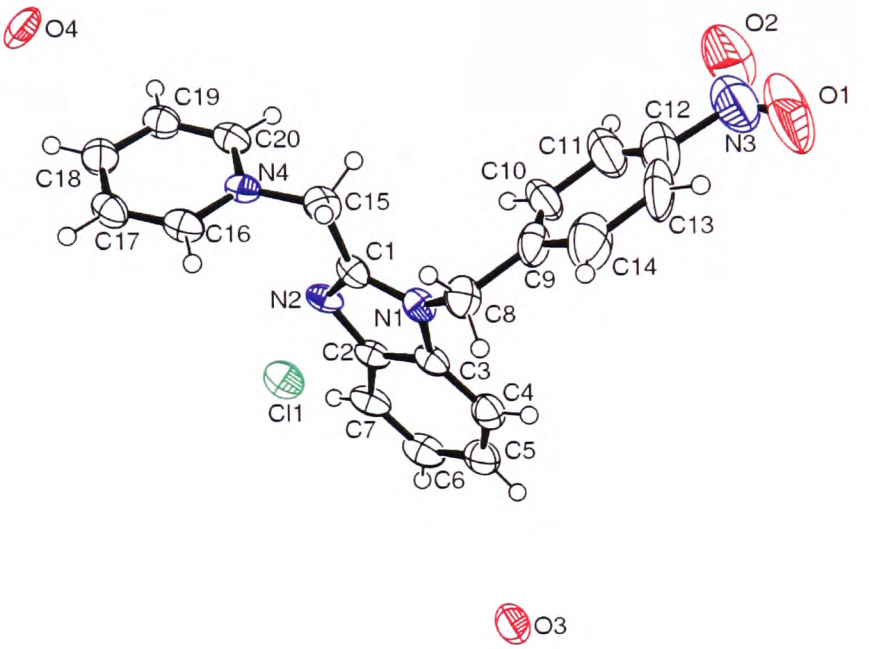

Identification code	sja21_07	
Empirical formula	C20 H17 Cl N4 O3	
Formula weight	396.83	
Temperature	150(2) K	
Wavelength	0.71073 Å	
Crystal system	Monoclinic	
Space group	P21/c	
Unit cell dimensions	a = 15.97(3) Å	α= 90°.
	b = 11.877(12) Å	β= 104.00(11)°.
	c = 10.922(16) Å	γ= 90°.
Volume	2010(5) $Å^3$	
Z	4	
Density (calculated)	1.311 Mg/m^3	
Absorption coefficient	0.218 mm^{-1}	
F(000)	824	
Crystal size	0.4 x 0.1 x 0.06 mm^3	
Theta range for data collection	3.10 to 34.87°.	
Index ranges	-25<=h<=25, -19<=k<=18, -17<=l<=15	
Reflections collected	67963	
Independent reflections	8682 [R(int) = 0.4112]	
Completeness to theta = 34.87°	99.3 %	
Absorption correction	None	
Refinement method	Full-matrix least-squares on F^2	
Data / restraints / parameters	8682 / 0 / 263	
Goodness-of-fit on F^2	0.691	
Final R indices [I>2sigma(I)]	R1 = 0.0751, wR2 = 0.1668	
R indices (all data)	R1 = 0.3175, wR2 = 0.2275	
Extinction coefficient	0.0030(12)	
Largest diff. peak and hole	0.727 and -0.348 $e.Å^{-3}$	

Table 23 Crystal data and structure refinement for **(9)**

C(1)-N(2)	1.306(4)	C(12)-N(3)	1.547(8)
C(1)-N(1)	1.366(5)	C(13)-C(14)	1.460(8)
C(1)-C(15)	1.486(5)	C(13)-H(13)	0.9300
C(2)-N(2)	1.388(5)	C(14)-H(14)	0.9300
C(2)-C(3)	1.391(6)	C(15)-N(4)	1.472(6)
C(2)-C(7)	1.407(5)	C(15)-H(15A)	0.9700
C(3)-C(4)	1.377(6)	C(15)-H(15B)	0.9700
C(3)-N(1)	1.388(5)	C(16)-N(4)	1.339(5)
C(4)-C(5)	1.393(6)	C(16)-C(17)	1.362(6)
C(4)-H(4)	0.9300	C(16)-H(16)	0.9300
C(5)-C(6)	1.384(7)	C(17)-C(18)	1.375(6)
C(5)-H(5)	0.9300	C(17)-H(17)	0.9300
C(6)-C(7)	1.368(6)	C(18)-C(19)	1.377(5)
C(6)-H(6)	0.9300	C(18)-H(18)	0.9300
C(7)-H(7)	0.9300	C(19)-C(20)	1.353(6)
C(8)-N(1)	1.447(5)	C(19)-H(19)	0.9300
C(8)-C(9)	1.523(6)	C(20)-N(4)	1.338(5)
C(8)-H(8A)	0.9700	C(20)-H(20)	0.9300
C(8)-H(8B)	0.9700	N(3)-O(1)	1.123(9)
C(9)-C(10)	1.361(7)	N(3)-O(2)	1.267(9)
C(9)-C(14)	1.367(7)	O(3)-O(4)	1.438(9)
C(10)-C(11)	1.391(7)	O(4)-O(3)	1.438(9)
C(10)-H(10)	0.9300		
C(11)-C(12)	1.275(9)		
C(11)-H(11)	0.9300		
C(12)-C(13)	1.334(9)		

Table 24 Bond lengths [Å] for **(9)**

N(2)-C(1)-N(1)	114.1(3)
N(2)-C(1)-C(15)	125.4(4)
N(1)-C(1)-C(15)	120.4(3)
N(2)-C(2)-C(3)	110.4(3)
N(2)-C(2)-C(7)	130.9(4)
C(3)-C(2)-C(7)	118.7(4)
C(4)-C(3)-N(1)	130.9(4)
C(4)-C(3)-C(2)	123.7(4)
N(1)-C(3)-C(2)	105.3(3)
C(3)-C(4)-C(5)	116.4(4)
C(3)-C(4)-H(4)	121.8
C(5)-C(4)-H(4)	121.8
C(6)-C(5)-C(4)	120.8(4)
C(6)-C(5)-H(5)	119.6
C(4)-C(5)-H(5)	119.6
C(7)-C(6)-C(5)	122.6(4)
C(7)-C(6)-H(6)	118.7
C(5)-C(6)-H(6)	118.7
C(6)-C(7)-C(2)	117.8(4)
C(6)-C(7)-H(7)	121.1
C(2)-C(7)-H(7)	121.1
N(1)-C(8)-C(9)	114.0(4)
N(1)-C(8)-H(8A)	108.8
C(9)-C(8)-H(8A)	108.8
N(1)-C(8)-H(8B)	108.8
C(9)-C(8)-H(8B)	108.8
H(8A)-C(8)-H(8B)	107.6
C(10)-C(9)-C(14)	118.4(5)
C(10)-C(9)-C(8)	123.3(4)
C(14)-C(9)-C(8)	118.3(5)
C(9)-C(10)-C(11)	122.1(6)
C(9)-C(10)-H(10)	119.0
C(11)-C(10)-H(10)	119.0
C(12)-C(11)-C(10)	118.3(7)
C(12)-C(11)-H(11)	120.8
C(10)-C(11)-H(11)	120.8
C(11)-C(12)-C(13)	125.5(6)
C(12)-C(13)-C(14)	116.9(5)
C(12)-C(13)-H(13)	121.5
C(14)-C(13)-H(13)	121.5
C(9)-C(14)-C(13)	118.6(6)
C(9)-C(14)-H(14)	120.7
C(13)-C(14)-H(14)	120.7
N(4)-C(15)-C(1)	111.5(3)
N(4)-C(15)-H(15A)	109.3
C(1)-C(15)-H(15A)	109.3
N(4)-C(15)-H(15B)	109.3
C(1)-C(15)-H(15B)	109.3
H(15A)-C(15)-H(15B)	108.0
N(4)-C(16)-C(17)	120.0(4)
N(4)-C(16)-H(16)	120.0
C(17)-C(16)-H(16)	120.0
C(16)-C(17)-C(18)	119.2(4)
C(16)-C(17)-H(17)	120.4
C(18)-C(17)-H(17)	120.4
C(17)-C(18)-C(19)	119.7(4)
C(17)-C(18)-H(18)	120.1
C(19)-C(18)-H(18)	120.1
C(20)-C(19)-C(18)	119.2(4)
C(20)-C(19)-H(19)	120.4
C(18)-C(19)-H(19)	120.4
N(4)-C(20)-C(19)	120.4(4)
N(4)-C(20)-H(20)	119.8
C(19)-C(20)-H(20)	119.8
C(1)-N(1)-C(3)	105.8(3)
C(1)-N(1)-C(8)	128.0(3)
C(3)-N(1)-C(8)	125.3(4)
C(1)-N(2)-C(2)	104.4(3)
C(20)-N(4)-C(16)	121.5(4)
C(20)-N(4)-C(15)	119.1(3)
C(16)-N(4)-C(15)	119.4(3)
O(1)-N(3)-O(2)	127.2(7)
O(1)-N(3)-C(12)	119.0(9)
O(2)-N(3)-C(12)	113.8(7)

Figure 164 Bond angles [°] for **(9)**

8.4 Crystallographic data for 1,4,7-tris(tert-butoxycarbonylmethyl)-10-(1-(4-nitrobenzyl)-2-methyl benzimidazole)-1,4,7,10-tetraazacyclododecane (32)

Crystals were grown by slow evaporation of a dichloromethane solution over a period of two weeks. Colourless blocks were separated from the solvent and a suitable crystal was selected and mounted on a glass fibre using perfluoropolyether oil.

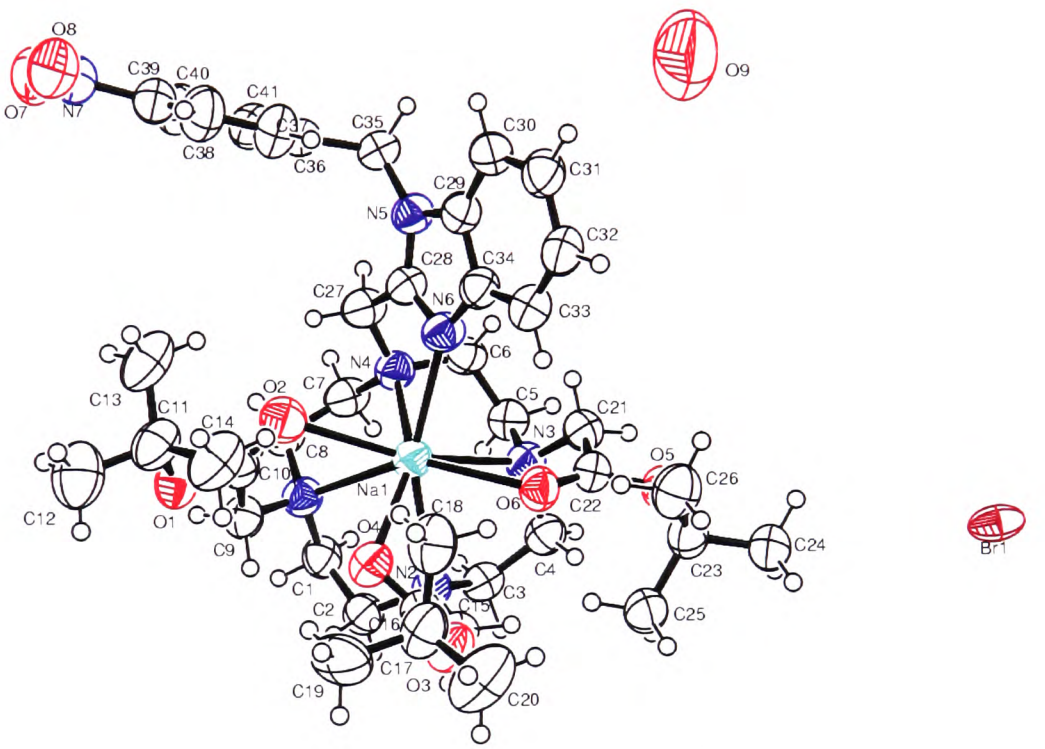

Identification code	sja06_07	
Empirical formula	C41 H61 Br N7 Na O9	
Formula weight	898.87	
Temperature	150(2) K	
Wavelength	0.71073 Å	
Crystal system	Monoclinic	
Space group	P21/n	
Unit cell dimensions	a = 18.5814(15) Å	α= 90°.
	b = 12.8752(8) Å	β= 96.745(7)°.
	c = 19.524(2) Å	γ = 90°.
Volume	4638.6(7) $Å^3$	
Z	4	
Density (calculated)	1.287 Mg/m^3	
Absorption coefficient	0.953 mm^{-1}	
F(000)	1896	
Crystal size	0.4 x 0.4 x 0.3 mm^3	
Theta range for data collection	2.63 to 34.96°.	
Index ranges	-29<=h<=29, -20<=k<=20, -30<=l<=31	
Reflections collected	143731	
Independent reflections	19992 [R(int) = 0.1222]	
Completeness to theta = 34.96°	98.1 %	
Absorption correction	None	
Refinement method	Full-matrix least-squares on F^2	
Data / restraints / parameters	19992 / 0 / 533	
Goodness-of-fit on F^2	0.876	
Final R indices [I>2sigma(I)]	R1 = 0.1059, wR2 = 0.2775	
R indices (all data)	R1 = 0.1938, wR2 = 0.3208	
Extinction coefficient	0.134(5)	
Largest diff. peak and hole	3.583 and -0.790 $e.Å^{-3}$	

Table 25 Crystal data and structure refinement for (32)

C(1)-N(1)	1.470(6)	C(23)-C(24)	1.476(6)
C(1)-C(2)	1.510(6)	C(23)-C(25)	1.518(7)
C(2)-N(2)	1.473(5)	C(23)-C(26)	1.532(7)
C(3)-N(2)	1.472(6)	C(27)-N(4)	1.446(6)
C(3)-C(4)	1.508(7)	C(27)-C(28)	1.499(6)
C(4)-N(3)	1.472(6)	C(28)-N(6)	1.312(5)
C(5)-N(3)	1.468(6)	C(28)-N(5)	1.372(6)
C(5)-C(6)	1.515(6)	C(29)-C(30)	1.388(7)
C(6)-N(4)	1.486(6)	C(29)-N(5)	1.399(6)
C(7)-N(4)	1.489(6)	C(29)-C(34)	1.405(6)
C(7)-C(8)	1.505(7)	C(30)-C(31)	1.386(7)
C(8)-N(1)	1.453(6)	C(31)-C(32)	1.401(7)
C(9)-N(1)	1.462(6)	C(32)-C(33)	1.358(7)
C(9)-C(10)	1.510(7)	C(33)-C(34)	1.385(6)
C(10)-O(2)	1.200(6)	C(34)-N(6)	1.402(6)
C(10)-O(1)	1.335(6)	C(35)-N(5)	1.454(5)
C(11)-C(12)	1.460(10)	C(35)-C(36)	1.500(6)
C(11)-O(1)	1.474(6)	C(36)-C(41)	1.357(7)
C(11)-C(14)	1.490(8)	C(36)-C(37)	1.397(7)
C(11)-C(13)	1.494(9)	C(37)-C(38)	1.361(7)
C(15)-N(2)	1.427(5)	C(38)-C(39)	1.363(8)
C(15)-C(16)	1.522(7)	C(39)-C(40)	1.359(9)
C(16)-O(4)	1.204(5)	C(39)-N(7)	1.460(7)
C(16)-O(3)	1.328(5)	C(40)-C(41)	1.405(8)
C(16)-Na(1)	3.022(5)	N(1)-Na(1)	2.632(4)
C(17)-C(19)	1.498(9)	N(2)-Na(1)	2.649(4)
C(17)-O(3)	1.505(7)	N(3)-Na(1)	2.596(4)
C(17)-C(18)	1.509(9)	N(4)-Na(1)	2.487(4)
C(17)-C(20)	1.526(7)	N(6)-Na(1)	2.498(4)
C(21)-N(3)	1.441(5)	N(7)-O(8)	1.223(8)
C(21)-C(22)	1.525(6)	N(7)-O(7)	1.252(7)
C(22)-O(6)	1.218(5)	O(2)-Na(1)	2.594(4)
C(22)-O(5)	1.314(5)	O(4)-Na(1)	2.451(4)
C(23)-O(5)	1.475(5)	O(6)-Na(1)	2.681(3)

Table 26 Bond lengths [Å] for **(32)**

N(1)-C(1)-C(2)	112.4(4)	O(5)-C(23)-C(26)	108.1(4)
N(2)-C(2)-C(1)	113.1(4)	C(24)-C(23)-C(26)	111.0(4)
N(2)-C(3)-C(4)	112.8(4)	C(25)-C(23)-C(26)	112.5(4)
N(3)-C(4)-C(3)	114.3(4)	N(4)-C(27)-C(28)	110.6(4)
N(3)-C(5)-C(6)	113.6(4)	N(6)-C(28)-N(5)	113.9(4)
N(4)-C(6)-C(5)	113.9(4)	N(6)-C(28)-C(27)	122.9(4)
N(4)-C(7)-C(8)	111.4(4)	N(5)-C(28)-C(27)	123.2(4)
N(1)-C(8)-C(7)	114.5(4)	C(30)-C(29)-N(5)	132.5(4)
N(1)-C(9)-C(10)	111.5(4)	C(30)-C(29)-C(34)	122.4(4)
O(2)-C(10)-O(1)	124.7(5)	N(5)-C(29)-C(34)	105.1(4)
O(2)-C(10)-C(9)	126.1(5)	C(31)-C(30)-C(29)	116.3(5)
O(1)-C(10)-C(9)	109.1(4)	C(30)-C(31)-C(32)	121.2(5)
C(12)-C(11)-O(1)	103.5(5)	C(33)-C(32)-C(31)	121.9(4)
C(12)-C(11)-C(14)	114.2(6)	C(32)-C(33)-C(34)	118.4(5)
O(1)-C(11)-C(14)	109.8(4)	C(33)-C(34)-N(6)	130.2(4)
C(12)-C(11)-C(13)	107.7(5)	C(33)-C(34)-C(29)	119.8(4)
O(1)-C(11)-C(13)	109.9(5)	N(6)-C(34)-C(29)	110.0(4)
C(14)-C(11)-C(13)	111.4(5)	N(5)-C(35)-C(36)	114.9(4)
N(2)-C(15)-C(16)	111.7(3)	C(41)-C(36)-C(37)	119.1(4)
O(4)-C(16)-O(3)	125.2(4)	C(41)-C(36)-C(35)	120.3(5)
O(4)-C(16)-C(15)	123.1(4)	C(37)-C(36)-C(35)	120.5(4)
O(3)-C(16)-C(15)	111.7(4)	C(38)-C(37)-C(36)	121.2(5)
O(4)-C(16)-Na(1)	51.0(2)	C(37)-C(38)-C(39)	118.8(6)
O(3)-C(16)-Na(1)	141.6(3)	C(40)-C(39)-C(38)	121.8(5)
C(15)-C(16)-Na(1)	84.4(2)	C(40)-C(39)-N(7)	118.7(6)
C(19)-C(17)-O(3)	107.7(5)	C(38)-C(39)-N(7)	119.5(6)
C(19)-C(17)-C(18)	113.3(5)	C(39)-C(40)-C(41)	119.1(5)
O(3)-C(17)-C(18)	111.0(4)	C(36)-C(41)-C(40)	119.9(5)
C(19)-C(17)-C(20)	112.7(6)	C(8)-N(1)-C(9)	111.7(3)
O(3)-C(17)-C(20)	102.1(4)	C(8)-N(1)-C(1)	111.6(4)
C(18)-C(17)-C(20)	109.4(6)	C(9)-N(1)-C(1)	110.3(4)
N(3)-C(21)-C(22)	109.1(4)	C(8)-N(1)-Na(1)	106.5(3)
O(6)-C(22)-O(5)	125.3(4)	C(9)-N(1)-Na(1)	105.7(3)
O(6)-C(22)-C(21)	122.5(4)	C(1)-N(1)-Na(1)	110.8(2)
O(5)-C(22)-C(21)	112.2(4)	C(15)-N(2)-C(3)	113.0(3)
O(5)-C(23)-C(24)	103.8(4)	C(15)-N(2)-C(2)	112.4(4)
O(5)-C(23)-C(25)	110.4(4)	C(3)-N(2)-C(2)	109.5(4)
C(24)-C(23)-C(25)	110.7(4)	C(15)-N(2)-Na(1)	101.5(3)

C(3)-N(2)-Na(1)	110.4(3)	N(4)-Na(1)-O(2)	87.35(13)
C(2)-N(2)-Na(1)	109.7(3)	N(6)-Na(1)-O(2)	81.13(13)
C(21)-N(3)-C(5)	112.5(4)	O(4)-Na(1)-N(3)	123.40(12)
C(21)-N(3)-C(4)	109.6(3)	N(4)-Na(1)-N(3)	73.13(12)
C(5)-N(3)-C(4)	110.8(4)	N(6)-Na(1)-N(3)	90.55(14)
C(21)-N(3)-Na(1)	105.1(3)	O(2)-Na(1)-N(3)	160.46(14)
C(5)-N(3)-Na(1)	106.7(2)	O(4)-Na(1)-N(1)	82.51(12)
C(4)-N(3)-Na(1)	111.9(3)	N(4)-Na(1)-N(1)	70.93(13)
C(27)-N(4)-C(6)	112.4(4)	N(6)-Na(1)-N(1)	127.02(13)
C(27)-N(4)-C(7)	109.8(3)	O(2)-Na(1)-N(1)	64.38(12)
C(6)-N(4)-C(7)	110.3(4)	N(3)-Na(1)-N(1)	108.58(13)
C(27)-N(4)-Na(1)	104.7(3)	O(4)-Na(1)-N(2)	64.50(12)
C(6)-N(4)-Na(1)	107.5(2)	N(4)-Na(1)-N(2)	109.66(14)
C(7)-N(4)-Na(1)	112.0(3)	N(6)-Na(1)-N(2)	158.37(14)
C(28)-N(5)-C(29)	106.3(3)	O(2)-Na(1)-N(2)	120.50(13)
C(28)-N(5)-C(35)	127.7(4)	N(3)-Na(1)-N(2)	68.86(12)
C(29)-N(5)-C(35)	126.1(4)	N(1)-Na(1)-N(2)	68.60(11)
C(28)-N(6)-C(34)	104.7(4)	O(4)-Na(1)-O(6)	80.06(11)
C(28)-N(6)-Na(1)	109.8(3)	N(4)-Na(1)-O(6)	126.96(12)
C(34)-N(6)-Na(1)	144.8(3)	N(6)-Na(1)-O(6)	80.95(11)
O(8)-N(7)-O(7)	123.9(5)	O(2)-Na(1)-O(6)	130.31(13)
O(8)-N(7)-C(39)	118.5(6)	N(3)-Na(1)-O(6)	64.74(11)
O(7)-N(7)-C(39)	117.5(6)	N(1)-Na(1)-O(6)	151.99(13)
C(10)-O(1)-C(11)	122.9(4)	N(2)-Na(1)-O(6)	84.09(11)
C(10)-O(2)-Na(1)	110.1(3)	O(4)-Na(1)-C(16)	22.46(11)
C(16)-O(3)-C(17)	120.1(4)	N(4)-Na(1)-C(16)	158.93(15)
C(16)-O(4)-Na(1)	106.5(3)	N(6)-Na(1)-C(16)	132.53(14)
C(22)-O(5)-C(23)	123.3(4)	O(2)-Na(1)-C(16)	97.46(13)
C(22)-O(6)-Na(1)	112.1(3)	N(3)-Na(1)-C(16)	101.15(13)
O(4)-Na(1)-N(4)	152.64(13)	N(1)-Na(1)-C(16)	92.61(13)
O(4)-Na(1)-N(6)	127.29(14)	N(2)-Na(1)-C(16)	50.45(12)
N(4)-Na(1)-N(6)	68.41(13)	O(6)-Na(1)-C(16)	63.95(11)
O(4)-Na(1)-O(2)	75.01(12)		

Symmetry transformations used to generate equivalent atoms:

Figure 165 Bond angles [°] for **(32)**

8.5 Physical data for europium(III) 1,4,7-tris(carboxymethyl)-10-(1-(4-nitrobenzyl)-2-methyl benzimidazole)-1,4,7,10-tetraazacyclododecane (34a)

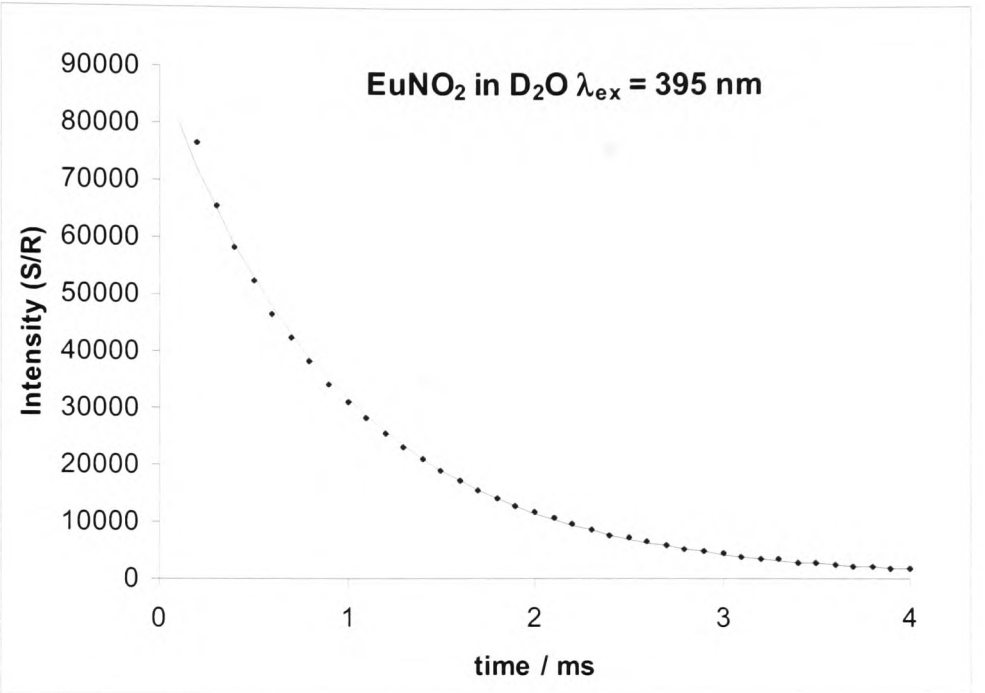

Figure 166 Fitted decay emission graph for **(34a)** in D_2O

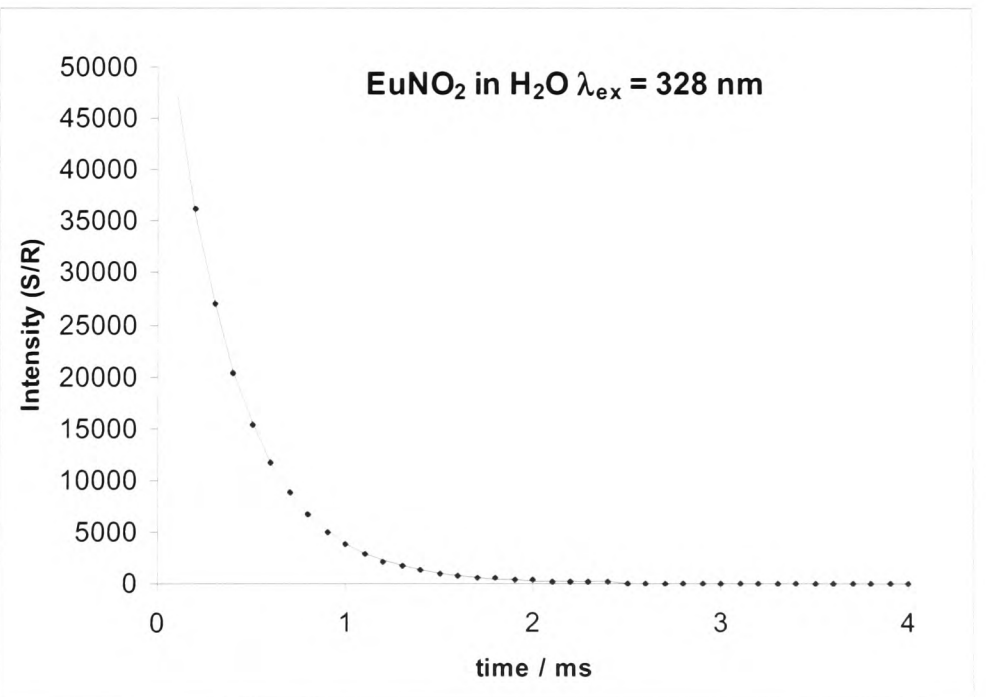

Figure 167 Fitted decay emission graph for **(34a)** in H_2O

8.6 Physical data for terbium(III) 1,4,7-tris(carboxymethyl)-10-(1-(4-nitrobenzyl)-2-methyl benzimidazole)-1,4,7,10-tetraazacyclododecane (34b)

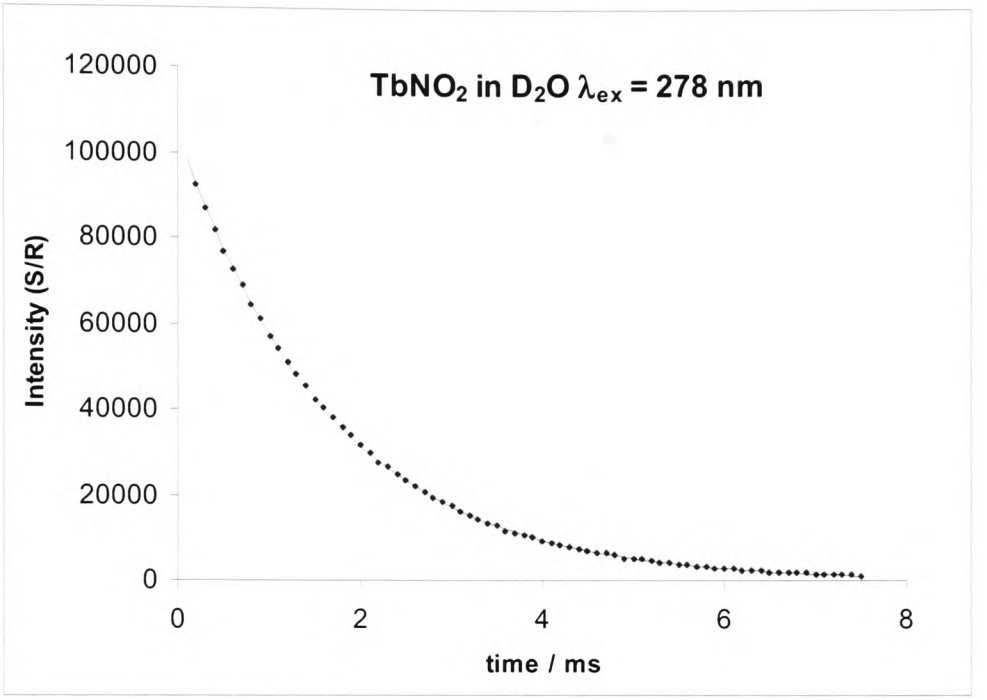

Figure 168 Fitted emission decay graph for **(34b)** in D_2O

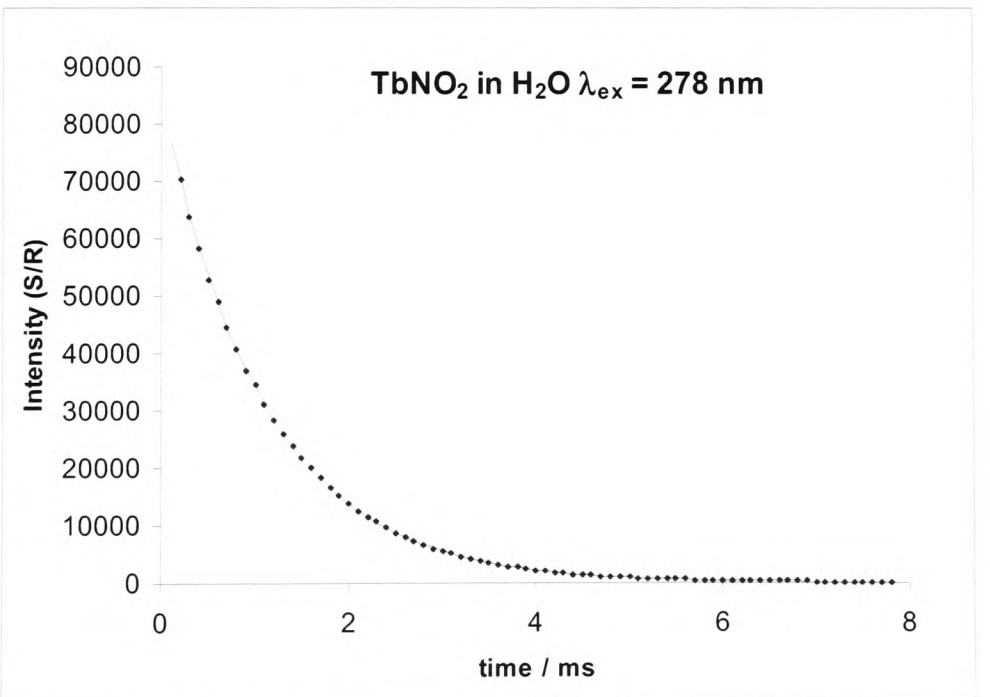

Figure 169 Fitted emission decay graph for **(34b)** in H_2O

8.7 Physical data for europium(III) 1,4,7-tris(carboxymethyl)-10-(1-(4-aminobenzyl)-2-methyl benzimidazole)-1,4,7,10-tetraazacyclododecane (37a)

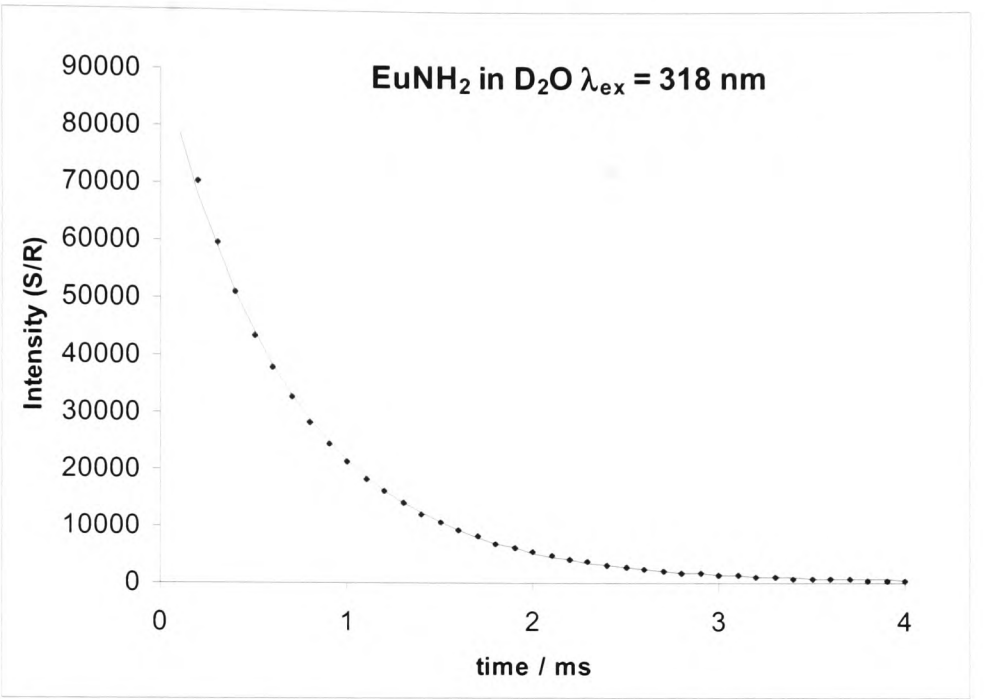

Figure 170 Fitted decay emission graph for **(37a)** in D_2O at λ_{ex} = 318 nm

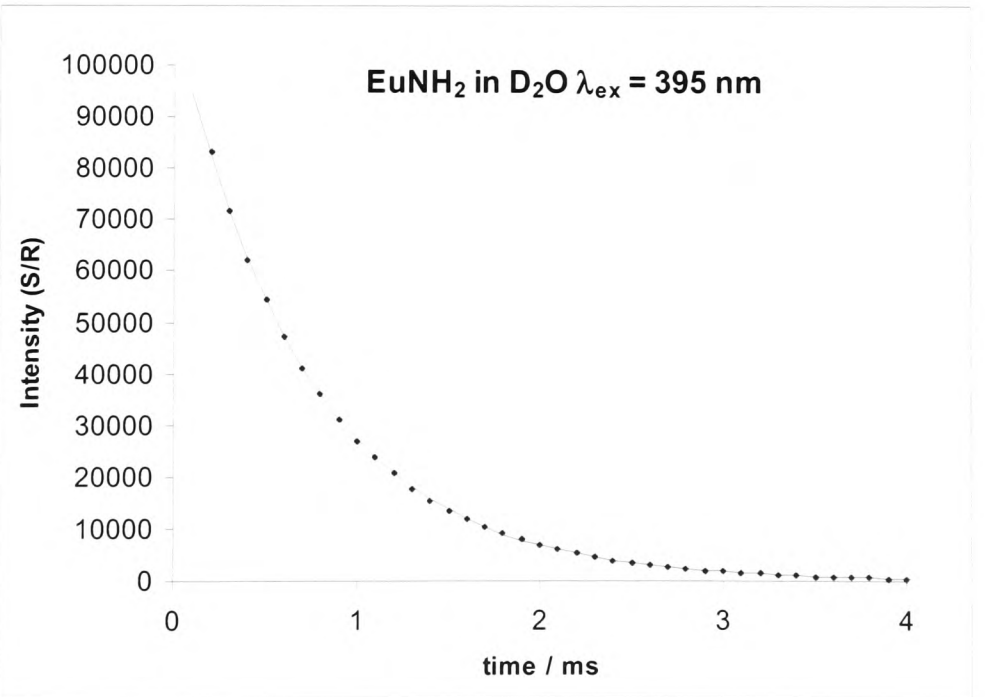

Figure 171 Fitted decay emission decay for **(37a)** in D_2O at λ_{ex} = 395 nm

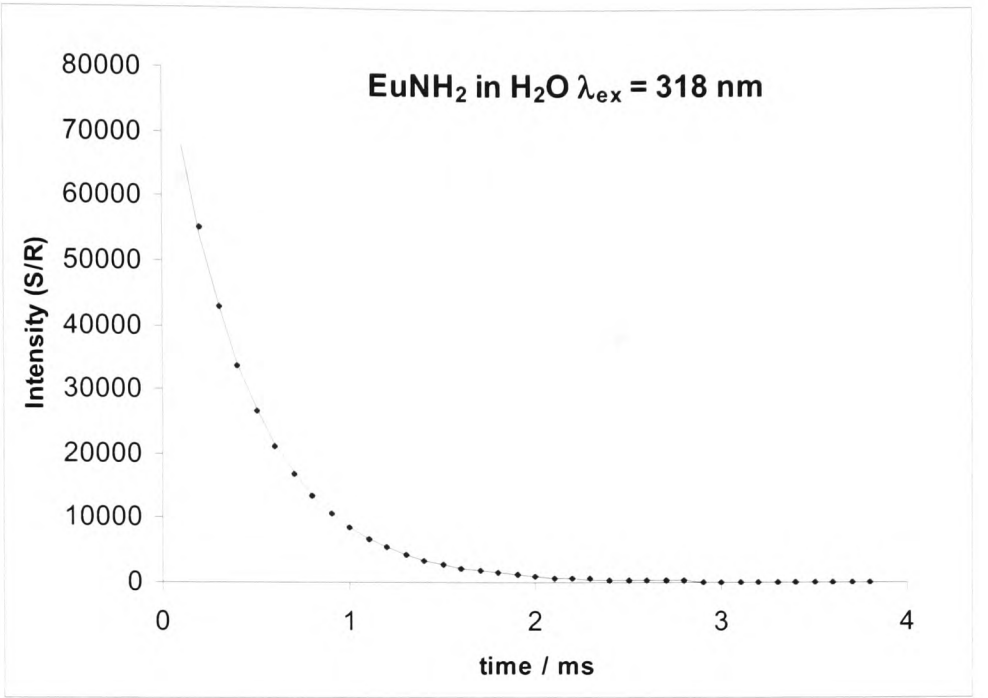

Figure 172 Fitted decay emission decay for **(37a)** in H_2O at λ_{ex} = 318 nm

8.8 Physical data for terbium(III) 1,4,7-tris(carboxymethyl)-10-(1-(4-aminobenzyl)-2-methyl benzimidazole)-1,4,7,10-tetraazacyclododecane (37b)

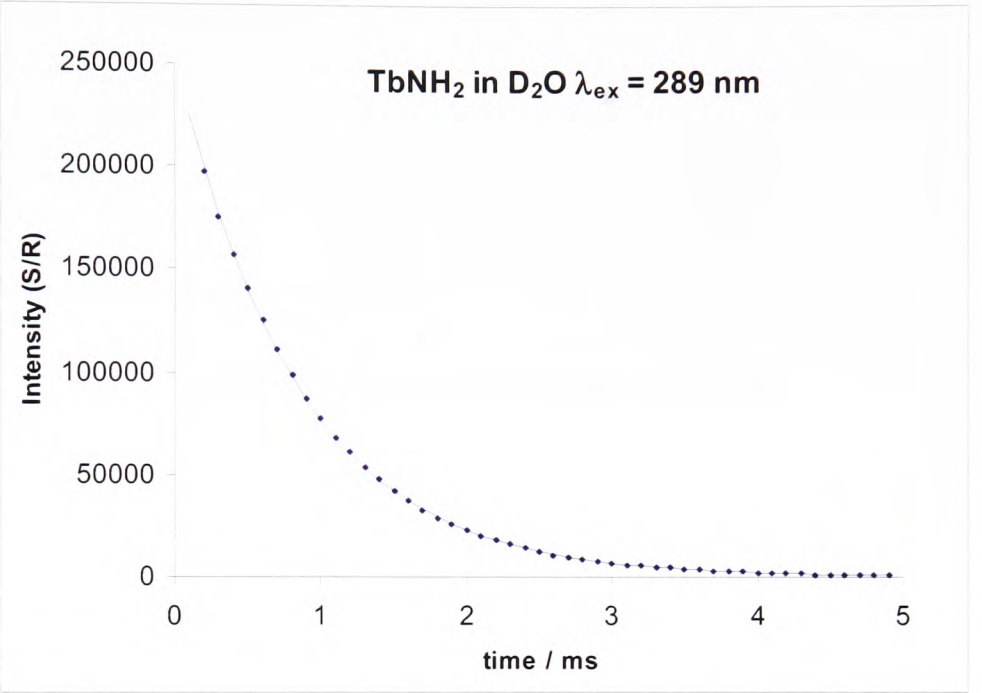

Figure 173 Fitted decay emission decay for (37b) in D_2O

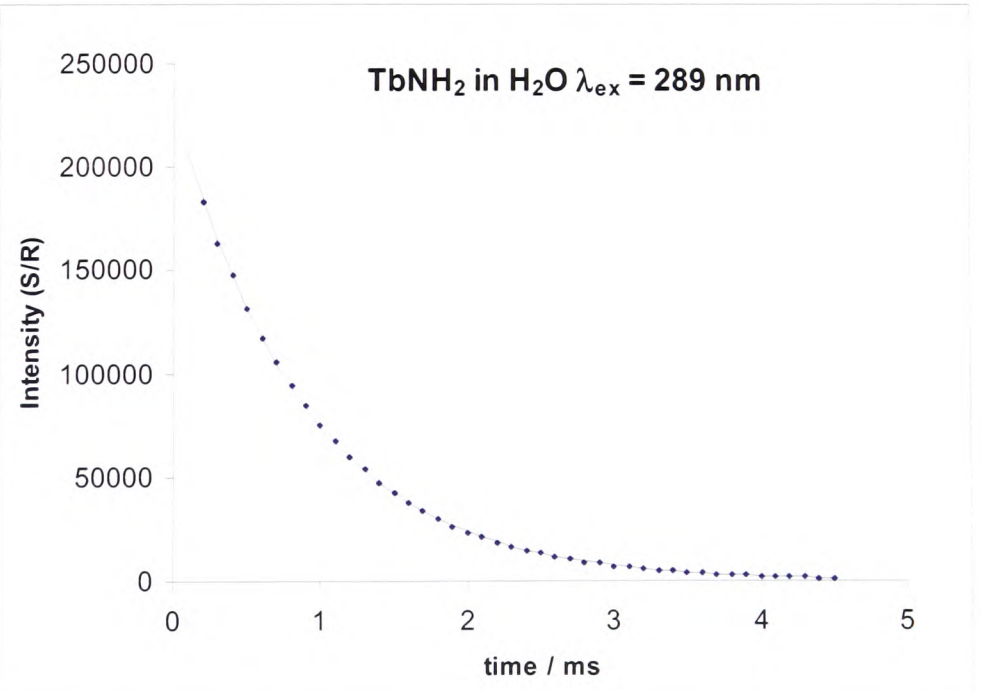

Figure 174 Fitted decay emission decay for **(37b)** in H_2O

8.9 Physical data for gadolinium(III) 1,4,7-tris(carboxymethyl)-10-(2-methyl benzimidazole)-1,4,7,10-tetraazacyclododecane (60)

Concentration (mM)	T_1 (s)	$1/T_1$ (s^{-1})
0.125	1.15	0.87
0.25	0.75	1.34
0.5	0.45	2.24
0.75	0.33	3.00
1.0	0.26	3.89

Table 27 Relaxivity data at pH 6.8 for **(60)**

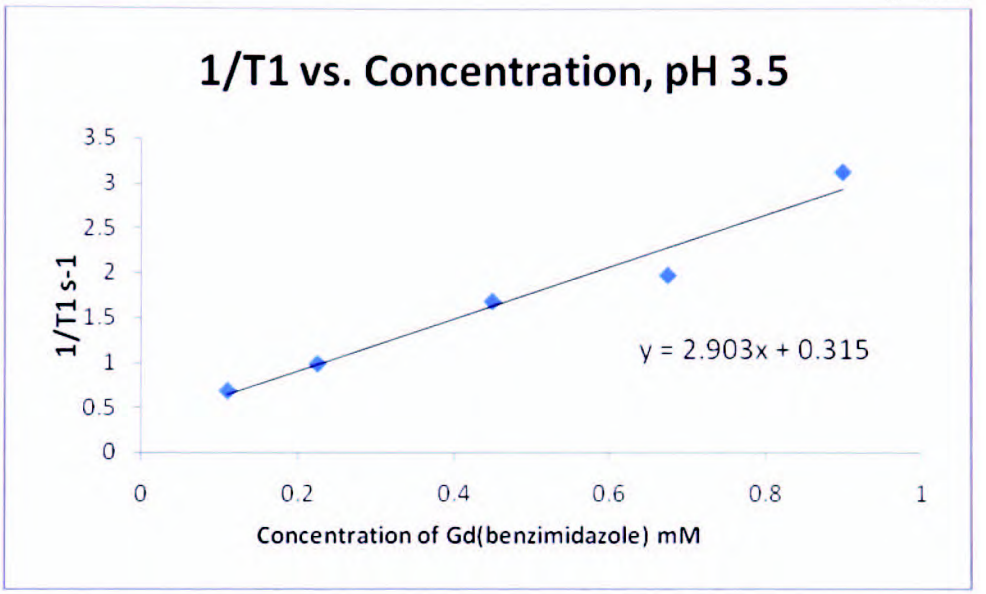

Figure 175 Graph to show $1/T_1$ vs. concentration at pH 3.5 for **(60)**

Concentration (mM)	T_1 (s)	$1/T_1$ (s^{-1})
0.11	1.47	0.68
0.225	1.02	0.98
0.45	0.60	1.68
0.675	0.51	1.96
0.9	0.32	3.12

Table 28 Relaxivity data at pH 3.5 for **(60)**

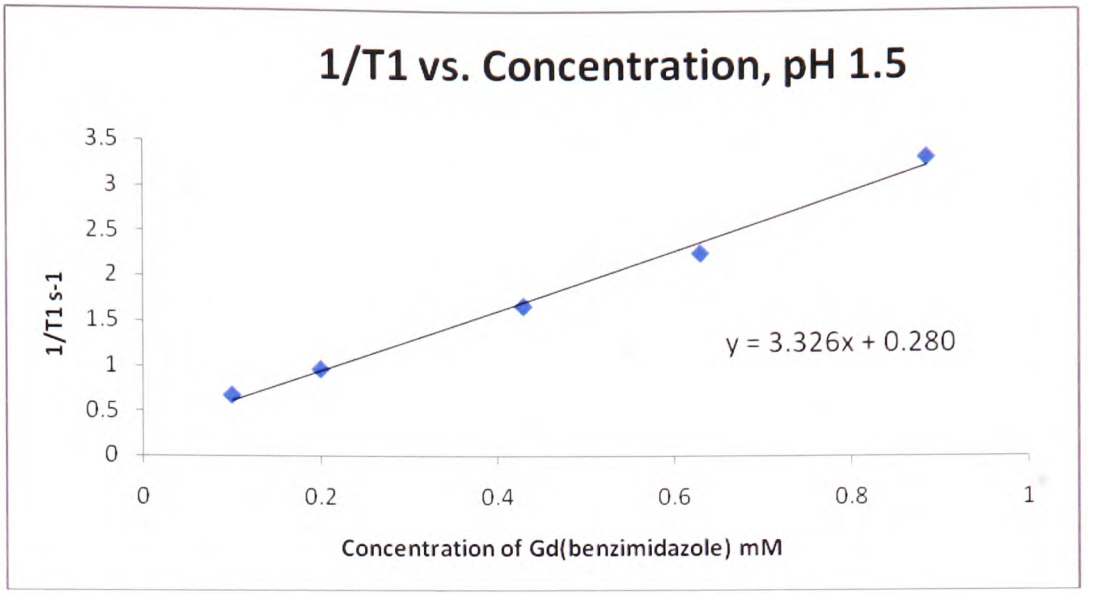

Figure 176 Graph to show $1/T_1$ vs. concentration at pH 1.5 for **(60)**

Concentration (mM)	$T_{1\,(s)}$	$1/T_{1\,(s^{-1})}$
0.11	1.5	0.67
0.225	1.04	0.96
0.45	0.60	1.67
0.675	0.44	2.26
0.9	0.30	3.32

Table 29 Relaxivity data at pH 1.5 for **(60)**

8.10 Physical data for gadolinium(III) 1,4,7-tris(carboxymethyl)-10-(1-(4-nitroobenzyl)-2-methyl benzimidazole)-1,4,7,10-tetraazacyclododecane (34c)

Concentration (mM)	$T_{1\,(s)}$	$1/T_{1\,(s^{-1})}$
0.125	1.08	0.93
0.25	0.64	1.56
0.5	0.34	2.94
0.75	0.23	4.32
1.0	0.15	6.50

Table 30 Relaxivity data at pH 4.6 for **(34c)**

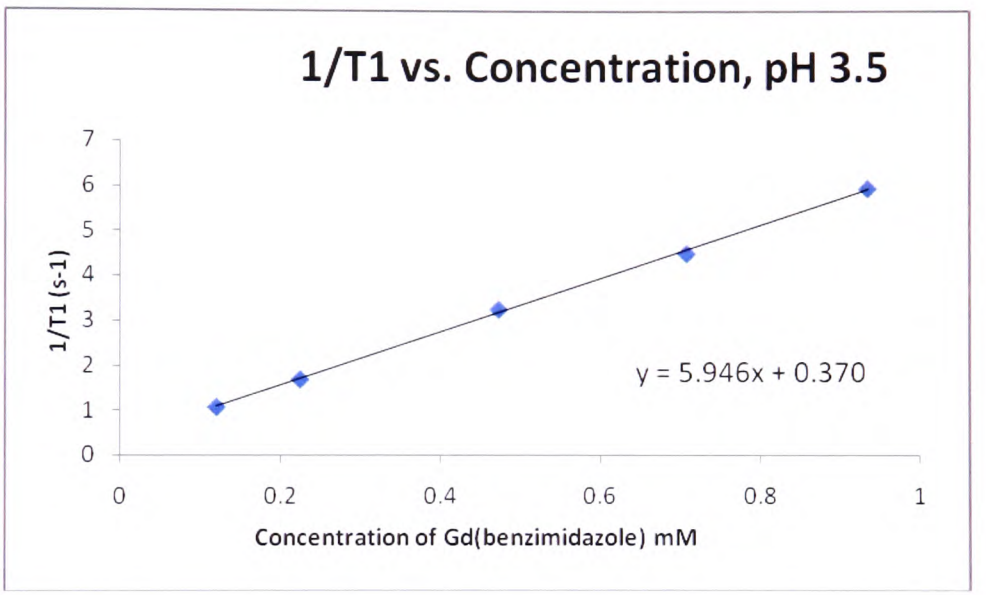

Figure 177 Graph to show $1/T_1$ vs. concentration at pH 3.5 for **(34c)**

Concentration (mM)	$T_{1\,(s)}$	$1/T_{1\,(s^{-1})}$
0.12	0.93	1.07
0.22	0.60	1.68
0.47	0.31	3.25
0.71	0.22	4.50
0.94	0.17	5.96

Table 31 Relaxivity data at pH 3.5 for **(34c)**

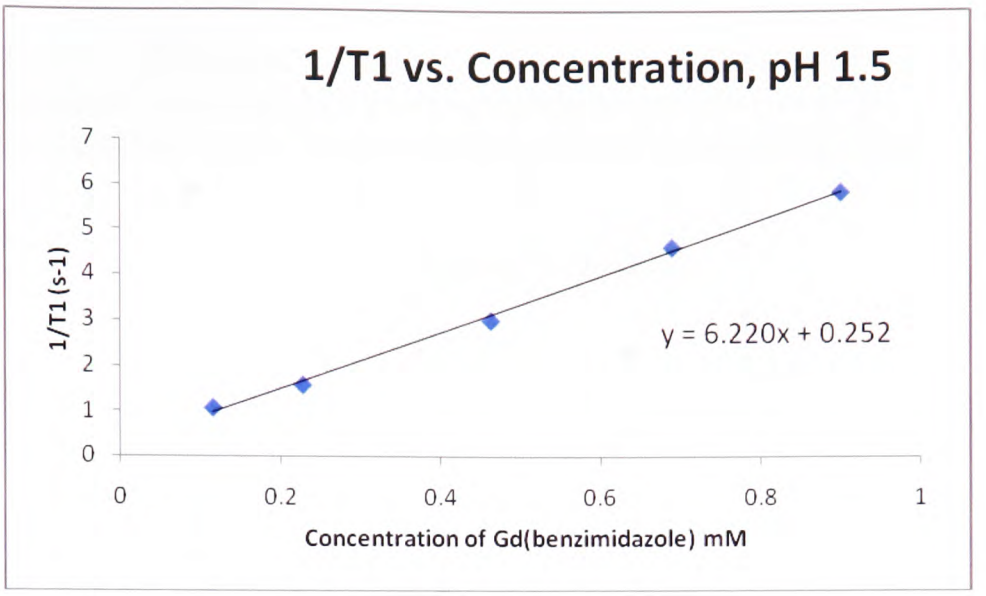

Figure 178 Graph to show $1/T_1$ vs. concentration at pH 1.5 for **(34c)**

Concentration (mM)	$T_{1\,(s)}$	$1/T_{1\,(s^{-1})}$
0.11	0.93	1.07
0.23	0.63	1.59
0.46	0.33	3.02
0.69	0.22	4.64
0.90	0.17	5.85

Table 32 Relaxivity data at pH 1.5 for **(34c)**

8.11 Physical data for gadolinium(III) 1,4,7-tris(carboxymethyl)-10-(1-(4-aminobenzyl)-2-methyl benzimidazole)-1,4,7,10-tetraazacyclododecane (37c)

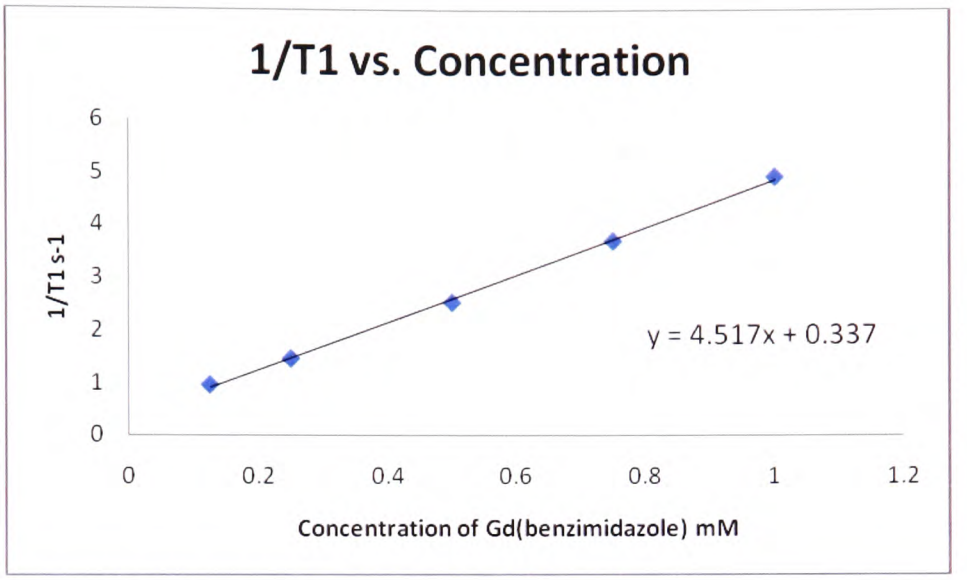

Figure 179 Graph to show $1/T_1$ vs. concentration for **(37c)**

Concentration (mM)	$T_{1\,(s)}$	$1/T_{1\,(s^{-1})}$
0.125	1.04	0.96
0.25	0.68	1.46
0.50	0.40	2.52
0.75	0.27	3.70
1.0	0.20	4.91

Table 33 Relaxivity data for **(37c)**

8.12 Physical data for gadolinium(III) 1,4,7-tris(carboxymethyl)-10-(4-aminobenzyl)-1,4,7,10-tetraazacyclododecane (41c)

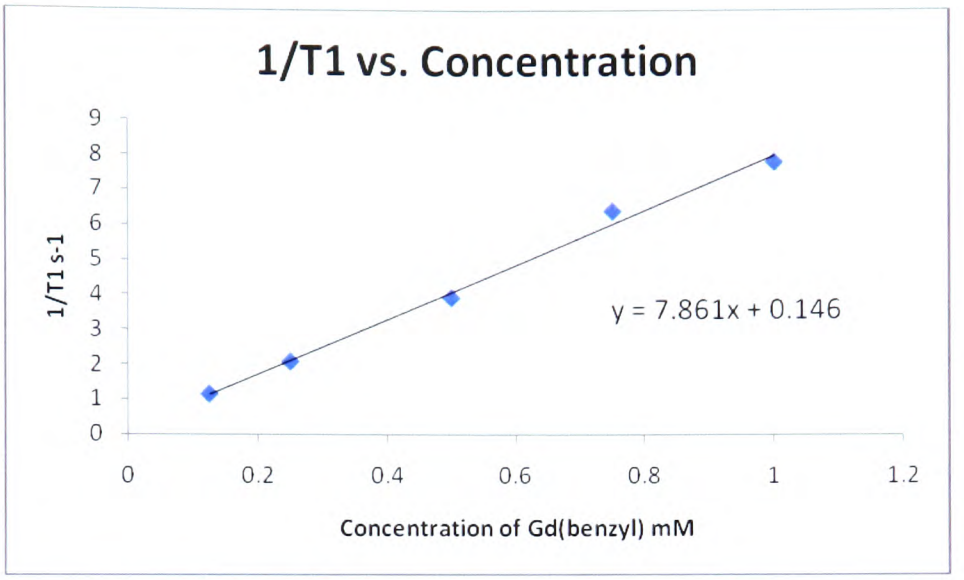

Figure 180 Graph to show $1/T_1$ vs. concentration for **(37c)**

Concentration (mM)	$T_{1\,(s)}$	$1/T_{1\,(s^{-1})}$
0.125	0.89	1.14
0.25	0.48	2.08
0.50	0.26	3.92
0.75	0.16	6.41
1.0	0.13	7.81

Table 34 Relaxivity data for **(37c)**

8.13 Physical data for Omniscan

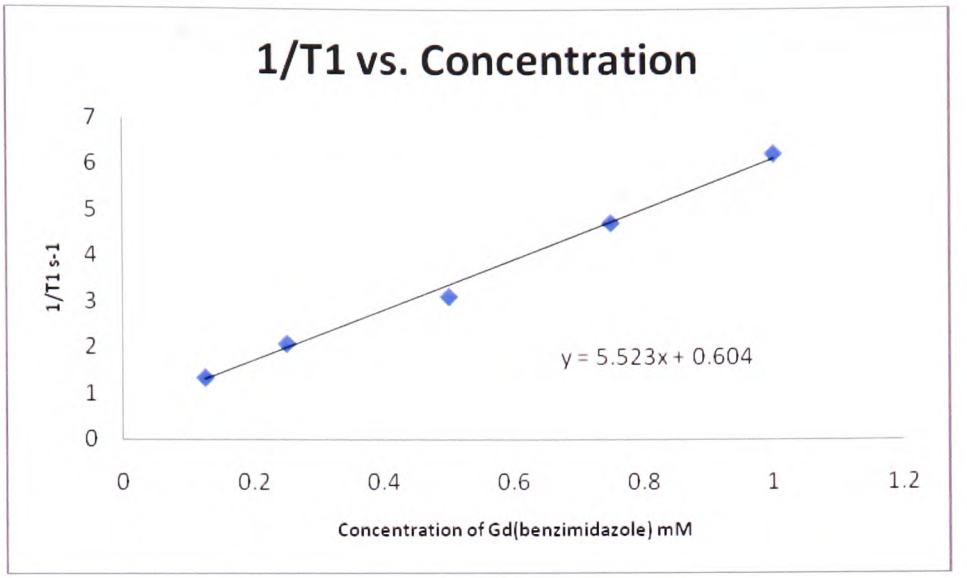

Figure 181 Graph to show $1/T_1$ vs. concentration for Omniscan

Concentration (mM)	$T_{1\,(s)}$	$1/T_{1\,(s^{-1})}$
0.125	0.74	1.35
0.25	0.48	2.09
0.50	0.32	3.12
0.75	0.21	4.73
1.0	0.16	6.23

Table 35 Relaxivity data for Omniscan

9. References

[1] I. Nasso, C. Galaup, F. Hvas, P. Tisnès, C. Picard, S. Laurent, L. Vander Elst, and R. N. Muller, *Inorg. Chem.*, 2005, **44**, 8293.
[2] M. M. Huber, A. B. Staubli, K. Kustedjo, M. H. B. Gray, J. Shih, S. E. Fraser, R. E. Jacobs, and T. J. Meade, *Bioconjugate Chem.*, 1998, **9**, 242.
[3] J. Costa, E. Tóth, L. Helm, and A. E. Merbach, *Inorg. Chem.*, 2005, **44**, 4747.
[4] J. M. Couchet, J. Azéma, P. Tisnès, and C. Picard, *Inorg. Chem. Commun.*, 2003, **6**, 978.
[5] S. Aime, M. Botta, and E. Terreno, *Adv. Inorg. Chem.*, 2005, **57**, 173.
[6] G. A. F. van Tilborg, W. J. M. Mulder, P. T. K. Chin, G. Storm, C. P. Reutelingsperger, K. Nicolay, and G. J. Strijkers, *Bioconjugate Chem.*, 2006, **17**, 865.
[7] D. F. Shriver and P. W. Atkins, 'Inorganic Chemistry-3rd Ed.' Oxford University Press, 1999.
[8] T. Gunnlaugsson and J. P. Leonard, *Chem. Commun.*, 2005, 3114.
[9] P. Caravan, J. J. Ellison, T. J. McMurray, and R. B. Lauffer, *Chem. Rev.*, 1999, **99**, 2293.
[10] J.-C. G. Bünzli and C. Piguet, *Chem. Soc. Rev.*, 2005, **34**, 1048.
[11] J. Kido and Y. Okamoto, *Chem. Rev.*, 2002, **102**, 2357.
[12] S. Faulkner, S. J. A. Pope, and B. P. Burton-Pye, *Appl. Spectrosc. Rev.*, 2005, **40**, 1.
[13] M. P. Lowe, *Curr. Pharm. Biotechnol.*, 2004, **5**, 519.
[14] J. Barkhausen, W. Ebert, J. F. Debatin, and H. J. Weinmann, *J. Am. Coll. Cardiol.*, 2002, **39**, 1392.
[15] R. Trokowski, S. Zhang, and A. D. Sherry, *Bioconjugate Chem.*, 2004, **15**, 1431.
[16] K. N. Raymond and V. C. Pierre, *Bioconjugate Chem.*, 2005, **16**, 3.
[17] S. Aime, S. G. Crich, E. Gianolio, G. B. Giovenzana, L. Tei, and E. Terreno, *Coordin. Chem. Rev.*, 2006, **250**, 1562.
[18] J. H. Hewhouse and J. I. Weiner, 'Understanding MRI - 1st Ed', Little Brown and Company, 1991.
[19] M. A. Brown and C. R. Semelka, 'MRI basic principles and Applications - 3rd Ed', John Wiley and Sons Inc, 2003.
[20] D. W. McRobbie, E. A. Moore, M. J. Graves, and M. R. Prince, 'MRI From Picture to Proton - 1st Ed', Cambridge University Press, 2003.
[21] P. Caravan, *Chem. Soc. Rev.*, 2006, **35**, 512.
[22] M. Bottrill, L. Kwok, and N. J. Long, *Chem. Soc. Rev.*, 2006, **35**, 557.
[23] C. Li, Y. X. Li, G. L. Law, K. Man, W. T. Wong, and H. Lei, *Bioconjugate Chem.*, 2006, **17**, 571.
[24] J. Xu, D. G. Churchill, M. Botta, and K. N. Raymond, *Inorg. Chem.*, 2004, **43**, 5492.
[25] E. J. Werner, S. Avedano, M. Botta, B. P. Hay, E. G. Moore, S. Aime, and K. N. Raymond, *J. Am. Chem. Soc.*, 2007, **129**, 1870
[26] J. B. Livramento, E. Tóth, A. Sour, A. Borel, A. E. Merbach, and R. Ruloff, *Angew. Chem., Int. Ed. Engl.*, 2005, **44**, 1480.
[27] D. A. Fulton, E. M. Elemento, S. Aime, L. Chaabane, M. Botta, and D. Parker, *Chem. Commun.*, 2006, 1064.
[28] M. Ito, H. Ogino, H. Oshima, N. Shiraki, Y. Shibamoto, H. Kassi, M. Mase, Y. Kawamura, and T. Miyati, *Magn. Reson. Imaging*, 2006, **24**, 625.

[29] B. Jebasingh and V. Alexander, *Inorg. Chem.*, 2005, **44**, 9434.
[30] P. Voisin, J. R. Ribot, S. Miraux, A. K. Bouzier-Sore, J.-F. Lahitte, V. Bouchaud, S. Mornet, E. Thiaudière, J.-M. Franconi, L. Raison, C. Labrugère, and M.-H. Delville, *Bioconjugate Chem.*, 2007, **18**, 1053
[31] H. Y. Lee, H. W. Jee, S. M. Seo, B. K. Kwak, G. Khang, and S. H. Cho, *Bioconjugate Chem.*, 2006, **17**, 700.
[32] J. Rudovský, M. Botta, P. Hermann, K. I. Hardcastle, I. Lukes, and S. Aime, *Bioconjugate Chem.*, 2006, **17**, 975.
[33] H. Kobayashi, S. Kawamoto, S. K. Jo, H. J. Bryant Jr, M. W. Brechbiel, and R. A. Star, *Bioconjugate Chem.*, 2003, **14**, 388.
[34] G. P. Yan, S. E. Bottle, R.-X. Zhuo, M.-L. Liu, and L.-Y. Li, *J. Bioact. Compat. Pol.*, 2004, **19**, 453.
[35] P. Lebdušková, A. Sour, L. Helm, E. Tóth, J. Kotek, I. Lukeš, and A. E. Merbach, *Dalton Trans.*, 2006, 3399.
[36] S. Laus, A. Sour, R. Ruloff, E. Tóth, and A. E. Merbach, *Chem. Eur. J.*, 2005, **11**, 3064.
[37] H. Xu, A. S. Regino, M. Bernardo, Y. Koyama, P. L. Choyke, and M. W. Brechbiel, *J. Med. Chem.*, 2007, **50**, 3185
[38] H. Kobayashi and M. W. Brechbiel, *Curr. Pharm. Biotechnol.*, 2004, **5**, 539.
[39] R. Hovland, C. Gløgård, A. J. Aasen, and J. Klaveness, *J. Chem. Soc., Perkin Trans. 2*, 2001, 929.
[40] S. Aime, F. Fedeli, A. Sanino, and E. Terreno, *J. Am. Chem. Soc.*, 2006, **128**, 11326
[41] R. A. Moats, S. E. Fraser, and T. J. Meade, *Angew. Chem., Int. Ed. Engl.*, 1997, **36**, 726.
[42] C. Carrera, G. Digillo, S. Baroni, S. Consol, F. Fedeli, D. Longo, A. Mortillaro, and S. Aime, *Dalton Trans.*, 2007, 4980.
[43] M. Woods, S. Zhang, V. H. Ebron, and A. D. Sherry, *Chem. Eur. J.*, 2003, **9**, 4634.
[44] I. Mamedov, A. Mishra, G. Angelovski, H. A. Mayer, L.-O. Pålsson, D. Parker, and N. K. Logothetis, *Dalton Trans.*, 2007, 5260.
[45] J. I. Bruce, R. S. Dickins, L. J. Govenlock, T. Gunnlaugsson, S. Lopinski, M. P. Lowe, D. Parker, R. D. Peacock, J. J. B. Perry, S. Aime, and M. Botta, *J. Am. Chem. Soc.*, 2000, **122**, 9674.
[46] S. Blair, M. P. Lowe, C. E. Mathieu, D. Parker, K. Senanayake, and R. Kataky, *Inorg. Chem.*, 2001, **40**, 5860.
[47] M. Woods, G. E. Kiefer, S. Bott, A. Castillo-Muzquiz, C. Eshelbrenner, L. Michaudet, K. McMillian, S. D. K. Mudigunda, D. Ogrin, G. Tircsó, S. Zhang, P. Zhao, and A. D. Sherry, *J. Am. Chem. Soc.*, 2004, **126**, 9248.
[48] F. K. Kálmán, M. Woods, P. Caravan, P. Jurek, M. Spiller, G. Tircsó, R. Király, E. Brucher, and A. D. Sherry, *Inorg. Chem.*, 2007, **46**, 5260.
[49] W. H. Li, G. Parigi, M. Fragai, C. Luchinat, and T. J. Meade, *Inorg. Chem.*, 2002, **41**, 4018.
[50] J. A. Duimstra, F. J. Femia, and T. J. Meade, *J. Am. Chem. Soc.*, 2005, **127**, 12847.
[51] L. M. Urbanczyk-Pearson, F. J. Femia, J. Smith, G. Parigi, J. A. Duimstra, A. L. Eckermann, C. Luchinat, and T. J. Meade, *Inorg. Chem.*, 2008, **47**, 56.
[52] M. Woods, Z. Kovacs, and A. D. Sherry, *J. Supramol. Chem.*, 2002, **2**, 1.
[53] S. Aime, Barge, A., Cabella, C., Crich, S. G., Ginanolio, E., *Curr. Pharm. Biotechnol.*, 2004, **5**, 509.

[54] D. Artemov, Z. M. Bhujwalla, and J. W. M. Bulte, *Curr. Pharm. Biotechnol.*, 2004, **5**, 485.
[55] H. J. Weinmann, W. Ebert, B. Misselwitz, and H. Schmitt-Willich, *Eur. Radiol.*, 2003, **46**, 33.
[56] G. M. Lanza, P. Winter, S. Caruthers, A. Schmeider, K. Crowder, A. Morawski, H. Zhang, M. J. Scott, and S. A. Wickline, *Curr. Pharm. Biotechnol.*, 2004, **5**, 495.
[57] I. Dijkgraaf, A. Y. Rijnders, A. Soede, A. C. Dechesne, G. W. Esse, A. J. Brouwer, F. H. M. Corstens, O. C. Boerman, D. T. S. Rijkers, and R. M. J. Liskamp, *Org. Biomol. Chem.*, 2007, **5**, 935.
[58] S. G. Crich, C. Cabella, A. Barge, S. Belfiore, C. Ghirelli, L. Lattuada, S. Lanzardo, A. Mortillaro, L. Tei, M. Visigalli, G. Forni, and S. Aime, *J. Med. Chem.*, 2006, **49**, 4926.
[59] T. Simor, B. Gaszner, J. N. Oshinski, S. M. Waldrop, R. I. Pettigrew, I. G. Horváth, G. Hild, and G. A. Elgavish, *J. Magn. Reson.*, 2005, **21**, 536.
[60] B. Gustafsson, S. Youens, and A. Y. Louie, *Bioconjugate Chem.*, 2006, **17**, 538.
[61] M. J. Allen and T. J. Meade, *J. Biol. Inorg. Chem.*, 2003, **8**, 746.
[62] W. Su, A. Mishra, J. Pfeuffer, K. H. Wiesmuller, K. Ugurbil, and J. Engelmann, *Contrast Media Mol. Imaging*, 2007, **2**, 42.
[63] J. Lee, J. E. Burdette, K. W. MacRenaris, D. Mustafi, T. K. Woodruff, and T. J. Meade, *Chem. Biol.*, 2007, **14**, 824.
[64] A. Dirksen, S. Langereis, B. F. M. de Waal, M. H. P. van Genderen, T. M. Hackeng, and E. W. Meijer, *Chem. Commun.*, 2005, 2811.
[65] S. G. Crich, A. Barge, E. Battistini, C. Cabella, S. Coluccia, D. Longo, V. Mainero, G. Tarone, and S. Aime, *J. Biol. Inorg. Chem.*, 2005, **10**, 78.
[66] T. N. Parac-Vogt, K. Kimpe, S. Laurent, L. V. Elst, C. Burtea, F. Chen, R. N. Muller, Y. Ni, A. Verbruggen, and K. Binnemans, *Chem. Eur. J.*, 2005, **11**, 3077.
[67] P. Caravan, N. J. Cloutier, M. T. Greenfield, S. A. McDermid, S. U. Dunham, J. W. M. Bulte, J. C. Amedio, R. J. Looby, R. M. Supkowski, W. D. Horrocks, T. J. McMurray, and R. B. Lauffer, *J. Am. Chem. Soc.*, 2002, **124**, 3152.
[68] Z. Tyeklár, S. U. Dunham, K. Midelfort, D. M. Scott, H. Sajiki, K. Ong, R. B. Lauffer, P. Caravan, and T. J. McMurray, *Inorg. Chem.*, 2007, **46**, 6621.
[69] P. Caravan, G. Parigi, J. M. Chasse, N. J. Cloutier, J. J. Ellison, R. B. Lauffer, C. Luchinat, S. A. McDermid, M. Spiller, and T. J. McMurray, *Inorg. Chem.*, 2007, **46**, 6632.
[70] R. P. Haugland, 'Handbook of fluorescent probes and research products - 9th Ed', Molecular Probes, 2002.
[71] K. Hanaoka, K. Kikuchi, H. Kobayashi, and T. Nagano, *J. Am. Chem. Soc.*, 2007, **129**, 13502.
[72] M. Shi, F. Li, T. Yi, D. Zhang, H. Hu, and C. Huang, *Inorg. Chem.*, 2005, **44**, 8929.
[73] D. Parker, R. S. Dickins, H. Puschmann, C. Crossland, and J. A. K. Howard, *Chem. Rev.*, 2002, **102**, 1977.
[74] M. H. Werts, J. W. Verhoeven, and J. W. Hofstraat, *J. Chem. Soc., Perkin Trans. 2*, 2000, 433.
[75] A. Beeby, L. M. Bushby, D. Maffeo, and J. A. G. Williams, *J. Chem. Soc., Dalton Trans.*, 2002, 48.

[76] J. Kotek, J. Rudovský, P. Hermann, and I. Lukes, *Inorg. Chem.*, 2006, **45**, 3097.
[77] A. Dadabhoy, S. Faulkner, and P. G. Sammes, *J. Chem. Soc., Perkin Trans. 2*, 2002, 348.
[78] D. Maffeo and J. A. G. Williams, *Inorg. Chim. Acta*, 2003, **355**, 127.
[79] A. J. Wilkinson, D. Maffeo, A. Beeby, C. E. Foster, and J. A. G. Williams, *Inorg. Chem.*, 2007, **46**, 9438.
[80] P. Atkinson, K. S. Findlay, F. Kielar, R. Pal, D. Parker, R. A. Poole, H. Puschmann, S. L. Richardson, P. A. Stenson, A. L. Thompson, and J. Yu, *Org. Biomol. Chem.*, 2006, **4**, 1707.
[81] B. H. Bakker, M. Goes, N. Hoebe, H. J. van Ramesdonk, J. W. Verhoeven, M. H. V. Werts, and J. W. Hofstraat, *Coordin. Chem. Rev.*, 2000, **208**, 3.
[82] E. G. Moore, C. J. Jocher, J. Xu, E. J. Werner, and K. N. Raymond, *Inorg. Chem.*, 2007, **46**, 5468.
[83] S. Petoud, G. Muller, E. G. Moore, J. Xu, J. Sokolnicki, J. P. Riehl, U. N. Le, S. M. Cohen, and K. N. Raymond, *J. Am. Chem. Soc.*, 2007, **129**, 77.
[84] S. I. Klink, H. Keizer, and F. C. J. M. van Veggel, *Angew. Chem., Int. Ed. Engl.*, 2000, **39**, 4319.
[85] A. Beeby, R. S. Dickens, S. Fitzgerald, L. J. Govenlock, C. L. Maupin, D. Parker, J. P. Riehl, G. Siligardi, and J. A. G. Williams, *Chem. Commun.*, 2000, 1183.
[86] S. G. Baca, H. Adams, D. Sykes, S. Faulkner, and M. D. Ward, *Dalton Trans.*, 2007, 2419.
[87] K. Sénéchal-David, S. J. A. Pope, S. Quinn, S. Faulkner, and T. Gunnlaugsson, *Inorg. Chem.*, 2006, **45**, 10040.
[88] K. Hanaoka, K. Kikuchi, H. Kojima, Y. Urano, and T. Nagano, *J. Am. Chem. Soc.*, 2004, **126**, 12470.
[89] K. Senanayake, A. L. Thompson, J. A. K. Howard, M. Botta, and D. Parker, *Dalton Trans.*, 2006, 5423.
[90] A. B. Dias and S. Viswanathan, *Chem. Commun.*, 2004, 1024.
[91] L. J. Charbonnière, S. Mameri, D. Flot, F. Waltz, C. Zandanel, and R. F. Ziessel, *Dalton Trans.*, 2007, 2245.
[92] T. Gunnlaugsson and A. J. Harte, *Org. Biomol. Chem.*, 2006, **4**, 1572.
[93] M. S. Tremblay, M. Halim, and D. Sames, *J. Am. Chem. Soc.*, 2007, **129**, 7570.
[94] S. Faulkner and S. J. A. Pope, *J. Am. Chem. Soc.*, 2003, **125**, 10526.
[95] D. Parker, *Chem. Commun.*, 1998, 245.
[96] K. Komatsu, Y. Urano, H. Kojima, and T. Nagano, *J. Am. Chem. Soc.*, 2007, **129**, 13447.
[97] S. Pandya, J. Yu, and D. Parker, *Dalton Trans.*, 2006, 2757.
[98] C. P. McCoy, F. Stomeo, S. E. Plush, and T. Gunnlaugsson, *Chem. Mater.*, 2006, **18**, 4336.
[99] B. Song, G. Wang, M. Tan, and J. Yuan, *J. Am. Chem. Soc.*, 2006, **128**, 13442.
[100] R. F. H. Viguier and A. N. Hulme, *J. Am. Chem. Soc.*, 2006, **128**, 11370.
[101] S. J. A. Pope, B. P. Burton-Pye, R. Berridge, T. Khan, P. J. Skabara, and S. Faulkner, *Dalton Trans.*, 2006, 2907.
[102] J. Yu, D. Parker, R. Pal, R. A. Poole, and M. J. Cann, *J. Am. Chem. Soc.*, 2006, **128**, 2294.
[103] J. C. Frias, G. Bobba, M. J. Cann, C. J. Hutchinson, and D. Parker, *Org. Biomol. Chem.*, 2003, **1**, 905.

104 R. A. Poole, C. P. Montgomery, E. J. New, A. Congreve, D. Parker, and M. Botta, *Org. Biomol. Chem.*, 2007, **5**, 2055.
105 S. Poupart, C. Boudou, P. Peixoto, M. Massonneau, P.-Y. Renard, and A. Romieu, *Org. Biomol. Chem.*, 2006, **4**, 4165.
106 S. D. Konda, M. Aref, S. Wang, M. W. Brechbiel, and E. C. Wiener, *Magn. Reson. Phys. Biol. Med.*, 2001, **12**, 104.
107 A. Mishra, J. Pfeuffer, R. Mishra, J. Engelmann, A. K. Mishra, K. Ugurbil, and N. K. Logothetis, *Bioconjugate Chem.*, 2006, **17**, 773.
108 H. C. Manning, M. Bai, B. M. Anderson, R. Lisiak, L. E. Samuelson, and D. J. Bornhop, *Tetrahedron Lett.*, 2005, **46**, 4707.
109 M. Modo, D. Cash, K. Mellodew, S. C. R. Williams, S. E. Fraser, T. J. Meade, J. Price, and H. Hodges, *Neuroimage*, 2002, **17**, 803.
110 G. A. F. van Tilborg, W. J. M. Mulder, N. Deckers, G. Storm, C. P. M. Reutelingsperger, G. J. Strijkers, and K. Nicolay, *Bioconjugate Chem.*, 2006, **17**, 741.
111 T. Lazarides, M. A. H. Alamiry, H. Adams, S. J. A. Pope, S. Faulkner, J. A. Weinstein, and M. D. Ward, *Dalton Trans.*, 2007, 1484.
112 N. V. Ivanova, S. I. Sviridov, and A. E. Stepanov, *Tetrahedron Lett.*, 2006, **47**, 8025.
113 J. B. Wright, *Chem. Rev.*, 1951, **48**, 397.
114 J. Gómez-Segura, M. J. Prieto, M. Font-Bardia, X. Solans, and V. Moreno, *Inorg. Chem.*, 2006, **45**, 10031.
115 F. A. Tanious, W. Laine, P. Peixoto, C. Bailly, K. D. Goodwin, M. A. Lewis, E. C. Long, M. M. Georgiadis, R. R. Tidwell, and W. D. Wilson, *Biochemistry*, 2007, **46**, 6944.
116 T. Ishida, T. Suzuki, S. Hirashima, K. Mizutani, A. Yoshida, I. Ando, S. Ikeda, T. Adachi, and H. Hashimoto, *Bioorg. Med. Chem. Lett.*, 2006, **16**, 1859.
117 X.-P. Yang, B.-S. Kang, W.-K. Wong, C.-Y. Su, and H.-Q. Liu, *Inorg. Chem.*, 2003, **42**, 169.
118 P. N. Preston, *Chem. Rev.*, 1974, **74**, 279.
119 J. Charton, S. Girault-Mizzi, M. A. Debreu-Fontaine, F. Foufelle, I. Hainault, J. G. Bizot-Espiard, D. H. Caignard, and C. Sergheraert, *Bioorg. Med. Chem.*, 2006, **14**, 4490.
120 T. Pandiyan, M. Palaniandavar, M. Lakshminarayanan, and H. Manohar, *J. Chem. Soc., Dalton Trans.*, 1992, 3377.
121 D. Hérault, K. Aelvoet, A. J. Blatch, A. Al-Majid, C. A. Smethurst, and A. Whiting, *J. Org. Chem.*, 2007, **72**, 71.
122 M. Raban, H. Chang, L. Craine, and E. Hortelano, *J. Org. Chem.*, 1985, **50**, 2205.
123 L. Casella, M. Gullotti, A. Pintar, F. Pinciroli, R. Viganò, and P. Zanello, *J. Chem. Soc., Dalton Trans.*, 1989, 1161.
124 T. Roth, M. L. Morningstar, P. L. Boyer, S. H. Hughes, R. W. Buckheit, and C. J. Michejda, *J. Med. Chem.*, 1997, **40**, 4199.
125 J. J. V. Eynde, F. Delfosse, P. Lor, and Y. V. Haverbeke, *Tetrahedron*, 1995, **51**, 5813.
126 E. Farrant and S. S. Rahman, *Tetrahedron Lett.*, 2000, **41**, 5383.
127 K. R. Hornberger, G. M. Adjabeng, H. D. Dickson, and R. G. Davis-Ward, *Tetrahedron Lett.*, 2006, **47**, 5359.
128 A. Abbotto, S. Bradamante, and G. A. Pagani, *J. Org. Chem.*, 1996, **61**, 1761.
129 B. Das, H. Holla, and Y. Srinivas, *Tetrahedron Lett.*, 2007, **48**, 61.

130 P. Gogoi and D. Konwar, *Tetrahedron Lett.*, 2006, **47**, 79.
131 J. H. Musser, D. M. Kubrak, J. Chang, S. M. Dizio, M. Hite, J. M. Hand, and A. J. Lewis, *J. Med. Chem.*, 1987, **30**, 400.
132 J. G. Wilson and F. C. Hunt, *Aust. J. Chem.*, 1983, **36**, 2317.
133 G. Solomons and C. Fryhle, 'Organic Chemistry - 7th Ed', John Wiley and Sons inc, 2000.
134 Y. Yasui, D. K. Frantz, and J. S. Siegel, *Org. Lett.*, 2006, **8**, 4989.
135 C. J. Wharton and R. Wrigglesworth, *J. Chem. Soc., Perkin Trans. 1*, 1981, 433.
136 S. M. McElvain and J. W. Nelson, *J. Am. Chem. Soc.*, 1942, **64**, 1825.
137 F. C. Schaefer and G. A. Peters, *J. Am. Chem. Soc.*, 1959, **81**, 1470.
138 A. Bloom and A. R. Day, *J. Org. Chem.*, 1939, **4**, 14.
139 K. Hofmann, 'The Chemistry of the Heterocyclic Compounds Imidazole and Derivatives Part 1 - 1st Ed', Interscience Publishers, 1953.
140 J. J. Paul, S. R. Kircus, T. N. Sorrell, P. A. Ropp, and H. H. Thorp, *Inorg. Chem.*, 2006, **45**, 5126.
141 J. P. H. Charmant, G. C. Lloyd-Jones, T. M. Peakman, and R. L. Woodward, *Eur. J. Org. Chem.*, 1999, 2501.
142 R. Iemura, T. Kawashima, T. Fukada, K. Ito, and G. Tsukamoto, *J. Heterocycl. Chem.*, 1987, **24**, 31.
143 Q. X. Li, Q. H. Luo, Y. Z. Li, C. Y. Duan, and Q. Y. Tu, *Inorg. Chim. Acta*, 2005, **358**, 504.
144 Y. Wang, K. Sarris, D. R. Sauer, and S. W. Djuric, *Tetrahedron Lett.*, 2006, **47**, 4823.
145 Y. F. Li, G. F. Wang, P. L. He, W. G. Huang, F. H. Zhu, H. Y. Gao, W. Tang, Y. Luo, C. L. Feng, L. P. Shi, Y. D. Ren, W. Lu, and J. P. Zuo, *J. Med. Chem.*, 2006, **49**, 4790.
146 S. J. Winston, P. J. Rao, B. Sethuram, and I. N. Rao, *Indian J. Chem. A*, 1989, **28**, 520.
147 A. P. Thomas, C. P. Allott, K. H. Gibson, J. S. Major, B. B. Masek, A. A. Oldham, A. H. Ratcliffe, D. A. Roberts, S. T. Russell, and D. A. Thomason, *J. Med. Chem.*, 1992, **35**, 877.
148 K.-L. Yu, Y. Zhang, R. L. Civiello, F. Kadow, C. Cianci, M. Krystal, and N. A. Meanwell, *Bioorg. Med. Chem. Lett.*, 2003, **13**, 2141.
149 S. P. Elmore, Y. Nishimura, T. Qian, B. Herman, and J. L. Lemasters, *Arch. Biochem. Biophys.*, 2004, **422**, 145.
150 R. C. Scaduto and L. W. Grotyohann, *Biophys. J.*, 1999, **76**, 469.
151 A. Minta, J. P. Kao, and R. Y. Tsien, *J. Biol. Chem.*, 1989, **264**, 8171.
152 T. E. Wood, N. D. Dalgeish, E. D. Power, A. Thompson, X. Chen, and Y. Okamoto, *J. Am. Chem. Soc.*, 2005, **127**, 5740.
153 A. C. Ribou, J. Vigo, and J. M. Salmon, *J. Photochem. Photobiol., A*, 2002, **151**, 49.
154 E. Peña-Cabrera, A. Aguilar-Aguilar, M. González-Dominguez, E. Lager, R. Zamudio-Vázquez, J. Godoy-Vargas, and F. Villanueva-García, *Org. Lett.*, 2007, **9**, 3985.
155 T. Nguyen and M. B. Francis, *Org. Lett.*, 2003, **5**, 3245.
156 S. C. Burdette and S. J. Lippard, *Inorg. Chem.*, 2002, **41**, 6816.
157 Y. Koide, Y. Urano, S. Kenmoku, H. Kojima, and T. Nagano, *J. Am. Chem. Soc.*, 2007, **129**, 10324.
158 Y. Xiang and A. Tong, *Org. Lett.*, 2006, **8**, 1549.

159 Y. K. Yang, K. J. Yook, and J. Tae, *J. Am. Chem. Soc.*, 2005, **127**, 16760.
160 Y. Shiraishi, R. Miyamoto, X. Zhang, and T. Hirai, *Org. Lett.*, 2007, **9**, 3921.
161 M. H. Lee, J.-S. Wu, J. W. Lee, J. H. Jung, and J. S. Kim, *Org. Lett.*, 2007, **9**, 2501.
162 J.-S. Wu, I.-C. Hwang, K. S. Kim, and J. S. Kim, *Org. Lett.*, 2007, **9**, 907.
163 R. W. Wagner and J. S. Lindsey, *Pure Appl. Chem.*, 1996, **68**, 1373.
164 C. Goze, G. Ulrich, L. J. Mallon, B. D. Allen, A. Harriman, and R. Ziessel, *J. Am. Chem. Soc.*, 2006, **128**, 10231.
165 G. Ulrich, C. Goze, S. Goeb, P. Retailleau, and R. Ziessel, *New J. Chem.*, 2006, **30**, 982.
166 T. Rohand, M. Baruah, W. Qin, N. Boens, and W. Dehaen, *Chem. Commun.*, 2006, 266.
167 M. Baruah, W. Qin, N. Basarić, W. M. D. Borggraeve, and N. Boens, *J. Org. Chem.*, 2005, **70**, 4152.
168 H. Sunahara, Y. Urano, H. Kojima, and T. Hagano, *J. Am. Chem. Soc.*, 2007, **129**, 5597.
169 X. Qi, S. K. Kim, S. J. Han, A. Y. Jee, H. N. Kim, C. Lee, Y. Kim, M. Lee, S. J. Kim, and J. Yoon, *Tetrahedron Lett.*, 2008, **49**, 261.
170 R. Ziessel, L. Bondari, and G. Ulrich, *Dalton Trans.*, 2006, 2913.
171 L. Porres, O. Mongin, and M. Blachard-Desce, *Tetrahedron Lett.*, 2006, **47**, 1913.
172 R. Ziessel, L. Bondari, P. Retailleau, and G. Ulrich, *J. Org. Chem.*, 2006, **71**, 3093.
173 N. Malatesti, R. Hudson, K. Smith, H. Savoie, K. Rix, K. J. Welham, and R. W. Boyle, *Photochem. Photobiol.*, 2006, **82**, 746.
174 I. Perillo, M. C. Caerina, J. López, and A. Salerno, *Synthesis*, 2004, 851.
175 G. S. Poindexter, D. A. Owen, P. L. Dolan, and E. Woo, *J. Org. Chem.*, 1992, **57**, 6257.
176 E. Biron and N. Voyer, *Chem. Commun.*, 2005, 4652.
177 M. Itoh, D. Hagiwara, and T. Kamiya, *Tetrahedron Lett.*, 1975, **16**, 4393.
178 J. M. Sutton, E. Rogerson, C. J. Wilson, A. E. Sparke, S. J. Archibald, and R. W. Boyle, *Chem. Commun.*, 2004, 1328.
179 Y. Zhang, A. Thompson, S. J. Rettig, and D. Dolphin, *J. Am. Chem. Soc.*, 1998, **120**, 13537.
180 K. Kumar, C. A. Chang, L. C. Francesconi, D. D. Dischino, M. F. Malley, J. Z. Gougoutas, and M. F. Tweedle, *Inorg. Chem.*, 1994, **33**, 3567.
181 E. Balogh, R. Tripier, P. Fousková, F. Reviriego, H. Handel, and E. Tóth, *Dalton Trans.*, 2007, 3572.
182 A. J. Mishra, K. Draillard, A. Faivre-Chauvet, J. F. Gestin, C. Curtet, and J. F. Chatal, *Tetrahedron Lett.*, 1996, **37**, 7515.
183 H. Tsukube, Y. Mizutani, S. Shinoda, T. Okazaki, M. Tadokoro, and K. Hori, *Inorg. Chem.*, 1999, **38**, 3506.
184 S. J. A. Pope and R. H. Laye, *Dalton Trans.*, 2006, 3108.
185 S. Aime, A. Barge, J. I. Bruce, M. Botta, J. A. K. Howard, J. M. Moloney, D. Parker, A. S. de Sousa, and M. Woods, *J. Am. Chem. Soc.*, 1999, **121**, 5762.
186 S. Aime, M. Botta, and G. Ermondi, *Inorg. Chem.*, 1992, **31**, 4291.
187 J. Rudovský, M. Botta, M. Hermann, A. Koridze, and S. Aime, *Dalton Trans.*, 2006, 2323.
188 I. Sircar, T. Winters, J. Quin, G. H. Lu, T. C. Major, and R. L. Panek, *J. Med. Chem.*, 1993, **36**, 1735.

189 K. Nwe, J. P. Richard, and J. R. Morrow, *Dalton Trans.*, 2007, 5171.
190 J. M. Lalancette, A. Frêche, J. R. Brindle, and M. Laliberté, *Synthesis* 1972, 526.
191 M. Maillet, C. S. Kwok, A. A. Noujaim, and V. Snieckus, *Tetrahedron Lett.*, 1998, **39**, 2659.
192 S. J. Kline, D. A. Betebenner, and D. K. Johnson, *Bioconjugate Chem.*, 1991, **2**, 26.
193 G. Quéléver, S. Burlet, C. Garino, N. Pietrancosta, Y. Laras, and J.-L. Kraus, *J. Comb. Chem.*, 2004, **6**, 695.
194 O. J. Clarke and R. W. Boyle, *Chem. Commun.*, 1999, 2231.
195 H. Heitsch, A. Wagner, B. A. Schölkens, and K. Wirth, *Bioorg. Med. Chem. Lett.*, 1999, **9**, 327.
196 M. H. B. G. Gransey, F. J. Steemers, W. Verboom, and D. N. Reinhoudt, *Synthesis*, 1997, 643.
197 U. C. Yoon, Y. X. Jin, S. W. Oh, C. H. Park, J. H. Park, C. F. Campana, X. Cai, E. N. Duesler, and P. S. Mariano, *J. Am. Chem. Soc.*, 2003, **125**, 10664.
198 R. R. Petrov, R. S. Vardanyan, Y. S. Lee, S. Ma, P. Davis, L. J. Begay, J. Y. Lai, F. Porreca, and V. J. Hruby, *Bioorg. Med. Chem. Lett.*, 2006, **16**, 4946.
199 C. Fisher, 'PhD thesis', University of Hull, 2005.
200 W. D. Horrocks and D. R. Sudnick, *J. Am. Chem. Soc.*, 1979, **101**, 334.
201 A. Beeby, I. M. Clarkson, R. S. Dickens, S. Faulkner, D. Parker, L. Royle, A. S. de Sousa, J. A. G. Williams, and M. Woods, *J. Chem. Soc., Perkin Trans. 2*, 1999, 493.
202 R. M. Supkowski and W. D. Horrocks, *Inorg. Chim. Acta*, 2002, **340**, 44.
203 T. J. Meade, A. K. Taylor, and S. R. Bull, *Curr. Opin. Neurobiol.*, 2003, **13**, 597.
204 M. J. Hall, L. T. Allen, and D. F. O'Shea, *Org. Biomol. Chem.*, 2006, **4**, 776.
205 L. M. Harwood, C. J. Moody, and J. M. Percy, 'Experimental Organic Chemistry- 2nd Ed', Blackwell Sciences, 1999.